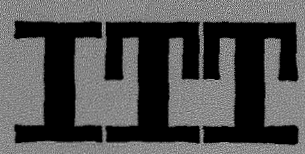


43 JAN 1956

4

TRANSISTOR DIVISION  
LIBRARY.

# **ELECTRICAL COMMUNICATION**

The logo for International Telephone and Telegraph (ITT), consisting of the letters 'ITT' in a bold, stylized, blocky font.

VOLUME 39 • NUMBER 1 • 1964

# ELECTRICAL COMMUNICATION

Technical Journal Published Quarterly by

INTERNATIONAL TELEPHONE and TELEGRAPH CORPORATION

320 Park Avenue, New York 22, New York

President: H. S. Geneen

Secretary: J. J. Navin

## CONTENTS

---

Volume 39	1964	Number 1
This Issue in Brief .....		2
Recent Achievements .....		7
Foreword on Satellite Communication by <i>H. Busignies</i> .....		23
Space-Research Ground Station by <i>B. Cooper and R. McCture</i> .....		25
Medium-Capacity Space-Communication Terminal by <i>L. Pollack, W. Glomb, and L. Gray</i> ..		37
System Configuration of Transportable Space-Communication Terminal by <i>D. Hershberg</i> ..		49
Antenna System for Transportable Space-Communication Terminal by <i>E. Singer and T. J. Vaughan</i> .....		58
Multifrequency High-Power Cassegrainian Antenna-Feed Systems for Satellite Ground Stations by <i>H. Scheiner, W. Spanos, and R. Edwards</i> .....		73
Transmitter for Satellite Ground Station by <i>H. Goldman, R. Graham, and L. Gray</i> .....		80
Communication Receiver for Satellite Ground Station by <i>M. Sassler and R. Surenian</i> .....		89
Satellite-Tracking Receiver by <i>W. Janeff</i> .....		98
Transportable-Station Operation with Telstar and Relay Satellites by <i>J. E. Drucker</i> .....		113
Satellite-Communication Ground Station in Germany by <i>Helmut Carl</i> .....		123
Transportable Satellite-Communication Ground Station in Brazil by <i>J. C. Fonseca and C. H. Moreira</i> .....		124
Radio Transmitter for Satellite Communication from Goonhilly Downs Station of the British Post Office by <i>E. A. Rattue</i> .....		129
Graphic Methods for Calculating Coverage Attainable with Communication Satellites by <i>R. Hepppe</i> .....		132
Spacecraft Technology for Satellite Communication Systems by <i>M. E. Brady</i> .....		144
Terrestrial Navigation by Artificial Satellites by <i>P. C. Sandretto</i> .....		155
Notes		
Duke Receives Honorary Doctorate .....		22
Barton Receives City and Guilds Award .....		36
Scarr and Aleksander Get Babbage Award .....		36

---

Copyright © 1964 by INTERNATIONAL TELEPHONE and TELEGRAPH CORPORATION

EDITOR, H. P. Westman

ASSISTANT EDITOR, M. Karsh

Subscription: \$2.00 per year

50¢ per copy

## This Issue in Brief

**Space-Research Ground Station**—Design studies during 1960 and 1961 used a fixed ground station to conduct narrow-band experiments using the moon as a reflector. These and later experiments with active satellites provided useful data on such parameters as terrestrial interference, atmospheric absorption, and satellite transmission characteristics.

A practical medium-capacity ground station includes a 10-kilowatt transmitter, a 40-foot (12.2-meter) paraboloidal antenna with cassegrainian feed system, and a radio-frequency equipment pod located near the apex of the primary reflector.

Voice and teleprinter communication via satellites have been demonstrated repeatedly. The ground station can be adapted to communicate with all present satellites, this flexibility being achieved primarily through use of a universal transmitting and receiving system with interchangeable front ends and antenna feed systems.

**Medium-Capacity Space-Communication Terminal**—The design of an air-transportable station for communication via satellites was based on experiments in reflecting narrow-band signals off the moon from a fixed station built for this purpose. Propagation conditions in space make the frequencies between 2 and 10 gigacycles per second most useful.

The signal-frequency equipments are in a single housing mounted at the vertex of the 30-foot (9.1-meter) primary paraboloidal reflector of a cassegrainian system. The remaining communication and control equipment is in a van. The reflectors are demountable for transport and are assembled without special tools or jigs to a surface tolerance within 0.08 inch (0.2 centimeter). The elevation-over-azimuth mount is hydraulically driven under control of a tracking system based on simultaneous-lobe-comparison operation. Parametric amplifiers are used for reception and a 10-kilowatt transmitter is provided.

Temperature control permits operation between

−20 and +129 degrees fahrenheit (−29 and +54 degrees centigrade). Tracking accuracy is maintained at wind speeds of 35 miles (56 kilometers) per hour and the antenna is controllable to the stow position at 60 miles (97 kilometers) with gusts of 90 miles (145 kilometers) per hour. An inflatable radome is required if heavy ice loading is encountered.

The 12 frequency-modulated frequency-division-multiplex voice channels are suitable for teleprinter, facsimile, and data communication. Other types of modulation and multiplexing could be accommodated.

The first transportable station was flown to Rio de Janeiro where it participated in the early tests of the Relay satellite. Two additional stations are working with Telstar and a fourth station, capable of immediate switching between Relay and Telstar, is for the German Bundespost. Estimated life is 10 years.

**System Configuration of Transportable Space-Communication Terminal**—The station is built into several vehicles of suitable size and weight for road or air transport. The antenna uses a cassegrainian arrangement of reflectors that are demountable. Three tracking receivers operate on a monopulse amplitude-sensing arrangement to produce both azimuth- and elevation-error signals to control the hydraulic drive that points the antenna. Parametric amplifiers are used for tracking and communication receivers.

Two klystron 10-kilowatt amplifiers operating between 2 and 10 gigacycles per second and all the microwave and frequency-determining equipment for transmission and reception are housed in an electronics package mounted on the paraboloidal reflector of the antenna. Connections to the equipment van are by coaxial cables at the intermediate frequency of 70 megacycles per second or lower.

Full control of the antenna and the apparatus in the electronics package, including monitoring of operations, is centralized in the radio van. Only four operators are required. Facilities for

measuring equipment performance, for prepass calibration, and for operation during a satellite pass are provided.

**Antenna System for Transportable Space-Communication Terminal**—Satellite communication requires highly maneuverable antennas for tracking a satellite either from a known ephemeris or by signal acquisition. In addition, transportability demands structures that can be carried by aircraft and assembled without heavy erection equipment.

A cassegrainian reflector system uses a demountable segmented primary reflector 30 feet (9.1 meters) in diameter and a secondary reflector 6 feet (1.8 meters) in diameter. The microwave equipment and associated waveguide feed systems are assembled in a package that is mounted at the vertex of the primary reflector.

The antenna is driven in both azimuth and elevation by hydraulic systems. Much of the paper is devoted to the servomechanisms that provide the precise adjustment for successful tracking of different satellites.

**Multifrequency High-Power Cassegrainian Antenna-Feed Systems for Satellite Ground Stations**—Ground-station antennas for satellite communication must provide large capture areas, contribute a minimum of noise, be capable of handling large powers, and track the target as well as communicate at several frequencies. Transmission and reception are respectively at 6 and 4 gigacycles per second for Telstar, at 2 and 4 for Relay, and at 8 and 2 for Syncom.

A cassegrainian system is used with a primary paraboloidal reflector 30 feet (9.14 meters) in diameter and a secondary hyperboloidal reflector 6 feet (1.8 meters) in diameter. For reception, the secondary reflector is coupled by 4 horns to the equipment through waveguides to provide lobe comparison for tracking in addition to communication. For transmission, only 2 waveguides are needed. Teflon polyrods are

used instead of flared horns to prevent blocking of the receiving ports while transmitting and to reduce the spacing of the two transmitting ports.

Data are given for the polyrod design and curves are presented of the performance of the feed system and of the antennas.

**Transmitter for Satellite Ground Station**—The 10-kilowatt transmitter used with Relay and Telstar has a 240-channel capability. Its microwave components are mounted in an equipment pod at the vertex of the antenna primary reflector. The exciter is crystal controlled and makes extensive use of varactor diodes as frequency multipliers.

The lower-frequency components for modulation, control, and power are contained in a van near the antenna base. A heat exchanger rounds out the installation.

Tuning and control are performed from the van with turn-on of the transmitter being automatically sequenced. Automatic fault protection plus self-clearing automatic reset for temporary failures are provided. The antenna-mounted control circuits remove all radio-frequency drive to the klystron within 10 microseconds after a fault occurs and maintain this condition long enough for the power to be shut off at the van.

Solid-state components throughout the transmitter permit substantial reduction in size and increase reliability. Nine transmitters have been placed in service through June 1963.

**Communication Receiver for Satellite Ground Station**—The microwave elements of the receiver are mounted at the vertex of the primary reflector of the antenna. A microwave hybrid system using 4 feed horns suitably positioned at the antenna provides signals for both tracking and communication. A 3-channel tracking receiver produces error signals for azimuth and elevation to control the pointing of the antenna. The dual communication receivers operate on the sum of all the horns.

The parametric amplifier, mixer, intermediate-frequency preamplifier, and local oscillator are also mounted in the antenna. The communication signals go to the demodulators in the van via 200 feet (61 meters) of coaxial cable.

In converting to baseband for either 6 or 12 channels, the frequency-modulation discriminator threshold is lowered by means of a phase-locked loop. Threshold extension of 3 to 4 decibels is obtained.

The receiver system noise temperature is 420 degrees Kelvin and produces a signal-to-noise ratio in the highest-frequency channel of 34.7 decibels for 6 channels and 38 decibels for 12 channels.

**Satellite-Tracking Receiver**—A satellite-tracking receiver is described that essentially consists of a front-end mixer mounted at the vertex of the paraboloidal reflector and a van-mounted receiver consisting of a sum channel and two difference channels, one for azimuth and the other for elevation signals. The sum channel supplies three signals to the difference channels: automatic gain control, reference signal, and voltage-controlled-oscillator signal. The voltage-controlled oscillator is part of a phase-locked loop in the sum channel.

The difference channels produce error signals that actuate a servo system to maintain proper antenna orientation toward the signal source.

The major portion of the paper is devoted to a discussion of error sources, pointing accuracy, and to tests proving the effectiveness of the design.

**Transportable-Station Operation with Telstar and Relay Satellites**—Operational experience with transportable space-communication terminals, using Telstar 1, 2, and Relay 1, has produced results closely correlated with expectations.

Tests showed that the primary causes of variation in signal level were the range and spin modulation of the satellite.

Tracking errors were held within  $\pm 0.03$  degree, and pointing errors within  $\pm 0.3$  degree, despite winds as high as 58 miles (93 kilometers) per hour.

Voice, teleprinter, facsimile, and medium-speed data communication were demonstrated successfully. Gain stability of more than  $\pm 0.5$  decibel was achieved for periods of many minutes, for radio-frequency levels above threshold.

The station may be transported by air or overland in as few vehicles as a 30-foot semitrailer van and two trailers, although ancillary equipment requirements may double this number.

**Satellite-Communication Ground Station in Germany**—A transportable ground station for communication via Telstar and Relay satellites was installed at Raisting, near Munich, Germany. A 120-channel microwave link connects the station to Munich.

**Transportable Satellite-Communication Ground Station in Brazil**—One of the transportable ground stations described in this issue was flown to Rio de Janeiro on 8 December 1962 and manually tracked the first orbit of Relay 1 five days later. It has since operated through that satellite with ground stations in Nutley, New Jersey, and Andover, Maine, in the United States; Goonhilly Downs in England; Pleumeur Bodou, France; and Fucino, Italy. The differences between predicted and actual tracking data have not reached 0.5 degree in elevation or azimuth. Testing intervals per pass have averaged 21 minutes with a maximum of 30 minutes. Telephone communication has been of commercial quality or better.

**Radio Transmitter for Satellite Communication from Goonhilly Downs Station of the British Post Office**—A 10-kilowatt 1725-megacycle-per-second radio transmitter is used to work with the Relay satellite from the experimental station of the British Post Office at Goonhilly Downs in Cornwall, England. Either of two types of klystrons may be used in the output

stage, only about 10 minutes being needed to substitute one for the other. An artificial load may be quickly connected to the output waveguide.

The extra-high-tension supply is turned on and off by push buttons. After being turned on, a vacuum tube in series with the output is adjusted by a single dial to set the output voltage. This tube also protects against excessive current flow, waveguide flash-over, and too high a standing-wave ratio, as well as a filter-capacitor discharge into the klystron.

A heat exchanger is fully monitored for water flow and temperature and will interrupt power if set limits are not maintained. An automatic valve keeps the outlet water within safe temperature limits.

**Graphic Methods for Calculating Coverage Attainable with Communication Satellites**—For a given orbital plane and altitude of a satellite and for a minimum receiving angle above ground of 7.5 degrees to reduce noise, graphic solutions indicate the period of satellite visibility at a ground station. For operations between two such stations, the satellite must be visible to both simultaneously.

For a circular polar orbit, a template permits any visibility area, which varies with latitude, to be plotted directly on a world map having equally spaced orthogonal latitude and longitude lines. Similar charts may be prepared for equatorial and inclined orbits. Polar satellites are most effective except for east-west links near the equator and north-south links that cross the equator.

Curves are given for the probability that a single satellite in circular polar orbit will be simultaneously in view of two stations in north-south and in east-west links and for the percent of time that 24 randomly spaced satellites will not provide service. For a given continuity of service, substantially fewer equally spaced than randomly spaced satellites are needed, but failures will penalize the former system more severely and tend to make it random.

Batteryless satellites are incapacitated in the shadow of the earth. For more-northerly links, the shadow overlaps the mutual-visibility area very little during most of the year.

**Spacecraft Technology for Satellite Communication Systems**—Full stabilization of a synchronous satellite requires attitude control so that on command from the ground tracking station the correcting propulsion thrusts may be properly directed. Attitude control permits use of directive antennas. Syncom depends on spin stabilization to keep one axis in fixed inertial space and an on-board logic system to control both orbit and a pencil-beam directive antenna pattern.

Our launch vehicles can now put about 700 pounds in synchronous orbit. The satellite transmitter, which is the limiting factor in the entire satellite communication system, may then have a power of about 25 watts. A small number of synchronous satellites will suffice but failures may cause substantial reduction in service.

Medium-altitude systems will use a relatively large number of randomly spaced spin-stabilized satellites in polar orbits. Toroidal antenna patterns will always lie in the plane of the orbit. Transmitting power will be about 4 watts. Failure of a satellite will cause only a small deterioration in service. Control of spacing can improve the reliability of the system.

For a 6-year period, a system that maintains at least 6 satellites in synchronous orbits, each having a mean-time-to-failure rate of 1 year and a launch probability for each satellite of 0.5, is estimated to cost \$470 million. A system maintaining at least 27 medium-altitude satellites in random orbits, each having a mean-time-to-failure rate of 3 years, and with a launch probability of 0.7 for 6 spacecraft per launch, is estimated to cost \$190 million. Costs will be lowered as larger launch vehicles become available.

Solar cells and batteries are limited to low powers. Nuclear-isotope heat sources with

thermoelectric converters can provide for medium powers, but nuclear reactors alone can produce powers in the kilowatt region. Natural and man-made radiations damage solar cells and transistors. Most-intense radiation is found about 2000 nautical miles (3704 kilometers) above the geomagnetic equator.

**Terrestrial Navigation by Artificial Satellites—**

A new system of navigation employs a stable oscillator in an orbiting satellite and a receiver at the point where position is to be determined. The receiver measures the doppler shift in the transmitted frequency as a function of the motion of the satellite. The exact position of the satellite being known, the position of the receiver can be calculated for the instant of closest approach when the doppler shift is zero.

In a typical satellite, a 3-megacycle-per-second quartz crystal, stable to within 1 part in  $10^8$ , controls the frequency of four transmitters operated at 54, 162, 216, and 324 megacycles per second. A ground station transmits corrections for both time and position to the satellite. Thus, the satellite constitutes a self-contained system in that it continually transmits a correction to its ephemeris as well as accurate time. The ground receiver differs from conventional designs in that it incorporates a phase detector

to limit noise, receives simultaneously on two harmonically related frequencies to compute a refraction correction, and records doppler frequency against real time on a paper tape that is inserted directly into a digital computer.

A position is determined from the exact time of zero doppler shift as broadcast from the satellite, an exact knowledge of the position and altitude of the satellite from an ephemeris and the broadcast correction, and the slant angle of the satellite from the horizon of the receiver as determined by the rate of change of doppler frequency.

Five Transit satellites have been orbited and three are still in service. As an example, the first one produced a signal on the surface of the earth on each side of its orbit over approximately 1600 miles. Its period of 1 hour and 36 minutes advanced its position eastward by 24 degrees or 1600 miles at the equator each pass. On the equator, 4 to 6 observations could be obtained each 24 hours. Measurements made at a fixed known location gave a maximum error of less than a mile.

Initial and maintenance costs are of the same order as for a ground-based radio system. Its greatest field of application appears to be with ships rather than aircraft.

## Recent Achievements

**Telex Automatic Transatlantic Switching**—The inauguration of a fully automatic telex subscriber-to-subscriber switching system linking Europe and North America occurred in November 1963. The initial exchange of telex messages was between P. H. Spaak, Belgian Minister of Foreign Affairs, in Brussels, and L. Hodges, United States Secretary of Commerce, in Washington. With Secretary Hodges were His Excellency Louis Scheyven, Belgian Ambassador to the United States, and Mr. B. B. Tower, President of American Cable & Radio Corporation.

The Brussels ceremony, shown in Figure 1, was attended by His Royal Highness Prince Albert of Liège; Mr. Theo Lefevre, Prime Minister; Mr. P. H. Spaak, Vice Prime Minister and Minister of Foreign Affairs; Mr. E. Anseele, Minister of Post, Telegraphs, and Telephones; Mr. A. Bertrand, Minister of Com-

munications; Admiral E. W. Stone, Chairman of the Board of American Cable & Radio Corporation and President of ITT Europe; Mr. C. Van Rooy, President and Managing Director of Bell Telephone Manufacturing Company, and Mr. D. Catlett, Economic Counselor to the United States Embassy.

After remarks by Minister Anseele, Admiral Stone, and Mr. Van Rooy, the official exchange of messages between Minister Spaak and Secretary Hodges took place. The audience watched the proceedings on television screens installed in the room. There then followed a fully automatically switched call from Washington to Brussels that was also witnessed by those present.

A transatlantic submarine cable provides the link over which this new facility operates. Belgium is thus the first country in Europe to be directly connected by automatic telex switching to the public network in the United States,



Figure 1—Present at the Brussels end of the inauguration of the first fully automatic subscriber-to-subscriber telex switching system linking Belgium and the United States were, from right to left, Messrs. E. W. Stone, A. Bertrand, P. H. Spaak, His Royal Highness Prince Albert, T. Lefevre, E. Anseele, and D. Catlett. The speaker is Mr. C. Van Rooy.

## Recent Achievements

access being provided to not only the telex subscribers of American Cable & Radio but to both the domestic telex subscribers of Western Union and the Bell System teletypewriter network. Outgoing calls from the latter two systems will be on a semiautomatic basis. Calls may be extended through Belgium to other European telex networks now connected with that country.

An outstanding feature is keyboard selection in which the calling subscriber uses the telex machine rather than a dial for calling an overseas number. A memory unit records electronically the calling and called numbers, length of call, and any other pertinent data. When the trunk circuit is released, a perforated tape record is made for billing.

The 7E automatic switching equipment for the system was manufactured by Bell Telephone Manufacturing Company, which also installed it in the Brussels, New York, and San Francisco terminals.

*Bell Telephone Manufacturing Company  
Belgium  
American Cable & Radio Corporation  
United States of America*

**Stimulated Emission of New Infrared Transitions of Helium and of Neon**—Spectrographic analysis of radiation from a gas laser shows stimulated emission for two new transitions. One at  $\lambda = 1.269$  microns belongs to the neon spectrum and the other at  $\lambda = 1.955$  microns was observed in pure helium. A note on this research was presented by Louis de Broglie in *Comptes Rendus of the French Academie des Sciences* in volume 257, number 5, pages 1044–1047; 29 July 1963.

The laser, shown in Figure 2, uses a discharge tube 4 meters (13 feet) long excited by an 800-watt continuous-wave high-frequency generator. The end faces of the tube are flat silicon windows set for Brewster incidence. The cavity is made with metallized silicon mirrors mounted on high-precision orientation heads. The beam is analyzed with a silica-prism spectrograph employing photomultiplier, lead-sulphide, and thermocouple detectors.

The laser tube is connected to a special ultra-vacuum and filling station to permit the study of a great variety of gas mixtures of extreme purity.

*Laboratoire Central de Télécommunications  
France*

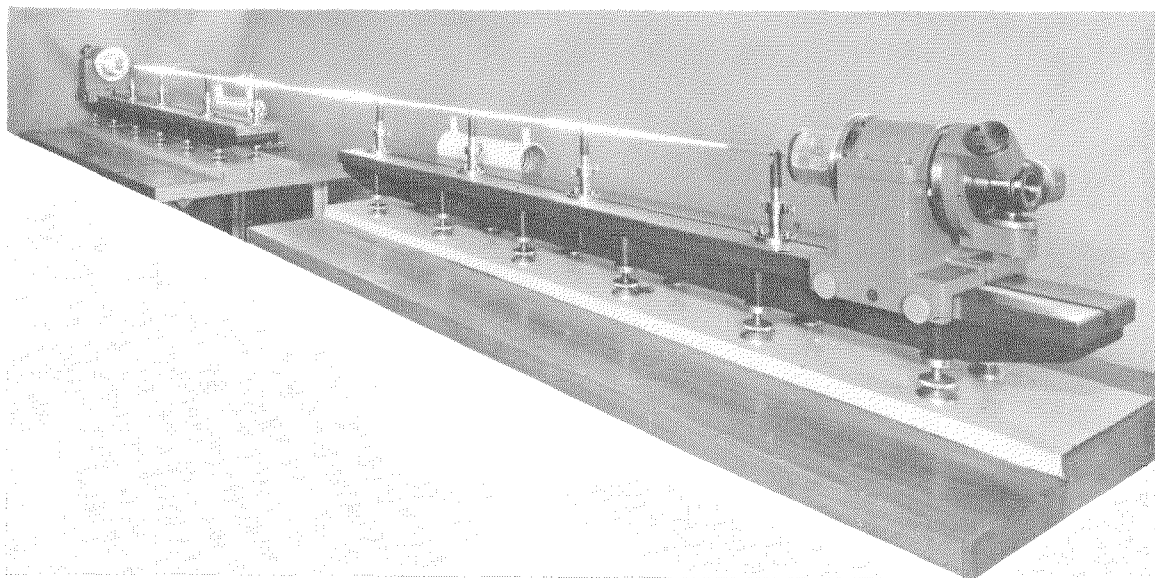


Figure 2—Laser tube 4 meters (13 feet) long used in spectrographic analysis of stimulated emission.

**Emergency Extension of Telephone Lines Via Radio**—The *SEM 27 KA* equipment, shown mounted in a motor vehicle in Figure 3, permits the extension of telephone lines via radio for emergency service.

Two *SEM 27* radio sets are provided together with the hybrid circuits required for connection to both local-battery and common-battery telephone systems. Switching facilities permit the 2 sets to serve up to 8 telephone lines or to be extended to either a private automatic branch exchange or to the public network. Provision is made also for simultaneous voice and teleprinter operation.

The radio sets may be operated independently and either can be quickly removed from the vehicle for separate service with its own hybrid circuits.

For relaying, each receiver is connected through its associated transmitter for simplex operation. Duplex operation requires use of both sets with the output of one receiver actuating the other transmitter, corresponding to a 4-wire circuit. The operator's set, or its extension through a telephone line, permits monitoring, including speech, for the equivalent of a conference connection. For remote control, a 2135-hertz signal will connect the receiver through the transmitter to operate as a relay for about 30 seconds. This call can be repeated any number of times. For normal operation, a 1750-hertz calling frequency is used.

The installation operates from a pair of 12-volt storage batteries with provision for charging from the mains or from the vehicle generator. The teleprinter is powered through a converter or may be operated from an emergency generator.

*Standard Elektrik Lorenz  
Germany*

**Portable Cartridge Recorder-Reproducer**—Designed for portable service under outdoor

conditions is the recorder-reproducer using cartridge loading of tape shown in Figure 4.

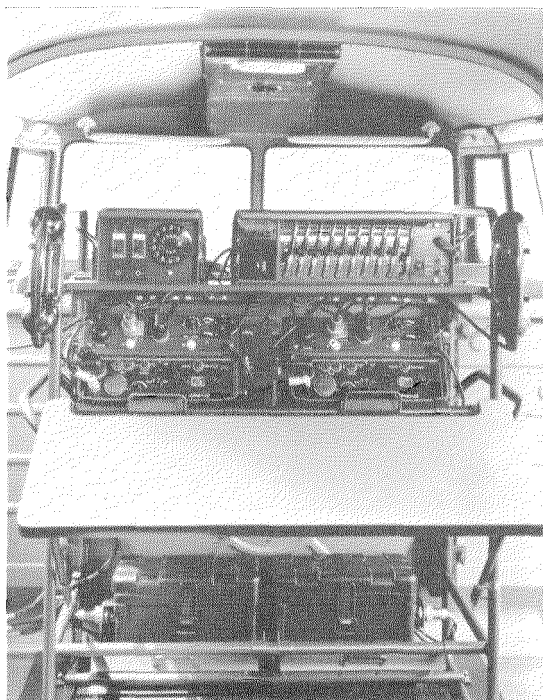


Figure 3—Mobile installation of 2 radio equipments and the required hybrid circuits to connect them to telephone lines for emergency service.

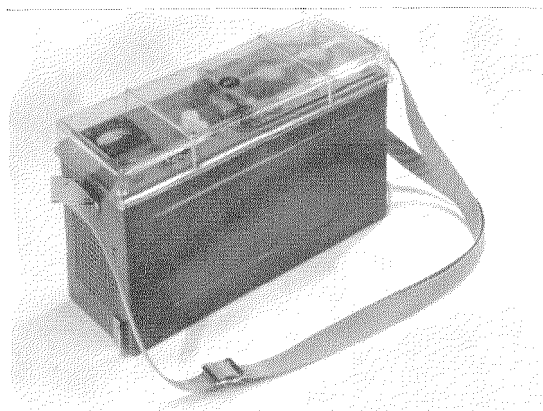


Figure 4—Portable tape recorder using cartridge magazine for tape storage. The transparent cover permits use in inclement weather.

## Recent Achievements

Enough magnetic tape for 40 minutes of recording is coiled in a plug-in cartridge within a plexiglass enclosure marked to indicate minutes of unused recording time. The transistor amplifiers for recording and reproducing and the stabilizing circuits for controlling the speed of the tape transport system are mounted on a plug-in circuit board.

The equipment is mounted in a compact watertight aluminum cabinet having a transparent cover through which the operating indicators may be seen. A plastic strap is adjustable for convenient carrying. The equipment, without batteries, weighs about 2 kilograms (4.4 pounds).

*Bell Telephone Manufacturing Company  
Belgium*

**Antenna Design for Jet Aircraft**—The growing amount of radio communication and navigation equipment carried by modern aircraft has increased the number of antennas and the prob-

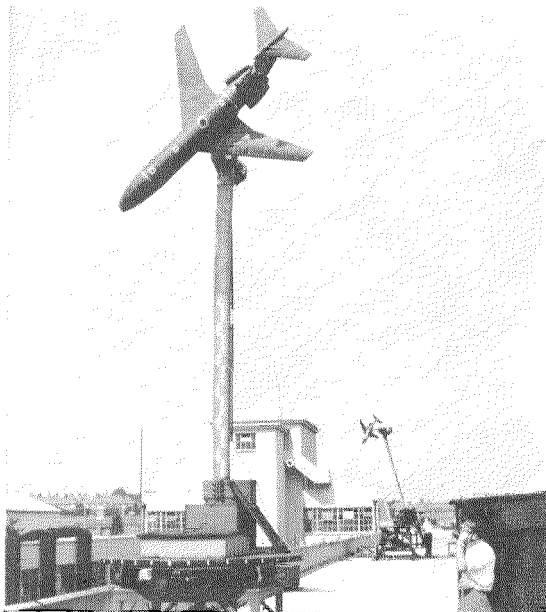


Figure 5—Aircraft models used for siting radio antennas to produce desired performance and avoid mutual interference.

lem of siting them not only to provide suitable performance, but to avoid damaging interaction among them. The Trident aircraft, for instance, has nearly 30 separate antennas.

Even before a new aircraft is built, the positions of all antennas can be established by working with small models covered with copper. If the model is  $\frac{1}{10}$  the size of the actual aircraft, the antennas will be tested at 10 times the frequency at which the actual antennas will operate. This frequency multiplication permits measurements to be made on a test range of less than 100 feet (30 meters).

The team of engineers working with models of the Hawker Siddeley Trident and 125 executive aircraft shown in Figure 5, also sited the antennas for the Argosy, Vanguard, Belfast, Buccaneer, and Britannia planes. The models are mounted about 20 feet (6 meters) above ground on fibre-glass poles. They may be remotely placed in any position relative to a fixed transmitting antenna 80 feet (24 meters) to the left in the figure. Field strength patterns are plotted automatically.

*Standard Telephones and Cables  
United Kingdom*

**Cool Stars Detected by Infrared Telescope**—An extremely sensitive infrared telescope has disclosed the existence of stars whose visible radiation is too faint to be seen. It has also indicated that some known stars emit much more infrared radiation than was previously estimated.

Sensitive enough to be disturbed by the heat of insects that fly by, the telescope can detect satellites by the heat they emit. To distinguish man-made heat sources from celestial bodies, the positions of the latter must be known; about 20 percent of the sky has already been mapped.

*ITT Federal Laboratories  
United States of America*

**Laser Range Finder**—An experimental laser range finder, shown in Figure 6, uses a single

light pulse from a ruby laser to illuminate the target. Some of the reflected light is collected by a telescope equipped with a photomultiplier. The time interval between transmitting the pulse and its reception determines the distance to the target.

The very-narrow beam of the laser permits it to be confined to a small target such as a vehicle without being disturbed by surroundings such as trees, poles, and houses. The measurement is accurate to within about 5 meters (16.4 feet) and is nearly independent of range. The operator aims at the target, presses a trigger, and the range is displayed immediately on numerical indicators.

A maximum range of about 10 kilometers (6.2 miles) is obtained in clear weather. In fog or mist, the range is about that of visibility.

*Laboratoire Central de Télécommunications  
France*

**Modulation of Gallium-Arsenide Lasers**—For optical communication, gallium-arsenide lasers must be modulated. If the radiations from two such diodes are collimated on the same optical path and the input modulation signals are 90 degrees apart in phase, the second-harmonic sidebands are balanced and a reduction in this distortion of more than 20 decibels can be obtained.

This technique may be considered to be an extension of push-pull electron-tube amplifiers in which the modulating signals are applied in phase opposition and extracted as the difference of the individual outputs. In the laser case, the light outputs are added rather than subtracted.

*ITT Federal Laboratories  
United States of America*

**Gas Laser of Reduced Size**—The gas laser shown in Figure 7 was presented at the International Aeronautic and Space Exhibition at Le Bourget on 7–16 June 1963. The laser ele-

ments are only 1 meter (40 inches) in length and weigh less than 10 kilograms (22 pounds).

A tube filled with helium and neon is mounted in an interferometer with preadjusted mirrors. A metal cylinder protects all of the elements and rigidly establishes their relative positions. By changing the mirrors, the emitted beam can be either visible ( $\lambda = 0.6328$  micron) or infrared ( $\lambda = 1.15$  microns).

The beam power is of the order of 5 milliwatts.



Figure 6—Range finder operating on a single pulse from a ruby laser.

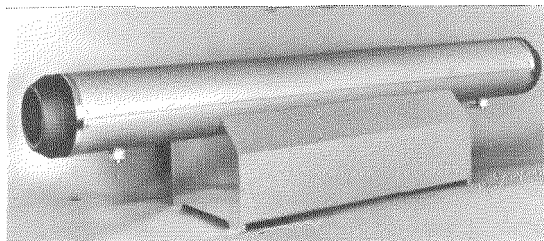


Figure 7—Gas laser for producing either visible or infrared radiation.

## Recent Achievements

Excitation is at 27.12 megahertz from a generator adjustable from zero to 100 watts. The unit provides a source of highly directive coherent radiation of narrow spectral response.

*Laboratoire Central de Télécommunications  
France*

**Multielement Infrared Detector**—To detect the radiation produced by ballistic missiles during midcourse and re-entry, a suitable detector is mounted in a jet aircraft that cruises at the re-entry altitude.

A 6-inch (15-centimeter) Dall-Kirkham cassegrainian telescope images the target on a 25-element array of thermoelectrically cooled lead-sulphide detectors. An oscillating mirror provides a 3-milliradian scan of the field. Any of 4 long-wavelength interference filters may be placed in the optical path.

For calibration, a sun shutter closes for 3 seconds and 6 attenuators are successively interposed between a quartz-lamp radiation source and the detector array. In operation, each detector individually delivers its signal through a transistor preamplifier to the processing console and recorder.

*ITT Federal Laboratories  
United States of America*



Figure 8—Push-button set in New York for making airline reservations in London via transatlantic telephone cable.

**Flight Reservations Via Transatlantic Cable**—British Overseas Airways Corporation New York ticket reservation desks are now linked via transatlantic cable with a central computer in London that provides immediate information on bookings on all its flights for the next 140 days.

The reservation desk, shown in Figure 8, using a push-button set will interrogate the computer regarding the flight requested by a customer. The reply appears within 4 seconds as an arrangement of colored lights indicating if seats are available, sold out, and whether there is a waiting list. If the desired flight is filled, the state of booking on 9 alternative flights on which seats are available will be shown. Several controller-type key sets permit up-dating of the booking information in the London computer on all flights of British Overseas Airways Corporation and its associated companies in and out of North America.

The New York installation is the latest in this electronic reservation network that serves Montreal, Frankfurt, Düsseldorf, and Zurich, in addition to all regional offices in the United Kingdom.

*Standard Telephones and Cables  
United Kingdom*

**Pentaconta Transit Exchange Opened in Rome**—One of the most-important centers in the telephone network of Italy was recently placed in service in Rome.

The new transit toll exchange handles all incoming communication to Rome or for transit through Rome. In addition, it handles all terminal and transit traffic from Rome to the toll and regional centers of the primary network and overflow traffic from transit lines whenever all direct circuits are busy.

All switching is by 4-wire Pentaconta equipment with two separate groups of registers, one for outgoing and the other for incoming and transit calls. There are 214 manual positions with push-button dialing, 360 each of incoming

and outgoing national toll lines, 40 junctions for transit service with manual lines, and 143 junctions toward the Rome local exchange.

*Fabbrica Apparecchiature per Comunicazioni  
Elettriche Standard  
Italy*

**100-Megawatt Hydrogen Thyatron**—The *KU-275A* ceramic-insulated hydrogen thyatron shown in Figure 9 has a peak power output of 100 megawatts. Operated with a moderate amount of air cooling, an average power output of 200 kilowatts is obtained. Maximum ratings are 50 kilovolts for both peak forward and reverse anode voltages, 4000 amperes peak anode current, and 8 amperes average anode current. The tube is 16 inches (41 centimeters) high and weighs 45 pounds (20.4 kilograms).

*ITT Electron Tube Division  
United States of America*

**Post Office Automation**—In its program of mechanizing the handling of mail, the German Bundespost has installed in the Hamburg post office 5 culling and 5 letter-facing machines as shown in Figure 10.

Each culling machine separates mixed mail into regular envelopes, large envelopes, bulky or stiff items, and parcels at a rate of 32 000 items



Figure 9—Ceramic-insulated thyatron capable of controlling a peak power of 100 megawatts.



Figure 10—Culling and facing machines in the Hamburg post office.

## Recent Achievements

per hour. The use of fluorescent ink on postage stamps permits each facing machine to arrange all envelopes with their addresses facing the same way at a rate of 26 500 items per hour. These two steps are preliminary to machine cancellation of the stamps and to sorting with automatic distribution to destination bins. These 10 machines can handle the entire collection of mail from the post boxes of the city. During the past 5 years, a substantial number of automatic mail-handling units have been supplied to the German post office including the first letter-facing machines that detect fluorescent postage stamps in their operation. Equipment has been installed in post offices in Italy, The Netherlands, and the United States.

*Standard Elektrik Lorenz  
Germany*

**Thin-Film Amplifier**—An intermediate-frequency amplifier for use in microwave systems has been designed for mass production by the thin-film technique. This 4-transistor unit employs a dozen capacitors and 16 resistors that, with their interconnecting leads, are deposited in successive thin films that can be produced



Figure 11—Localized radio-frequency heating is used in zone refining of material held in a water-cooled silver crucible.

quickly and economically. Weighing but  $\frac{1}{4}$  ounce (7 grams), the unit is about 1 percent of the size of a corresponding vacuum-tube device.

*ITT Federal Laboratories  
United States of America*

**White-Hot Metal in a Cold Crucible**—Chemically reactive materials may be melted and processed at high temperatures without contamination by using radio-frequency heating and water-cooled metal crucibles. Molybdenum, iron, vanadium, and boron, besides materials like ferrites, may be melted without either wetting the cold surface with the molten charge or forming a solid skin.

The crucibles are generally made of silver and can assume various forms. For zone refining as in Figure 11, an elongated “boat” crucible and means for moving the melt region along

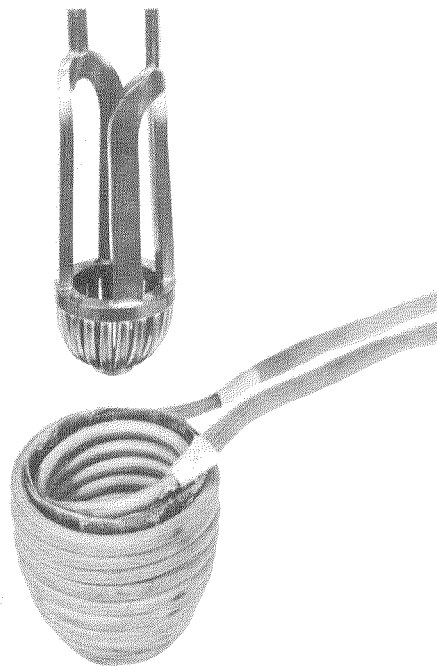


Figure 12—For growing single crystals, material melted by radio-frequency currents stays within this water-cooled cage of silver probably by a combination of surface tension and pinch effect.

the crucible is required. The cage and heating coil shown in Figure 12 are used for growing single crystals from a melt. The molten charge is held in this cage probably by a combination of surface tension and pinch effect.

*Standard Telecommunication Laboratories  
United Kingdom*

**Frequency Dividers for Time-Pulse Metering**

—For billing purposes, metering of calls over the Swiss automatic telephone network is based on a number of pulses, determined by the zoned distance between stations, being registered in the subscriber's meter at the start of every 3-minute interval. It is planned to replace this with a system that supplies pulses at time intervals that become shorter as the call distance increases.

The first metering impulse must be registered not more than 6 seconds after the start of conversation. Pulses will be supplied at short time

intervals by a master generator. To provide for the pulse frequency corresponding to the present 3-minute tariff in use, the 16:1 frequency divider shown in Figure 13 has been developed. They will be installed in each of 45 000 metering control circuits throughout the country. The frequency divider uses a 2-stage magnetic counter and is economical of both components and space.

*Standard Téléphone et Radio  
Switzerland*

**Sound-Recognition Machine**—The basic phonetic elements of human speech are called phonemes and a machine has been developed to distinguish among such sounds within a selected class.

The machine first “learns” the characteristics of the phonemes it is to recognize and later will identify those that occur among sounds presented to it. Such recognition is not limited to speech but could include sounds of vehicles such as automobiles and aircraft.

*ITT Federal Laboratories  
United States of America*

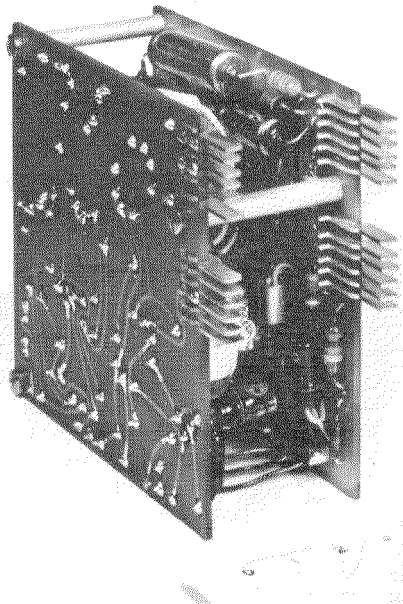


Figure 13—Frequency divider for new telephone metering system in Switzerland.

**Remote Control and Signalling**—An electronic system for both remote control and signalling has been put in service at Nieuwe Vaart for the electricity administration of Ghent in Belgium.

The Digitel 140 remote signalling system operates at 50 bauds over a 120-hertz telegraph channel and reports on the operating states of 140 units every 3.6 seconds. Five such systems are employed to care for 100 circuit breakers, 300 section breakers, and 200 alarms. Each uses a distinctive frequency so that all may transmit over a single telephone pair. A message consists of 14 information groups and one synchronization group. Parity checks protect against transmission errors.

The remote control system uses a duplex 100-baud telegraph channel over a telephone pair.

## Recent Achievements

One control order is handled at a time and there is capacity to control 600 units. At present, 60 circuit breakers are being controlled from Nieuwe Vaart.



Figure 14—Stantec 2000 warehouse stock control and handling system.

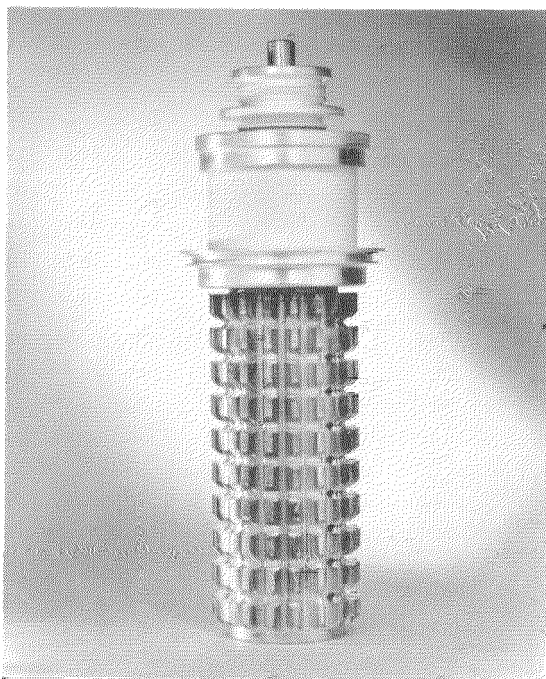


Figure 15—Evaporation-cooled triode capable of dissipating 100 kilowatts.

The code address of the specific piece of apparatus to be controlled is first transmitted to the substation, where it serves to select the appropriate control relay. The code address is then retransmitted to the master station for verification, after which the control order is transmitted. The time required for such a control operation does not exceed 800 milliseconds.

*Bell Telephone Manufacturing Company  
Belgium*

**Gyroscope Gas-Lubricated Bearings**—On page 13 of volume 38, number 1, of this publication appeared a brief description of a gyroscope consisting of a fused-quartz sphere enclosed within a metal sphere. Both spheres are driven by high-pressure air jets that also float the inner sphere to provide a nearly frictionless bearing and a highly flexible coupling between the two spheres that rotate at the same speed.

Conventional inertial platforms using the finest mechanical bearings have too much friction to permit the full possibilities of this new gyroscope to be realized. A special gas transfer system has therefore been developed to provide gas lubrication to the platform and gimbal bearings for smooth minute positioning of the gyroscope with very-low expenditure of power.

*ITT Federal Laboratories  
United States of America*

**Stantec Warehouse Stock Control**—The first of ten installations of a new warehouse stock control and handling system for groceries based on the Stantec computer is shown in Figure 14. It was completed in Nürnberg for Kaspar, K.G., a member of the international Spar group. The remaining installations for Spar and independent warehouse operators will be in the Nürnberg, Frankfurt, Essen, and Heidelberg areas.

Based on a Stantec computer and an integrated system of handling goods, the installation is the result of nearly two years of operation of

a pilot plant at the Johan Drexel warehouse in Dornbirn, Austria, which quickly showed a dramatic increase in turnover of stock and an equally impressive speed-up in the handling of goods in the warehouse. A very-substantial reduction in stock is permitted as the computer automatically prints orders, fully addressed and ready for mailing to the suppliers, for every item for which only a predetermined minimum safe quantity remains in stock.

Standard Elektrik Lorenz has cooperated closely in this project.

*Standard Telephones and Cables  
United Kingdom*

**100-Kilowatt Evaporation-Cooled Triode**—The *F-8388* is a general-purpose amplifier, oscillator, and modulator having plate dissipation of 100 kilowatts with evaporation cooling.

A thoriated-tungsten cathode is used. Amplification factor is 25. The maximum continuous-wave ratings up to 30 megahertz are a plate voltage of 17 000, grid voltage of  $-3000$ , plate current of 19 amperes, grid current of 3.5 amperes, and plate input of 250 kilowatts. The tube, shown in Figure 15, uses ceramic insulation and is approximately 25 by 7 inches (63.5 by 17.8 centimeters).

*ITT Electron Tube Division  
United States of America*

**Radiotelephone Selective Calling**—A fully electronic selective calling unit for mobile radiotelephone networks, coded *SRS 37*, is shown in Figure 16. It is based on the simultaneous transmission of 2 frequencies out of 10 to select any one of 45 called stations or in two stages to care for  $45 \times 44 = 1980$  stations.

The 10 audio frequencies are related by the factor 1.224. In the receiver, each of the two desired frequencies passes through a *T*-type band-pass filter to actuate a trigger circuit, the

operating threshold of which can be adjusted for the particular operating conditions. The outputs of these two triggers operate a third buffer trigger through an AND gate. If a second pair of frequencies are required to complete the selection, the corresponding tone filters are then connected and respond in the same way.

The operation of the final buffer trigger by the designated calling frequencies controls a flip-flop circuit that actuates a call lamp, a bell, and turns on the transmitter. After the initial ring for a controlled time, the call lamp goes out and a service lamp lights. A press-to-talk button in the handset then controls the transmitter. At the end of the conversation, the mobile-station operator presses a button that restores the equipment to normal.

To avoid interference from other calling stations when operation with one station has been established, a noise-controlled speech-blocking circuit is used. As propagation can exceed the normal radio horizon at times, one of a series of audio frequencies may be used to provide audio selectivity in addition to the radio channel selectivity in calling a particular fixed station.

The selective calling unit is operated from a 12-volt battery or from a 6-volt battery through



Figure 16—Fully electronic selective call unit for mobile radiotelephone networks. As many as 1980 separate stations may be called individually.

## Recent Achievements



Figure 17—Double-spiral antenna for 2.5 to 11 gigahertz. This receiving unit is only 2.5 inches (6.3 centimeters) in diameter.

a built-in transistor converter. For remote-control operation, a blocking-tone receiver is available.

*Standard Elektrik Lorenz  
Germany*

**Lightweight Spiral Antenna**—A small lightweight double-spiral antenna operating over a band from 2.5 to 11 gigahertz is shown in Figure 17. It is circularly polarized and the directivity pattern is 65 degrees wide between the half-power points. Standing-wave ratio is less than 2.5 to 1. For reception, the unit is only 2.5 inches (6.3 centimeters) in diameter; larger designs for transmission are available. The units can be used with paraboloidal reflectors or in arrays to increase the directivity.

*ITT Kellogg Communications Systems  
United States of America*



Figure 18—Demonstration equipment for converting 6-, 7-, and 8-unit code groups into 5-unit code for transmission over a conventional 5-unit start-stop telegraph system.

**Converting 6-, 7-, and 8-Unit Codes Into 5-Unit Code**—Telegraph systems using the conventional 5-unit start-stop code are usually unable to handle data in code combinations containing more than 5 elements. A code converter or regrouper to change 6-, 7-, and 8-unit codes into the 5-unit code permits transmission of data over such systems.

A 7- or an 8-unit code combination is converted into two 5-unit characters while two 6-unit combinations form three 5-unit characters. The first pulse of the first of the two or three 5-unit combinations is used for synchronization.

A demonstration model is shown in Figure 18. At the left is the tape reader of the regrouper handling 6-, 7-, or 8-unit code and its transmit terminal, while on the right of the 5-unit monitoring teleprinter is the receive terminal, regrouper, and tape punch producing 6-, 7-, or 8-unit output.

*Standard Telecommunication Laboratories  
United Kingdom*

**Television Program Switching**—The equipment shown in part in Figure 19 permits television network switching and program distributing over radio links that use 70-megahertz intermediate frequencies. Providing for 13 inputs and 17 outputs, it corresponds to a crossbar system using latching coaxial dry-reed relays that maintain their operated positions without electric power.

Without disturbing an existing switching pattern, a future rearrangement may be stored in relays and then be actuated by a master change-over switch. Both the existing and proposed switching patterns are displayed on signal lamps. An electric interlock prevents accidental operation.

Isolation amplifiers and attenuators prevent a fault in one channel from affecting others. The impedance of 75 ohms varies by not more than 4 percent from 58 to 82 megahertz and 6 percent from 55 to 85 megahertz. Over this wider

band, the insertion loss does not exceed 0.8 decibel and the response-versus-frequency is within 0.6 decibel. The differential phase change is within 0.5 degree. The input and output levels are approximately 0.5 volt.

*Standard Elektrik Lorenz  
Germany*

**Solid-State Microwave Power Source**—The microwave power source shown in Figure 20 produces an output within 1 decibel of 0.8 watt over a range from 4181 to 4395 megahertz. A 67-megahertz driver with a built-in frequency-modulation facility is followed by 6 band-pass-coupled frequency-doubling stages using voltage-sensitive capacitor diodes.

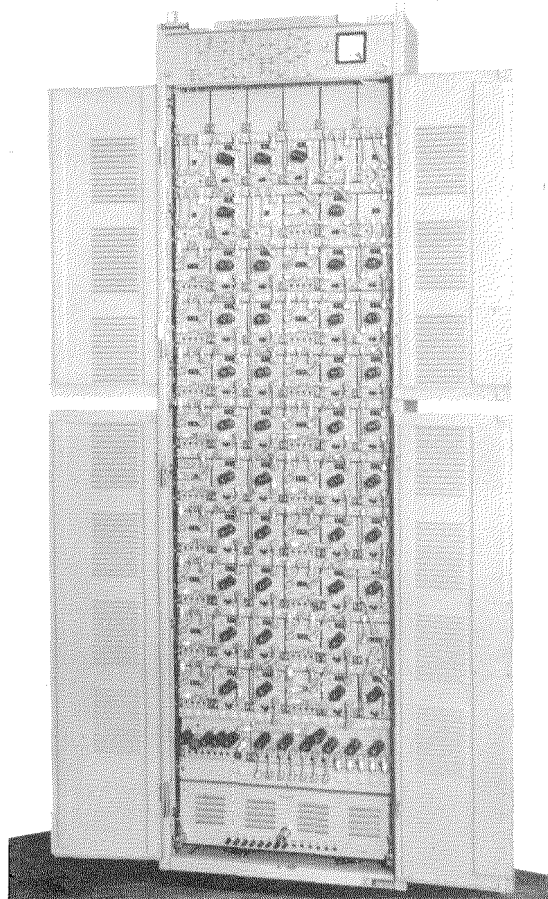


Figure 19—Distribution panel for television programs.

## Recent Achievements

A direct-current power supply of 28 watts is required. The unit is 10 by 2 by 2 inches (25 by 5 by 5 centimeters) and weighs 4 pounds (1.8 kilograms).

*Standard Telecommunication Laboratories  
United Kingdom*

**Filter-Detector for S and C Bands**—A series of filters and video detectors for the *S* and *C* radar bands are now available. Transmission is flat to within 1 decibel in the pass band, which may be as wide as 25 percent of the center frequency. A typical 5-resonator filter and detector for use in the *S* band measures 3 by  $\frac{7}{8}$  by  $\frac{5}{8}$  inches (76 by 22 by 16 millimeters) and weighs only 1.5 ounces (43 grams).

*ITT Kellogg Communications Systems  
United States of America*

**Improved Semiconductor Power Devices**—By virtually eliminating the possibility of surface breakdown, which makes semiconductor rectifiers and power transistors highly sensitive to reverse voltage transients, particularly at high temperatures, it is possible to make greater use of the inherent properties of the *p-n* junction. Not only is the tolerance to reverse overload increased but power rectifiers can be used as surge protectors and for stabilization of extra-high-tension supplies. The voltage ratings of controlled rectifiers can also be extended.

Using these new techniques, Standard Telephones and Cables has developed a new rectifier, coded *RAS 300*, production of which is shown in Figure 21. Nominally rated at 1000 volts and 1 ampere, it can absorb peak reverse transients of 4 kilowatts provided the mean power dissipation is within its thermal overload capacity. The rectifiers need not be derated grossly for parallel operation and voltage-distributing resistors are no longer needed for series working.

*Standard Telecommunication Laboratories  
United Kingdom*

**Transistor Video-Frequency Amplifier**—A transistor amplifier having an adjustable gain of 80 decibels is shown in Figure 22. The wiring connections are welded. It is designed for use with multiple-antenna receiving systems employing crystal detectors and video-frequency amplification. It operates from 12 volts and consumes less than 70 milliwatts.

*ITT Kellogg Communications Systems  
United States of America*

**High-Fidelity Loudspeaker System**—Two recently developed loudspeaker units mounted in a suitable sound-absorbing enclosure will provide virtually linear response over the frequency range of modern electroacoustic systems.

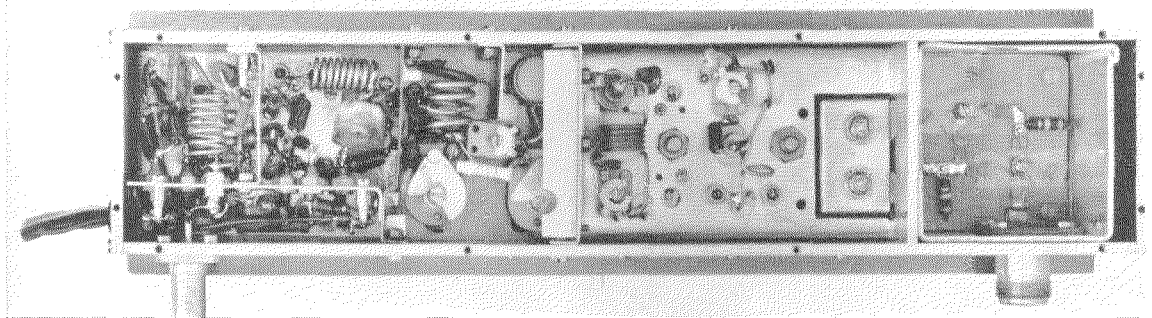


Figure 20—Solid-state source of 0.8 watt in the band from 4181 to 4395 megahertz.

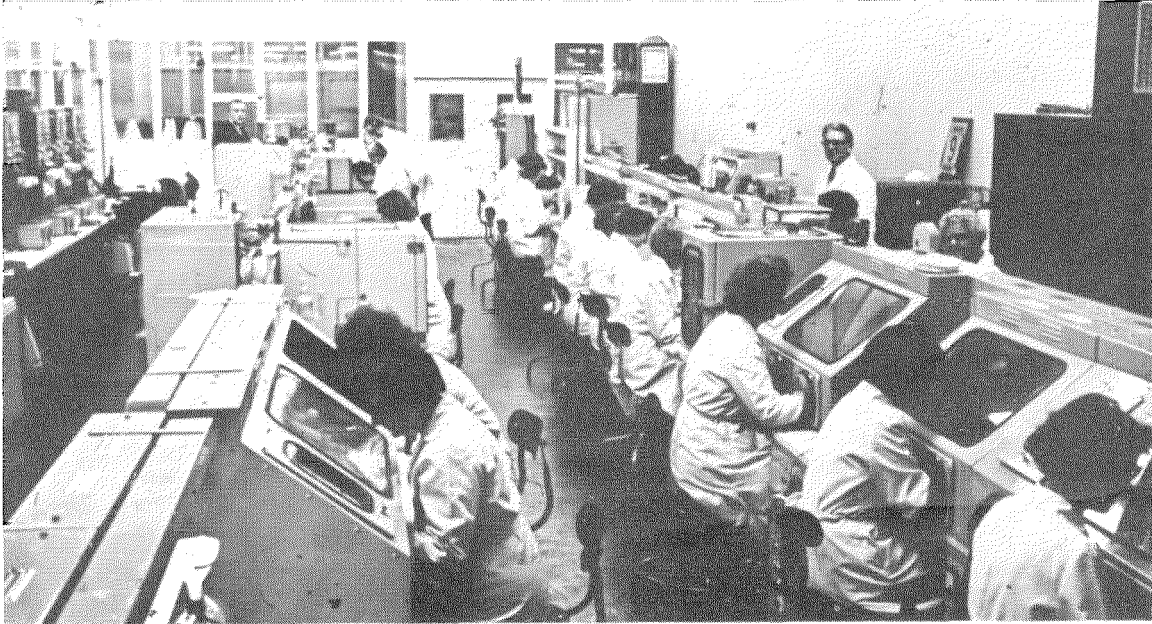


Figure 21—Production line for *RAS 300* semiconductor rectifiers.

The low-range loudspeaker, *LPT245*, has a circular cone resonating at about 25 hertz, which will increase to 40 to 60 hertz when enclosed, and a cutoff frequency of 9 kilohertz. It will handle about 15 watts.

The combined mid-range and tweeter unit, *LPMH 1318*, shown in Figure 23, has an oval radiator that resonates at 300 hertz and cuts off at 20 kilohertz. It will handle about 5 watts.

Both units employ ferrite magnets producing 10 500 gauss. Their impedances at 1 kilohertz are 4.5 ohms.

*Standard Elektrik Lorenz  
Germany*

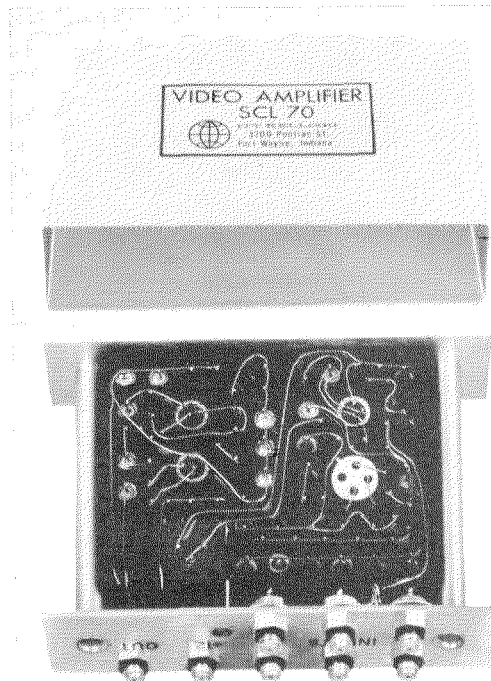
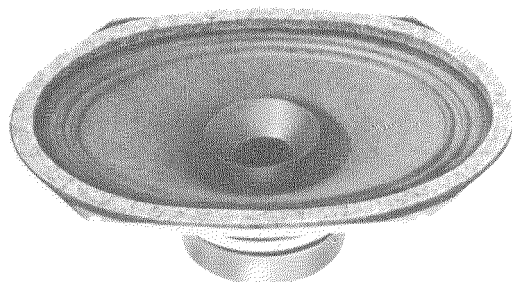


Figure 22—This transistor video-frequency amplifier has welded wiring connections.

## Recent Achievements

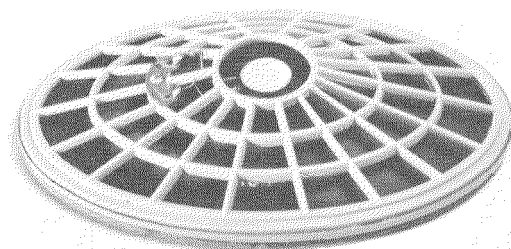
Figure 23—High-quality loudspeaker for mid and high acoustic ranges.



**Space-Saving Loudspeaker for Portable Receivers**—An oval loudspeaker, shown in Figure 24, has been developed for use in portable broadcast receivers. A ferrite magnet producing a magnetic flux of 10 500 gauss is mounted within the diaphragm chamber to reduce the mounting depth to 27 millimeters (1.06 inch). The basket dimensions are 143 by 95 millimeters (5.63 by 3.74 inches). The use of plastics permits weight to be held to 125 grams (4.4 ounces), which is important in portable equipment. The resonant frequency is 200 hertz and upper cutoff is at 8000 hertz. Power capacity is a half watt. The voice-coil impedance is 5 ohms.

*Standard Elektrik Lorenz  
Germany*

Figure 24—Thin loudspeaker for portable sets.



**Scanning Spectrometer**—For the testing of photoemissive surfaces, there has been developed an instrument producing monochromatic radiation of constant-energy output in the wavelength region from 0.5 to 2.0 microns with an output of the order of  $10^{-7}$  to  $10^{-8}$  watt per square centimeter.

The source can scan linearly over three wavelength ranges, from 0.35 to either 1.0, 1.5, or 2.0 microns. The rate of scanning may be adjusted to any interval between 5 and 50 seconds per sweep.

The current from a photoemissive surface is measured on a picoammeter and may be recorded on paper with suitable wavelength markers.

*ITT Federal Laboratories  
United States of America*

## Duke Receives Honorary Doctorate

William Meng Duke received from Clarkson College of Technology on 2 June 1963 an honorary degree of Doctor of Engineering.

The citation for talented engineering and leadership includes references to his contributions to applied mechanics, engineering analysis, ex-

perimentation, and design in missile technology; to his leadership in the Thor, Atlas, Titan, and Minuteman projects; and as vice-president of International Telephone and Telegraph Corporation to his present direction of its defense group in the United States.

## Foreword on Satellite Communication

This issue is dedicated to one of the most-challenging developments in electrical communication, one that offers the greatest promise for the spread of understanding, tolerance, and progress among men and nations.

Signals have been sent to and relayed by radio repeaters and reflectors orbiting the earth, and very-long-distance wide-band communications of high quality and stability have been established experimentally. Operational systems are in the planning stage.

Early published descriptions of possible systems involved orbits of low, medium, and synchronous altitudes having polar, inclined, equatorial, and random paths, and with controlled spacing, et cetera. The very availability of so-many solutions can cause some confusion for a while but the future is obviously bright.

The experimental results were correctly predicted as soon as it became apparent that artificial satellites could be launched in orbit. Technical solutions are available for most radio and electronic problems except in two areas that require further research and development; the first is that of ensuring long life for the satellite repeater under space and radiation conditions, and the second is the need for a reliable source of power for this repeater. There is no doubt that solutions will be found to these problems.

As far as space mechanics are concerned, the problems of synchronous satellites are not solved yet but are certainly solvable. The capabilities of launching medium-altitude satellites have been well demonstrated.

We in the International Telephone and Telegraph Corporation have been actively working on the development of the electronic side of satellite communication and have followed closely the space mechanics and the vehicle aspects of the problem. We are very confident that the tremendous effort that is being applied to space mechanics will provide early solutions to the problems of synchronous and other orbits of great interest for communication purposes.

I am less concerned about the ability of space scientists to place a satellite in synchronous orbit than I am concerned about making the right decision as to the best purpose of such a communication system and of defining properly the services it is supposed to render, because these services have a considerable bearing on the choice of the orbit and of the channeling principle.

It is known that existing and new submarine telephone cables can provide for the future traffic between North America and Europe, which represents the largest share of international communications. The satellites would add television but this is a supplementary feature rather than a prime requirement of a worldwide communication system. It is also clear that the satellite system can solve the problem of complete intercommunication among all the free nations of the world in a way that no cable system could ever aim at solving economically. It also seems clear that the system best adapted to provide global communication would make use of synchronous satellites. The availability and quality of communication among peoples is of paramount importance to the free world. Before proceeding with the development and construction of an operational system, it is essential to determine what kind of service it is to provide and how universal the system is desired to be. This raises many economic questions that require deep study. The problems of modulation and channel assignment for global applications are closely related to the decisions reached on the universality of the system.

As the following articles show, our efforts were directed to the needs of the free world by developing medium and small ground stations for satellite communication that provide for up to 60 voice channels and television reception. An experimental ground station for satellite communication was developed and constructed on the grounds of ITT Federal Laboratories in Nutley, New Jersey. It was completed in 1960. A demountable version of

## Foreword on Satellite Communication

this station can be air transported to any part of the world and set up in a few days.

The first commercial license for experimentation using the moon as a reflector was obtained from the Federal Communications Commission on 11 January 1961. Using a 10-kilowatt transmitter and parametric amplifiers, various experiments to demonstrate bandwidth capabilities were carried out in cooperation with Standard Telecommunication Laboratories, one of our associate companies in England.

The Nutley station was used in 1962 and 1963 as one of the ground radio terminals for Project Relay. It was also used by the National Aeronautics and Space Administration as part of a control center for experiments with the Relay satellite. Based on experience with this first ground terminal, a demountable and transportable radio terminal was constructed; the first unit of this type was installed in Rio de Janeiro, Brazil, during November 1962.

The first satellite communication between North and South America was established between the Nutley and Rio de Janeiro radio terminals on 6 January 1963 as part of the Relay program. Many more contacts have been established since then and also with England and France through the Relay satellite. A number of demountable stations have been produced for further satellite experimentation. They can be transported by aircraft to any accessible part of the world and installed in a matter of days. Such a system has been placed in use by the German Bundespost. Other installations in other countries are in planning.

We are glad to present in this issue of Electrical Communication some of the theoretical and practical results of our activities that bear on this most-challenging subject. I welcome this opportunity to thank the authors for their kind cooperation and valuable contributions.

*H. Busignies*

# Space-Research Ground Station

B. COOPER  
R. McCLURE

ITT Federal Laboratories, A Division of International Telephone and Telegraph Corporation; Nutley, New Jersey

## 1. Introduction

Satellite technology has presented the communication-system engineer with a transmission medium of unprecedented range and bandwidth. The satellite transponder is a broadband microwave repeater that can relay information between ground stations as far apart as 10 000 miles (16 090 kilometers). Such experiments have been performed via the Telstar and Relay satellites.

Large ground stations each engage the entire capacity of the satellite in its trunking mode. In the ultimate system, the satellite may be time shared.

These ground stations appear to be potential gateways to large, highly developed communication complexes. Except for television, which originates at a single source (studio) and terminates at a single destination (broadcast transmitter), the traffic originates in many discrete sources spread over a large area. A supporting ground network is required to collect and distribute this traffic.

Such extensive telephone systems exist now chiefly in Europe and the North American continent. However, there are many potential subscribers throughout the world who need from one channel to several dozen telephone and data channels. The Pacific islands and the major cities of South America and Africa are excellent examples.

Their real, though limited, need cannot be satisfied economically with the trunking concept. Two major modifications are required. The ground station must first be reduced in cost and complexity to levels that the traffic can support (less than \$50 000 per telephone channel). Second, an operating concept must be developed that will use the satellite efficiently for simultaneous exchange of telephone, telegraph, and television traffic.

Investigation of both of these problems began early in 1959. The experimental station described represents one aspect of this study. It is designed for low- and medium-capacity

transmissions via both active and passive satellites and is a useful research tool for examining terrestrial interference, atmospheric absorption, and the transmission characteristics of space-communication media.

## 2. Station Requirements

Communication and analytical tests were the two broad classes of experiments considered in establishing the station requirements. For the analytical tests, the station was equipped to measure and record frequency, power, and modulation.

For the communication tests, transmitters, receivers, and traffic terminal equipment were installed. These were compatible with several existing and planned satellites, including the moon. As indicated in Figure 1, the transmitter

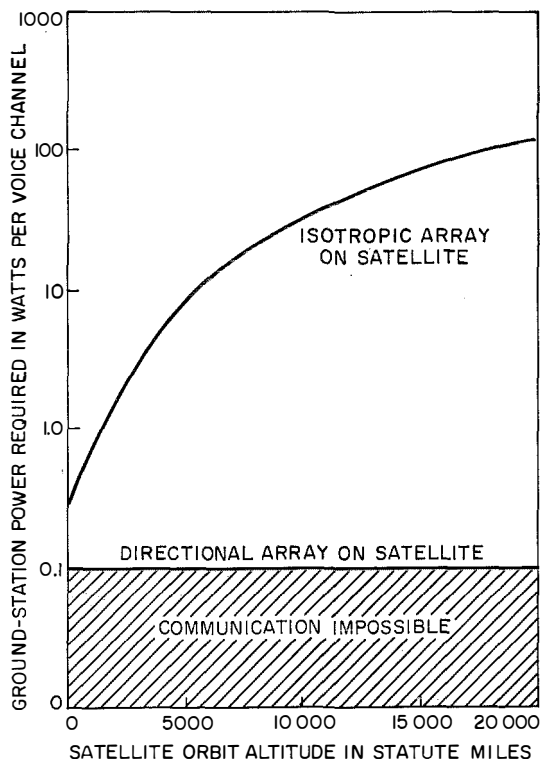


Figure 1—Required transmitter power as a function of the orbit altitude. Assumed ground-station parameters are antenna diameter, 40 feet; satellite noise figure, 8 decibels; and satellite carrier-to-noise ratio, 30 decibels.

## Space-Research Ground Station

power required for active satellites is nominal, ranging from 0.1 to 10 watts per voice channel. However, to accommodate passive satellites, such as using the moon for store-and-forward teleprinter transmission, considerably higher powers are required. Further, economical antenna size requires transmitters of higher power than indicated by the active-satellite analysis. For these reasons, a 10-kilowatt transmitter and a 40-foot (12.2-meter) antenna were selected. Estimates of the station performance with passive satellites are given in Table 1.

The limiting transmission parameter in satellite communication systems is the sensitivity of the ground-station receiving system. The quotient of antenna gain over system noise temperature becomes a figure of merit of communication system capabilities.

The first installation contained an uncooled parametric amplifier that operated at 2300 megacycles per second with a noise temperature of 300 degrees Kelvin and was mounted in the equipment shelter.

Table 2 gives the details of station performance with Relay and Telstar, based on later experiments at 1725 megacycles per second with an uncooled parametric amplifier having an improved noise temperature of 250 degrees Kelvin. A 40-foot cassegrainian antenna was used and the parametric amplifier was relocated at its paraboloidal vertex.

Cooled parametric amplifiers and masers being developed will improve the system sensitivity further.

### 3. Station Description

There are 6 major equipment categories in the ground station: transmitter, communication receiver, terminal equipment, antenna and tracking system, coordinating facilities, and special test equipment.

#### 3.1 TRANSMITTER

The transmitting system includes the local oscillator, frequency modulator, and 10-kilowatt power amplifier. The local oscillator and frequency modulator are part of an ultra-high-frequency exciter similar to the one used in the Courier satellite program. The local oscillator uses a vacuum-tube multiplier chain to generate a frequency 70 megacycles per second above the required carrier frequency from an oven-controlled crystal accurate to 5 parts in  $10^6$ . The frequency modulator generates a 70-megacycle-per-second carrier with a peak-to-peak deviation of up to 2 megacycles per second. A 12-channel pre-emphasis network that meets the requirements of the International Consulting Committee on Radio is included in the modulator input circuit.

The exciter is also used at 2300 megacycles

TABLE 1  
ESTIMATED PERFORMANCE WITH PASSIVE SATELLITES

	Moon	Echo
Frequency in megacycles per second	6390	6390
Transmitter power in decibels referred to 1 watt	+40	+40
Transmitter antenna gain in decibels	+52	+52
Two-way path loss in decibels	-290	-284
Receiver antenna gain in decibels	+52	+52
Net loss in decibels	-186	-180
Received power in decibels referred to 1 watt	-146	-140
Noise power in decibels referred to 1 watt per cycle of bandwidth	-202	-202
Receiver bandwidth in kilocycles per second	1	1
Receiver noise power in decibels referred to 1 watt	-172	-172
Carrier-to-noise ratio in decibels	26	32

per second for moon reflection experiments, with the substitution of an appropriate oven-controlled crystal.

The power amplifier uses a Varian type-800E klystron to generate a continuous-wave output of 10 kilowatts from the 50-milliwatt carrier input. To minimize local interference and satisfy the Relay system requirement for harmonic content of the transmitter output, a

3-gigacycle-per-second low-pass filter has been inserted in the waveguide. The output frequencies of the power amplifier are 1723.33 and 2299.5 megacycles per second, respectively, for Relay and moon reflection experiments. The klystron is connected to the antenna by WR-430 waveguide through wide-band rotary joints and operates within the band from 1720 to 2400 megacycles per second. The waveguide

TABLE 2  
STATION PERFORMANCE WITH CURRENT ACTIVE SATELLITES

	Relay	Telstar
Altitude in nautical miles (kilometers)	500 to 3000 (926 to 5555)	500 to 3000 (926 to 5555)
Inclination in degrees	45	45
Maximum slant range in nautical miles (kilometers)	7200 (13 332)	6000 (11 110)
Ground to Satellite		
Frequency in megacycles per second	1725	6390
Modulation	Frequency modulation	Frequency modulation
Transmitter power in decibels referred to 1 milliwatt	+70	+70
Transmitter antenna gain in decibels	+43.5	+52
Maximum path loss in decibels	-177.7	-188.4
Miscellaneous losses in decibels	-2	-1
Receiver antenna gain in decibels	-1	0
Received power in decibels referred to 1 milliwatt	-67.2	-67.4
Received noise in decibels referred to 1 milliwatt per megacycle of bandwidth	-101.5	-101.0
Receiver bandwidth in megacycles per second	2.3	0.576*
Received noise power in decibels referred to 1 milliwatt	-97.9	-103
Carrier-to-noise ratio in decibels	+30.7	+35.6
Satellite to Ground		
Frequency in megacycles per second	4170	4170
Modulation	Frequency modulation	Frequency modulation
Transmitter power in decibels referred to 1 milliwatt	+36	+30
Transmitter antenna gain in decibels	-1	0
Maximum path loss in decibels	-186.2	-186.2
Miscellaneous losses in decibels	-2	-1
Receiver antenna gain in decibels	+51.1	+51.1
Received power in decibels referred to 1 milliwatt	-102.1	-106.1
Received noise in decibels referred to 1 milliwatt per cycle of bandwidth	-173	-173
Receiver bandwidth in megacycles per second	1.3	0.576*
Received noise power in decibels referred to 1 milliwatt	-111.8	-115.4
Carrier-to-noise ratio in decibels	9.7	9.3
Threshold level in decibels	7.2	7.2
Margin in decibels	2.5	2.1
Frequency-division-multiplex channel capacity (full duplex)	12	6
Estimated channel signal-to-noise ratio in decibels	39	30
* Ground-receiver intermediate-frequency bandwidth was used in linear-repeater calculations.		

TABLE 3  
COMMUNICATION-RECEIVER PERFORMANCE

Moon-experiment frequency in megacycles per second	2299.5
Receiver noise figure in decibels	2.5
Intermediate-frequency bandwidth in kilocycles per second	0.2 to 50
Postdetection bandwidth in kilocycles per second	0.001 to 25
Relay-experiment frequencies in megacycles per second	4165 and 4175
System noise temperature in degrees Kelvin	360
Intermediate frequencies in megacycles per second	60 and 70
Carrier-to-noise ratio at threshold in decibels	7.2
Intermediate-frequency peak-to-peak deviation in megacycles per second	1.2
Acquisition range in kilocycles per second	±800
Baseband width in kilocycles per second	0.3 to 70
Intermodulation noise-power ratio in decibels (12 channels)	50

system is pressure dehydrated at 0.5 pound per square inch gauge. Power is radiated with right-hand circular polarization for Relay and linear or circular polarization for moon reflection experiments.

The transmitter output can be switched to a water-cooled dummy load for testing and for standing by. The power amplifier is designed to turn on semiautomatically and has fully automatic fault detection and protective action.

### 3.2 COMMUNICATION RECEIVER

Two types of communication receivers are used, one for Relay and one for moon reflection experiments. Performance of both types is summarized in Table 3.

The equipment used with Relay includes a parametric amplifier and a dual communication receiver. The parametric amplifier with its associated mixer-preamplifier and local oscillator is mounted in an air-conditioned enclosure close to the apex of the 40-foot paraboloidal reflector. This minimizes the length of waveguide between feed and amplifier and eliminates lossy rotary joints. As a result, the system noise temperature is 360 degrees Kelvin. The parametric amplifier and its mixer-preamplifier have a combined 1-decibel-down bandwidth of 14 megacycles per second, centered at 4170 megacycles per second. Thus both carriers, one at 4165 and the other at 4175 megacycles per second, can be accommodated without band switching. The local-oscillator

frequency is 4105 megacycles per second, giving intermediate frequencies of 60 and 70 megacycles per second after conversion. These are supplied to the dual communication receiver where they are separated and then amplified. Demodulation takes place in a phase-locked loop and a wide-band limiter-discriminator.

The communication equipment used in the moon reflection experiments includes a parametric amplifier and two receivers connected in cascade. The system has selectable predetection bandwidths of from 200 cycles to 13 kilocycles per second. In addition, a very-narrow-band phase-locked loop is available with bandwidths adjustable from 1 to 50 cycles per second. The parametric amplifier and its mixer-preamplifier are connected to the antenna via a waveguide switch and the same waveguide run used for the transmitter. To minimize problems associated with frequency drift, the same local oscillator is used for both transmitter and receiver. This system has a noise threshold of -131 decibels referred to 1 milliwatt with a noise bandwidth of 8 kilocycles per second.

### 3.3 TERMINAL EQUIPMENT

The terminal equipment (Figure 2) includes multiplex, recorders, signal generators, meters, and patching facilities.

The multiplex equipment is a 24-channel unit. Presently, only the 12-channel group from 12 to 60 kilocycles per second is in use for Project Relay.

A 7-track Ampex tape recorder will respond directly to frequencies as high as 50 kilocycles per second. Using frequency modulation, it will record signal frequencies as high as 4 kilocycles per second. It records experimental data for later analysis.

An 8-channel Sanborn recorder registers antenna pointing errors, received signal strengths, and other pertinent data.

For teleprinter experiments, 3 audio-frequency-tone keyers with matching demodulators are used. The keyers can be operated from a keyboard or a punched-tape reader. The demodulators can supply either of two page printers or a tape punch.

To handle telephone conversations via the satellite, eight 2-wire telephone lines are connected to the multiplex equipment through 4-wire terminations.

A 4-wire data line connects the station at Nutley to American Cable and Radio Corporation in New York City. This link is used for high-speed data-transmission experiments and multichannel teleprinter experiments with the satellite.

### 3.4 ANTENNA AND TRACKING SYSTEM

The antenna and tracking system may be divided into

- (A) Antenna structure,
- (B) Servo control system, and
- (C) Automatic-tracking receiver.

The antenna uses a 40-foot (12.2-meter) paraboloidal reflector with a cassegrainian feed system. The horns are located at the apex of the reflector and can be replaced or supplemented for transmission at either 6 or 8 gigacycles per second. A hyperboloidal secondary reflector provides a virtual focus near the apex. An air-conditioned microwave-electronics package is mounted close to the horn structure and moves with the antenna. Table 4 summarizes the performance of the antenna and tracking system.

The tracking-receiver and communication-receiver front ends are mounted in the microwave-electronics package. All receiver frequencies are converted to an intermediate frequency of 60 or 70 megacycles per second before they leave the microwave-electronics package. In addition, there is space for a 10-kilowatt power amplifier covering the 6-gigacycle-per-second band.

There are two feed systems presently in use. One is the 2-horn transmitting feed. The other is a 4-horn monopulse receiving system with three outputs. One is the sum of the outputs from all 4 horns and the other two are the algebraically derived elevation and azimuth difference outputs, which are used in a simultaneous amplitude-comparison technique to generate antenna pointing-error information. The sum output, at 4165 and 4175 megacycles per second, goes to the communication-receiver parametric amplifier through one arm of a duplexing filter and, at 4080 megacycles per second, to the tracking-receiver sum-channel mixer through the second arm of the filter. The two difference outputs, at 4080 megacycles per second, go directly to their respective difference-channel mixers with no preamplification. The noise figure of the mixer and intermediate-frequency preamplifier is 8 decibels.

To obtain an acquisition sensitivity at 4080

Figure 2—Terminal equipment.



TABLE 4  
ANTENNA AND TRACKING-SYSTEM PERFORMANCE

Tracking System	
Operational modes	Automatic (normal or rate memory) and manual tracking
Maximum rates along each axis in degrees per second	10
Maximum accelerations along each axis in degrees per second per second	6
Maximum operational wind speed in miles per hour	35 (with gust factor of 1.25)
Tracking accuracy along each axis in degrees:	
Automatic tracking	0.15
Programmed tracking	0.3
Angle-tracking receiver:	
Signal frequency in megacycles per second	4080
Local-oscillator frequency in megacycles per second	4010
Output frequency in megacycles per second	70
Mixer type	Crystal, nonlinear resistance
Conversion loss in decibels	10
Noise figure in decibels	8
Average signal level in decibels referred to 1 milliwatt	-120
Local-oscillator signal level in milliwatts	1
Bandwidth in megacycles per second	2
Impedance level in ohms	50
Minimum isolation in decibels between signal and local-oscillator circuits	30
Spurious output in decibels	-60
Frequency search modes	Open loop, manual; closed loop, manual; closed loop, automatic
Frequency search characteristics:	
Maximum excursion in kilocycles per second	150 (manual) 200 (automatic)
Maximum rate in megacycles per second	1.5 (automatic)
Antenna System	
Ultra-high-frequency antenna:	
Reflector diameter in feet (meters)	40 (12.2)
Type	Cassegrainian
Mount	Elevation over azimuth
Frequency range in megacycles per second:	
Transmit	1710 to 2300
Receive	4000 to 4200
Gain in decibels:	
Transmit	43.5
Receive	51.1
Beamwidth at 3-decibel-down points in degrees:	
Transmit	1
Receive	0.45
Side lobes in decibels:	
First-order	-15 or lower
Higher-order (beyond 4th)	-30 or lower
Polarization	Circular (right-hand or left-hand) or linear
Transmitter power in kilowatts	10
Antenna control:	
Boresight collimation in degrees	0.05
Tracking accuracy in degrees	0.1 (3 $\sigma$ error)
Static pointing accuracy in degrees	0.2 (3 $\sigma$ error)
Maximum tracking speed in degrees per second	10
Maximum angular acceleration in degrees per second per second	6
Minimum tracking speed in degrees per second	0.01
Maximum operational wind speed in miles per hour	35

TABLE 4—Continued

Operation modes	Manual Beacon automatic tracking with acquisition scan Programmed tracking Rate memory and reacquisition
Very-high-frequency receiver:	
Operating frequency in megacycles per second	55 to 260
Noise figure in decibels	6
Intermediate-frequency bandwidth in kilocycles per second	50
Image rejection in decibels	45
Dynamic range in decibels	60
Very-high-frequency antenna:	
Frequency range in megacycles per second	135 to 138 (receive only)
Gain in decibels (at 136 megacycles per second)	+16
Bandwidth in degrees (at 136 megacycles per second)	20
Side lobes in decibels:	
First-order	−15 or lower
Higher-order (beyond 4th)	−30 or lower
Polarization	Circular (right-hand or left-hand) or linear

megacycles per second of  $-128$  decibels referred to 1 milliwatt, the sum or reference signal is detected in a narrow-band phase-locked loop centered at 9.8 megacycles per second. A quadrature phase detector provides automatic gain control.

The phase-locked oscillator in the sum channel acts as the local oscillator for all three channels of the tracking receiver, thereby reducing frequency-modulation noise in the difference channels. Coherent detection with post-detection filtering to 10 cycles per second is used in the difference channels to achieve a low-noise tracking error signal.

The antenna is driven along each axis of its mount by a pair of contrarotating constant-speed alternating-current motors with eddy-current clutches on their output shafts. A 2-speed synchro system provides high-accuracy position feedback with a static pointing accuracy of  $\pm 4$  minutes of arc.

A very-high-frequency receiver is available to acquire a 136-megacycle-per-second beacon signal from a satellite before line-of-sight acquisition is achieved. Orbit prediction accuracy has made this receiver superfluous at Nutley since very-reliable direct acquisition has been possible at ultra-high frequencies. However,

the very-high-frequency technique is being studied for application to mobile and transportable stations in uncharted areas.

The very-high-frequency antenna is a crossed dipole mounted in front of the 6-foot (1.8-meter) secondary reflector. This proximity to the primary focus of the 40-foot (12.2-meter) paraboloid yields a gain of 16 decibels at the beacon frequency.

### 3.5 COORDINATING FACILITIES

Coordinating facilities are used mainly during satellite passes to regulate operations with other stations and National Aeronautics and Space Administration headquarters.

These include the following.

(A) The communication control console, which allows its operator to turn the exciter on and off, to insert test signals into the system before a pass, to monitor received signal strength and receiver phase lock, and to turn the paper recorder on and off. It also has a 24-hour digital clock indicating universal time.

(B) An intercommunication and public-address system.

(C) A tape recorder for the intercommunication system.

## Space-Research Ground Station

(D) A telephone handset connected to one of the multiplex channels during a pass to coordinate experiments with the remote station.

(E) A direct telephone link to National Aeronautics and Space Administration headquarters for real-time test coordination.

### 3.6 SPECIAL TEST EQUIPMENT

A test mode generator provides a signal at 4080 megacycles per second to check tracking-receiver operation. Also, when supplied with a 1723-megacycle-per-second communication signal, it produces an output at either 4165 or 4175 megacycles per second having 3 times the frequency-modulation deviation of the input signal, for testing the dual communication receiver. These signals are coupled directly to the 3 antenna outputs by directional couplers to simulate received signals in the presence of antenna noise.

A replica of the equipment in the Relay satellite is mounted on the 88th floor of the Empire State Building in New York City with receiving

and transmitting antennas oriented toward Nutley. This enables a complete system check, including performance of the dynamic tracking system, receiver system, and modulator-transmitter.

### 4. Station Applications

Initially, the ground station (Figure 3) was used in tracking and acquisition experiments, and in communication experiments using the moon as a passive reflector. At present, under contract to the National Aeronautics and Space Administration, the station operates as a medium-capacity experimental communication terminal with the Relay satellite. To meet the requirements of this program, the station has been modified and expanded. Frequencies have been changed and telemetry, command, and control added (the latter government supplied). The expanded station is shown in Figure 4.



Figure 3—Initial ground station.



Figure 4—Ground station expanded to include command and control facilities.

#### 4.1 MOON BOUNCE TESTS

The 2300-megacycle-per-second system was used in propagation studies with the moon as a passive reflector. A continuous-wave pulse was transmitted for 1.2 seconds and the duplex switch was then transferred to the receive position. The reflected signal was recorded (see Figure 5) 2.41 seconds after the start of the transmitted pulse. This sequence was repeated at 5.2-second intervals.

The receiver was adjusted for maximum sensitivity to the expected return signal ( $-118$  decibels referred to 1 milliwatt) by having it limit at about  $-105$  decibels referred to 1 milliwatt. Initially, a signal generator was used as a reference input level, but its frequency stability was inadequate for use with the 3-kilocycle-per-second-bandwidth system.

Therefore, reference levels were recorded just before each transmission, to help in estimating the level of the return signal, which was about  $-119$  decibels referred to 1 milliwatt.

#### 4.2 INTERFERENCE TESTS

In December 1961, measurements of field strength were made at great-circle distances up to 136 miles from the Nutley site. These measurements showed that if the Nutley antenna and that of another station illuminated a common area at the same frequencies, interference could result. However, since the power received by forward scatter falls off sharply with increasing elevation angle, both antennas would have to be at low elevation angles, typically less than 3 degrees. As operation with the satellite is restricted by other considerations to elevations higher than 5 degrees, this type of interference seems unimportant.

#### 4.3 PROJECT RELAY TESTS

In Project Relay, two major areas were studied. First, the Nutley station performed narrow-band experiments on the quality of the

Relay 12-channel telephone link. The tests included the following measurements.

- (A) Continuous random noise.
- (B) Impulse noise.
- (C) Periodic noise.
- (D) Band-pass characteristics.
- (E) Envelope delay distortion.
- (F) Received carrier power.
- (G) Harmonic distortion.
- (H) Noise loading (cross-modulation noise).
- (I) Round-trip time delay.
- (J) Crosstalk.

Second, the Nutley station provided support for the adjacent National Aeronautics and Space Administration test station. This support consisted of

- (A) Ultra-high-frequency antenna and tracking facilities for communication via Relay.
- (B) Plant facilities for installation and maintenance.

Figure 6 shows a recording of a typical experiment. It can be seen that the beacon carrier level varies from  $-114$  to  $-121$  decibels referred to 1 milliwatt. The monitor carrier level extends from  $-97$  to  $-103$  decibels referred

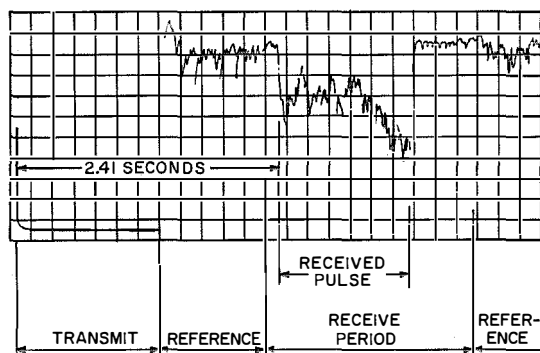


Figure 5—Typical moon echo sequence. The recording speed was 0.2 second per division and the received pulse averaged  $-119$  decibels referred to 1 milliwatt.

to 1 milliwatt and the periodicity of its signals is due to the stabilizing spin of the satellite.

The major emphasis of the narrow-band communication experiments is in the areas of thermal noise, intermodulation distortion, and harmonic distortion. Theoretical and experimental results of threshold-level and signal-to-noise-ratio tests appear to agree.

The theoretical threshold level for the communication receiver is  $-104.1$  decibels referred to 1 milliwatt with a baseband of 12 to 60 kilocycles per second. The threshold level determined by experiments lies between  $-103$  and  $-104$  decibels referred to 1 milliwatt. The experimentally determined signal-to-noise ratio of 43 decibels at a carrier level of  $-99$  decibels referred to 1 milliwatt confirms this threshold figure. The majority of mean communication carrier levels have been within the range from  $-94$  to  $-104$  decibels referred to 1 milliwatt. The maximum and minimum levels recorded were  $-81$  and  $-109$  decibels referred to 1 milliwatt, respectively.

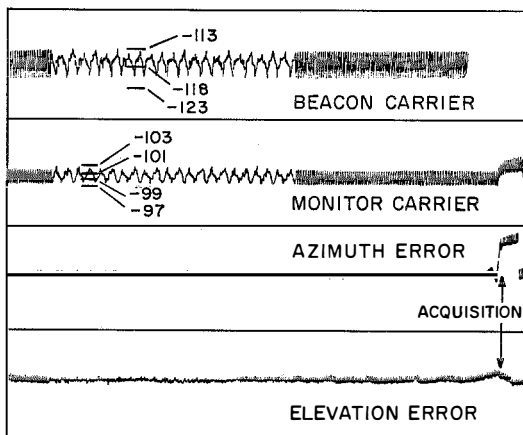


Figure 6—Recording of typical experiment with Relay satellite. The signal levels shown superimposed on traces are in decibels referred to 1 milliwatt. The spin pattern can be examined more closely by increasing the recording speed by 10 times to 25 millimeters per second for approximately 4 seconds, as shown in the center of the recording.

Tests of intermodulation distortion using noise loading show that the receiving system is limited by thermal noise, that is, the intermodulation products are below the thermal-noise level. Tests of intermodulation using 2 tones show a level of second-order products at least 40 decibels down, with third-order products about 55 decibels down.

Noise measurements via the satellite using a peak-reading meter show a peak-to-peak noise voltage more than 18 decibels above the root-mean-square noise voltage. This difference appears to be caused by noise peaks resulting from spin modulation.

Investigation of tracking performance during January 1963 showed a total of 55 tracking operations. Of these, 23 were communication experiments and 32 were in support of the National Aeronautics and Space Administration test station. The slant ranges of various passes were from 3418 to 7146 miles (5500 to 11 500 kilometers). Operation was satisfactory with spin-modulation noise up to 6 decibels. The range of signal levels extended from  $-126$  to  $-105$  decibels referred to 1 milliwatt.

Results of operations during January 1963 tend to confirm that radio-frequency interference is not a significant problem in narrow-band operation and tracking. There has been no evidence of it in communication experiments. Spurious signals appeared to cause tracking difficulty once. These did not prevent successful tracking, although the monitoring equipment did indicate the presence of interference.

In addition to engineering experiments, a number of public demonstrations were performed via the satellite. On January 26, three tape-recorded messages prepared by the Voice of America, one each in English, Portuguese, and Spanish, were transmitted from Nutley to Rio de Janeiro, Brazil. During the second half of this pass, Rio de Janeiro transmitted three other tapes, one in each language, to Nutley. The quality of the received messages was good,

with slight spin-modulation noise appearing on each channel.

During several passes, teleprinter tapes were transmitted from Nutley to Rio de Janeiro.

Voice has been transmitted via the satellite many times. The quality has generally equalled or bettered that of commercial telephony. During each communication pass, voice is used to coordinate the experiment between the two participating stations. In one case, the commercial high-frequency circuits to Brazil were unusable because of atmospheric disturbances. Rio de Janeiro had previously received pointing data for the pass. When Nutley began to transmit, Rio de Janeiro received the instructions to turn on their transmitter and proceed with the experiment. They did so, and the experiment proceeded normally.

A 4-channel telephone experiment used calls originated at 3 lines in Maryland and 1 in Nutley. These were routed to the Nutley station, patched through the satellite back to Nutley, and routed to other telephones in Maryland, Virginia, and California.

## 5. Summary and Outlook

The space-research ground station has provided information on terrestrial interference, moon-communication parameters, and general propagation parameters between 1 and 10 gigacycles per second. In addition, it has served as a proving ground for space-communication techniques and equipment.

A medium-capacity satellite communication system has been tested as part of a National Aeronautics and Space Administration program. The data provide valuable information with which to plan systems. Acquisition and tracking requirements, noise and distortion characteristics, experimental techniques, and the type of data to be taken are a few of the areas under study.

The research operation has resulted in a number of new equipment designs, which have been combined in a transportable ground station ca-

pable of supporting the medium-capacity satellite system. This equipment is described elsewhere in this issue.

The major emphasis in this facility is on flexibility. It has the capability to participate in any of the major government-sponsored space-communication programs, as well as to do independent research.

This flexibility is achieved primarily by providing a universal transmitting and receiving system with interchangeable front ends and antenna feed systems. The terminal equipment and test equipment are of laboratory quality and are capable of supporting a variety of communication experiments.

With this research facility, we continue to evaluate operational techniques and ground-equipment designs to improve our capabilities in the field of space communications.

## 6. Acknowledgments

The authors are indebted to Mr. W. Glomb for his assistance and critical review of the material in this paper.

**Bernard Cooper** was born in Brooklyn, New York, on 17 January 1929. He received a B.E.E. in 1950 and M.E.E. in 1956 from Polytechnic Institute of Brooklyn.

From 1951 to 1952, he was associated with Allen B. Dumont Laboratories. In 1953, he joined ITT Federal Laboratories where he is now directing operations of the space-communication research and tracking station.

Mr. Cooper is a Member of the Institute of Electrical and Electronics Engineers.

**Richard McClure** was born in Yonkers, New York, on 22 November 1935. He received a B.E.E. degree from New York University in 1959.

## Space-Research Ground Station

From 1955 to 1958, he was with the Electric Boat Division of the General Dynamics Corporation. From 1958 to 1959, he was employed by Sterns Control Company to design industrial measurement and control systems.

He joined ITT Federal Laboratories in 1959, where he worked on the design of transmitters

and the operation of a station for experimental communication via natural and artificial satellites. He is now assistant manager of the satellite-communication ground station at Nutley, New Jersey.

Mr. McClure is a Member of the Institute of Electrical and Electronics Engineers.

## Barton Receives City and Guilds Award

J. F. Barton has received the Insignia Award of the City and Guilds of London Institute for his thesis on "Filiform Corrosion." This is the highest award in Great Britain in the field of paint technology and is conferred only on rare

occasions. The recipient is a senior paint technologist in the New Southgate Process Engineering Group of Standard Telephones and Cables Limited.

## Scarr and Aleksander Get Babbage Award

R. W. A. Scarr and I. Aleksander were the recipients of the 1962 Charles Babbage Award from the Council of the British Institution of Radio Engineers for their paper on "Tunnel Devices as Switching Elements." The paper appeared in the Journal of that organization, volume 23, number 3, pages 177-192; March 1962.

Both authors were with Standard Telephones and Cables Limited when the paper was published; Mr. Aleksander has since joined the staff of West Ham College of Technology as a lecturer.

# Medium-Capacity Space-Communication Terminal

L. POLLACK  
W. GLOMB  
L. GRAY

ITT Federal Laboratories, A Division of International Telephone and Telegraph Corporation; Nutley, New Jersey

## 1. Introduction

During 1960 and 1961, our studies indicated the need for a unique satellite-communication terminal. Its principle characteristics were:

- (A) Medium traffic capacity.
- (B) Economic accessibility to users requiring a modest number of voice channels.
- (C) Transportability to and operability in a variety of environments.

A research program was undertaken in which a fixed experimental station was constructed and narrow-band experiments were performed using the moon as a reflector. A theoretical analysis and paper design were initiated in June 1961, directed toward the formulation of a transportable design meeting a series of commercial and military operational requirements. The ultimate users of the equipment were considered to be both commercial and military organizations. Voice, teleprinter, facsimile, and data traffic were to be transmitted.

Propagation considerations for space communication determined that the frequencies between 2 and 10 gigacycles per second were most useful. A number of designs covering this range were considered, and a review of various reasonable configurations indicated many areas of similarity. A system configuration was conceived that placed the signal-frequency components in a single mechanical structure mounted directly on the paraboloidal reflector. This arrangement conserved signal energy and minimized noise.

A review of the remaining equipments indicated that they could be common for all of the proposed configurations. In particular, the antenna, antenna control servos, transmitter power supplies and controls, tracking receiver, communication receiver, and support instrumentation designs were conceived as universally applicable components.

## 2. Requirements

The operational requirements of the station as originally conceived were based on a satellite-communication-system concept described in earlier studies [1-4]. In these studies, it was determined that the satellite-communication system could support a large number of ground stations simultaneously, each representing an entry to a multiple-user system. Analyses of world communication trends indicated that many of these entries would require between 12 and 120 voice-channel capacities during the 1965-1970 time frame. It was accepted further that the system design should be sufficiently flexible so that it could be expanded to accommodate television, high-speed data, and other wide-band traffic.

The station was required to operate in a variety of environments from polar to tropical, to operate with a minimum staff, and to require a minimum of communication and logistic support. It was considered desirable that no more than 4 personnel be required to operate the ground terminal.

### 2.1 ECONOMIC REQUIREMENTS

The economics of satellite-communication systems indicate that the larger investment and maintenance costs reside in the satellite because of launch costs and the considerable research and development investment necessary to assure a long useful life in orbit. For ground stations, however, equipment life of the order of 10 years is now feasible so that first cost is dominant. Many analyses have been performed to determine the optimum ground-station configuration for least cost per voice channel of capacity. In each case, the results are grossly affected by the state of the art of ground-station technology, particularly that associated with large steerable antenna systems.

The results of one typical analysis are demonstrated in Figure 1. Since the curve has a broad

## Medium-Capacity Space-Communication Terminal

minimum, it can be assumed that antenna diameters between 30 and 60 feet (9.144 and 18.288 meters) represent a satisfactory compromise between initial investment and optimum cost per channel. A minimum cost per channel is indicated for antenna diameters between 40 and 60 feet (12.192 and 18.288 meters).

The station cost is made up of 3 parts. The first is fixed and includes the cost of site, support facilities, buildings, transmitter, receiver, and common terminal equipment. The second stems from the per-line cost of equipment and is directly proportional to capacity. The third is a summation of all components, contributing a cost that is proportional to channel capacity raised to an exponent greater than 1. The total costs, therefore, can be represented by  $C = a + bw + cw^n$  where  $C$  is the total cost,  $w$  is the capacity of the station, and  $a, b, c$  are constants of proportionality.

For communication via satellites, the principal contribution to the third term is the cost of the antenna. Antenna costs have been estimated to vary as the 2.5-to-3.0 power of diameter. Capacity, assuming that surface tolerance does not significantly compromise theoretical gain, is proportional to the square of the diameter. Therefore, the exponent  $n$  is expected to vary from 1.25 to 1.5. Dividing the above equation by the number of channels and differentiating

to determine the minimum cost per channel, it can be demonstrated that this minimum is achieved when

$$C_{\text{antenna}} = cw^n = \frac{a}{n-1} = \frac{C_{\text{fixed}}}{n-1}$$

Assuming the variation in  $n$  cited above, the antenna cost should equal 2 to 4 times the fixed-cost part of station cost.

### 2.2 PHYSICAL REQUIREMENTS

A review of the physical requirements of the system indicates that the operating frequencies would be limited to between 2 and 10 gigacycles per second. The limits are fundamental and arise from the atmospheric absorption and cosmic noise that reduce system sensitivity at other frequencies.

Orbit altitudes between 6000 and 22 300 miles (9654 and 35 881 kilometers) are expected to be useful in space-communication systems. These altitudes respectively represent the minimum altitude at which a reasonable 5000-mile (8045-kilometer) communication link can be supported and the maximum useful altitude (the synchronous altitude that is generally recognized as the optimum location for a communication satellite).

### 2.3 TECHNOLOGICAL LIMITATIONS

The satellite radiated power will probably be limited to between 1 and 100 watts and will be the costliest parameter in the system.

Based on this premise, analysis of the propagation path both to and from the satellite indicates that the limiting link is that from satellite to ground and, therefore, it is essential that maximum receiver sensitivity be achieved in this link. Given an antenna of a size consistent with economic and transportability considerations, an increase in system sensitivity can be achieved only by reduction in noise temperature. It was decided that the initial model would use an uncooled parametric

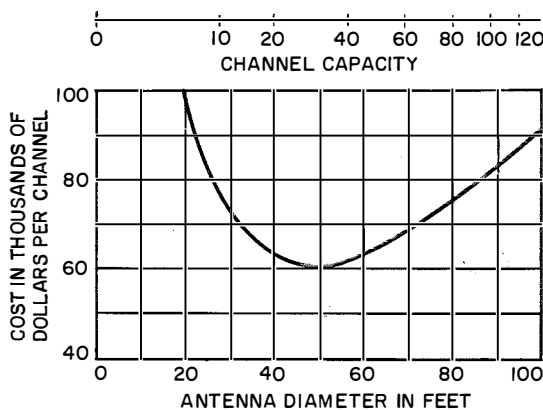


Figure 1—Space-communication ground-station cost per channel.

amplifier having a noise temperature of about 300 degrees Kelvin. As the development of cryogenic generators progresses, it is expected that a new parametric amplifier with a reliable closed-cycle cooler will achieve an amplifier noise temperature of 50 degrees Kelvin or less.

The link from ground to satellite, however, enjoys a considerable margin and can be supported in most instances by a 1-kilowatt ground transmitter. However, experience has shown that a number of effects (primarily degradation of satellite noise figure and reduction in antenna gain at the satellite because of unfavorable satellite look angle) demand considerable reserve power. Accordingly, a 10-kilowatt ground transmitter was specified as there are a number of klystrons for the desired frequency range that do not require excessive drive for this power and use essentially identical power-supply and heat-exchanger equipment.

2.4 OPERATIONAL REQUIREMENTS

In addition to the economic and physical constraints on the system specification, several operational considerations ultimately established the over-all weight, size, and configuration of the ground station. The main limitation is the requirement for transportability in cargo aircraft. A review of the capacity of existing cargo aircraft shown in Table 1 indicates that:

- (A) No single package should exceed 26 000 pounds (11 794 kilograms) in weight.
- (B) Maximum height should be limited to 9 feet (2.74 meters).

(C) Maximum length should be limited to 40 feet (12.19 meters).

(D) Maximum width should be limited to 10 feet (3.05 meters).

The major equipments were specified as antenna mount, antenna parts carrier, radio-equipment van, and heat exchanger, all of which satisfied the above requirements. (To satisfy the C-130 height limitation, a removable under-carriage must be designed for the standard equipment van.)

Furthermore, it was recognized that the applicability of the proposed station would be worldwide and a survey of potential operating environments was made. It appeared that tracking requirements under various wind conditions were almost universal and that the tracking accuracy would have to be maintained at wind speeds as high as 35 miles (56 kilometers) per hour with gusts to 50 miles (80 kilometers) per hour. It was also recognized that the antenna should remain controllable at substantially higher speeds and a specification of 60 miles (97 kilometers) per hour with gusts to 90 miles (145 kilometers) per hour was established for these operating conditions. Survival in winds higher than 100 miles (161 kilometers) per hour was also required.

While the above wind specifications satisfied the operating requirements in almost any part of the world, they could not be met economically if the antenna were loaded with ice. It was therefore assumed that in arctic environments the antenna would be surrounded by an inflatable radome that could also be used in unique

TABLE 1  
AIR-TRANSPORTATION CAPABILITIES

Type of Transport	Payload in Pounds (Kilograms)	Size in Inches (Centimeters)			Range in Miles (Kilometers)
		Length	Width	Height	
C-133	80 000 (36 288)	982 (2494)	144 (366)	144 (366)	3000 (4827)
C-124	50 000 (22 680)	884 (2245)	136 (345)	139 (353)	3000 (4827)
C-130	26 000 (11 794)	492 (1250)	123 (312)	109 (277)	1840 (2961)

temperate and tropic areas where the proposed wind specifications would be exceeded.

It was recognized also that the operating personnel and equipment required a controlled environment under extreme climatic conditions. The radio-equipment trailer and antenna-equipment pod include heating and cooling facilities capable of maintaining a temperature of 70 degrees fahrenheit (21 degrees centigrade) with external variations from  $-20$  to  $+129$  degrees fahrenheit ( $-29$  to  $+54$  degrees centigrade).

### 3. Evolution of Specifications

The specifications that evolved from the system study reflected a compromise among the various factors enumerated above. For example, though the operational requirements would imply a larger antenna, a 30-foot (9.14-meter) diameter was the largest size consistent with the transportation requirements. A paraboloidal surface of this size could be manufactured in segments having a surface tolerance of 0.08 inch (0.2 centimeter) root-mean-square or better and could maintain this tolerance after repeated assembly and disassembly. The assembly procedure could be accomplished without elaborate templates. Larger antennas would probably exceed the load capacity of the specified aircraft since the total weight of such structures varies approximately as the cube of the diameter. Furthermore, assembly and disassembly of these larger structures could not be accomplished with simple hand tools.

A paraboloidal reflector was chosen with a ratio of focal distance to diameter of 0.4, which reduced the moment of inertia of the structure and minimized drive power. A cassegrainian system was chosen so that the port to the radio equipment could be located at the vertex of the reflector. This minimized transmission-line losses, which is particularly important for receiving. The transmission-line contribution to system noise temperature is now approximately 30 degrees Kelvin but would be in excess of

150 degrees Kelvin if a focus feed were used. Alternatively, the equipment pod would be mounted at the focus; however, this was rejected because of the difficulty in servicing and the increase in the moment of inertia of this configuration. The cassegrainian geometry also allows an additional degree of freedom in beam forming since the secondary reflector can be shaped to reduce side lobes and antenna noise temperature.

Evaluation of tracking-system parameters indicated that an elevation-over-azimuth mount represented the most-compact mechanical structure that could satisfy the transportability requirements. Some consideration was given to the problem of tracking through zenith, which is the principal shortcoming of such a configuration. It can be shown that in an elevation-over-azimuth mount the azimuth rate required for a satellite in a given orbit varies as the secant of the elevation angle. This implies an infinite azimuth velocity at 90-degree elevation. In this instance the antenna moves only in elevation until the satellite is directly overhead, at which instant it must execute a 180-degree azimuth shift whereupon it again becomes stationary in azimuth and tracks only in elevation.

Recognizing that the antenna beam width is of the order of 0.6 degree at 4000 megacycles per second, the instantaneous rotation of the antenna through 180 degrees is not necessary. With a 6000-mile (9654-kilometer) orbit, an azimuth speed of only 6 degrees per second would be required to track within 1/2 beam width of zenith. It can be demonstrated that any satellite in a 6000-mile (9654-kilometer) or higher orbit can be tracked with a 30-foot antenna having an azimuth slew capability of 6 degrees per second (including directly through zenith). In the extreme case, namely a zenith pass, it is necessary that the antenna sense this some moments before zenith is reached and execute an offset that passes within 1/2 beam width of zenith. Under these conditions, the received signal strength will vary 3

decibels at most; however, track will be maintained through zenith.

Other considerations regarding maximum speeds required for stow and acquisition operations under manual control established the requirement for a maximum azimuth rate of 10 degrees per second and a maximum elevation rate of 6 degrees per second, plus accelerations of the order of 6 degrees per second per second in both axes.

An analysis of the available drive systems indicated that for the most part electromechanical drive devices of the eddy-current clutch type (which was used in the fixed research station), the amplidyne and its derivatives, or straight direct-current motor type were all bulky and heavy and thus not generally applicable to transportable designs. It was therefore decided that a hydraulic-drive system would be used, with a 40-horsepower pump driving a 10-horsepower azimuth-drive motor and a 20-horsepower elevation-drive motor.

Hydraulic drive and control are commonly applied to artillery and naval gun mounts, but have not been extensively used for antenna-tracking systems. Considerable effort was expended in developing related technology and the ultimate design has met all requirements.

It was decided early in the program that minimum tracking-equipment complexity would be achieved by relying entirely on automatic tracking of a beacon on the satellite. It was recognized that programmed tracking, while desirable in a large fixed installation, requires an increase in equipment (in the form of a local computer) and a substantial communication channel to a central computer for the transmission of ephemerides. Recognizing that beam widths as low as 0.3 degree were possible (at 8 gigacycles per second), a tracking accuracy of  $\pm 0.05$  degree was specified in the automatic-tracking mode. Tracking accuracies in manual control and in programmed tracking were relaxed to  $\pm 0.1$  degree as these were not considered primary tracking techniques.

The maximum wind speeds indicated earlier became the limiting parameters in determining system power. At 60 miles (97 kilometers) per hour the torque profiles, as a function of antenna attitude, were found to require essentially the full drive capacity of the system.

Considerable study of the automatic-tracking method resulted in the following trade-off analysis. Conical-scan or sequential-lobing techniques generally suffer a limitation in performance if a significant amount of amplitude modulation is present on the beacon signal. This amplitude modulation could arise in the spin modulation of the satellite and in fact has been noted in most of the experiments to date. Furthermore, sequential lobing cannot be made to operate with a diffuse scatterer that exhibits severe fading, particularly if the fading rates include the lobe-scanning rate and harmonics thereof.

The monopulse, or simultaneous-lobing, techniques however are capable of tracking both discrete and distributed targets and those exhibiting high-speed fading, because the comparison of 4 lobes is simultaneous. A review of the various monopulse techniques indicated that amplitude error sensing correlated with the sum channel represented the technique least sensitive to phase and amplitude variations in the tracking-receiver amplifiers.

The transmitter, for reasons discussed above, was specified to have a 10-kilowatt final amplifier. Each range of interest for satellite communication given in the recommendations of the International Consulting Committee on Radio could be covered with one of three series of tubes. The selection of frequency modulation was consistent with the first-generation systems. However, the system power, bandwidth, and linearity have been specified to accommodate other types of modulation, for example digital, that may be used in future systems.

The receiver is characterized by two parameters, namely its noise temperature (which for the first-generation system is specified as 400 degrees Kelvin for the total receiving system)

## Medium-Capacity Space-Communication Terminal

and its demodulation technique (which for the first-generation system is frequency demodulation with feedback, using a phase-locked detector). The demodulation technique arises from the requirement in a satellite-communication system to achieve high (40-decibel) signal-to-noise ratios with minimum-power-threshold performance.

Command, control, and telemetry facilities have been designed and supplied as part of one station to date. In establishing the requirements, several factors were considered: First, all command, control, and telemetry at the time the specifications were prepared used frequencies in the range from 100 to 150 megacycles per second. This permitted a certain universality in the design and in fact prompted the installation of a crossed dipole tuned to approximately 130 megacycles per second and located forward of the cassegrainian secondary reflector in the receiving-antenna system. While not at the prime focus, this antenna, combined with the reflector, yielded a gain of about 12 decibels, which was consistent with the helical arrays currently in use in satellite command and control. This modification, however, possesses one advantage not characteristic of the helical arrays, namely that its bandwidth is sufficient to encompass both the lowest and highest possible frequencies (107 and 148 megacycles per second) and can therefore be duplexed for control transmission and telemetry reception.

Associated with this system is a 200-watt transmitter operating at 122 megacycles per second (for Telstar operation); a 4-decibel-noise-figure receiver at 136 megacycles per second (for both Telstar and Relay operation); and a command code generator and a telemetry demodulator which, with minor modifications, are applicable to both programs.

A summary of the station specifications appears in Table 2.

In addition to the transmission and reception equipment described above, each station was

specified to have a minimum complement of terminal equipment and calibration instrumentation. Transmission analyses indicated that the first-generation stations could easily support 12 voice channels in frequency-division multiplex with either the Telstar or the Relay satellite in its contemplated orbit. Furthermore, each telephone channel would be of sufficiently high quality to permit multiplexing teleprinter, facsimile, or data information. The specification therefore included, as minimal equipment, a transistor-operated 12-channel frequency-division-multiplex telephone equipment, a teleprinter modulator and demodulator with provision for additional units as required, and an automatic send-receive teleprinter machine. The latter also facilitated the handling of operational traffic including the reception of ephemerides from the various computation centers that supported the programs.

A review of the essential requirements of a satellite-communication terminal indicated that the special multiplex equipment (for example, facsimile and data) as well as command, control, and telemetry are unique requirements not generally characteristic of a communication terminal. These were therefore segregated in a separate equipment van and became optional equipment if a specific program had such requirements.

### 3.1 POTENTIAL APPLICATIONS

The above specifications anticipate the potential applicability of the proposed station to military and commercial satellite-communication programs. The configuration was arranged with the major subsystems divided into plug-in interchangeable chassis, racks, or major subsystems to accommodate various satellite programs. Since the system gain (the product of free-space loss and gain of a fixed ground paraboloid) is independent of frequency, the 30-foot dish can support approximately the same traffic independent of operating frequency. Multilens arrays were designed as

primary radiators that would cover the frequency range from 2 to 8 gigacycles per second and in fact could permit simultaneous operation on 2, 4, and 6 gigacycles per second as required by the composite Telstar and Relay programs. Specifications were evaluated against the foreseeable satellite systems to test their universal applicability. The predicted performance using Relay, Telstar, and the moon as repeaters was calculated and is shown in Table 3.

The calculated performance was subsequently measured and agreed with these predictions.

**4. Equipment**

The station has been divided into four major packages. The antenna moves on two trailers when dismantled. The equipment van and heat exchanger each comprise another package. When command, control, telemetry, and/or special terminal equipment are required, these

TABLE 2  
MEDIUM-CAPACITY SPACE-COMMUNICATION-STATION SPECIFICATION

Antenna System	
Reflector Surface tolerance Geometry	30-foot (9.144-meter) diameter 0.08 inch (0.2 centimeter) root-mean-square Paraboloidal reflector with cassegrainian feed
Tracking System	
Coordinate system Drive Maximum rate Accuracy Maximum wind speed Maximum elevation for tracking Automatic tracking method	Elevation over azimuth Hydraulic 10 degrees per second in azimuth and 6 degrees per second in elevation 0.05 degree in automatic-tracking mode 35 miles (56 kilometers) per hour, full specification, and 60 miles (97 kilometers) per hour, drive to stow 89 degrees for 1000-mile (1609-kilometer) orbit Amplitude-sensing monopulse
Transmitter	
Power Modulation Frequency bands in gigacycles per second (klystron used)	10 kilowatts Frequency modulation, with deviation of $\pm 1$ megacycle per second 2 (VA 800E) 6 (VA 867) 8 (VA 863)
Receiver	
Noise temperature Frequency bands in gigacycles per second Demodulation	400 degrees Kelvin 1.7-2.4, 3.8-4.2, and 7.1-8.5 Frequency-modulated feedback (phase locked)
Command, Control, and Telemetry	
Transmitter Receiver Command code Telemetry	200 watts at 122 megacycles per second 4-decibel noise figure at 136 megacycles per second 3-out-of-6 digital Amplitude-modulated, frequency-shift-keyed, and pulse-code-modulated signaling

## Medium-Capacity Space-Communication Terminal

are included in a fifth package. Other optional additions are diesel generators, a boresight tower, a radome for severe environments, and a maintenance van where local logistic support is not available.

The radio-frequency components are divided between the antenna-equipment pod and the van so that all components operating at radio frequencies are located at the antenna. This includes the transmitter exciter and power amplifier, receiver low-noise amplifier, and communication- and tracking-receiver local oscillators, mixers, and preamplifiers. The transmitter modulator, receiver intermediate-frequency am-

plifiers, and demodulators are in the van; interconnections between van and antenna are accomplished in the 60-to-80 megacycle-per-second band.

Automatic tracking by simultaneous-lobe comparison requires four waveguide ports, comparators to generate sum and difference signals, and three receivers to amplify and detect these signals.

A test-mode generator was provided to simulate signals received from the satellite. On command, this unit accepts a small amount of modulated energy from the transmitting antenna and processes it the same way the satel-

TABLE 3  
MEDIUM-CAPACITY GROUND STATION PRESENT PERFORMANCE

Satellite	Relay 1	Telstar 1	Moon
Maximum range in miles (kilometers)	7000 (11 263)	6000 (9654)	220 000 (353 980)
Power in watts	4*	1†	0
Ground-to-Satellite Path			
Frequency in megacycles per second	1725	6390	2300
Power in kilowatts	10	10	10
Transmitting-antenna gain in decibels	40.2	52	41
Path loss in decibels	176.5	187	276
Power at satellite in decibels referred to 1 milliwatt	-66.3	-65	—
Radio-frequency bandwidth in megacycles per second	2.3	0.57	—
Carrier-to-noise ratio in decibels	28	35	—
Satellite-to-Ground Path			
Frequency in megacycles per second	4170	4170	—
Path loss in decibels	184	184	—
Receiving-antenna gain in decibels	48	48	41
Miscellaneous losses in decibels	2	2	—
Received power in decibels referred to 1 milliwatt	-102	-107	-124
Receiver bandwidth in megacycles per second	1.3	0.57	0.001
Noise figure in decibels	2	2	3
Carrier-to-noise ratio in decibels	9	8	23
Threshold in decibels	7	7	20
Margin in decibels	2	1	3
Channel capacity	12 (voice or frequency-division-multiplex)	6 (voice or frequency-division-multiplex)	4 (teleprinter)
Quality	Signal-to-noise ratio = 39 decibels	Signal-to-noise ratio = 30 decibels	Error = 1 part in 10 <sup>5</sup>
* 4 watts for each of 2 channels, both operated 2-way in the equivalent of a 4-wire system; 10 watts in wide-band 1-way operation.			
† 1 watt for each of 2 channels, both operated 2-way in the equivalent of a 4-wire system; 2.5 watts in wide-band 1-way operation.			

lite does. Its output is inserted into the receiver antenna transmission line. This permits a complete check of the transmitter and communication receiver immediately before satellite acquisition. The generator also contains a tracking-frequency beacon and can be used to check tracking-receiver sensitivity.

The terminal and test equipment include the multiplex equipment described in Section 3 as well as service and calibration equipment. The calibration equipment includes a multichannel paper recorder and one magnetic recorder. Signal generators and frequency-measuring equipment are also included for testing receiver and transmitter components. A noise-figure meter integral to the pod permits checking the receiver front-end components. A 10-kilowatt calorimetric dummy load is supplied for checking and calibrating the power amplifier.

### 5. Program Implementation

The present design of the transportable space-communication terminal was part of a 2-phase effort starting in 1958 with preliminary studies and resulting in the construction of a fixed space-research station. This facility, shown in Figure 2, was completed in late 1960 and a series of propagation tests were undertaken using the moon as a passive reflector. The space-research station served as a proving ground for equipment technologies and provided verification of propagation characteristics in space, which were found to be essentially those in vacuo. The product design studies for the transportable station were undertaken concurrently. Late in 1961, work was started at company expense to implement the design and fabrication of two transportable stations. The first transportable station (Figure 3) was instrumented for Project Relay and was ultimately sent to Rio de Janeiro as the South American participant in the Relay program. It is now operated by the engineering staff of one of our associate companies, Companhia Rádio Internacional do Brasil. It has provided the first operational test of the station in a field environment. Subse-

quently, two additional systems were constructed and have been operated with the Telstar satellite under lease to the United States Department of Defense. A fourth station has been constructed for the German Bundespost. The latter station is equipped for both Relay and Telstar operation and can be switched from one satellite to the other on command from the operator's console.

Operation with Telstar and Relay indicates that predicted performance has been achieved. The few operational problems encountered were solved and appropriate design modifications incorporated in the original equipments. The equipment line now includes the basic station configuration with radio-frequency equipment pods to satisfy the Telstar, Relay, and Syncom programs. Designs exist for moon-bounce and other passive-communication applications.

### 6. Future Plans

Completion of the initial phase of the design of the transportable communication-satellite equipment indicates that initial objectives



Figure 2—Fixed space-research station.

## Medium-Capacity Space-Communication Terminal

have been achieved. The advance of equipment technology in the interim has suggested improvements that are being undertaken in continuing programs. Among these are an increase in system capacity by the development and incorporation of supercooled parametric amplifiers and the reduction in antenna temperature by beam-shaping techniques.

The composite effect of these modifications will be a fourfold increase in system sensitivity. This will be accomplished by a reduction in system noise temperature from 400 to 100 degrees Kelvin, half of the latter noise temperature to be from the parametric amplifier and half from the antenna. The result of these changes will be to increase the system capacities of Table 3 to those of Table 4. Included in these figures is a hypothetical synchronous satellite of the 1970 era.

Emphasis is now being placed on the specification and design of a compatible line of de-

modulation and terminal equipments, with particular emphasis on the multiple-access mode of operation.

### 7. Summary and Conclusions

We now have a medium-capacity transportable satellite-communication terminal that is applicable to most satellite-communication-system configurations foreseeable in the near future. This equipment has been designed specifically for medium traffic capacity, as current studies indicate that this will be the principal application in future multiple-access systems. Also, the design has the capability of expansion to larger capacities by the combination of two or more tracking antennas into phased arrays having larger effective apertures. Current effort is directed toward incorporating into the basic design technological improvements that will maintain its sensitivity, tracking accuracy, and modulation equipment consistent with the

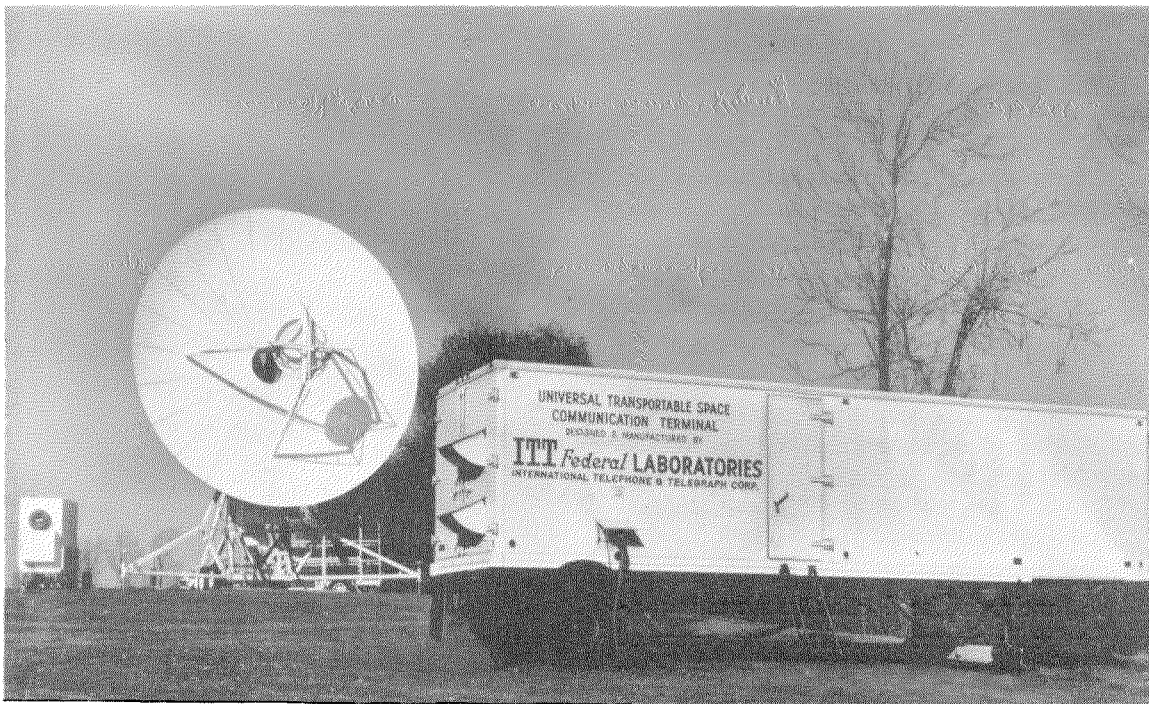


Figure 3—The first universal transportable space-communication terminal, which was air transported to Rio de Janeiro for tests with the Relay satellite.

TABLE 4  
PROJECTED PERFORMANCE WITH COOLED PARAMETRIC AMPLIFIER

	Relay	Telstar	Moon	Future 25-Watt Synchronous Satellite
Noise temperature in degrees Kelvin	100	100	400*	100
Channel capacity	60 (voice, frequency-division multiplex)	36 (voice, frequency-division multiplex)	1 (voice, single sideband)	600 (voice, frequency-division multiplex, or television)
Quality in decibels	40	30	30	30

\* Assume moon noise temperature to be 275 degrees Kelvin.

state of the art. It is believed that the basic configuration will remain unchanged and will be applicable to the forthcoming commercial satellite system.

**8. Acknowledgments**

Many persons, including the authors of the other articles in this issue, have contributed to the accomplishments described in this paper.

The program materialized primarily through the exceptional leadership of Mr. A. G. Kandorian, of ITT Federal Laboratories, and the hearty support of Dr. H. Busignies, of International Telephone and Telegraph Corporation headquarters.

**Louis Pollack** was born in New York, New York, on 4 November 1920. He received a B.S. degree in electrical engineering from the College of the City of New York in 1953.

From 1941 to 1943, he was with the Fort Monmouth Signal Laboratory and the Alaska Defense Command.

He joined ITT Federal Laboratories in 1943 and is now director of the Space Communica-

**9. References**

1. L. Pollack, "Radio Communication Using Earth-Satellite Repeaters," *Electrical Communication*, volume 36, number 3, pages 180-188; 1960.
2. L. Pollack, "World-Wide Communication with Artificial Satellites," presented at Fourth Global Communication Symposium in Washington, District of Columbia, in August 1960.
3. W. Glomb, J. Granlund, and L. Pollack, "Application of Satellites to Global Communications," *Signal*, volume 15, pages 55-59; August 1961.
4. "Universal Space-Communication Terminal," ITT Federal Laboratories Technical Memorandum 796-7; October 1961.

tion and Tracking Systems Laboratory, responsible for the design of communication systems utilizing spaceborne repeaters. Operation of the space-communication research station maintained by ITT Federal Laboratories is under his cognizance.

He is a Senior Member of the Institute of Electrical and Electronics Engineers and of the American Institute of Aeronautics and Astronautics.

## Medium-Capacity Space-Communication Terminal

**Walter L. Glomb** was born in Glen Ridge, New Jersey, on 7 February 1925. Columbia University bestowed on him a B.S. degree and the Illing medal in 1946 and an M.S. degree in 1948, both degrees in electrical engineering.

From 1946 to 1950, he was associated with Paramount Pictures, Inc., on the design of television recording and theater television equipment.

In 1950, he joined ITT Federal Laboratories where he has been involved in microwave, forward scatter, and satellite communication system analysis and aerospace equipments relating thereto.

He has four patents issued to him. Mr. Glomb is a Member of the Institute of Electrical and Electronics Engineers, and Tau Beta Pi.

**Laurence F. Gray** was born in Victoria, British Columbia, on 15 December 1915. He

received a B.S. degree in electrical engineering from the University of British Columbia in 1938.

From 1938 to 1943, he worked for the Canadian Marconi Company on broadcast and communication transmitters. During the second World War, he served with the Canadian Navy as a radar and communication officer.

He joined ITT Federal Laboratories in 1945, where he has been engaged in the design, development, and production of various types of transmitters, including frequency modulation and commercial television equipment. He is presently concerned with satellite ground stations.

Mr. Gray is co-author of the book *Radio Transmitters*.

He is a Member of the Institute of Electrical and Electronics Engineers.

# System Configuration of Transportable Space-Communication Terminal

D. HERSHBERG

ITT Federal Laboratories, A Division of International Telephone and Telegraph Corporation; Nutley, New Jersey

A space-communication terminal has many equipments in common with a conventional microwave forward-scatter system, such as large-diameter antennas, high-power transmitter amplifiers, and low-noise receivers. It differs in that steerable tracking antennas are used and, because there is no limitation in bandwidth imposed by the medium, high frequency-modulation deviations are used with ultra-low-noise receivers that take advantage of the cool sky temperatures at elevations exceeding 7.5 degrees above the horizon. The implementation of these systems differs considerably. A block diagram of the equipment for working with the Relay and Telstar satellites is shown in Figure 1.

## 1. General

The antenna system uses a 30-foot (9.1-meter) solid-panel paraboloidal reflector and a 6-foot (1.8-meter) hyperboloidal secondary reflector in a cassegrainian arrangement. The antenna is steerable in azimuth and elevation and is capable of being pointed to a position in space to within  $\pm 0.15$  degree. It will automatically track a satellite with errors not exceeding  $\pm 0.05$  degree once radio acquisition of the satellite is effected. The antenna system operates at approximately 40-percent efficiency at frequencies up to 8 gigacycles per second. The antenna drive system is hydraulic and capable of turning at 10 degrees per second in azimuth and 6 degrees per second in elevation.

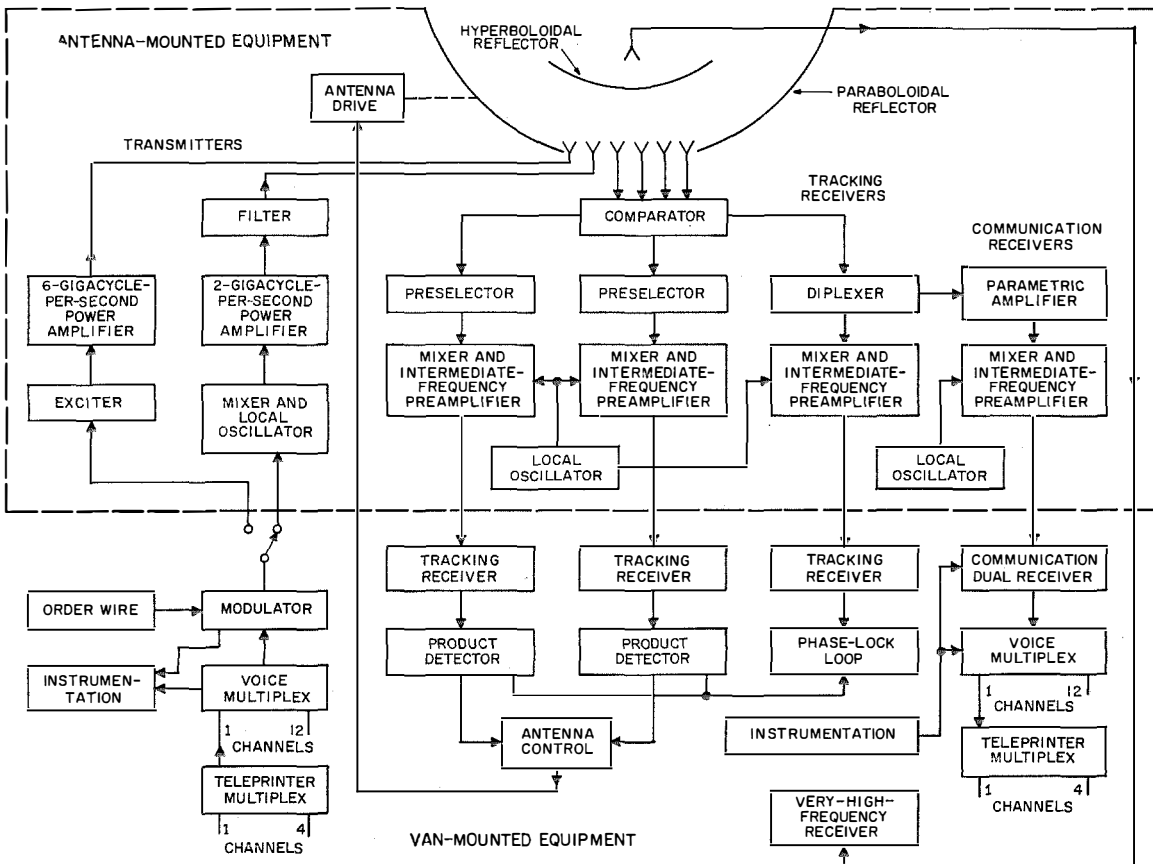


Figure 1—Equipment for working with Relay and Telstar satellites.

## Configuration of Transportable Terminal

The communication receiver consists of a low-noise parametric amplifier, local oscillator, and intermediate-frequency amplifier and demodulator. The receiver microwave components are located on the antenna assembly. Cooled parametric amplifiers with a 1-decibel noise figure and uncooled units with a 3-decibel noise figure have been developed for various satellite systems. The outputs of these amplifiers are connected to an intermediate-frequency system at a nominal 70-megacycle-per-second frequency. The radio-frequency bandwidth is 20 megacycles per second and narrower bandwidths are selected at the intermediate frequencies by the use of plug-in filters. Threshold-extension demodulators have been used exclusively with selectable bandwidths for 12, 6, and 2 channels. The threshold of these units occurs at a 7.2-decibel carrier-to-noise ratio. Two intermediate-frequency demodulator chassis are used in each station, one to receive distant communication signals and one to monitor transmissions from the station.

Tracking-error signals are generated by using an amplitude-sensing monopulse system having 4 identical feeds as shown in Figure 2. To generate azimuth tracking information, the signals received on *A* and *B* are added as are those received on *C* and *D*, giving the pattern shown in Figure 3. The two resultant signals are combined 180 degrees out of phase, forming

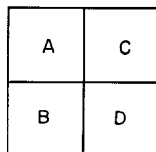


Figure 2—Arrangement of waveguide receiving horns for monopulse direction sensing.

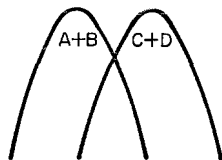


Figure 3—Effect of combining *A* and *B* as a pair and *C* and *D* as a separate pair for azimuth tracking.

the azimuth difference pattern of Figure 4. This difference pattern and the sum pattern of all 4 inputs shown in Figure 5 are multiplied in a detector, the output of which is the direct-current error voltage used to control the antenna position. The pairing of *A* and *C* and of *B* and *D* generate elevation-error signals. The sum pattern is also used for receiving the communication signal.

The tracking receiver inputs consist of balanced mixers and intermediate-frequency preamplifiers having noise figures of 8 decibels. The sum channel consists of a phase-lock-loop receiver located in the radio-equipment van. The frequency search rate and loop bandwidth of the receiver are variable so that it may be adapted to a variety of satellite systems.

Because the transportable ground station was designed for universal operation, the intermediate-frequency section of the communication receiver must accommodate a wide variation of bandwidths. The choice of 70 megacycles per second allowed the use of radio-frequency amplifiers with bandwidths of up to 20 megacycles per second. Plug-in filters can narrow the bandwidth to 1 megacycle per second and the phase-

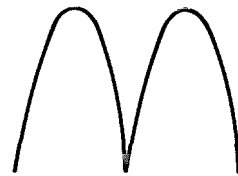


Figure 4—This difference pattern is produced by combining the *AB* pair and the *CD* pair 180 degrees out of phase.  $(A + B) - (C + D)$ .



Figure 5—The sum of all 4 inputs,  $A + B + C + D$ , is used for the communication channel and also for tracking. When it is multiplied by the difference pattern of Figure 4 in a detector, a direct-current error voltage is produced.

## Configuration of Transportable Terminal

lock demodulator further narrows the effective noise bandwidth of the system. The tracking receiver uses a double-conversion scheme from 70 to 9.8 megacycles per second. The second local oscillator is phase locked to the received beacon signal. The 9.8-megacycle-per-second intermediate frequency permits bandwidths of 30 kilocycles per second by using crystal filters. Further effective noise-bandwidth reduction is obtained by the filters in the phase-locked feedback loop.

Local-oscillator crystal frequencies were chosen in the 50-megacycle-per-second region, the highest range in which the specified stability can be achieved. This reduces the frequency multiplication required and spurious harmonics will be spaced this frequency apart. The tracking-receiver local oscillator supplies all three mixers. Isolation is provided in the sum channel to insure that no power from the sum channel is coupled into the difference channels through this path.

The transmitter can be equipped with either one or two 10-kilowatt amplifiers employing high-gain klystrons. They are located in the antenna package and are driven by all-solid-state exciters. The klystrons are monitored and remotely controlled from the radio equipment van. An 18-kilovolt 2-ampere power supply capable of being switched to either klystron is also located in the van. The station requires 150 kilovolt-amperes at 0.9 power factor from a 208-volt 3-phase 4-wire system. Maximum line voltage surge is 600 amperes on starting of the antenna pump motor.

### 2. Layout and Major Units

The basic transportable ground station is contained in a 31-foot (9.45-meter) semitrailer van, a 20-foot (6.1-meter) antenna trailer, and a 7-foot (2.1-meter) heat-exchanger trailer. An additional trailer of 17-foot (5.2-meter) length transports the disassembled reflector parts. These units in position at the site are

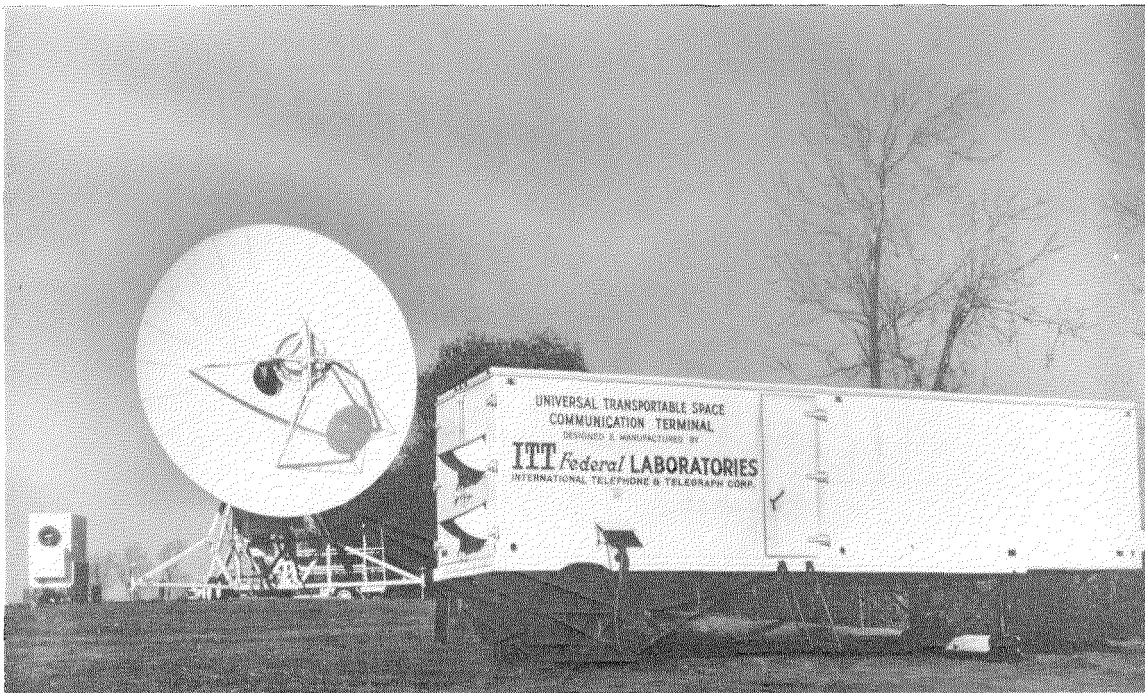


Figure 6—Semitrailer equipment van, antenna, and heat-exchanger trailer for a transportable ground station.

## Configuration of Transportable Terminal

shown in Figure 6. A typical arrangement with interconnections is shown in Figure 7.

All microwave and frequency-determining portions of the system are located at the antenna. These include the receiver front-end components, local oscillator, antenna feeds, klystron amplifier, and exciter local-oscillator components. They are in an antenna electronics package that is easily accessible for servicing. The package is shown in an extended position in Figure 8.

The antenna-mounted electronic modules are all completely self-contained with their independent power supplies. Only the power supply for the 10-kilowatt klystron amplifiers is omitted from this package. All the modules are mounted on slides and are easily accessible for servicing on the antenna platform or can be

removed to a laboratory location and completely tested without any additional power sources. Remote control and indications are provided for monitoring and on-off control of the power supplies in each module. The upper half of the electronics package contains all modules except the power amplifier and is moisture sealed and thermally insulated. A combination air conditioner and heater maintains the package temperature at  $70 \pm 3$  degrees fahrenheit. This reduces failure rates and instability of equipment.

Positioning the microwave components in the antenna eliminates rotary joints. The intermediate-frequency signals are transmitted to the radio van via coaxial lines in a single cable assembly. This also allows quick changeover between satellite systems by simply removing

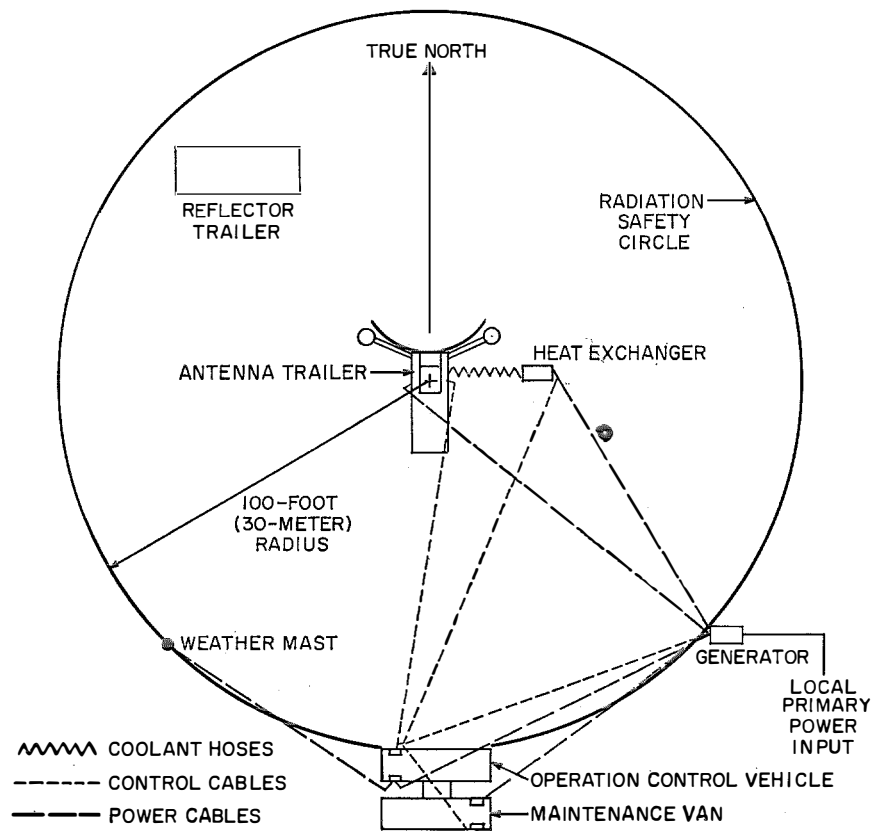


Figure 7—Typical arrangement of equipment for a transportable station.

## Configuration of Transportable Terminal

one electronics package and inserting a new one. This changeover normally requires about 4 hours.

The radio equipment van accepts and generates intermediate-frequency signals that remain essentially unchanged for all present satellite systems. It contains the receiver intermediate-frequency sections, modulator, transmitter control and power supply, terminal-equipment instrumentation, and antenna-control equipment. Two views of the radio equipment van are shown in Figures 9 and 10, and a layout is shown in Figure 11.

The 10-kilowatt-transmitter controls and power supply are located across the back axle of the van, a placement dictated by weight and size. The two receivers are located together next to the receiver test cabinet. This allows a convenient means of receiver adjustment and calibration of the recorder located across the aisle. The control console is located between the terminal and radio-frequency equipments. The console consists of a facilities panel, which controls and monitors all important station functions, and an antenna-control panel. A window is provided above the antenna-control panel for observation of the antenna during test. The

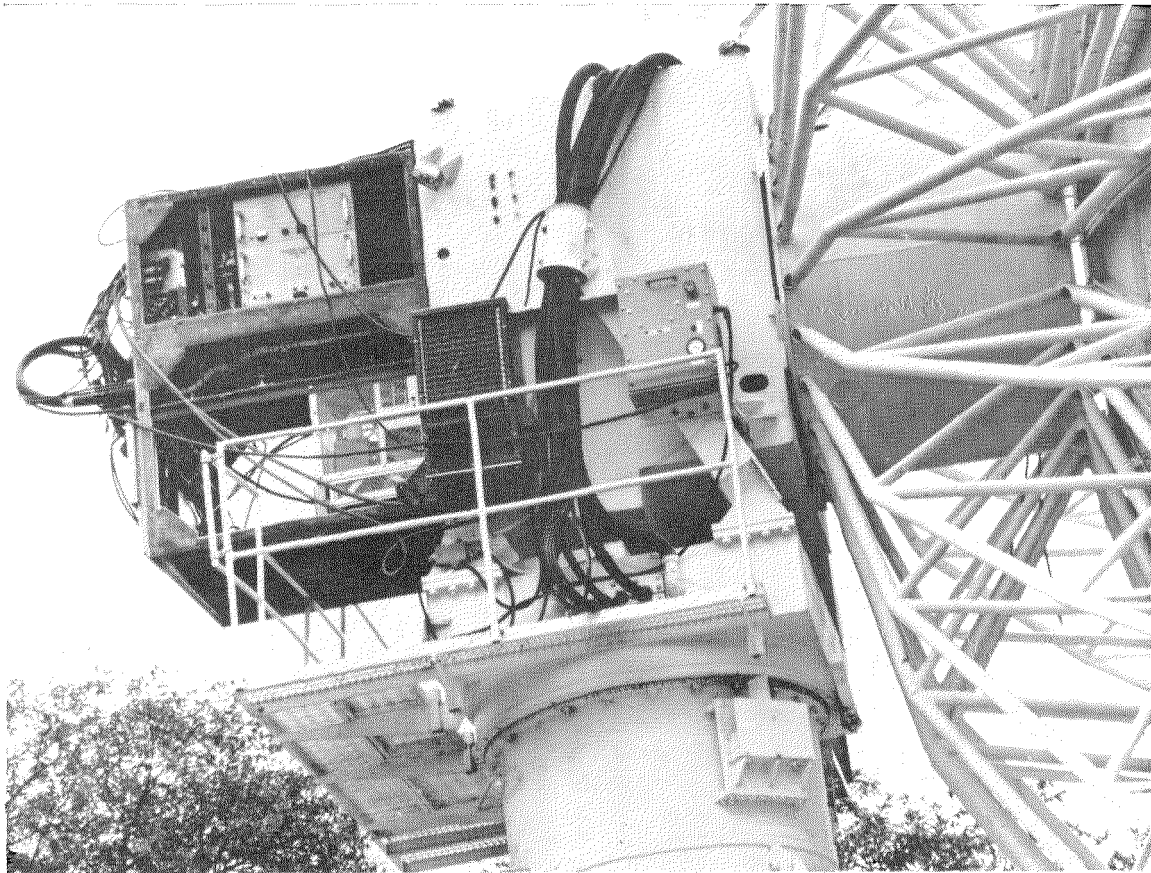


Figure 8—Electronics package containing all microwave and frequency-determining equipment is shown withdrawn from its housing at the vertex of the primary paraboloidal reflector of the antenna system.

## Configuration of Transportable Terminal

antenna-servo amplifiers and control circuits are next to the antenna-control panel. The terminal equipment and additional test equipment are located in the front of the van.

The station can be operated by personnel in the positions indicated in Figure 11. A station manager sits at the facilities panel and directs operation during a pass. The antenna-control operator positions the antenna until automatic acquisition occurs.

Another operator monitors the receiver and transmitter and a fourth operator prepares patch-panel arrangements for tests and records data.

The radio van is located approximately 100 feet (30 meters) from the antenna to assure operator safety from radiation.

The heat-exchanger van is placed next to the antenna and is controlled from the radio van. It provides coolant to the klystron amplifier mounted on the antenna and in this case slip joints are used. The antenna-reflector trailer is stored near the antenna.

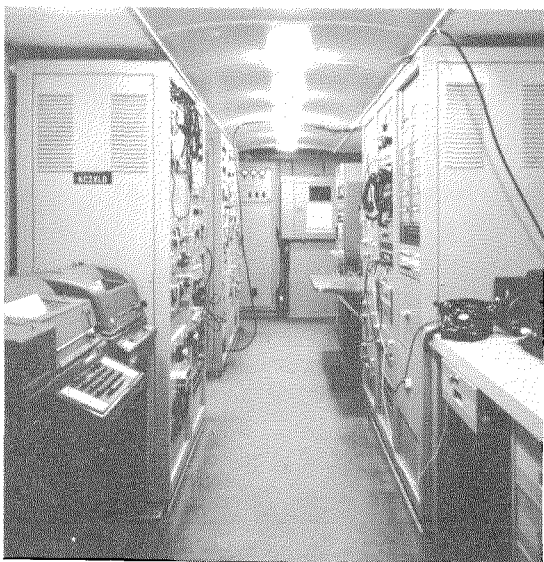


Figure 9—One end of radio equipment van.

### 3. Operation

Satellite operation begins with a prepass station checkout and calibration. This includes calibrating the received-signal levels and antenna error on the paper recorder. The antenna is directed at a boresight tower-mounted beacon, the error-signal detector slope is adjusted, and antenna position readouts are checked. A complete loop test is performed utilizing the test-mode generator and performing the experiments that will be made with the satellite. The results are recorded for comparison with those obtained through the satellite.

The antenna is then aimed at the predicted satellite position at time of turn-on. If the satellite position is not known precisely, a sector scan may be initiated around the predicted satellite position. Satellite acquisition occurs by sensing a received beacon signal in the tracking receiver phase-lock loop. When signal voltage is received, a relay switches the antenna-servo input from manual control to the tracking receiver and automatic tracking begins. The

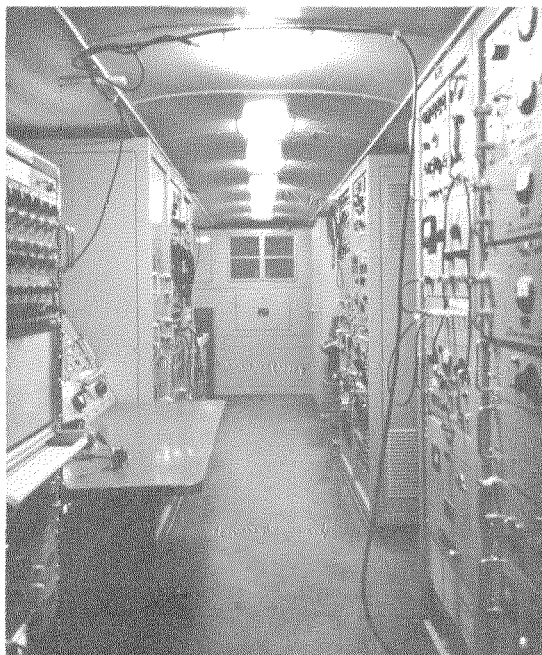


Figure 10—Other end of radio equipment van.

## Configuration of Transportable Terminal

microwave transmitter and receiver then complete the communication link. An order-wire channel is provided so that tests may be coordinated between the two stations. Operation of the system has included telephone, teleprinter, facsimile, and high-speed-data demonstrations. Experiments involving channel signal-to-noise measurements, baseband response, periodic noise, noise power ratios, 2-tone intermodulation distortion, and level stability have also been conducted.

### 4. Instrumentation

Instrumentation is provided to calibrate all important station parameters, keep a permanent record of pass activity, and completely check out the system. The station manager monitors and controls all important station operations during an active satellite pass from a central console position shown in Figure 12.

A test-mode generator is used for completely checking out the system. It simulates the satellite by sampling a small amount of transmitter output power, converting it to the receiver frequency, and coupling it into the receiver close to the feed system. An output at the beacon frequency is used to check the tracking receiver.

A noise-figure test set checks the performance of the receiver front-end components by automatically measuring the noise contribution of the receiver. The noise tube is always connected to the receiver front ends through directional couplers.

Solid-state multiplex equipment provides for 12 channels in the band from 12 to 60 kilocycles per second. The use of individual channel oscillators permits channel capacity to be changed readily. Teleprinter multiplex can be accommodated to work into any of the multiplex channels and up to 20 teleprinter channels can be accommodated on each voice channel.

Sufficient test equipment to calibrate and maintain the station is permanently provided. This includes frequency-measuring equipment, signal generators, voltmeters, power meters, and noise-measuring equipment.

An 8-channel recorder is used to keep a permanent record of all important station parameters such as received-signal level, antenna pointing errors, transmitter turn-on time, et cetera. A digital clock utilizing a 100-kilocycle-per-second standard with a stability of 1 part in  $10^7$  is used as a time reference for positioning the antenna and providing time marks on the recorder paper tapes.

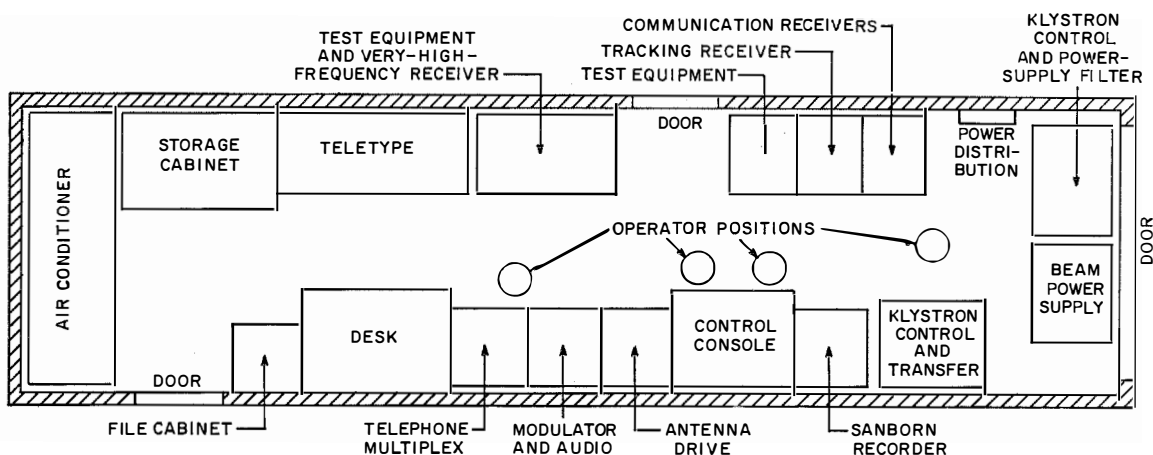


Figure 11—Plan view of radio equipment van. Outside dimensions are approximately 8-by-30 feet (2.4-by-9.1 meters).

## Configuration of Transportable Terminal

Patch panels provide for conveniently connecting voice and teleprinter landline circuits. To facilitate operations, channel and baseband inputs and outputs may be connected through patch panels to signal generators, meters, recorders, and amplifiers.

To accurately calibrate the antenna-position indicators and the receiver error-slope sensitivity, a signal source must be provided in the far field of the antenna and at a known azimuth bearing. The elevation of the source must be sufficient to eliminate the effect of ground reflections. Each transportable ground station is supplied with a crystal-controlled signal source at the tracking-receiver frequency with adjustable power output to allow its placement from 1.5 to 10 miles (2.4 to 16 kilometers) from the station. A feedhorn is also supplied.

In two installations, the feedhorns were mounted on 150-foot (46-meter) towers.

An accurate calibration of received-signal level is essential in evaluating station performance and obtaining useful data on satellite-to-ground operation. A coaxial cable is connected from the van to the input of the parametric amplifier via a directional coupler. The noise figure of the system and noise bandwidth are known. By integrating the noise over this bandwidth, the total noise-power contribution of the receiver front end is known. A signal generator is then connected to the test cable and the level adjusted until a 3-decibel increase in receiver output is observed. This indicates that the amount of signal-generator power is equal to the front-end noise power. By subtracting the known noise level from the signal-generator level, the cable attenuation is now known. This loss can be checked easily before every signal-level cali-

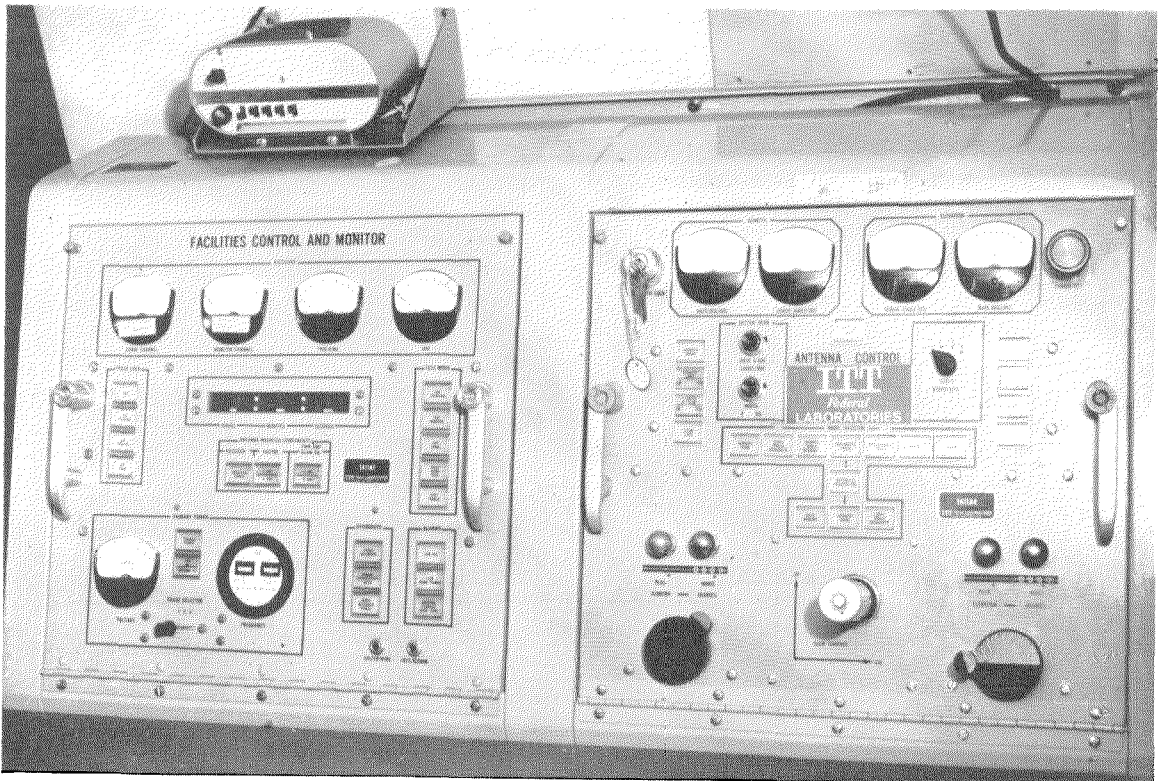


Figure 12—The station manager monitors and controls operations during a pass from this control console.

## Configuration of Transportable Terminal

bration. A system loop test can now be conducted at known input levels before each experiment with the satellite at the expected received-signal strengths and the performance compared with that of the entire system through the satellite at equal levels.

An intercommunication system is included in each equipment cabinet and at convenient places in the antenna system to assist in maintenance and operation of the terminal. One circuit includes a loudspeaker and the other uses headsets.

### 5. Installations

Four transportable ground stations have been constructed and are in service. Two additional stations are under construction. Table 1 is

a listing of the capabilities and deployment of each.

	Capability	Location
1	Telstar 1 and 2	Camp Roberts, California
2	Relay	Rio de Janeiro, Brazil
3	Telstar 1 and 2, Syncom	Lakehurst, New Jersey
4	Telstar 1 and 2, Relay	Raisting, Germany
5	Telstar 1 and 2, Relay	To be determined
6	Telstar 1 and 2, Relay	To be determined

### 6. Acknowledgment

I would like to thank Mr. L. Pollack and Mr. L. Gray of the Space Communication and Tracking Systems Laboratory for their assistance on this paper.

**David Hershberg** was born in Albany, New York, on 31 May 1937. In electrical engineering, he received a B.S. degree from Rensselaer Polytechnic Institute in 1959 and an M.S. degree from Columbia University in 1963.

He joined ITT Federal Laboratories in 1959, and has been active in the design, installation, and testing of satellite-communication ground stations and high-power microwave transmitters. He presently is responsible for system design and testing of the universal transportable ground stations.

Mr. Hershberg is a Member of the Institute of Electrical and Electronics Engineers and of the American Institute of Aeronautics and Astronautics.

# Antenna System for Transportable Space-Communication Terminal

E. SINGER

ITT Federal Laboratories, A Division of International Telephone and Telegraph Corporation; Nutley, New Jersey

T. J. VAUGHAN

Antenna Systems, Incorporated; Manchester, New Hampshire

## 1. Introduction

For operation with satellites, including natural satellites such as the moon, it is necessary to provide each ground terminal with an antenna system that can acquire and track the satellite. Alternatively, the antenna can be controlled by a real-time computer or a program stored on tape.

Among the design considerations for a ground-terminal antenna system are the following.

(A) The frequency bands allocated or intended for the system. Their selection is influenced by receiver sensitivity, terrestrial noise, galactic noise, atmospheric attenuation, and directional interference. The range from approximately 1.5 to 10 gigacycles per second is most suitable.

(B) The intended service such as television, telephone, telegraph, et cetera. Economic factors dictate a minimum capacity of 6 to 12 duplex voice channels. These must have commercial quality with low-orbit satellites of the Telstar and Relay types. Government or military requirements may be substantially less, particularly when using passive reflectors or satellites under emergency conditions.

(C) The operating site for the ground terminal. While high-capacity operation requires a fixed installation, a properly designed terminal of more-modest capacity is feasible as a transportable configuration. This materially decreases installation time and cost. The military applications of such a transportable station, which can be quickly set up in any part of the world, are obvious.

Assessing these and other considerations, it was decided to design the ground terminal around a trailer-mounted antenna with a 30-foot-diameter primary reflector.

## 2. Requirements

### 2.1 MECHANICAL

The antenna had to meet exacting weight and size allowances for transport by truck, ship, and aircraft. The latter requirement was most stringent, being based on load factors of the C-124 aircraft because of its general availability, although larger aircraft such as the C-133 could have been specified.

A second important mechanical requirement concerned packaging and assembly. A segmented configuration was selected that allows a 4-man team to assemble and place the system in operation within 16 hours. Most of the parts had to be capable of being lifted by only two men, which implied relatively light backframe members and primary-reflector segments.

A third important mechanical design requirement was that the antenna pedestal be erected by a power drive integral with the pedestal trailer frame; this requirement was imposed to speed the over-all assembly time and eliminate the need for heavy construction cranes.

The final stringent mechanical requirement was that the pedestal design include a generously sized trunnion box capable of enclosing a microwave-electronics package on the focal axis behind the primary reflector. This concept appeared very attractive because all of the microwave equipment could be close to the feeds, thereby reducing microwave losses, transmitter dissipation losses, and the need for a complex system of microwave rotary joints. The electrical interface between the antenna system and the radio equipment van is a set of flexible control and coaxial cables with no signal frequencies exceeding approximately 70 megacycles per second. Inside the tower section of the pedestal, the cables have sufficient slack to permit 300 degrees of

pedestal rotation in either direction from reference.

## 2.2 ELECTRICAL

The electrical design is based on the universality concept, which involves rapid interworking with all satellites. Switchover has been provided between Relay and Telstar with no down time at the antenna system and relatively short delays in switching power, control, and liquid coolant from one transmitter to the other. This implies simultaneous illumination of the antenna primary reflector by an array of feeds covering the transmitting frequencies of 1.72 and 6.39 gigacycles per second for Relay and Telstar, respectively. Reception for communication and tracking covers from 4.08 to 4.17 gigacycles per second, which is common to both Relay and Telstar. One microwave-electronics package can be replaced by another within 4 hours to permit operation with another communication satellite operating at different frequencies.

The requirements for multiple feeds and quick changeover of the microwave-electronics package made the choice of prime-focus illumination extremely unattractive from the following viewpoints.

(A) Poor accessibility for feed changeover, requiring removable staging or platforms.

(B) Laborious disassembly of waveguides and their terminating feeds, with possible loss of pressure and resultant contamination.

(C) The need to circulate coolant around the transmitter waveguides above 6 gigacycles per second.

(D) Unfavorable weight concentration of feeds, power splitters, microwave hybrid structure, filters, and receiver front ends far out on the focal axis.

These factors made any arrangement except an integral microwave-electronics package with short straight runs of waveguide very unattractive. Consequently, a cassegrainian system was chosen. The real focus was placed

at the vertex of the primary reflector; this made it feasible to transport the antenna-pedestal trailer with one of the microwave-electronics packages in place.

The size of the secondary reflector and its blockage of the primary reflector are determined by the lowest frequency and the feed-system beam width. In this case, for 1.72 gigacycles per second, the secondary reflector was made 6 feet (1.8 meters) in diameter. Of course, this size is more than adequate for illumination at the high-frequency end of the range.

The linear blockage ratio  $D_s/D_p$  is 0.2, where  $D_s$  is the diameter of the secondary reflector and  $D_p$  is the diameter of the primary reflector. The percentage of aperture area blocked is given by

$$A_b = (D_s/D_p)^2 + 4A_s/\pi D_p^2 \quad (1)$$

where  $A_s$  = projected area of support spars.

For the design contemplated,  $A_b$  was approximately 0.055. The loss of antenna gain with a tapered illumination may be found from the approximate relation

$$\delta G \approx 20 \log (1 - 2A_b) \quad (2)$$

which yields approximately 1 decibel.

The effect on the close-in side-lobe levels is given by the approximate expression

Blocked side-lobe ratio

$$\approx 20 \log \left[ \frac{(E_s/E_m) + 2A_b}{1 - 2A_b} \right] \quad (3)$$

where  $E_s/E_m$  is the unblocked side-lobe voltage ratio. The design value for  $E_s/E_m$  is  $-23$  decibels, or 0.07. Therefore, with blockage, the side-lobe ratio was expected to be degraded to  $20 \log (0.18/0.89)$  or  $-14$  decibels. Actual patterns of the antenna system at 4 and 8 gigacycles per second showed first-side-lobe levels between  $-14$  and  $-15.5$  decibels. However, higher-order side lobes and back lobes, which are most important in determining noise temperature of the antenna, are more than 35 decibels below the main lobe.

## Antenna for Transportable Terminal

The surface tolerance of the reflector system was specified as 0.080 inch (0.2 centimeter) ( $1\sigma$  value) for the 30-foot (9.1-meter) paraboloidal primary reflector and 0.032 inch (0.08 centimeter) ( $1\sigma$  value) for the 6-foot (1.8-meter) hyperboloidal secondary reflector. The tolerances refer to root-mean-square deviations from theoretical contour under static conditions and symmetrical gravity loading (zenith pointing).

### 2.3 SERVO POSITIONING AND TRACKING

The tracking or programming capability of an elevation-over-azimuth mount is tested most severely in traverse motion (motion at right angles to the planes defined by the line of sight and the gravity vector) as the elevation angle approaches 90 degrees (zenith track). This is due to the transformation equation relating the two systems of axes.

$$\theta_{az} = \theta_{tr} \sec \phi \quad (4)$$

where  $\theta_{az}$ ,  $\theta_{tr}$ , and  $\phi$  are the azimuth, traverse, and elevation angles.

Approximate relations, valid only for relatively high peak elevation angles and limited angle range about these values, are

$$\dot{\theta}_{az} = (v_s/h) \tan \phi_p \cos^2 \theta_{az} \quad (5)$$

$$\ddot{\theta}_{az} = 2[(v_s/h) \tan \phi_p]^2 \sin \theta_{az} \cos^3 \theta_{az} \quad (6)$$

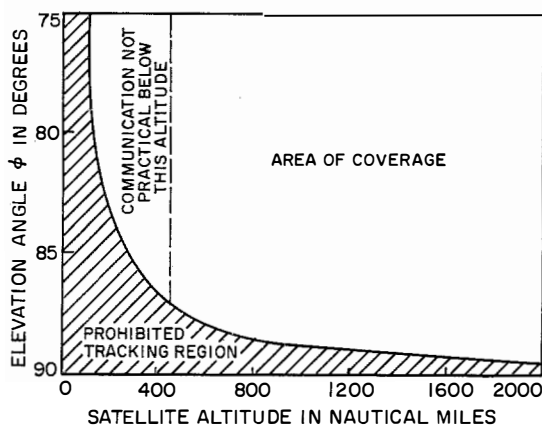


Figure 1—Elevation coverage as a function of satellite altitude for maximum azimuth speed of 10 degrees per second. Communication via satellites below 450 nautical miles (832 kilometers) is not practical.

where  $\dot{\theta}_{az}$  = azimuth speed,  $\ddot{\theta}_{az}$  = azimuth acceleration,  $\phi_p$  = peak elevation angle (at  $\theta_{az} = 0$ ),  $v_s$  = satellite orbital speed, and  $h$  = satellite height.

Using 450 nautical miles (833 kilometers) as minimum altitude for a low-level active-repeater satellite in circular orbit, the orbital speed is 4.03 nautical miles (7.46 kilometers) per second. As the satellite passes through zenith, it will move at maximum angular speed and will also appear to change its azimuth direction by 180 degrees. The servo design must provide for this rapid change. Any deficiency in this performance will leave a "cone of blindness" that can result in loss of tracking.

The maximum azimuth speed specified was 10 degrees per second under peak wind loading of 35 miles (56 kilometers) with gusts to 40 miles (64 kilometers) per hour. This value assures that the antenna will achieve the peak azimuth speeds required for passes reaching peak elevation angles of 87.1 degrees, which leaves a blind-zenith-cone angle of 5.8 degrees. It is possible to track into this cone, with the improvement in zenith coverage depending on the instantaneous orbit and the induced azimuth speeds and accelerations, provided the inequality (7) is satisfied.

$$\frac{1}{k_v} \dot{\theta}_{az}(t) + \frac{1}{k_a} \ddot{\theta}_{az}(t) \leq 0.3\theta_b \quad (7)$$

where  $k_v$  = the speed constant,

$k_a$  = the acceleration constant, and

$\theta_b$  = the 3-decibel-down beam width.

This is based on the very-laborious computation of actual coverages obtained beyond the values of peak elevation angle given and would ordinarily be done with the aid of a computer. However, coverages given by (5) and plotted in Figure 1 give a conservative value of the peak elevation coverage as a function of satellite altitude independent of beam width, providing that  $k_v$  and  $k_a$  for the azimuth channel can be set high enough. For fastest tracking response, a hydraulic servo-drive

system was specified. During actual operation, the antenna has tracked Relay and Telstar passes through elevations as high as 89.6 degrees without loss of track.

Maximum orbit-induced elevation rate occurs at zenith. With minimum satellite altitude of 450 nautical miles (833 kilometers), the elevation rate at zenith is approximately 0.009 radian per second or 0.52 degree per second. This speed is very low compared with the capability desired for peak azimuth rate; the elevation acceleration is correspondingly very low. However, to maintain a consistent design on each of the two axes and to facilitate rapid slewing for acquisition, it is desirable to have comparable speeds in both axes; consequently the peak elevation-rate capability of the mount was specified at 5 degrees per second.

Azimuth sector scan, adjustable in both scan rate and sector width, was specified to provide

sufficient flexibility for acquisition of communication satellites at any altitude. An automatic-acquisition-mode control was also specified to terminate the scan and transfer the hydraulic power servo to control by the tracking-receiver error channels. Manual and automatic positioning were also specified as overrides for any other preselected mode of control.

Except for automatic tracking via the tracking-receiver error inputs, all modes of control of the tracking mount were to be produced by controlling the mount with a high-performance instrument servo system. Fail-safe brakes, controlled by an operator or by limit switches, were specified for safety of both equipment and personnel. Finally, rate memory computation and injection were to be included to permit continued track for preset periods to compensate for possible temporary loss of tracking-receiver signals.

2.4 SUMMARY

An abbreviated summary of the specification developed for the antenna follows.

(A) Physical

Maximum number of trailers	2
Maximum combined length in feet (meters) minus removable tow bars	37 (11.3)
Maximum combined weight in pounds (kilograms)	38 000 (17 337)
Maximum clearance requirements in feet (meters):	
Width	8 (2.4)
Height	11.5 (3.5)

(B) Electrical

Primary power	50–60 cycles per second, 208 volts, 3-phase, 4-wire
Control	Local and console

(C) Environmental

Ambient temperature in degrees fahrenheit (centigrade)	–25 (–32) to +128 (+53)
Relative humidity in percent	97
Maximum altitude in feet (meters)	8000 (2438)
Maximum wind conditions in miles (kilometers) per hour:	
Track	35 (56)
Stow	60 (97)
Survive (in stowed condition)	100 (161)

## Antenna for Transportable Terminal

<b>(D) Reflector System</b>		
Illumination	Cassegrainian	
Primary reflector:		
Type	Paraboloidal	
Diameter in feet (meters)	30 (9.1)	
Focal length in feet (meters)	12.5 (3.9)	
Focal length over diameter	0.417	
Surface tolerance in inches (centimeters) root-mean-square	0.080 (0.2) ( $1\sigma$ value)	
Secondary reflector:		
Type	Hyperboloidal	
Diameter in feet (meters)	6 (1.8)	
Eccentricity	1.581	
Surface tolerance in inches (centimeters) root-mean-square	0.032 (0.08) ( $1\sigma$ value)	
Real-focus location	Vertex of primary reflector	
Feed angle in degrees	15.4	
Magnification ratio of feed	4.442	
Gain in decibels and beam width in degrees at frequency in gigacycles per second	40.3 and 1.4 at 1.72 48.2 and 0.6 at 4.08 52 and 0.39 at 6.39 53 and 0.31 at 8.00	
Maximum side-lobe levels in decibels:		
First 3	-15	
Higher-order	-30	
<b>(E) Servo System</b>		
	Azimuth	Elevation
Maximum tracking speed in degrees per second	10	5
Maximum angular acceleration in degrees per second per second	6	3
Static pointing accuracy in degrees	$\pm 0.04$	$\pm 0.04$
Automatic-tracking accuracy in degrees	0.1 ( $3\sigma$ )	0.1 ( $3\sigma$ )
Dynamic-pointing accuracy in degrees (maximum combined speed, acceleration, and 35-mile wind)	0.1 ( $3\sigma$ )	0.1 ( $3\sigma$ )
Dynamic-positioning accuracy in degrees	0.12 ( $3\sigma$ )	0.12 ( $3\sigma$ )
Lowest smooth tracking rate in degrees per second (equal to sidereal motion)	0.004	0.004
Servo system dead zone in degrees	$< 0.04$	$< 0.04$
Azimuth sector scan limits in degrees	0 to 5	
Azimuth sector scans per minute	0 to 200	
Rate memory duration in seconds	6 to 60 (adjustable)	6 to 60 (adjustable)
Automatic-tracking acquisition scan	automatic or manual	automatic or manual
Angle readout resolution in degrees	0.01	0.01

### 3. Design Implementation

#### 3.1 STRUCTURAL

The pedestal trailer employs a stepped chassis with tandem axles, as shown in Figure 2. The support during operation is through a modified tripod arrangement (Figure 3). A pair of closely spaced leveling jacks are affixed to the side rails near the towing end and a leveling jack is affixed to each of two outriggers clamped at 120-degree angles from the trailer axis. The tower and tracking mount are raised to operating position by a single hydraulic cylinder, operating from the hydraulic pump for the servo system.

The entire reflector system in Figure 4, including back structure and spars, is of aluminum. The primary reflector is assembled from 24 stretch-formed panels 0.060-inch (0.15-centimeter) thick. The contour of the individual panels is preserved by riveting the skin sections on all four sides to channel sections. The panels are then assembled to a fabricated truss-section on each radial-joint line. The trusses are built from straight and formed aluminum pieces that are butt-welded. To attain maximum surface accuracy, the entire primary reflector is assembled and fitted under a swing template before the bolt holes are drilled at each truss ear. Matching station marks are then formed on the back-

frame hub, truss members, and panel flanges to identify the order of assembly. The secondary reflector is die-formed from a single sheet and riveted to a peripheral flange.

Figure 3—Antenna dish mounted on pedestal.

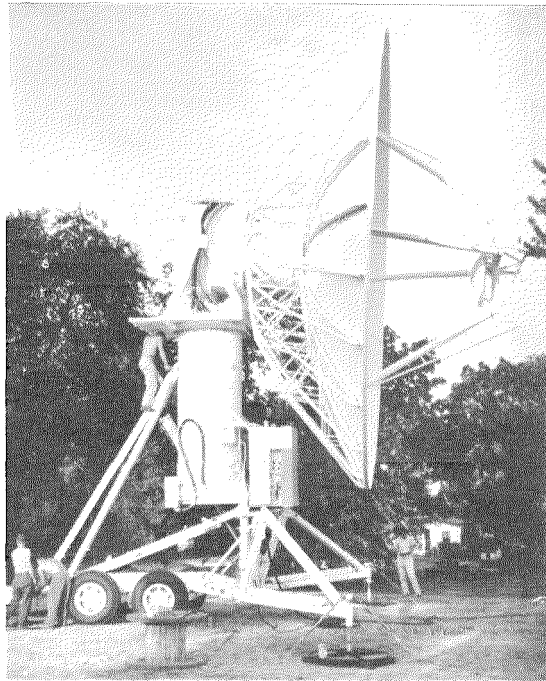


Figure 4—Disassembled reflector system mounted on trailer for transport.

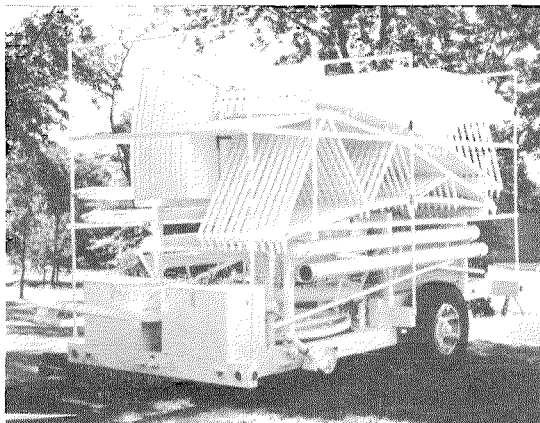
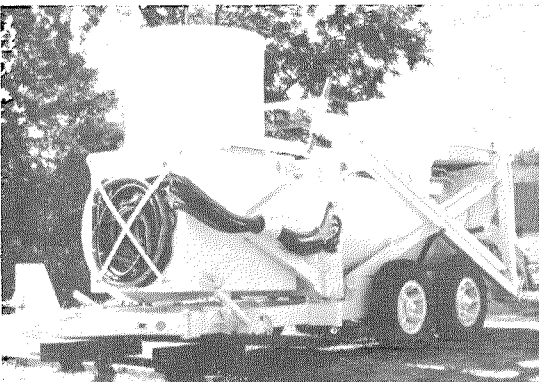


Figure 2—Antenna pedestal trailer ready for towing.



# Antenna for Transportable Terminal

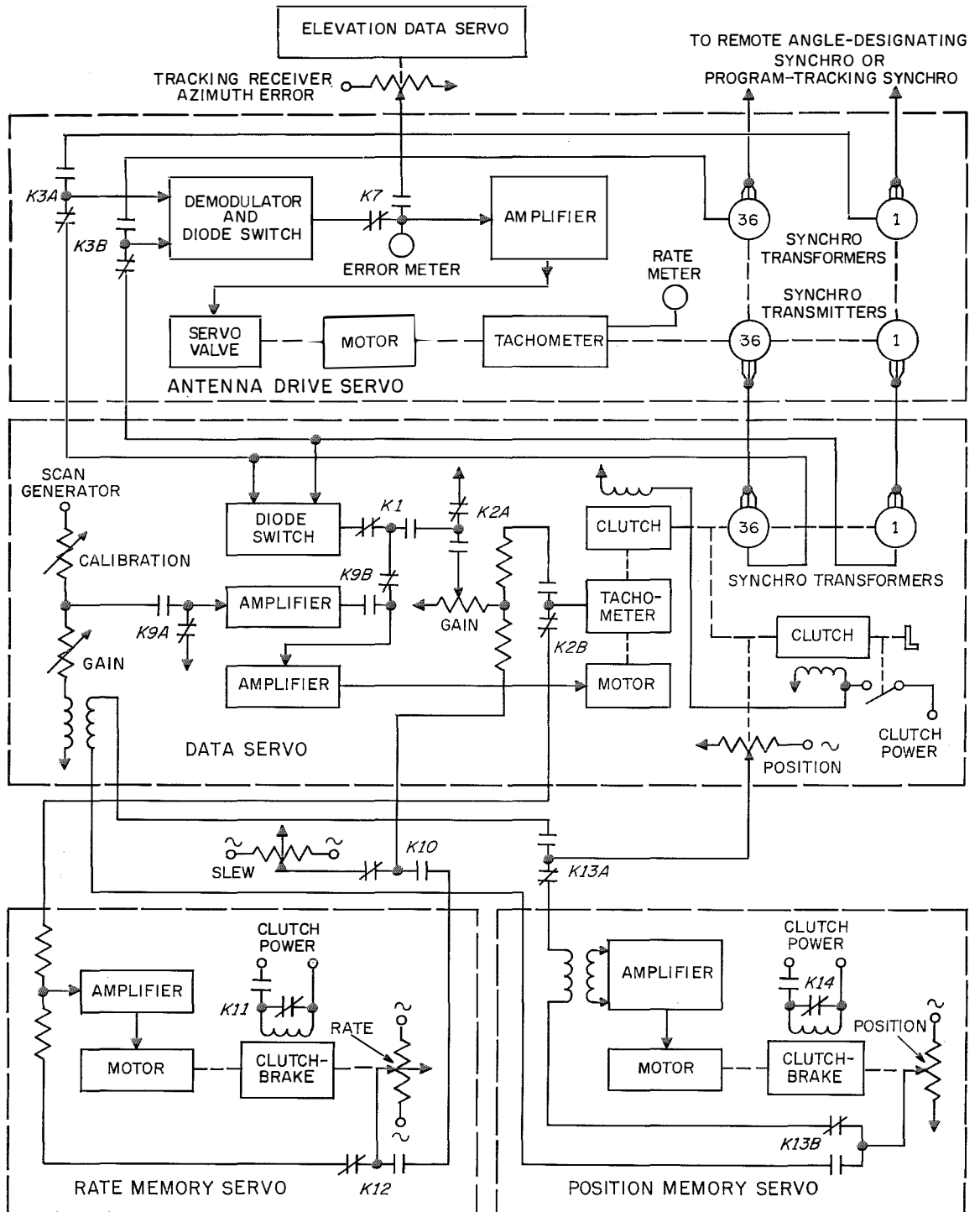


Figure 5—Simplified diagram of the azimuth-control system.

### 3.2 ELECTRICAL AND HYDRAULIC CONTROL

Figure 5 is a simplified diagram of the azimuth servo system. For manual tracking or setting, the crank handle at the right of the data servo section is adjusted to the desired azimuth setting for both the coarse 1-to-1 and the fine 36-to-1 synchro transformers. The diode switch in that section alternately connects the synchro electric outputs through the amplifier to the control motor to maintain that setting. The electric output also goes to the input of the antenna drive servo to drive the antenna to the designated position. When the satellite signal operates the automatic gain control of the tracking receiver, relay *K7* is energized and the antenna drive is under control of the tracking receiver.

In the azimuth-control system, memory servos continuously compute and store azimuth rate and position. The position memory servo holds the azimuth position for summation with the sector-scan signal so that the center of the scan does not drift. Its output signal is supplied to the input of a data servo on pre-selection of azimuth scan either as a principal mode or as a submode for loss of track in the principal mode.

In the latter case, it is supplied without delay if another submode has been preselected, or it is supplied as the instantaneous value generated by a rate memory when rate memory operation is terminated by a timer. The tracking-receiver azimuth-error signal is ex-

citation for an adjustable secant-correction voltage-divider resistor, the wiper being positioned by the elevation data servomotor. The azimuth loop gain for the automatic-tracking mode is varied in this way to maintain the requisite constant gain for the traverse plane; the secant function is generated only up to 80 degrees so that the traverse gain actually drops off above this elevation. For all other modes of azimuth control (manual positioning, slew positioning, data input from remote angle-designate synchros, or data input from external program-tracking synchros), the azimuth servo loop gain is kept independent of elevation angle. The azimuth drive servo is a direct-current-coupled system using stabilized operational amplifiers; all other loops and amplifiers are alternating-current units.

The elevation control system is basically the same as the azimuth control system except that a sector-scan generator and a position memory servo are not supplied.

### 3.3 SERVO

The servo comprises three loops, as shown in Figure 6. The load may be approximated by a quadratic lag, in which the natural frequency is determined by the combined moments of inertia and the combined compliances of the movable parts of the antenna, gear train, and hydraulic motor. Damping is accomplished by the viscous friction of the motor, gears, and

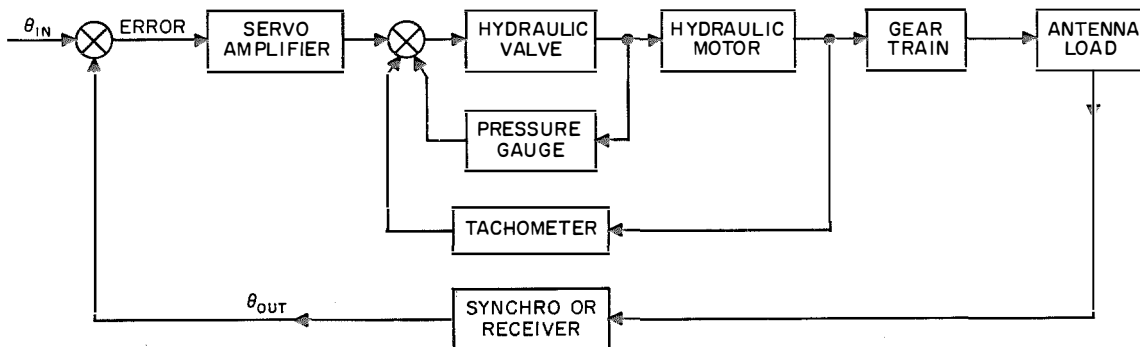


Figure 6—The antenna drive servo has 3 feedback loops.

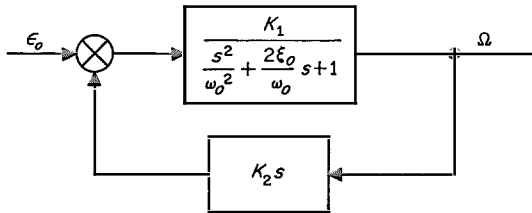


Figure 7—Pressure feedback loop.

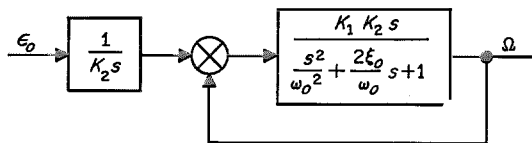


Figure 8—Equivalent circuit of the pressure feedback loop.

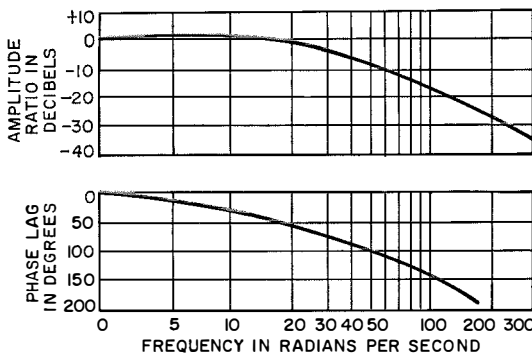


Figure 9—Transfer function of antenna load and hydraulic drive with pressure feedback loop closed.

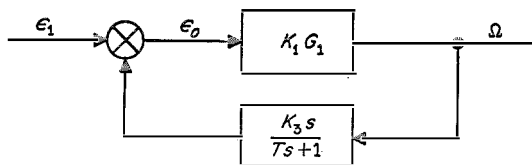


Figure 10—Tachometer feedback loop.

bearings, and by hydraulic leakage, but is very small.

### 3.3.1 Transfer Function

The inner feedback loop measures the pressure drop across the motor and its output goes through a high-pass filter. This loop serves solely to increase the load damping factor. In Figure 7, the motor-load natural frequency is  $\omega_o$  and the damping factor is  $\zeta_o$ . Using its equivalent, Figure 8, we may write

$$\frac{\Omega}{\epsilon_o} = \frac{1}{K_2s} \left( \frac{KG}{1 + KG} \right) = \frac{1}{K_2s} \frac{K_1K_2s}{\frac{s^2}{\omega_o^2} + \left( \frac{2\zeta_o}{\omega_o} + K_1K_2 \right) s + 1} \quad (8)$$

where  $\Omega = s\theta_o =$  output angular speed.

If we define  $\omega_1 = \omega_o$  and  $\zeta_1 = \zeta_o + \frac{1}{2}K_1K_2\omega_o$ , the closed-loop transfer function is

$$\frac{\Omega}{\epsilon_o} = \frac{K_1}{\frac{s^2}{\omega_1^2} + \frac{2\zeta_1}{\omega_1}s + 1} \quad (9)$$

which is the same form as the original quadratic, but with the damping term increased by the gain of the pressure feedback loop. However, a high-pass filter must be cascaded in  $K_2$  so as not to reduce the torque-error constant.

The closed loop is then approximately

$$K_1G_1 = \frac{\Omega}{\epsilon_o} \frac{K_1(T_1s + 1)}{\frac{s^2}{\omega_1^2} + \frac{2\zeta_1}{\omega_1}s + 1} \quad (10)$$

Values of  $T_1 = 1/6.4$ ,  $\omega_1 = 9.5$ , and  $\zeta_1 = 0.77$  were selected for  $\omega_o = 50$  radians per second, equivalent to 8 cycles per second. The transfer function is plotted in Figure 9 and has a 45-degree frequency of 15 radians per second and a 90-degree frequency of 50 radians per second.

The natural frequency is increased by the tachometer loop, shown in Figure 10, and its equivalent in Figure 11. The open- and closed-loop transfer functions are shown in Figure 12. A loop gain,  $\alpha = K_1K_3$ , of 18 decibels can be

obtained with  $\zeta = 0.8$ . The closed tachometer loop can be expressed by

$$K_m G_m = \frac{\alpha s}{(\alpha T s + 1) \left( \frac{s^2}{\omega_n^2} + \frac{2\zeta}{\omega_n} s + 1 \right)} \quad (11)$$

where  $\alpha = 8$   
 $T = 1/3.2$   
 $\omega_n = 90$   
 $\zeta = 0.8$ .

The tracking loop is formed by cascading an undercompensated integral network with the tachometer loop. The over-all open-loop function is

$$KG = \frac{\theta_o}{\epsilon} = K_o G_o \frac{T s + 1}{K_3 s} K_m G_m \frac{1}{R s} \quad (12)$$

where  $K_o G_o (T s + 1) / K_3 s$  is the integral network transfer function and  $R$  is the gear ratio. Then

$$KG = \frac{K_o}{K_3 R} \times \frac{T_o s + 1}{\alpha_o T_o s + 1} \times \frac{T s + 1}{\alpha T s + 1} \times \frac{1}{s \left( \frac{s^2}{\omega_n^2} + \frac{2\zeta}{\omega_n} s + 1 \right)} \quad (13)$$

Thus, the servo dynamically consists of two lag networks and a quadratic lag.

The servo bandwidth is adjustable with four settings: 5, 2.5, 1.25, and 0.625 cycles per second. The bandwidth control adjusts  $T$ ,  $T_o$ , and  $\alpha_o$  to maintain the velocity-error constant (loop gain,  $K_v$ ) greater than 300 (second)<sup>-1</sup>. For the 5-cycle-per-second bandwidth, the open- and closed-loop frequency responses are shown in Figure 13.

### 3.3.2 Error Constants

The important parameters required in the servo-error analysis are the error constants for velocity, acceleration, and torque. The velocity-error constant is the servo loop gain, and is given by

$$K_v = \alpha_o \alpha \omega_c \quad (14)$$

where  $\omega_c$  is the servo bandwidth, defined as the

frequency at which the open-loop gain is unity (gain crossover).

For the 5-cycle-per-second bandwidth,  $K_v = 2.5 \times 8 \times 5 \times 2\pi \approx 600$  (second)<sup>-1</sup>.

The acceleration-error constant  $K_a$  is found

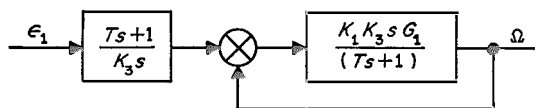


Figure 11—Equivalent circuit of tachometer feedback loop.

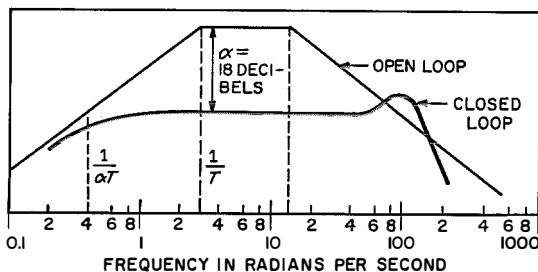


Figure 12—Tachometer functions with both open and closed feedback loops.

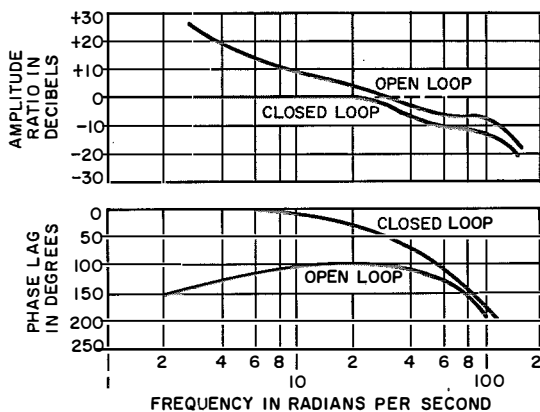


Figure 13—Transfer functions of complete antenna servo for both open and closed feedback loops.

## Antenna for Transportable Terminal

from a Taylor's series expansion of the error/ input ratio

$$\frac{\epsilon}{\theta_i} = \frac{1}{1 + KG} = e_1s + e_2s^2 + \dots = \frac{1}{K_v} s + \frac{1}{K_a} s^2 + \dots \quad (15)$$

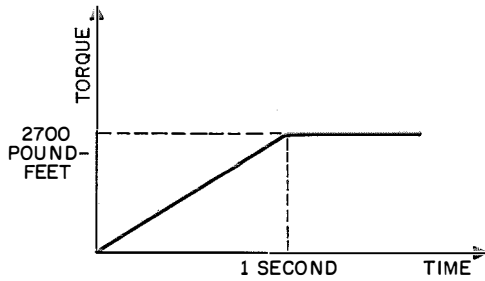


Figure 14—Specified wind gust.

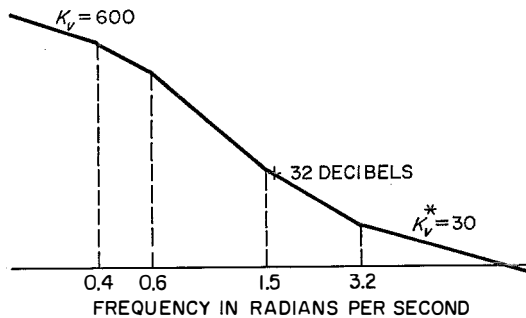


Figure 15—Asymptotic open-loop transfer function.

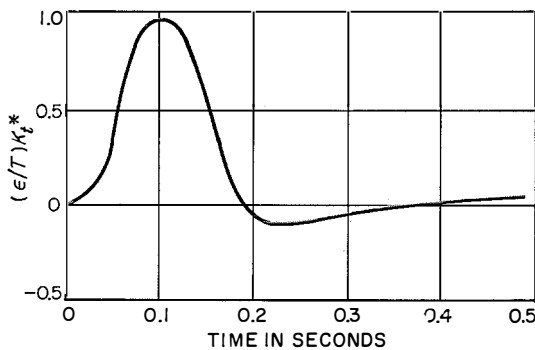


Figure 16—Transient response to a step gust of wind for  $K_t^* = 2.84 \times 10^7$  pound-feet per radian and  $T = 2700$  pound-feet. The peak error is 0.095 milliradian.

The transfer function may be expressed as the polynomial

$$KG = K_v \frac{n_1s^i + \dots + n_2s^2 + n_1s + 1}{d_1s^j + \dots + d_2s^2 + d_1s + 1} \quad (16)$$

Solving for  $K_a$

$$K_a = \frac{K_v^2}{K_v(d_1 - n_1) - 1} \quad (17)$$

From Section 3.3.1,

$$KG = K_v \times \frac{T_oTs^2 + (T_o + T)s + 1}{s \left[ 1 + \left( \frac{2\zeta}{\omega_n} + \alpha T + \alpha_o T_o \right) s + \dots \right]} \quad (18)$$

and

$$K_a = \frac{K_v^2}{\left[ \frac{2\zeta}{\omega_n} + \alpha T + \alpha_o T_o - (T_o + T) \right] K_v - 1} = \frac{K_v^2}{\left[ \frac{2\zeta}{\omega_n} + (\alpha - 1)T + (\alpha_o - 1)T_o \right] K_v - 1} \quad (19a)$$

For the 5-cycle-per-second bandwidth, the constants are

$$\begin{aligned} \alpha &= 8 & \zeta &= 0.8 \\ \alpha_o &= 2.5 & \omega_c &= 30 \\ T &= 1/3.2 & 2\zeta/\omega_n &= 0.016 \\ T_o &= 1/1.5 & (\alpha - 1)T &= 2.19 \\ \omega_n &= 100 & (\alpha_o - 1)T_o &= 1. \end{aligned}$$

$$K_v = \alpha_o \alpha \omega_c = 2.5 \times 8 \times 30 = 600 \text{ (second)}^{-1}.$$

$$K_a \approx \frac{K_v}{(\alpha - 1)T + (\alpha_o - 1)T_o} = \frac{600}{3.19} = 188 \text{ (second)}^{-2}.$$

The static torque-error constant  $K_t$  (see Section 3.3.3) is a function of hydraulic leakage and  $K_v$ . Since the open-loop gain decreases with increasing frequency, dynamic torque-error constant  $K_t^*(j\omega)$  may be conveniently determined by multiplying  $K_t$  by the ratio of the gain at the desired frequency to  $K_v$ . The wind gust specified is shown in Figure 14. It may be approximated by a sine wave having a period of 4 seconds and an amplitude of 2700 pound-feet. A more-exact expression

could be obtained by fitting a Fourier series to the given function, but the approximation is simpler and gives a conservative result.

The asymptotic open-loop transfer function is plotted in Figure 15. At the wind-gust frequency,  $\omega = (2\pi/4) = 1.59$  radians per second, the gain is 12 decibels ( $\times 4$ ) above the basic speed constant of 30. Then the servo stiffness to wind gusts is

$$K_t^* = \frac{30 \times 4}{600} \times K_t \quad (20)$$

$$= \frac{1}{5} \times 18 \times 10^8 = 3.6 \times 10^8$$

pound-feet per radian for azimuth

$$= \frac{1}{5} \times 36.7 \times 10^8 = 7.34 \times 10^8$$

pound-feet per radian for elevation.

For an applied step-function of torque, the dynamic torque-error constant is

$$K_t^* = J\omega_{cp}\omega_{cr} \quad (21)$$

where  $J$  is the system moment of inertia,  $\omega_{cp}$  is the position-loop crossover frequency, and  $\omega_{cr}$  is the tachometer-loop crossover frequency. Then,  $K_t^* = 8000 \times 2\pi \times 5 \times 2\pi \times 18 = 2.84 \times 10^7$  pound-feet per radian. Figure 16 shows an approximate transient response to a step gust. The error magnitudes for a wind gust as specified in Figure 14 are

$$\text{Azimuth: } \frac{2700 \times 1000}{3.6 \times 10^8} = 0.0075 \text{ milliradian}$$

$$\text{Elevation: } \frac{2700 \times 1000}{7.34 \times 10^8} = 0.0037 \text{ milliradian.}$$

The error constants may now be summarized. To maintain a  $K_v$  of at least 300, the servo design adjusts  $K_o$ ,  $T$ ,  $T_o$ , and  $\alpha_o$  for each bandwidth setting. The specified  $K_a$  of 50 is exceeded for both 5- and 2.5-cycle-per-second bandwidths. The error tabulation includes tracking errors for the normal 5-cycle-per-second bandwidth. Errors for other bandwidths may be computed from the coefficients tabulated in Table 1.

### 3.3.3 Static Torque Errors

The static torque-error constant is determined by the hydraulic leakage and the loop gain  $K_v$ . A static applied torque requires sufficient error to establish enough flow to develop a compensating pressure drop across the leakage path. For the hydraulic motor

$$Q = K_s \epsilon$$

$$\Omega = K_v \epsilon$$

$$d_p = Q/R\Omega \quad (22)$$

- where  $Q$  = motor flow
- $\epsilon$  = servo error
- $\Omega$  = angular speed at the antenna
- $d_p$  = motor displacement per radian
- $R$  = gear ratio.

Then

$$K_s = \frac{Q}{\epsilon} = K_v \frac{Q}{\Omega} = K_v R d_p. \quad (23)$$

TABLE 1  
ERROR COEFFICIENTS

$f_c$ in Cycles Per Second	$\omega_c$ in Radians Per Second	$T$ in Seconds	$T_o$ in Seconds	$\alpha$	$\alpha_o$	$K_v$ (Second) <sup>-1</sup>	$K_a$ (Second) <sup>-2</sup>	$K_t^*$ in Pound-Feet Per Radian
5	31.4	1/3.2	1/1.5	8	2.5	600	188	$2.84 \times 10^7$
2.5	15.7	1/1.6	1/1.5	8	2.5	300	56	$1.42 \times 10^7$
1.25	7.8	1/0.8	1/0.4	8	10	600	19	$0.72 \times 10^7$
0.625	3.9	1/0.4	1/0.4	8	10	300	7.5	$0.36 \times 10^7$

\* For torque applied as a step function, the static  $K_t = 9.31 \times 10^8$  for azimuth and  $18.3 \times 10^8$  for elevation.

## Antenna for Transportable Terminal

The leakage flow  $Q_L$  is laminar and thus proportional to the pressure drop across the motor  $P$ .

$$Q_L = K_L P. \quad (24)$$

The output torque  $T$  is

$$T = PR d_p. \quad (25)$$

Then if the error with an applied torque  $T$  is  $\epsilon_T$

$$\epsilon_T = \frac{Q_L}{K_s} = \frac{K_L}{K_s} P = \frac{K_L}{K_s} \frac{T}{R d_p} = \frac{K_L}{K_s R^2 d_p^2} T.$$

The torque-error constant is

$$k_t = \frac{T}{\epsilon_T} = \frac{K_s R^2 d_p^2}{K_L}. \quad (26)$$

For the azimuth servo

$K_L = 1.53$  cubic inches per second per 1000 pounds per square inch

$K_s = 600$  (second)<sup>-1</sup>

$R = 1600$

$d_p = 0.92$  cubic inch per revolution

$$k_t = \frac{600(1600)^2(0.92/2\pi)^2}{1.53 \times 10^{-3} \times 12} = 18 \times 10^8$$

pound-feet per radian.

The azimuth error calculated for a wind load of 11 000 pound-feet and an elevation angle of zero degrees is 0.0061 milliradian. For a wind load of 2530 pound-feet and an elevation

TABLE 2  
CLASSIFICATION OF TRACKING SYSTEM ERRORS

Independent Tracking Errors (Static and Dynamic)		
Systematic	Bias	Noise
Gravity Alignment Readout Post-comparator phase shift Pre-comparator unbalance Reference alignment Leveling (above items removable at boresight)	Wind (steady-state) Gravity Solar heating Leveling Lean-in backlash Orthogonality of axes Readout Pre-comparator phase shift Servo unbalance Servo dead zone	Wind gusts Receiver noise Gear-tooth inaccuracies Variable phase shift in radio-frequency receiver Data gear nonlinearity and backlash Readout (operator reading error)
Dependent Tracking Errors (Dynamic)		
	Dynamic lag Multipath signal and other interfering errors	Glint Vehicle tumbling Compliance (acceleration) Hunting
Propagation Errors		
Predictable atmospheric behavior	Average atmospheric behavior	Atmospheric turbulence Scintillation
Instrumentation Errors		
Inherent accuracy of optical equipment	Optical parallax Inherent accuracy of optical equipment	Reference instability Reading error

angle of 80 degrees, the azimuth error is 0.0014 milliradian.

For the elevation servo

$K_L = 1.28$  cubic inches per second per 1000 pounds per square inch

$R = 3200$

$d_p = 0.6$  cubic inch per revolution

$k_t = \frac{600(3200)^2(0.6/2\pi)^2}{1.28 \times 10^{-3} \times 12} = 36.7 \times 10^8$   
pound-feet per radian.

The elevation error determined for a wind load of 11 000 pound-feet is 0.0030 milliradian and the gravity load of 14 000 pound-feet gives an elevation error of 0.0039 milliradian.

#### 4. Angular Accuracies

In the design phase, error flow charts were prepared and the contributions to angular error in each of the principal control modes were budgeted such that the "worst case" summation of all of the effects imposed by structural compliance, component linearities, environmental conditions (wind, solar heating), gravitational effects, inertial effects, et cetera, would not exceed the  $3\sigma$  accuracy values specified. The  $3\sigma$  errors in each of these modes were computed for combined effects due to satellite motion, component deflections of reflector and support structure, servo unbalance, servo dead zone, power gearing errors and noise, data gearing errors and noise, monopulse 4.08-gigacycle-per-second receiver dead zone and noise, drive-motor noise, and synchro errors.

Table 2 lists and classifies the error sources affecting any or all of the control modes. Although identified as sources of error, propagation anomaly (refraction and scintillation) and target glint and tumbling were not actually evaluated. Extensive tests were made for automatic-track beam errors, automatic-track pointing errors, and dynamic synchro positioning errors (manual or program). Results were consistent with design values presented in Section 3 and structural-deformation

errors in the reflector system, pedestal, and base supports. The only discrepancy noted in actual field measurement is that the forward loop gain cannot be adjusted for stable values of  $K_v$  above 300 (second)<sup>-1</sup>. This problem is still being studied. The effect on tracking to elevation angles as high as 87 degrees has not been significantly impaired, however.

#### 5. Acknowledgments

The active support and efforts of Mr. Paul Smith and Mr. Herbert Bradwin of Feedback Controls, Inc., and of Mr. Emery St. George of Cornell and St. George, Inc., during the development program are gratefully acknowledged.

**Emanuel Singer** was born on 8 September 1920, in Brooklyn, New York. He received a B.S. degree, cum laude, in electrical engineering from the College of the City of New York in 1942, and an M.S. degree from Rutgers University in 1955.

He joined ITT Federal Laboratories in 1943. From 1944 to 1946 he served in the United States Navy, returning to ITT Federal Laboratories until 1948. After a brief period with Freed Radio Corporation, he was employed by the Signal Corps Engineering Laboratories.

He rejoined ITT Federal Laboratories in 1955, where he has been concerned with the design, development, and evaluation of electronic systems in fields of communication, missile guidance, and precision-tracking radar.

Mr. Singer is a Member of the Institute of Electrical and Electronics Engineers.

**Thomas J. Vaughan** was born in Somerville, Massachusetts, on 30 September 1928. In 1950, he received a B.S. degree from the American Television Institute.

## Antenna for Transportable Terminal

He has been engaged in the design and development of microwave systems, testing, and components from 1950 to 1951 for Raytheon Manufacturing Company, from 1951 to 1954 for Sylvania Electric Corporation, from 1954 to 1958 for Goodyear Aircraft Corporation, and from 1958 to 1961 for I-T-E Circuit Breaker Company. He is now Manager of Engineering for Antenna Systems, Incorporated.

Mr. Vaughan is a Member of the Institute of Electrical and Electronics Engineers and past chairman of the Philadelphia chapter of its Professional Technical Group on Antennas, Propagation, and Microwave Theory and Techniques. He is a member of the standards committees of the Electronic Industries Association dealing with transmission lines and waveguide flanges.

# Multifrequency High-Power Cassegrainian Antenna-Feed Systems for Satellite Ground Stations

H. SCHEINER  
W. SPANOS  
R. EDWARDS

ITT Federal Laboratories, A Division of International Telephone and Telegraph Corporation; Nutley, New Jersey

## 1. Introduction

The antenna system of the transportable space-communication terminal must transmit to, receive from, and track the satellite. An antenna capable of being transported with the complex feed system intact would greatly reduce the erection time. For this reason a cassegrainian antenna design was chosen. The slight reduction in gain resulting from blockage by the hyperboloidal secondary reflector is offset by two advantages. The waveguide runs have been reduced to a foot or two at most and antenna temperature resulting from the cassegrainian design is reduced. The first transportable ground terminal was designed to operate with the Relay satellite.

For Relay, the ground-antenna requirements are to transmit right-hand circularly polarized signals from 1720 to 1730 megacycles per second and to receive left-hand circularly polarized signals from 4079 to 4180 megacycles per second.

The satellite emits a beacon signal at the low end of the reception band for tracking.

## 2. Antenna

The antenna is cassegrainian with the feeds located at the vertex of the main paraboloidal reflector. The main reflector is 30 feet (9.144 meters) in diameter with a focal length of 12.5 feet (3.81 meters). The receiving feed is a 4-horn cluster that provides simultaneous lobe comparison for beacon tracking in addition to communication reception. The transmitting feed is two polyrods placed on either side of the receiving-horn cluster. Polyrod radiators are used rather than flared horns to prevent blockage of the receiving feeds while simultaneously minimizing the center-to-center spacing of the two transmitting feeds. Nominally, the crossover level in an amplitude-comparison system is between 1 and 3 decibels;

this system is designed to have a 1-decibel crossover. Here again, the size of the receiving-feed cluster was minimized to further reduce the separation of the polyrod feeds.

Geometrical ray optics was used to determine the feed separation required at the paraboloidal vertex. As shown in Figure 1, a source  $S$  is displaced a distance  $Y_0$  from the primary focus of the hyperboloidal reflector, which focus is at the vertex of the main paraboloidal reflector. Consider the two reflected rays; 1 is derived from a ray directed toward the vertex of the hyperboloid and 2 is from a ray directed toward the secondary focus of the hyperboloidal reflector, which focus is located at the focus of the paraboloidal reflector. It is assumed that the displacement of  $P$  from the plane tangent to the vertex of the hyperboloid is negligible, and  $P$  can be considered to lie in the tangent plane. The equations of the two reflected rays can be derived using the 2-coordinate equation for a straight line and the virtual source is then determined by the intersection of the two reflected rays.

Equation for path 1 is

$$Y = \frac{Y_0}{a + c} (X - a).$$

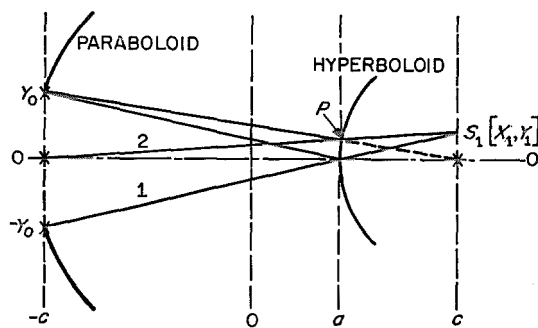


Figure 1—Determination of the virtual source.

## Cassegrainian Antenna for Ground Stations

Coordinates of  $P$  are

$$\left[ a, \frac{Y_0(c-a)}{2c} \right].$$

Equation for path 2 is

$$Y = \frac{Y_0(c-a)}{2c(c+a)}(X+c).$$

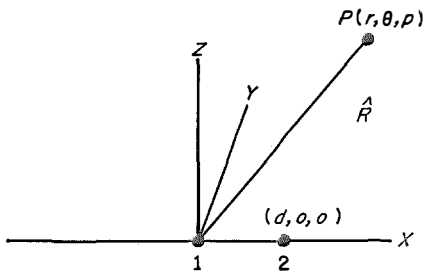


Figure 2—Determination of polyrod design.

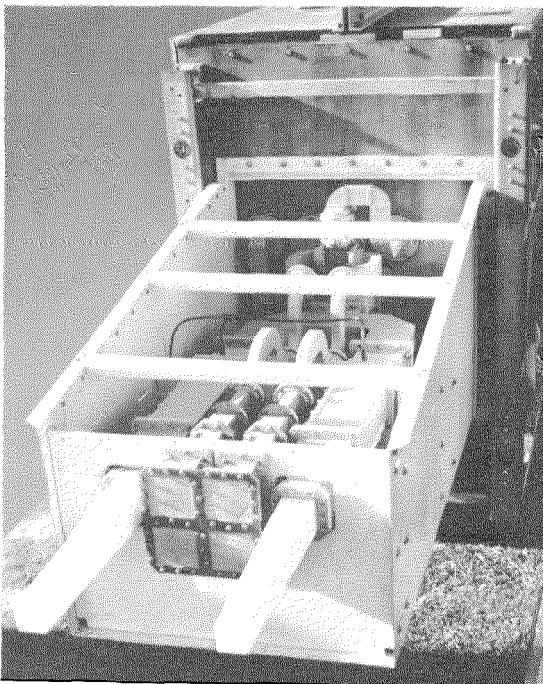


Figure 3—Feed system of transportable ground station used with Relay.

At  $S_1$  both equations are equal.

$$\frac{Y_0}{a+c}(X_1-a) = \frac{Y_0(c-a)}{2c(c+a)}(X_1+c)$$

or  $X_1 = c$

and

$$\frac{Y_0}{Y_1} = \frac{c+a}{c-a} = \frac{e+1}{e-1} = m.$$

As seen from the results, to a first-order approximation, the virtual source is located in the plane of the secondary focus of the hyperboloidal reflector and the displacement is equivalent to the source displacement divided by the magnification of the hyperboloid. Therefore, knowing the feed displacement necessary to produce a required beam displacement for a front-feed paraboloid, the amount of feed displacement necessary for a cassegrainian antenna can then be determined.

Based on the required feed separations for proper reception crossover, configurations were determined for various sizes of secondary reflectors to determine the best compromise between transmitting and receiving characteristics, with emphasis on receiving performance. As a result, the size of the secondary reflector was optimized at 6 feet (1.83 meters), which subtends an angle of 30 degrees from the paraboloidal vertex.

### 2.1 POLYROD DESIGN

For 10-kilowatt transmission, the up-path margin is approximately 15 decibels so that some compromise in illumination characteristics is possible. Calculations were made of spillover and blockage loss as a function of secondary-reflector illumination taper. See Figure 2.

$$\begin{aligned} \text{Array, } E_P &= g(\theta)[1 + \exp(jk\hat{p} \cdot \hat{R})] \\ &= g(\theta)\{1 + \exp[j(2\pi/\lambda)d \sin \theta \cos \phi]\}. \end{aligned}$$

$$\begin{aligned}
 \text{Power}_\theta &= K_2 \int_0^{2\pi} \int_0^\theta E_P E_P^* \sin \theta \, d\theta \, d\phi \\
 &= K_3 \int_0^\theta g(\theta)^2 \sin \theta \\
 &\quad \times \left\{ \int_0^{2\pi} [1 + \cos(Z \cos \phi)] \, d\phi \right\} d\theta \\
 &= K_4 \int_0^\theta g(\theta)^2 \sin \theta \\
 &\quad \times \left[ 1 + J_0 \left( \frac{2\pi}{\lambda} d \sin \theta \right) \right] d\theta \\
 \text{Power}_{\text{total}} &= K_4 \int_0^\pi g(\theta)^2 \sin \theta \\
 &\quad \times \left[ 1 + J_0 \left( \frac{2\pi}{\lambda} d \sin \theta \right) \right] d\theta
 \end{aligned}$$

where  $d$  = separation of polyrods

$$g(\theta) = \frac{\sin(K\theta)}{K\theta}$$

= individual source amplitude distribution

$$k = 2\pi/\lambda$$

$$\hat{p} = d\hat{i}$$

$$\hat{R} = \sin \theta \cos \hat{i} + \sin \theta \sin d\hat{j} + \cos \theta \hat{k}$$

$$Z = 2\pi d \sin \theta / \lambda$$

$\frac{\text{Power}_\theta}{\text{Power}_{\text{total}}}$  = fractional power contained in solid angle  $\theta$ .

The individual polyrod intensity distribution was assumed to follow a  $[\sin(K\theta)]/K\theta$  variation. By choosing the proper value of  $K$ , the intensity at the secondary-reflector edge could be varied. The percentage of signal loss because of spillover and blockage for various edge-illumination tapers, was determined graphically with the aid of a planimeter. The loss for a 3-decibel taper was 0.5 decibel more than for a 10-decibel taper. The additional loss for a 2-decibel taper was 1.4 decibels and for a 1-decibel taper it was 4.2 decibels. A polyrod with a 2-decibel edge-illumination taper was chosen as a good compromise, because it will provide sufficient antenna gain for television transmission at a later date.

### 3. Testing

The feed system of the transportable ground station used with Relay is shown in Figure 3. The polyrod length required to produce a 2-decibel illumination taper across the secondary reflector is quite long. To determine the effect of the polyrods on the 4-horn receiving feed, primary radiation patterns using only the horns and no reflectors were taken. The sum and difference patterns for the azimuth and elevation planes, taken without the polyrods, are shown in Figures 4 and 5, respectively. The sum pattern is obtained with all four horns operating in phase. The difference patterns are with one pair of horns out of phase with the other pair. Figure 6 shows the effect of the transmitting polyrods on the 4-gigacycle-per-second sum and difference primary patterns in the azimuth plane. The null depths are filled in and the first side lobes

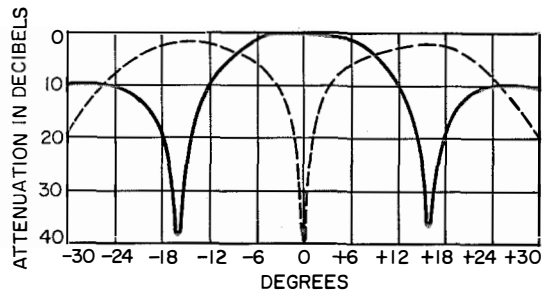


Figure 4—Azimuth sum (solid line) and difference (broken line) patterns at 4165 megacycles per second without polyrods or reflectors.

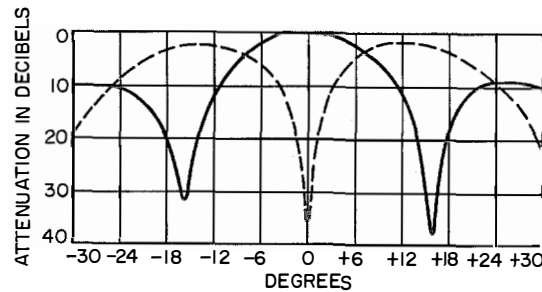


Figure 5—Elevation sum (solid line) and difference (broken line) patterns at 4165 megacycles per second without polyrods or reflectors.

## Cassegrainian Antenna for Ground Stations

are perturbed; however, within the  $\pm 15$ -degree sector subtended by the secondary reflector, the change is negligible. Since the transmitting polyrods are arrayed in the azimuth plane, the 4-gigacycle-per-second primary elevation pattern in the presence of the polyrods was unchanged. The azimuth-plane primary pattern of the 2-gigacycle-per-second polyrod array is shown in Figure 7. The separation of the two polyrods was slightly greater than required to satisfy the relation  $d \sin 15^\circ / \lambda \leq 0.5$  so that a small fraction of the first side lobe illuminates the secondary reflector.

The secondary 4-gigacycle-per-second sum and difference patterns for the azimuth and elevation planes are shown in Figures 8 and 9, respectively. These secondary patterns are for the 4-horn feed with the 30-foot (9.144-meter) cassegrainian antenna. The beam width was

0.55 degree and the measured gain was 48.4 decibels.

A typical secondary azimuth pattern for the dual-polyrod feed at 1725 megacycles per second is shown in Figure 10. This pattern was taken using a 40-foot (12.192-meter) paraboloidal antenna retrofitted with the identical feeds and hyperboloidal secondary reflector used on the 30-foot (9.144-meter) transportable antenna. Since the focal length of the 40-foot (12.192-meter) antenna was 16 feet (4.877 meters), the feeds were displaced 3.5 feet (1.067 meters) from the vertex. Also, the 6-foot (1.829-meter) secondary reflector was slightly smaller than required, which resulted in illuminating a diameter aperture of 38.5 feet (11.735 meters). The antenna pattern is a point-by-point plot, measured with the 40-foot (12.192-meter) antenna transmitting to a receiving antenna located on the 88th floor of the Empire State Building. The azimuth

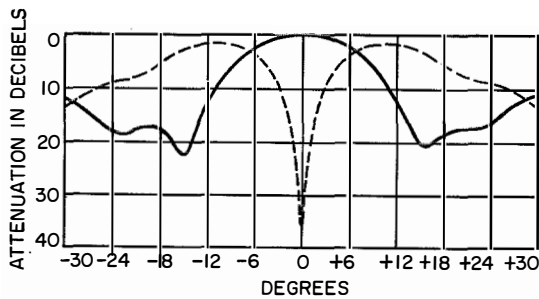


Figure 6—Azimuth sum (solid line) and difference (broken line) patterns at 4080 megacycles per second with 2-gigacycle-per-second polyrod array.

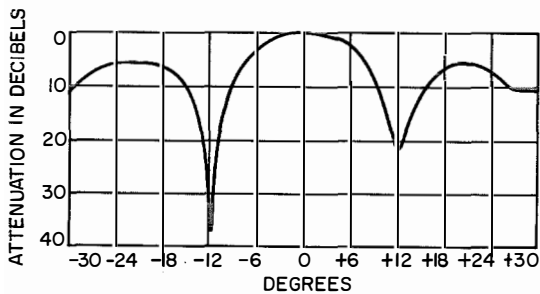


Figure 7—Azimuth-plane sum pattern of 2-gigacycle-per-second polyrod array, with separation of polyrods slightly greater than required to satisfy the relation  $d \sin 15^\circ / \lambda \leq 0.5$ .

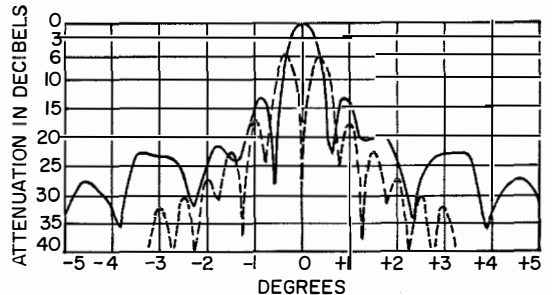


Figure 8—Azimuth sum and difference patterns at 4080 megacycles per second with reflectors.

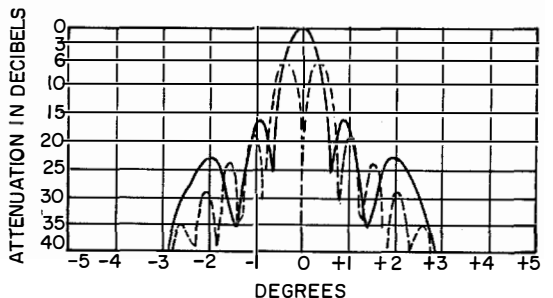


Figure 9—Elevation sum and difference patterns at 4080 megacycles per second with reflectors.

TABLE 1  
COMPARISON OF 6 GIGACYCLE-PER-SECOND RADIATION CHARACTERISTICS

Polarization	Polyrod Cluster			Free Space		
	3-Decibel Beam Width in Degrees	10-Decibel Beam Width in Degrees	Axial Ratio in Decibels	3-Decibel Beam Width in Degrees	10-Decibel Beam Width in Degrees	Axial Ratio in Decibels
Vertical	20	36	Less than 1	19.8	35	Less than 1
Horizontal	21.5	36	Less than 1	16.5	32	Less than 1

angles were read by a theodolite mounted on the antenna. The beam width of 1.2 degrees is slightly broader than the value of 1.05 degrees given in most antenna nomographs.

A right-hand circularly polarized transmission from 6380 to 6400 megacycles per second is required for Telstar. By changing the 4-giga-

cycle-per-second receiving cluster to polyrod end-fire radiators, sufficient space was made available to place a 6-gigacycle-per-second polyrod feed in on-axis alignment. The 4 receiving polyrods have the same illumination characteristics as the original horns. Primary sum and difference patterns of the 4-gigacycle-per-second polyrod feed cluster with and without the 6-gigacycle-per-second on-axis feed are shown in Figures 11 and 12, respectively.

The figures show that the effect of the polyrod on-axis feed on the 4-gigacycle-per-second pattern is negligible, especially with regard to the on-axis null depth. Table 1 compares the 6-gigacycle-per-second polyrod radiation characteristics of the cluster with the radiation characteristics in free space. The slight broadening of the primary beam has a negligible effect on transmission performance. The feed system for the transportable antenna

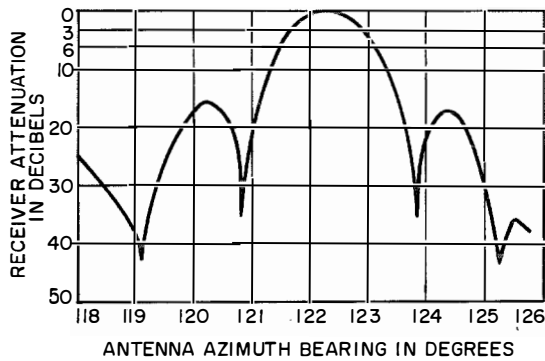


Figure 10—Azimuth radiation pattern at 1725 megacycles per second with reflectors.

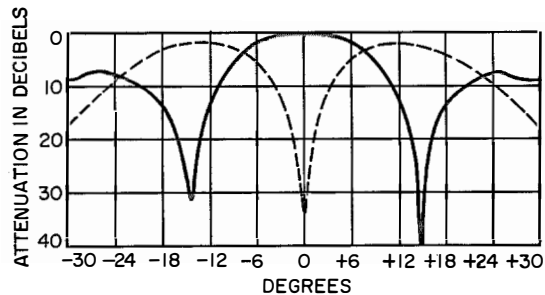


Figure 11—Azimuth sum (solid line) and difference (broken line) patterns at 4080 megacycles per second with on-axis 6-gigacycle-per-second polyrod feed but no reflectors.

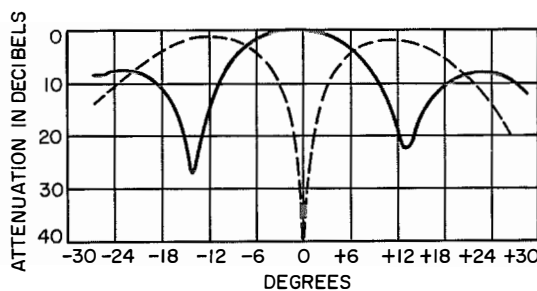


Figure 12—Elevation sum (solid line) and difference (broken line) patterns at 4080 megacycles per second using polyrod radiators without on-axis feed and without reflectors.

## Cassegrainian Antenna for Ground Stations

used with Telstar is shown in Figure 13. The waveguide for the on-axis 6-gigacycle-per-second polyrod feed, shown in Figure 14, is water-cooled to permit transmission of 10-kilowatt continuous-wave power.

The feed system designed to operate with both the Telstar and Relay communication satel-

ites is shown in Figure 15. Since the receive bands are identical, the receivers within the electronic-equipment pod can be used with either Relay or Telstar. Power amplifiers for 10-kilowatt continuous-wave signals at 2 and 6 gigacycles per second are also mounted within the enclosure.

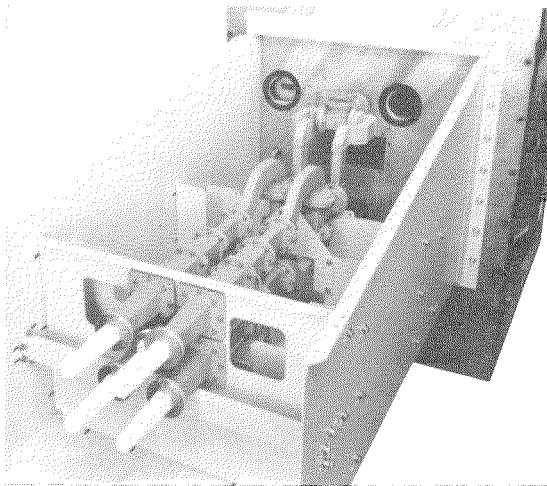


Figure 13—Transportable-antenna feed system used with Telstar satellites.

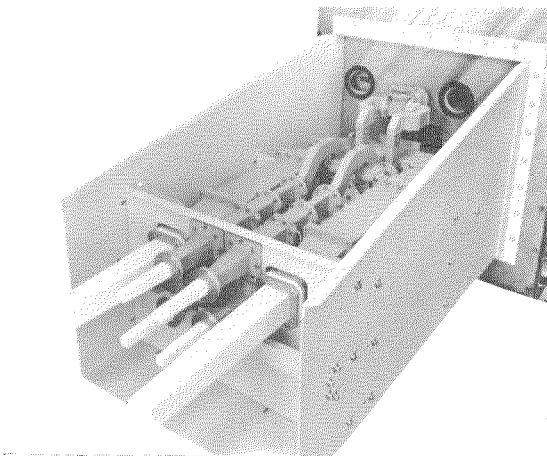


Figure 15—Feed system designed for operation with both Telstar and Relay satellites.

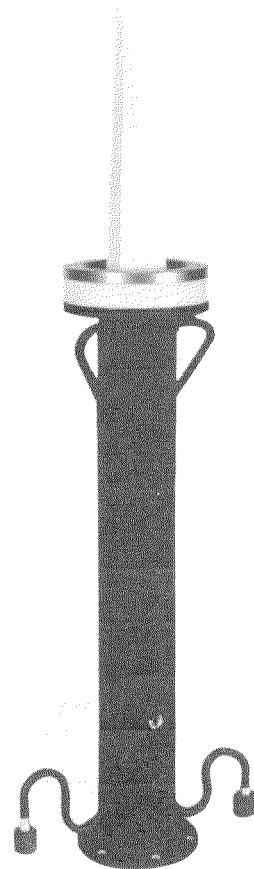


Figure 14—Waveguide for the on-axis 6-gigacycle-per-second polyrod feed.

## Cassegrainian Antenna for Ground Stations

**Harry Scheiner** was born on 23 November 1931, in Brooklyn, New York. He received a B.S. degree in physics from the College of the City of New York in 1954.

He then entered the armed services and after release from active duty in 1956, he attended graduate school full-time until 1957.

In 1957, he was employed by General Electric Company and in 1960 by Lockheed Electronics Company.

He joined ITT Federal Laboratories in 1960, where he has been engaged in the design of antenna systems. He is now concerned with the system for the transportable satellite-communication ground terminal.

**William M. Spanos** was born on 17 April 1927, in Orlando, Florida. In 1951, he received a B.S. degree in electrical engineering from Rensselaer Polytechnic Institute.

He joined ITT Federal Laboratories in 1951, where he is now engaged in work on multi-frequency high-power feed systems for satellite-communication transportable ground stations.

Mr. Spanos is a Member of the Institute of Electrical and Electronics Engineers.

**Robert A. Edwards** was born in Detroit, Michigan, on 23 August 1920. He received in electrical engineering a B.S. degree from the University of Michigan in 1943 and an M.S. degree from Stevens Institute of Technology in 1956.

In 1952, he joined ITT Federal Laboratories, where he has been engaged in the development of microwave antennas and equipment. He is presently responsible for developing ultra-high-frequency antenna systems for satellites.

Mr. Edwards is a Member of the Institute of Electrical and Electronics Engineers.

# Transmitter for Satellite Ground Station

H. GOLDMAN  
R. GRAHAM  
L. GRAY

ITT Federal Laboratories, A Division of International Telephone and Telegraph Corporation; Nutley, New Jersey

## 1. Introduction

This paper describes the transmitting system used in the universal transportable space-communication terminal developed for communication over long distances via satellites orbiting the earth.

## 2. Dual Transmitting System

A dual transmitting system (Figure 1) permits changing the transmitter frequency for Relay or Telstar easily and quickly.

The exciter, power amplifier, and transmitting horns are designed for 2-gigacycle-per-second operation with Relay; comparable units operate at 6 gigacycles per second with Telstar. The

modulator, heat exchanger, and power supplies are common for both frequencies.

The transmitting frequency is controlled from the operations control van by switching power and modulation to the desired exciter and power amplifier. This is accomplished within 30 seconds.

Transmitters operating at still-other frequencies can be accommodated. For example, the transmitter for use with Syncom operates in the band from 7 to 8 gigacycles per second. By proper selection of units, the ground station can operate with any pair among Relay, Telstar, and Syncom.

All 3 transmitters are similar. They use 10-kilowatt liquid-cooled klystrons manufactured

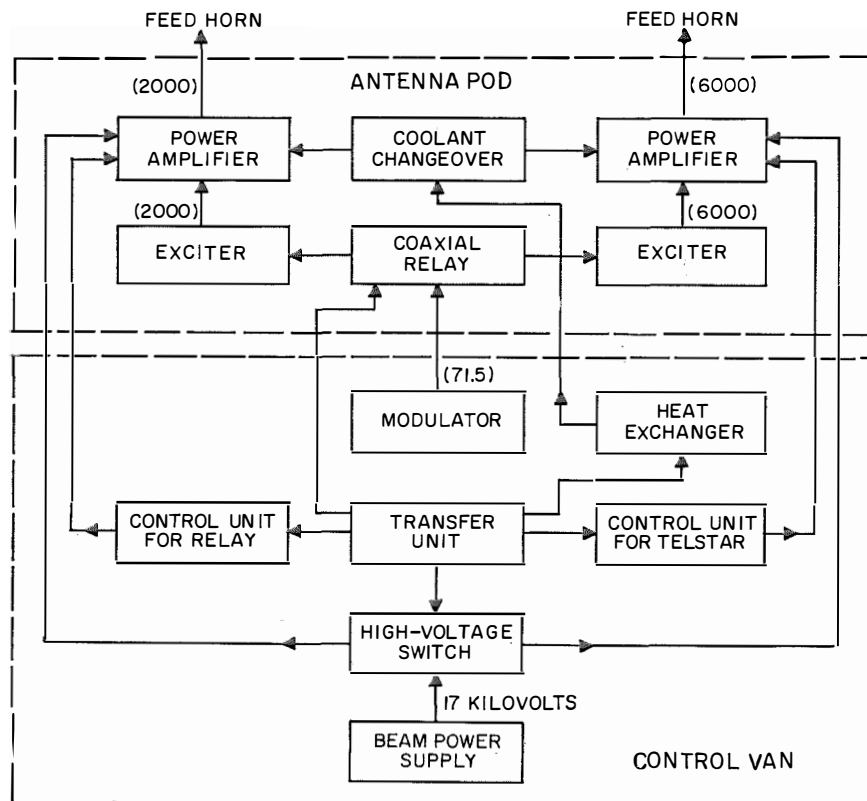


Figure 1—Diagram of dual-transmission system for Relay or Telstar. Frequencies within parentheses are in megacycles per second.

by Varian Associates. This paper describes the units used in 6-gigacycle-per-second operation.

### 3. Major Components

The major components of the transmitter are the modulator, exciter, power amplifier, heat exchanger, control unit, and beam power supply. To minimize transmission losses and avoid using rotary joints, the exciter and power amplifier are located in a microwave-electronics package mounted on the antenna behind the vertex of the primary reflector. The modulator, control unit, and power supply are located in the equipment van. The heat exchanger, which handles a large volume of air, is normally located near the base of the antenna. The klystron coolant, a mixture of ethylene glycol and water, is supplied to the microwave-electronics package through flexible metal hoses.

#### 3.1 MODULATOR

The present transmitter uses frequency-division multiplex with frequency modulation of the carrier by the subcarriers. The modulator has a 240-channel capability but multiplex terminal equipment for only 12 channels was used in the Relay and Telstar experiments. The modulator output frequency is 71.5 megacycles per second. It is designed to accept a level of -40 decibels referred to 1 milliwatt per channel

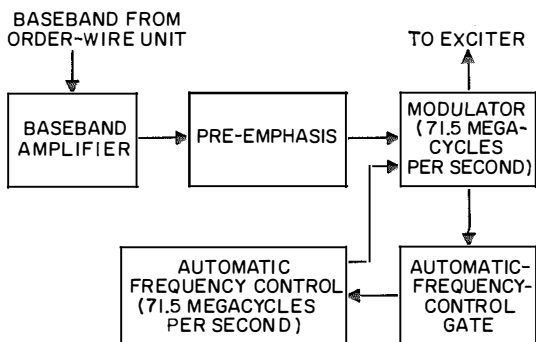


Figure 2—Modulator diagram.

with a maximum deviation capability of 50 kilocycles per second per wire channel. The per-channel root-mean-square deviations with Relay and Telstar are 29 and 42 kilocycles per second, respectively.

The modulator uses solid-state components and includes a video amplifier, automatic frequency control, and integral power supplies. Figure 2 is a diagram of the unit. Interchannel distortion when operating with 36 channels is better than 50 decibels below the reference level in each channel.

#### 3.2 EXCITER

The exciter is in the antenna-mounted equipment housing. It uses solid-state components and generates 0.05 watt to drive the klystron power amplifier. Figure 3 is a diagram of the unit.

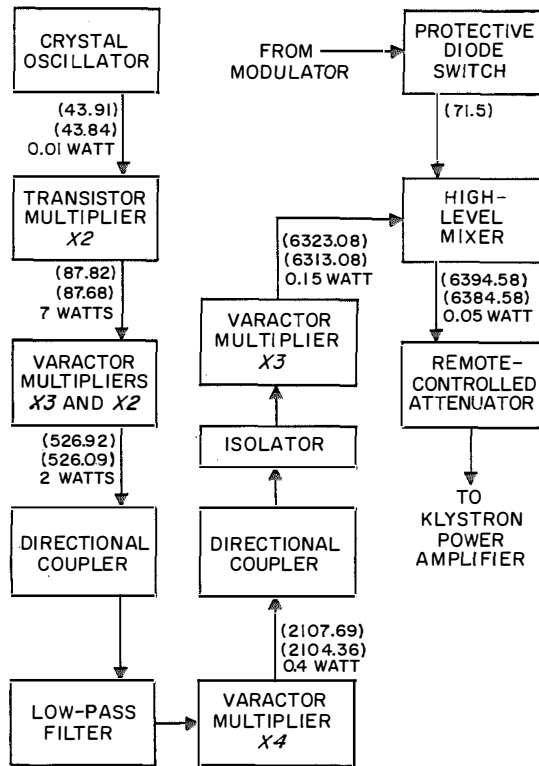


Figure 3—Exciter diagram. Frequencies within parentheses are in megacycles per second.

## Transmitter for Satellite Ground Station

A crystal-controlled oscillator determines the transmitter frequency. It has a vernier adjustment that allows the frequency to be set within  $\pm 1$  part in  $10^6$ . The crystal and its transistor circuit are packaged in a plug-in oven.

After amplification, the signal is multiplied in a transistor frequency doubler, then passed through a 3-stage amplifier. The last amplifier is operated class-C, with an output of approximately 7 watts at the nominal frequency of 87 megacycles per second. The variable-reactance multiplier stages that follow have no gain so

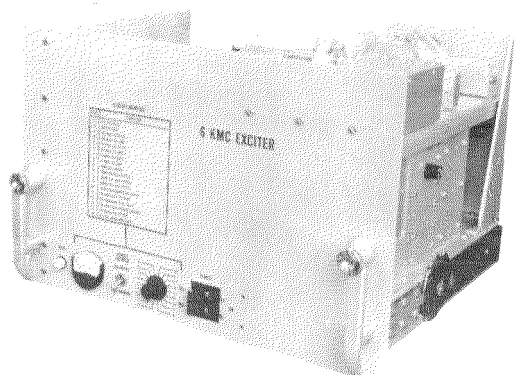


Figure 4—Exciter front view.

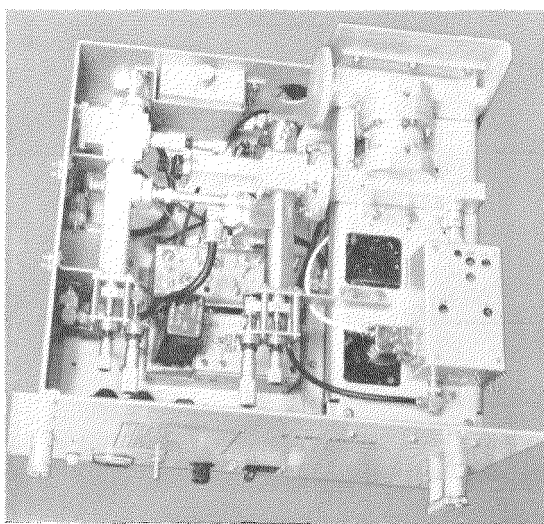


Figure 5—Interior of exciter.

that considerable power is required from the amplifier chain [1].

The output from the amplifier is passed to a tripler stage using two varactors in a balanced circuit with an untuned idler to permit third-harmonic currents to flow. Although this is more complex than a single-varactor circuit, the increased stability warrants its use. The following doubler stage uses a balanced circuit to provide good rejection of the fundamental frequency. Its output is 2 watts at a nominal frequency of 525 megacycles per second.

The quadrupler uses a single varactor in a coupled coaxial-resonator configuration. The input and output resonators are tuned respectively to 525 and 2100 megacycles per second, nominal. The output is 0.4 watt. No idlers are used in the quadrupler.

A ferrite isolator is inserted between the quadrupler and the second tripler, which uses a third-harmonic idler, a coaxial-resonator input cavity, and a waveguide resonant-iris output. A loss of 3 decibels occurs in this tripler, the output being 0.15 watt at 6300 megacycles per second, nominal.

The varactor multipliers have a combined 1-decibel-down bandwidth of 6 percent.

The output of the final tripler is passed to a high-level mixer that also receives the 71.5-megacycle-per-second signal from the modulator in the radio van. The sum frequency, nominally 6400 megacycles per second, is forwarded to the klystron power amplifier.

The output of the high-level mixer is 0.05 watt at the center of the frequency range.

To change transmitter frequency, the required crystal is inserted in the crystal oven. No exciter tuning controls need be adjusted. The mixer uses a fixed-tuned band-pass filter covering from 6383 to 6397 megacycles per second.

The amplitude variation of the exciter over a  $\pm 5$ -megacycle band centered at 6390 megacycles per second is less than  $\pm 0.25$  decibel and the 3-decibel-down bandwidth is  $\pm 7$  mega-

cycles per second. The rejection of spurious signals in the exciter output is greater than 60 decibels.

The exciter operates from 115 volts alternating current. An integral power supply provides the required direct voltages. Where necessary, current-limiting circuits are used to protect the power transistors during tune-up. Voltage regulation is used to minimize ripple. Direct metering points in the low-frequency stages and directional couplers in the high-frequency stages are provided for tuning and maintenance. Figures 4 and 5 show the exciter used in the transportable ground station.

### 3.3 POWER AMPLIFIER

The power amplifier (Figure 6) in the antenna microwave-electronics package contains the following items.

- (A) Klystron and magnet.
- (B) Input and output directional couplers.
- (C) Klystron motor-tuning drive mechanism.
- (D) Filament transformer.
- (E) Current transformer for remote filament-current metering.
- (F) Current transformer for remote filament-current interlock.
- (G) High-voltage interlocks and access-door short-circuiting switches.
- (H) Motor drive and clutch mechanism for tuning the klystron. This is monitored at the transmitter control panel in the operations control van.

The following items are also contained in the microwave-electronics package.

- (A) Coolant manifold for the klystron collector, body, magnet, and waveguide. The manifold incorporates flow interlock switches and high-temperature interlock switches for all cooled circuits.
- (B) Waveguide arc-detector assemblies.

- (C) Waveguide protective-circuits assembly.
- (D) Waveguide bends and sections to connect the output of the waveguide protective-circuits assembly through the pod bulkhead to the antenna-feed support structure.
- (E) Waveguide power-flow monitor assembly.

A continuously adjustable power control is provided on the transmitter control panel in the operations control van. This permits adjustment of the transmitter power-output level from 250 watts to 10 kilowatts.

The following is a brief summary of power-amplifier performance.

Signal power output in watts	250 to 10 000
Signal power input (minimum) in milliwatts	5
Antenna reflected power in watts	Less than 200
Beam voltage in kilovolts	17.5
Beam current in amperes	1.8
Body current in milliamperes	Less than 25
Bandwidth in megacycles per second at 3-decibel-down points	±2.5

#### 3.3.1 Transmission-Line Components

The klystron output is supplied through the adjacent main directional coupler to the

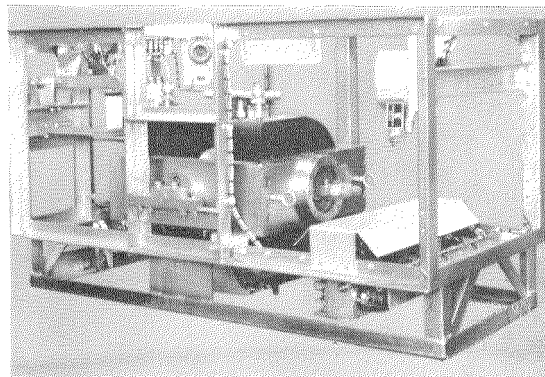


Figure 6—Microwave portion of power amplifier. It is located in the antenna pod.

## Transmitter for Satellite Ground Station

transmitting-horn system. All waveguide components in the radio-frequency transmission-line feed are liquid cooled.

The waveguide assembly that precedes the main directional coupler contains a light-sensi-

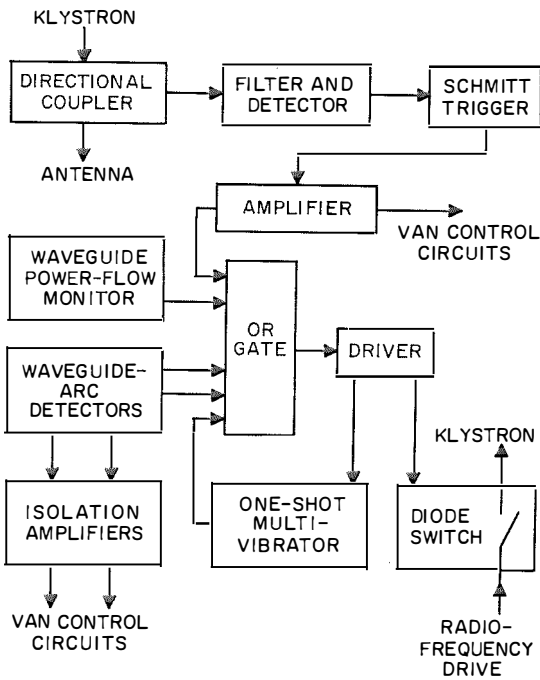


Figure 7—Antenna-mounted waveguide protective circuits.

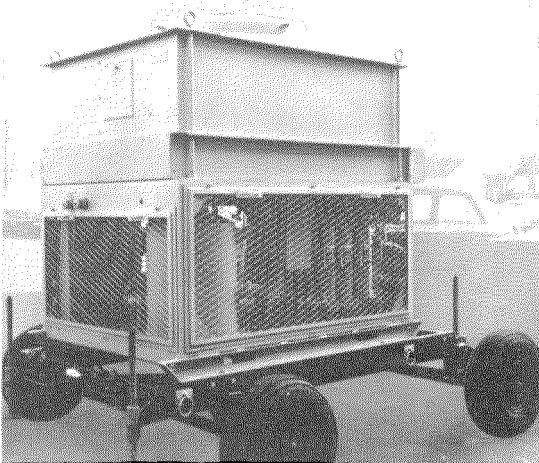


Figure 8—Heat exchanger on its trailer.

tive silicon controlled rectifier to detect any arcs near the klystron. An additional waveguide-arc detector is located near the horn assembly.

### 3.3.2 Klystron Protection

Figure 7 is a diagram of the antenna-mounted waveguide protective circuits for the power amplifier. These solid-state circuits protect the klystron window against waveguide arcs and excessive standing waves.

The standing-wave ratio is monitored through a directional coupler. The signal from the coupler is filtered to bar harmonics that could cause inaccurate measurements. It is then detected and if a preset level of reflected power is exceeded, a Schmitt trigger will be operated. Through an amplifier, the trigger provides an output to the van-mounted control circuits to remove the high-voltage power supply and, through the OR gate, to the antenna-mounted control circuits to remove the drive signal from the klystron.

Waveguide-arc protection is provided by the two light-actuated silicon controlled rectifiers. A lens mounted in the waveguide wall concentrates the light from an arc onto its associated rectifier, which operates through the OR gate to remove the klystron drive and also through the isolation amplifier to remove the high-voltage power supply.

The output of the OR gate provides a signal to the driver that controls the bias on a diode switch in the exciter. If a malfunction is sensed, the polarity of the bias is reversed, turning the diode switch off to remove the radio-frequency drive to the klystron.

The polarity-reversal signal also triggers a one-shot multivibrator that allows time for removing the high voltage from the klystron through other switches. This prevents rapid on-and-off switching of the driver as a fault is alternately sensed and removed.

Test functions are provided to check the operation of all circuits. These tests are made at the

operations control van before the klystron is turned on.

Removal of the radio-frequency drive from the klystron is necessary because the power-supply filter prevents rapid removal of high voltage from the klystron. The antenna-mounted control circuits are designed to remove all radio-frequency output from the power amplifier in less than 10 microseconds.

### 3.4 HEAT EXCHANGER

The heat exchanger (Figure 8) includes a circulating pump, blower, and coolant-purifying system. The heat-exchanging coils are automatically bypassed until the proper operating temperature of 60 degrees centigrade (140 degrees fahrenheit) is reached. The purifying unit removes dissolved oxygen, carbon dioxide, and minerals.

The heat exchanger is controlled from the operations control van and the coolant is circulated for two minutes after the klystron filaments are switched off. To provide the necessary pressure at the klystron and to lift the coolant to antenna level, the circulating pump is rated at 125 pounds per square inch.

### 3.5 CONTROL UNIT

The control unit (Figure 9) provides the power amplifier with radio-frequency and direct-current fault protection and control. Modular control circuits are integrated with the radio-frequency monitoring and protective circuits to respond within microseconds to provide protection for the klystron and the associated waveguide components. The control circuits are self-clearing with automatic reset for sporadic and nonrecurring faults.

Solid-state printed-circuit cards (Figure 10) minimize downtime by enabling entire control functions to be replaced at once.

The front-panel indicators make fault location easy, changing from green to red for a faulty or inoperative function. Each indicator is

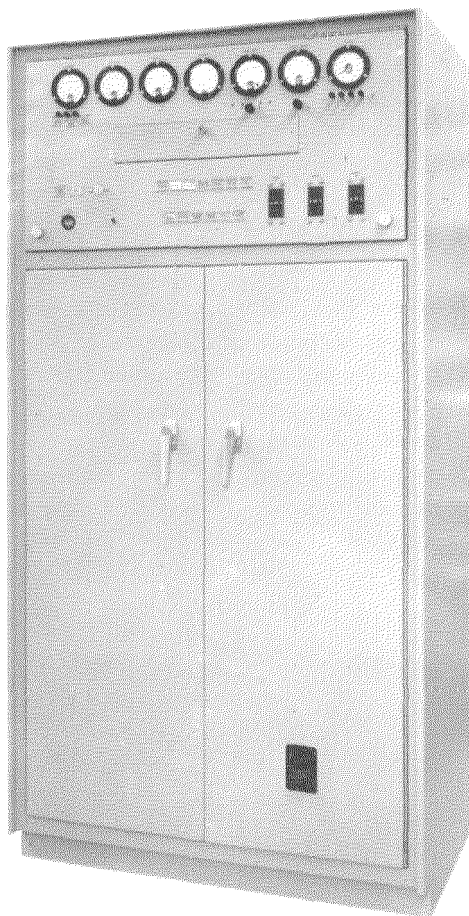


Figure 9—Control unit. Dimensions are 24 by 36 by 72 inches (61 by 91 by 183 centimeters).

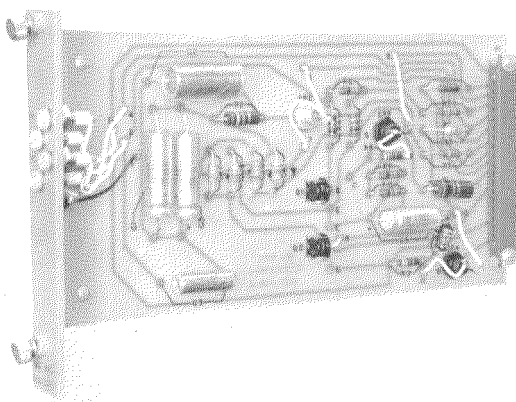


Figure 10—Control card.

## Transmitter for Satellite Ground Station

labelled for the function it monitors. In normal service, the only control needed to turn the equipment on is the lighted main-power indicator button. The adjacent beam indicator button controls the beam voltage. If the protective circuit breakers (at the power-supply panel) are all closed and the beam button has been pressed, the beam voltage will be applied automatically at the end of the starting sequence.

If the alarm for low power output from the klystron sounds, pressing the reset button will stop the bell; however, alarm functions for overload or other conditions remain in effect. The alarm will automatically reset without sounding again whenever the radio-frequency output returns to normal.

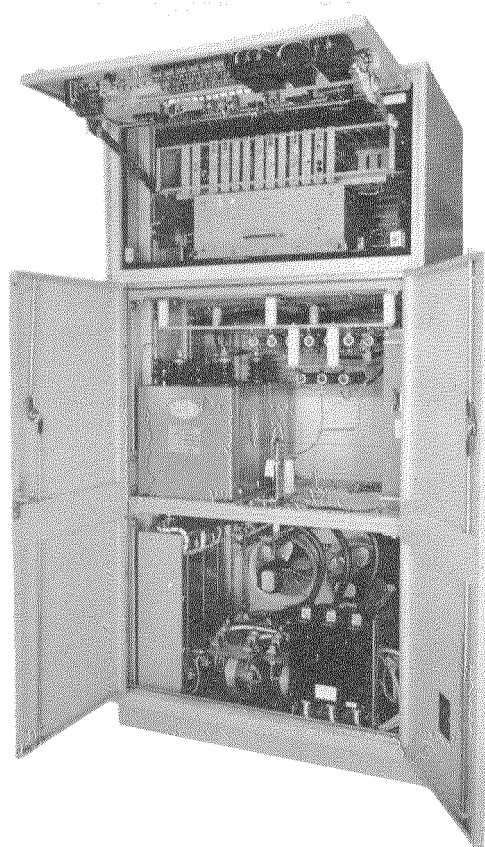


Figure 11—Interior of control unit.

The interior of the control unit is shown in Figure 11. At top is the control section, which houses the printed-circuit cards and klystron focus-magnet power supply. The top panel holds the meters, low-level circuit breakers, control-circuit-sequence indicators, and overload and fault indicators. The box below the cards contains infrequently used adjustments for focus-magnet current, calibration of meters for beam and body circuits, radio-frequency monitoring, beam-voltage control, and wave-guide-arc test.

The lower portion of the control unit contains the primary beam-voltage-control components, high-voltage filter capacitors, bleeder resistors, and beam-meter multiplier resistors, and is interlocked for safety.

### 3.5.1 Klystron Remote Tuning

For personnel safety and operating convenience, all normal adjustments of the antenna-mounted klystron are accomplished from the operations control van. These include adjustment of the klystron cavity, focus-magnet current, filament voltage, beam voltage, and radio-frequency drive.

Klystron-cavity frequency setting is indicated on a front-panel meter. The arrangement is sufficiently accurate to permit radio-frequency power output to be obtained when the klystron cavities are initially set using the tuning meter. This is a 270-degree meter with an arbitrary scale from 0 to 100. The cavity frequency for any reading is given by a chart prepared for the particular klystron in use.

The switch for raising and lowering the resonant frequency for each cavity is located behind the small subpanel on the upper portion of the control unit (Figure 9).

### 3.5.2 Control and Status

The control and status panel is shown in Figure 9. It uses rectangular push-button indi-

## Transmitter for Satellite Ground Station

cators either for control and response or simply for status of equipment. Each indicator has two green lamps to signify normal operation and two red lamps to warn of failure. The twin lamps provide redundancy for reliability; if one fails, the uneven illumination pattern is evident.

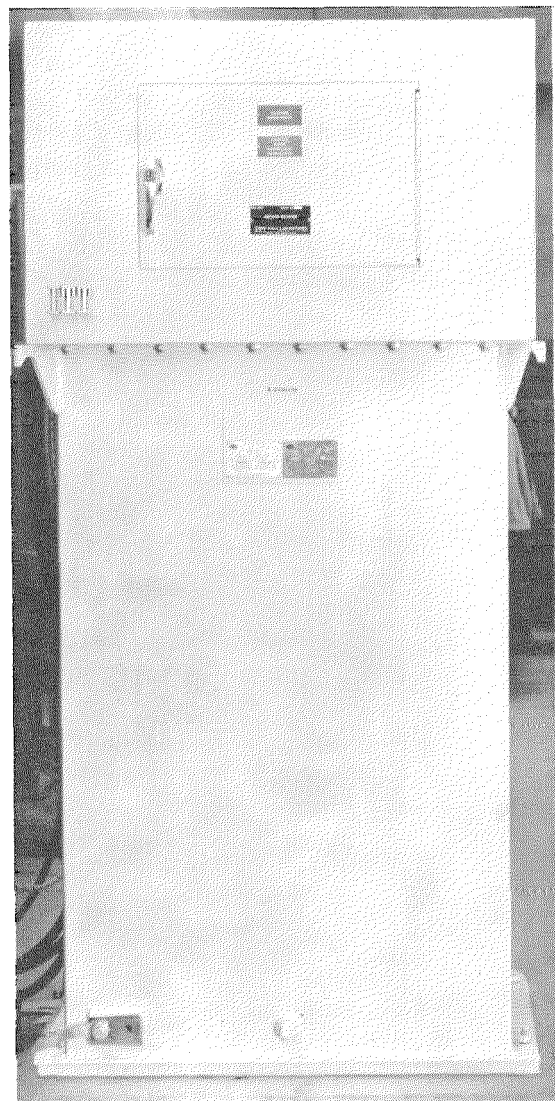


Figure 12—Beam power supply. Dimensions of this unit are 23 by 36 by 68 inches (57 by 91 by 173 centimeters).

### 3.6 BEAM POWER SUPPLY

The beam power supply for the power amplifiers consists of a single askarel-filled unit housing the high-voltage transformer and filter choke. This unit is shown in Figure 12. It is capable of delivering 17.5 kilovolts at 2.0 amperes. Silicon rectifiers are used for high-voltage rectification. They are located at the top of the beam-power-supply cabinet and are shown in Figure 13. This compartment is protected by high-voltage grounding switches and control-circuit interlocks. In addition, red warning signs are on the front of the door adjacent to the handle.

### 4. Conclusion

Nine transmitters, using the design described in this paper, have been built and placed in service through June 1963. The operation to date has clearly demonstrated the feasibility of mounting the microwave components on the antenna.

### 5. Acknowledgments

The authors are indebted to the following persons for their contributions to the transmitter design and development.

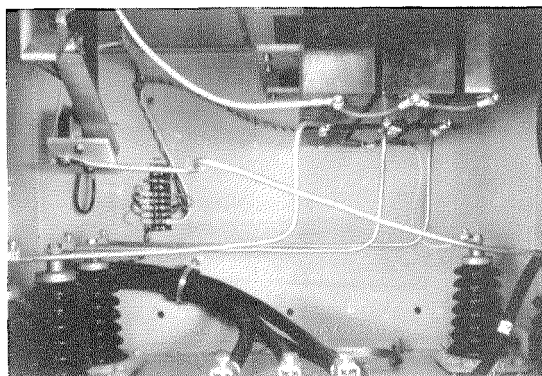


Figure 13—Silicon-rectifier compartment in top of beam power supply.

## Transmitter for Satellite Ground Station

Mr. L. Pollack for system guidance; Mr. W. Wasylkiwskyj for design work on the exciter; Messrs. K. Meyers and C. Fioretti for work on crystal oscillators and intermediate-frequency amplifiers; Mr. F. Kupersmith for the design and construction of the frequency modulator; and Mr. R. Kirsche for design work on the klystron protective circuits and power-amplifier test circuits.

### 6. References

1. W. Janeff, "Variable-Reactance Frequency Multipliers," *Electrical Communication*, volume 38, number 1, pages 106-118; 1963.

**Richard Graham** was born in New York, New York, on 13 September 1927. He received a B.S. degree in electrical engineering from Newark College of Engineering in 1950.

He was employed as a radio engineer for Wickes Engineering and Construction Company during 1950. From 1951 to 1953, he was

a technical representative for Bendix Aviation Corporation.

In 1953, he joined ITT Federal Laboratories where he has been working on transmitting equipment. He is presently responsible for the development of high-power amplifiers for forward-scatter and space-communication ground stations.

Mr. Graham is co-author of the book *Radio Transmitters*.

**Hyman Goldman** was born in Malden, Massachusetts, on 11 April 1922. From 1943 to 1946, he served with the United States Navy.

In 1942, he joined ITT Federal Laboratories, returning there after his navy duty. He has been engaged in the design and development of radio transmitters for various services. He is presently responsible for directing the transmitter development for satellite ground stations.

Mr. Goldman is a Member of the Institute of Electrical and Electronics Engineers.

**L. Gray.** Biography appears on page 48.

# Communication Receiver for Satellite Ground Station

M. SASSLER  
R. SURENIAN

ITT Federal Laboratories, A Division of International Telephone and Telegraph Corporation; Nutley, New Jersey

## 1. Introduction

The ground-station communication receiver for a satellite system has a number of constraints imposed on it. As the signal power radiated by the satellite is necessarily low, the ground-station receiver must achieve the best possible noise figure. To use signals having minimum carrier-to-noise ratios, some form of threshold extension is required. As the frequency of the incoming signals may vary by an amount considerably greater than the bandwidth required for the modulation, automatic frequency control must be used. For multichannel telephony, intermodulation distortion must be minimized.

The receiver shown in Figure 1 meets all of these requirements. Some of its performance characteristics are given in Table 1. The low noise temperature is achieved by use of a parametric amplifier located on the antenna as close as possible to the waveguide output of the sum channel from the 4-horn feed system. The threshold extension is provided by a phase-locked loop. To minimize intermodulation distortion in this type of circuit, it is necessary to stabilize the frequency at the input to the phase-locked loop so that a 90-degree phase angle can easily be maintained between the incoming signal and the phase-locked oscillator.

This is achieved by applying automatic frequency control to one of the local oscillators.

## 2. Input Waveguide Assembly

The input circuits of the receiver are shown in Figure 2 and consist of three waveguide runs that connect the monopulse microwave comparator outputs to the tracking and communication receiver inputs. The three tracking runs



Figure 1—Receiver for satellite ground station.

TABLE 1  
CHARACTERISTICS OF 4.2-GIGACYCLE-PER-SECOND RECEIVER

	6 Channels	12 Channels
Noise temperature in degrees Kelvin	420	420
Bandwidth in kilocycles per second	560	1300
Threshold signal level in decibels referred to 1 milliwatt	-107	-103
Threshold extension in decibels	3	4
Signal-to-noise ratio for highest-frequency channel in decibels	34.7	38

## Communication Receiver for Ground Station

are for the sum, azimuth-error, and elevation-error channels.

Each tracking channel terminates in a resistive diode mixer that converts the 4080-megacycle-per-second beacon to a 70-megacycle-per-second intermediate frequency. The mixers are crossed-guide units that provide good isolation between the signal and local-oscillator ports. This is important since all three tracking mixers use a common local oscillator. Any coupling between channels results in the generation of false tracking errors and therefore must be held to  $-50$  decibels relative to the sum-channel output.

The three mixers are connected to separate low-noise preamplifiers by short lengths of coaxial cable. Each preamplifier has a nominal gain of 48 decibels with an intermediate-frequency noise figure of 2 decibels. The total gain of the mixer-preamplifier combination from radio frequency to intermediate frequency is 42 decibels. The single-sideband noise figure ranges between 7 and 9 decibels. The preamplifiers at the antenna are connected to the angle-tracking receiver in the radio van via 200 feet of coaxial cable.

The tracking local oscillator is an all-solid-state device consisting of a nominally 50-megacycle-

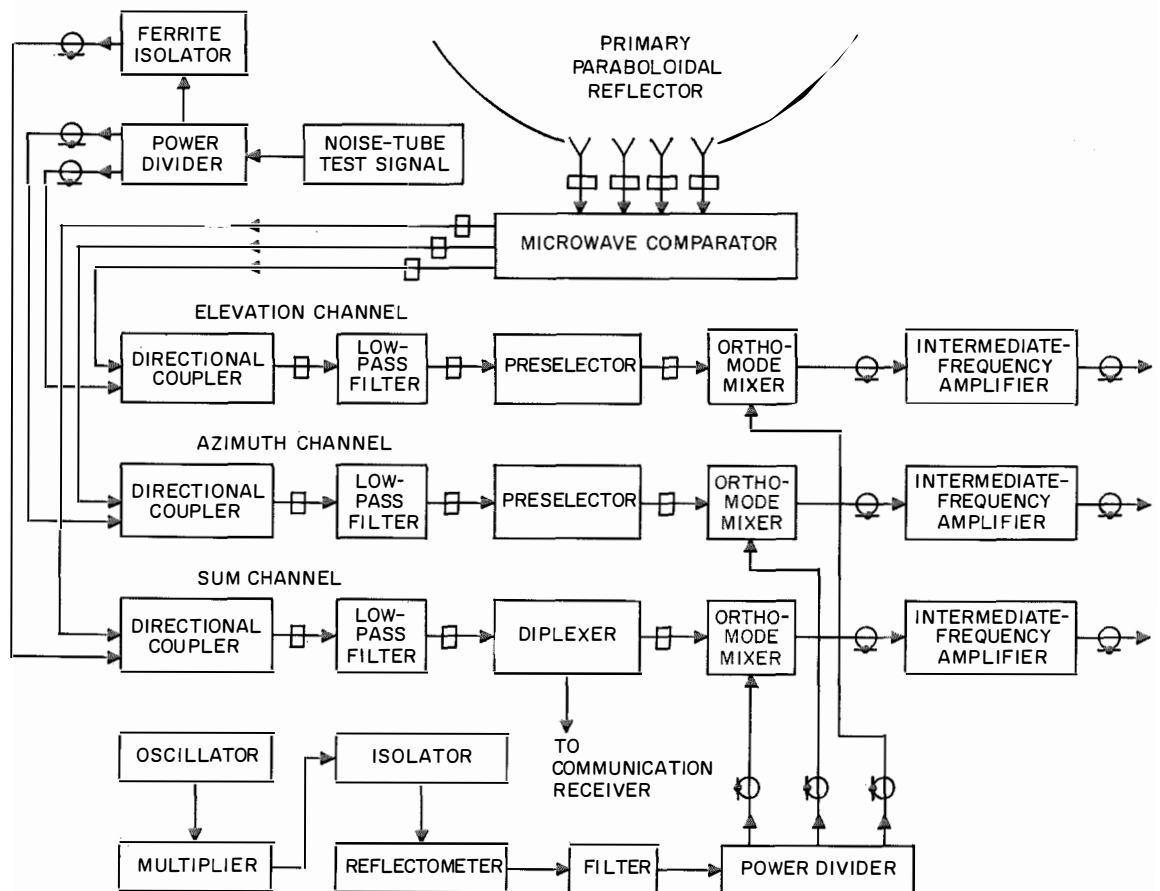


Figure 2—Input circuits include separate channels for elevation and azimuth tracking errors and their sum. The communication receiver is connected to the diplexer in the sum channel.

per-second crystal oscillator, power amplifier, and varactor-diode frequency multiplier. The oscillator long-term stability is 1 part per million. All spurious outputs are at least -60 decibels relative to the output, and peak deviation of the residual frequency modulation is less than 100 cycles per second. Both the residual frequency modulation and its rate are of importance in tracking-receiver applications since the tracking-signal demodulator uses a very-narrow-band synchronous detector. The residual frequency modulation of both the beacon and local oscillator appears as hum on the detected output signal.

Each of the three waveguide runs incorporates calibrated couplers for injecting test signals, a preselector for rejecting image noise and spurious signals, and a low-pass filter to reject the 6-gigacycle-per-second transmitter signal. The sum channel contains a diplexer that separates the tracking and communication signals. The diplexer is basically two band-pass filters connected by a *T* junction. The tracking signal is directed to the tracking front end through a band-pass filter identical to the preselector used in the azimuth- and elevation-error channels. The communication signals go to the parametric amplifier through a band-pass filter similar to the preselector. The band-pass filters are fixed-tuned three-section iris-coupled waveguide units. Losses in the waveguide assembly are held to a minimum since they degrade the receiving-system sensitivity. In addition to rejecting image noise and spurious signals, the filters must protect the sensitive receiver front end from the transmitter power, which is coupled in through the receiver feed-horn assembly. This power is of the order of 100 watts at a transmit power level of 10 kilowatts.

While the 2-gigacycle-per-second separation between transmit and receive frequencies eases the filtering problem, a transmit-frequency rejection of 75 decibels is still required to protect the parametric-amplifier diode. Most of this rejection is provided by a low-pass filter, since the iris-coupled band-pass filter tends to propa-

gate the transmit signal with little loss as a spurious mode.

### 3. Parametric Amplifier, Second Stage, and Local Oscillator

A varactor-diode parametric amplifier and a conventional diode mixer-preamplifier assembly make up the communication-receiver first and second stages, respectively. The parametric amplifier operates in the nondegenerate mode with a single idler below the pump frequency. A four-port circulator is used to isolate the varactor from both the second stage and the input. This unit has single-knob tuning and a remotely controlled motor-driven pump-power attenuator.

The parametric amplifier has a 1-decibel-down bandwidth of 15 megacycles centered at 4170 megacycles per second. Two independent carriers separated by 10 megacycles per second, each modulated with 12-channel frequency-division-multiplex information, are amplified by one parametric amplifier. The intermodulation distortion and crosstalk that results from amplifying both signals in one unit is immeasurably low.

The noise figure of the parametric amplifiers is 2.7 to 2.9 decibels. The second-stage mixer-preamplifier is connected to the parametric amplifier by a short length of *RG-9* coaxial cable. The mixer-preamplifier combined noise figure is 7.5 to 8.5 decibels. The over-all noise figure of the parametric amplifier and the second stage is 3.0 to 3.2 decibels. The received signals at 4175 and 4165 megacycles per second are converted to 70- and 60-megacycle-per-second intermediate frequencies and amplified in a common wide-band preamplifier. The preamplifier output is connected to the communication demodulator via 200 feet of *RG-9* coaxial cable.

The local oscillator is an all-solid-state unit consisting of a crystal oscillator and a varactor-diode frequency-multiplier chain. Lumped-

## Communication Receiver for Ground Station

parameter circuits give way to distributed-parameter circuits above 600 megacycles per second. The frequency stability of the local oscillator is better than 1 part per million. Spurious outputs are at least 40 decibels below

the desired output. The maximum power is 25 milliwatts into a matched load.

In addition to the receiver components already mentioned, there are two power supplies in the antenna pod. One supplies the communication preamplifier, and the other is for the pump klystron of the parametric amplifier.

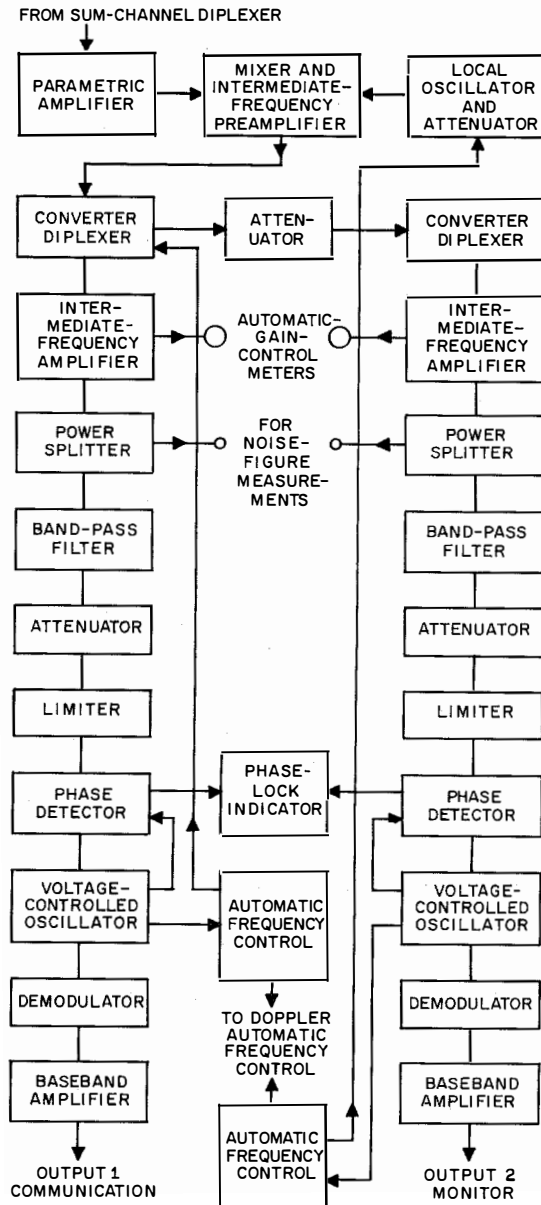


Figure 3—Communication and monitor channels.

### 4. Front-End Monitor and Control

A monitor and control panel is provided to tune the communication-channel parametric amplifier from the radio van.

The parametric-amplifier gain is measured by the noise density at the input to the intermediate-frequency demodulator. The response of the parametric amplifier is indicated by the relative noise densities at the two received-signal frequencies. While this indication is no guarantee that the parametric response is flat over the required 10 megacycles per second, it does indicate the response at the frequencies being used. Experience with parametric amplifiers of this type has shown that a dip in response of not more than 1 decibel occurs between any two points of equal gain.

The monitor and control panel provides metering facilities to indicate reflected and incident pump power, absolute pump power, and pump klystron reflector voltage. The power to the associated mixer-preamplifier and the currents to the mixer crystals are also metered at this location.

Another function of the monitor and control panel is to display the phase-lock status of each threshold-extension circuit. The receiver operate-standby switches as well as the main circuit breaker for the entire communication-receiver rack are located on the monitor and control panel.

### 5. Communication Demodulator

The two signals that are amplified and converted in the front end are separated and de-

modulated in the radio van. The 70- and 60-megacycle-per-second signals are separated in the converter-diplexer module and the 60-megacycle-per-second signal is converted to 70 megacycles per second so that two identical intermediate-frequency amplifiers and demodulators may be used. The drawer tuned to the locally transmitted signal that is returned by the satellite contains the monitor channel and the drawer tuned to another ground-station signal being received via the satellite contains the communication channel. A diagram of the communication and monitor systems from the diplexer in the tracking unit to the baseband outputs is shown in Figure 3. An intermediate-frequency amplifier and demodulator drawer is shown in Figure 4.

A 70-megacycle-per-second amplifier follows the converter module. This amplifier has 6 broad-band stages with fixed-tuned interstage coupling. A log-linear automatic gain control is used to indicate signal strength. Since the automatic-gain-control detector is not a coherent detector, it does not require a phase-lock circuit to interpret the received signal level. The intermediate-frequency amplifier gain is 60 decibels maximum with a 3-decibel-down bandwidth of 15 megacycles per second and 30 decibels of automatic gain control. A switch is provided to select automatic or manual gain control.

A two-pole filter follows the intermediate-frequency amplifier. This filter has a Butterworth response and a 2-megacycle-per-second noise bandwidth. The intermediate-frequency bandwidth is thereby reduced to improve the signal-to-noise ratio before limiting.

A 70-megacycle-per-second limiter follows the two-pole filter. The signal level is adjusted by the attenuator so that the limiter is normally operated just below the threshold of limiting. Noise peaks estimated to be 12 decibels greater than the root-mean-square signal level are limited and cannot reach the threshold-extension circuit.

The threshold-extension circuit consists of two

modules. One module is a voltage-controlled oscillator and the other module contains two phase detectors, the loop filter, and a buffer amplifier. The voltage-controlled oscillator has two outputs, one to the demodulator and the other to the phase detector. The phase-detector output is connected to the input of the voltage-controlled oscillator. The signal output of the limiter is connected to the second input of the phase detector. The frequency of the voltage-controlled oscillator is a linear function of the bias voltage applied to a diode. The diode is in the collector circuit of a 2-stage transistor oscillator. Changing the bias on the diode varies the phase shift in the oscillator. The oscillator frequency changes to maintain the feedback in the proper phase. Several limiter stages follow the oscillator to ensure that the output amplitude does not vary as the oscillator frequency changes. The limiters also serve to isolate the oscillator from the load.

The phase detector contains two product detectors, one of which supplies a signal to the voltage-controlled oscillator to produce phase lock between it and the input to the phase detector. The other product detector operates

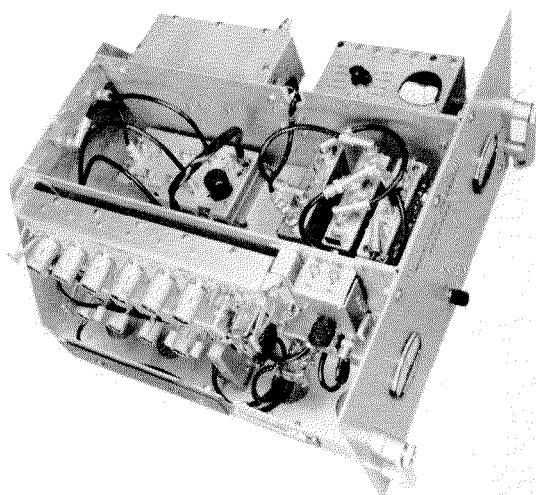


Figure 4—Intermediate-frequency amplifier and demodulator drawer.

in quadrature to produce a phase-lock indication. The voltage-controlled-oscillator signal is shifted by 90 degrees before going to the second product detector. The phase-locked product detector drives the loop filter, which is isolated from the output by a buffer amplifier. The loop filter is a conventional lag network. There are two loop filters in the phase-detector module. Either filter may be selected by means of a switch located on the module.

The demodulator has 4 wide-band limiter stages followed by a Foster-Seely discriminator. A cathode-follower isolates the discriminator from the load. The limiter consists of 4 amplifier stages using 5847 vacuum tubes with a back-to-back diode limiter between adjacent stages. The amplifier stages have screen and cathode degeneration to ensure uniform characteristics over the useful life of the tube. The interstage coupling networks have printed-circuit mutual-inductance coupling coils for stability and uniformity. The discriminator is also of printed-circuit construction.

The baseband amplifier is a 4-stage solid-state circuit with a response within  $\pm 0.5$  decibel

from 30 to 300 000 cycles per second. The gain is adjustable from 0 to 40 decibels.

Each amplifier stage consists of a complementary pair of transistors in a circuit that provides negative local voltage feedback for high input impedance. The combination of low output impedance and high input impedance results in a flat response over a wide band. This amplifier has several built-in de-emphasis characteristics, which may be selected by a switch.

The communication receiver uses the following direct-current power supplies.

- +150 volts at 600 milliamperes
- +24 volts at 200 milliamperes
- +15 volts at 200 milliamperes
- 15 volts at 200 milliamperes
- +6 volts at 400 milliamperes
- 6 volts at 400 milliamperes

The +150-volt plate supply is a commercial unit, using a vacuum-tube series voltage regulator. All of the low-voltage supplies are transistor-regulated units. Each supply has automatic overload protection.

### 6. Phase-Locked Loop

A phase-locked-loop type of threshold-extension circuit is used to improve the predetection carrier-to-noise ratio of the received signal. A second-order loop with minimal circuitry provides uniform performance with little adjustment and maintenance.

Basically the phase-locked loop operates as follows. In Figure 5, the frequencies of the incoming signal and the voltage-controlled oscillator are compared in the phase detector. When both frequencies are equal, the phase-detector output contains a double-frequency term and a direct-current term, the latter being proportional to the cosine of the phase angle between the two inputs. This direct-current term in the output of the phase detector changes the phase of the voltage-controlled oscillator in a direction that tends to reduce the phase-detector output to zero. Suppose the signal is frequency modu-

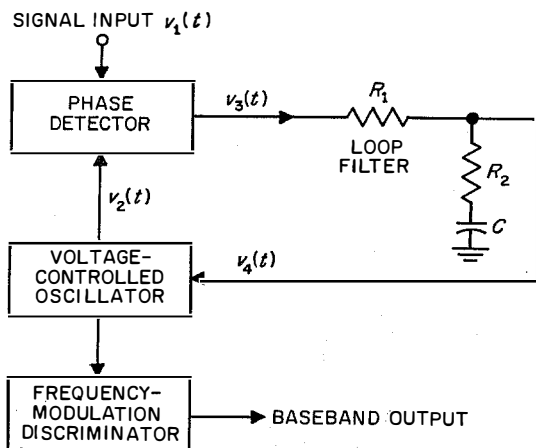


Figure 5—Threshold extension by means of a phase-locked loop.  $v_1(t) = A \sin(\omega t + \theta)$  and  $v_2(t) = B \sin(\omega t + \phi)$ . The phase-detector direct-current output  $= (-AB/2) \cos(\theta - \phi)$ . The filter time constants are  $T_1 = (R_1 + R_2)C$  and  $T_2 = R_2C$ .

lated. The output of the phase detector, which represents the loop phase error, will vary at a rate equal to the modulating frequency. The amplitude of the phase-detector output will be proportional to the frequency deviation of the frequency-modulated signal. The phase-locked loop thus demodulates a phase- or frequency-modulated signal. The addition of a low-pass filter between the phase detector and the voltage-controlled oscillator restricts the band of frequencies that the oscillator will follow. If this filter is made wide enough to pass the highest modulating frequency (without introducing appreciable amplitude or phase distortion) but narrower than the root-mean-square deviation, then the voltage-controlled oscillator will track a narrower band of noise than a conventional frequency-modulation detector. Under these conditions it is possible to obtain an extension of the detection threshold relative to a conventional frequency-modulation detector.

Figure 6 illustrates the threshold characteristics of a frequency-modulation system. This curve shows the relationship between the carrier-to-noise ratio at the input to the demodulator and the signal-to-noise ratio at the output of the demodulator. Above threshold, the curves are straight lines of unity slope. The threshold is defined as the carrier-to-noise ratio at which the slope of the curve deviates from unity [1]. As the deviation ratio  $m$  increases, the output signal-to-noise ratio increases and the threshold occurs at higher carrier powers.

The linear portion of the characteristic may be extended to a lower threshold through the use of a phase-locked loop as shown by the dashed addition to  $m = 8$ . The threshold of the phase-locked loop is also defined as the carrier-to-noise ratio at which the slope of the characteristic departs from unity. The amount of threshold extension is the difference between the two thresholds.

The bandwidth used in computing the carrier-to-noise ratio should be related to the signal being demodulated; otherwise the amount of

threshold extension is arbitrary. Bandwidth values commonly used for this purpose are (A) the minimum radio-frequency bandwidth required to pass the maximum deviation plus all of the significant sidebands; (B) twice the highest frequency in the baseband; and (C) the highest frequency present in the baseband. The threshold carrier-to-noise ratio of any frequency-modulation detector occurs when the envelope of the noise exceeds the signal for a long enough time to cause loss of information. The threshold carrier-to-noise ratio varies with the modulation, but is of the order of 10 to 12 decibels for sinusoidal modulation [2].

Threshold extension is theoretically possible only if the deviation ratio is greater than unity. It is practical with the phase-locked loop only if the deviation index is 3 or greater. A phase-locked loop designed to demodulate a signal with a Gaussian spectrum should have a closed-loop 3-decibel-down bandwidth of  $\frac{1}{4}$  the desired radio-frequency noise bandwidth [3]. This large factor is assumed for the simple lag filter shown in Figure 5 to keep the distortion generated by the loop at a low level.

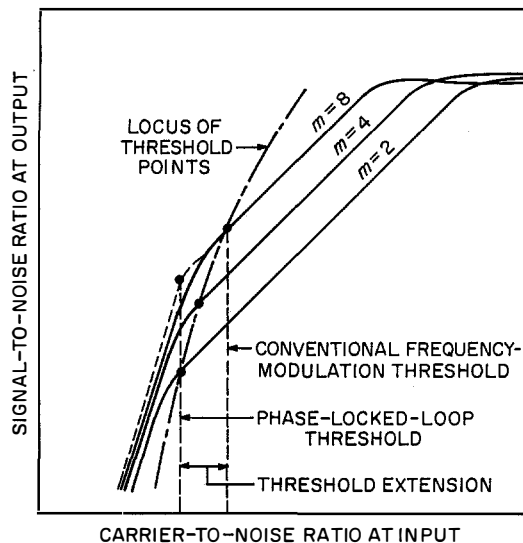


Figure 6—Threshold characteristics of frequency-modulation systems for three deviation ratios  $m$ .

## Communication Receiver for Ground Station

The following values of threshold extension are obtainable with the given values of deviation ratio.

Deviation Ratio	Threshold Extension in Decibels
3	0
4	1
8	3
16	5.5
24	7

The above values assume sinusoidal modulation and a conventional frequency-modulation demodulator threshold carrier-to-noise ratio of 10 decibels.

Ideally the noise bandwidth of the phase-locked loop is just twice the highest modulating frequency. The amount of threshold extension possible is then  $10 \log B_{rf}/2f_m$  where  $B_{rf}$  is the radio-frequency bandwidth required to pass the carrier and all significant sidebands, and  $f_m$  is the highest modulating frequency present in the baseband. In practice, any noise bandwidth may be achieved with the phase-locked loop, but when this bandwidth is made less than about  $4.2f_m$ , the total distortion generated by the loop nonlinearities and thermal noise begins to rise rapidly. The total distortion of the phase-locked loop increases with decreasing carrier-to-noise ratio as it does with the conventional frequency-modulation discriminator, but the

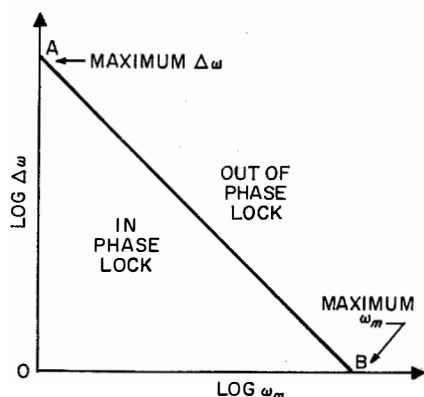


Figure 7—Closed-loop response of a phase-locked loop.

mechanism is different. Figure 7, the closed-loop response of the phase-locked loop, illustrates this.

This is not the usual response in which the loop gain is plotted on the vertical axis. Instead, the deviation, which is directly proportional to the gain, is plotted. For simplicity, we will assume that the transfer function of the loop filter is unity. The straight line  $AB$  is the locus of the values of  $\Delta\omega$ , the angular-deviation frequency, and  $\omega_m$ , the angular rate of deviation or modulated frequency, for which the closed-loop phase error is at its maximum value of  $\pi/2$  radians. The loop will be locked at any point within the area  $OAB$  and will be out of lock outside this area. The line  $AB$  represents the maximum rate of change of frequency that the loop will tolerate.

If two or more signals are applied to the loop, the sum of the  $(\Delta\omega \omega_m)$  products must not exceed the maximum value. The loop response to a given signal is then seen to be dependent on other signals entering the loop. Thus the law of superposition may not be applied to the loop, since it implies that the total response is the sum of the responses to individual driving functions.

The phase-locked oscillator is normally operated at a value of the  $(\Delta\omega \omega_m)$  product that produces a loop error much less than  $\pi/2$  radians. The reason for this is that the phase detector is linear only for small phase errors. At low carrier-to-noise ratios, the sum of the  $(\Delta\omega \omega_m)$  noise products causes the loop phase error to increase, thus increasing the non-linearity of the phase detector. It should be noted that while the distortion so generated has a Gaussian spectral distribution [4], it is generated by the same mechanism that produces intermodulation distortion in a passive linear filter. Another result of  $\sum \Delta\omega_n \omega_{mn} \leq K$  is that a static frequency error caused by doppler or frequency drift in an oscillator can, if not corrected, generate enough distortion to cancel all the threshold-extension advantage.

## 7. Acknowledgments

The authors wish to acknowledge the technical contributions of Mr. L. F. Gray, Mr. Ed Imboldi, and Mr. L. Jankovich, and are indebted to Mr. D. Hershberg and Mr. M. Sparrow for their assistance in making measurements.

## 8. References

1. Article 4.6.1 on page 71 of reference 2.
2. E. F. Florman and J. J. Tary, United States National Bureau of Standards Note 100; 1962.
3. R. C. Booton, Jr., and J. A. Develet, Jr., "Coherent FDM/FM Telephone Communication," Space Technology Laboratories Report 8614-6004-NU-000; January 1962: page 18.
4. D. Middleton, "An Introduction to Statistical Communication Theory," McGraw-Hill Book Company, New York; 1960: page 624.

**M. L. Sassler** was born in Cleveland, Ohio, on 6 August 1932. In 1955, he received a B.S. degree in electrical engineering from Case Institute of Technology.

In 1955, he joined ITT Federal Laboratories and developed a narrow-band receiver to measure path loss of forward-scatter links. He is presently responsible for the design of ultra-high-frequency receivers.

**Rouben Surenian** was born in Kermanshah, Iran, on 11 August 1936. He received in electrical engineering a B.S. degree from Northeastern University in 1960 and an M.S. degree from Polytechnic Institute of Brooklyn in 1962.

Mr. Surenian joined ITT Federal Laboratories in 1961 and is presently engaged in the development and manufacture of communication and tracking receivers.

# Satellite-Tracking Receiver

W. JANEFF

ITT Federal Laboratories, A Division of International Telephone and Telegraph Corporation; Nutley, New Jersey

## 1. Introduction

The instantaneous position of a moving target is uniquely determined by the coordinates of its projection on two planes perpendicular to each other. A tracking system, therefore, consists of an arrangement capable of sensing the coordinates of the projections of the target in both planes, plus a positioning mechanism that, directed by the signal supplied by the sensors, follows the target's projections.

In a monopulse amplitude-sensing system, the sensing function is performed by two pairs of horns, each pair defining one plane. Each horn pair senses the coordinates of one target projection while being, ideally, insensitive to the coordinates of the target projection on the other plane. Targets located along the boresight axis of the antenna (determined by the line of intersection of the two planes) reflect equal amounts of energy into one pair of horns. The difference signal for this target location is ideally zero. A target located off boresight, on the other hand, reflects unequal amounts of radio-frequency energy into the two horns of a given pair. The difference signal now yields a quantity, the magnitude and phase of which define the target location in the respective plane.

It is the purpose of the tracking receiver to process the microwave signals supplied by the radio-frequency comparator, that is, to amplify them, and to convert them into a form acceptable to the following servo amplifier. Magnitude and polarity of the supplied signals are an exact analog of the angle between target position and antenna boresight axis. The van-mounted part of the receiver consists, therefore, of essentially two difference or error channels that process the target positioning signals for the horizontal (azimuth) and vertical (elevation) planes, plus a reference or sum channel.

The front end of the receiver is mounted at the vertex of the paraboloidal reflector and its purpose is to convert the three signals supplied by the radio-frequency comparator from 4080 to 70 megacycles per second.

## 2. Tracking Receiver

The block diagram of the tracking receiver is shown in Figure 1. The sum channel supplies three signals to the difference channels: a 60.2-megacycle-per-second signal derived from the voltage-controlled oscillator, which is part of the phase-locked loop; a 9.8-megacycle-per-

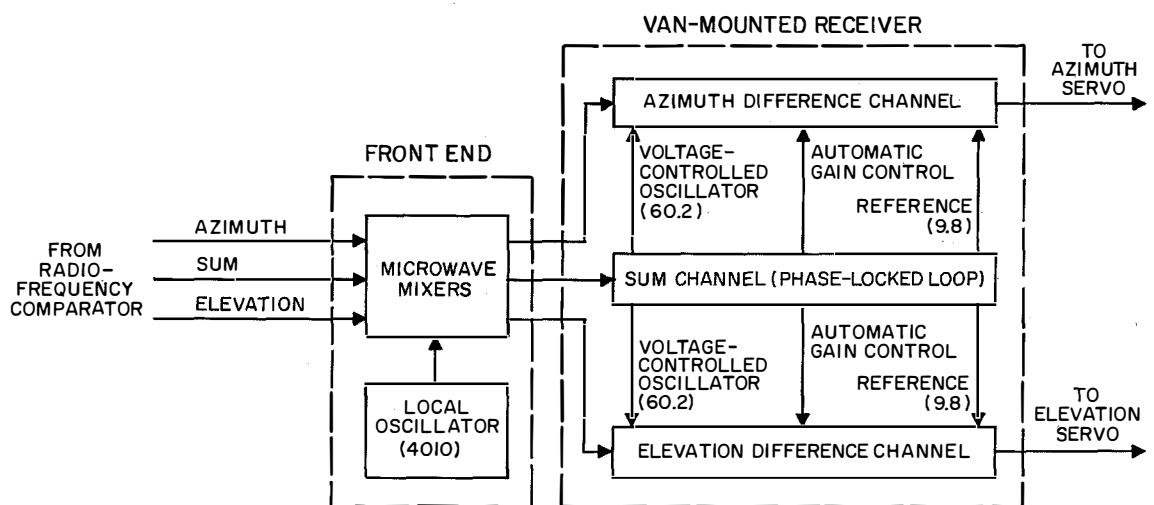


Figure 1—Tracking receiver block diagram. The frequencies shown in parentheses are in megacycles per second.

second locally generated reference signal; and an automatic-gain-control signal.

2.1 SUM CHANNEL

The sum channel consists of a phase-locked loop, the purpose of which is threefold.

(A) It provides a means for tracking the input signal, the frequency of which is subject to variations because of doppler shift, limited frequency stability of the satellite beacon transmitter, and frequency shifts of the receiver front-end local oscillator.

(B) It provides a means to identify and extract the signal from the noise environment.

(C) It provides automatic gain control for the sum and difference channels.

The block diagram of the phase-locked loop is shown in Figure 2. Its performance is based on:

(A) A conventional phase detector, the output signal of which is proportional to the sine of the phase difference between the applied signals.

(B) A passive proportional-plus-integral 2-time-constant network  $F(s)$ .

Furthermore, the loop contains the intermediate-frequency amplifier followed by a crystal narrow-band-pass filter centered at the intermediate frequency. No limiter is used; instead, a slow-acting automatic-gain-control signal derived from and controlled by the phase-locked loop is applied to both the sum and difference channels. Frequency search and acquisition are obtained by applying a sinusoidal signal to the voltage-controlled oscillator under closed-loop conditions and removing this signal as soon as phase lock is obtained.

This arrangement offers several advantages when compared with the simple loop where phase comparison is performed at the signal frequency.

(A) When phase locked, the loop maintains a constant 9.8-megacycle-per-second frequency

despite the frequency variations of the input signal. The choice of a low intermediate frequency allows the insertion of a fixed-tuned narrow-band-pass filter after the amplifier that limits the noise presented to the phase detector. The latter is operated far enough from the point where saturation effects would cause degradation in performance. The operating limits are set by the requirement that the predetection filter  $F$  should not introduce any appreciable time delays, that is, that the filter bandwidth should be at least one order of magnitude larger than the loop bandwidth.

(B) The chosen loop arrangement calls for the use of a local oscillator that supplies the reference signal to the sum- and difference-channel phase detectors. This reference signal, locally generated, can be made large enough (compared to the root-mean-square value of the predetection noise) to permit the phase

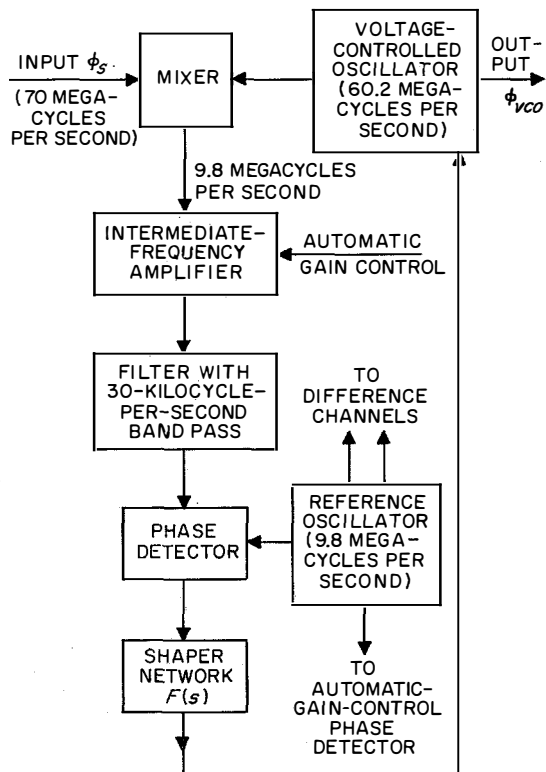


Figure 2—Block diagram of the phase-locked loop.

detector to be operated most advantageously, that is, linearly, without threshold, and with no degradation in the output signal-to-noise ratio. The signal-to-noise advantage is important and applies not only to the phase-locked loop, but also to the coherent detectors in the error channels and in the automatic-gain-control loop.

(C) Low predetection noise is of prime importance during the frequency-search operation; high noise-to-signal ratios significantly degrade the acquisition capability of the phase-locked loop.

A heterodyning process is performed within the loop and, as a consequence, input and output frequencies differ by the intermediate frequency of 9.8 megacycles per second. The phase comparison is performed at this frequency and the generated error is a sine function of the instantaneous phase difference between the two waveforms. If the fundamental frequencies of these waveforms are within the lock-on range of the loop, the generated error voltage is of constant magnitude or zero and the loop is in lock. If the frequency of the input waveform differs significantly from that of the voltage-controlled oscillator, the alternating error voltage frequency-modulates the voltage-controlled oscillator, but cannot drive its frequency close enough to the input signal to achieve phase lock and the loop is unlocked, or unstable.

The signal generated by the phase detector is amplified and applied to a shaper network  $F(s)$ . The output of the shaper network at a time  $t$  is the weighted average of the input signal from time  $t$  to approximately one time constant earlier.

The phase detector, the shaper, and the voltage-controlled oscillator compose the path along which the error is generated, amplified, and shaped to be ultimately impressed on the voltage-controlled oscillator. Their properties and limitations determine the loop performance most significantly, and can be summarized briefly as follows.

The phase detector is a nonlinear device; its output voltage is a sine function of the instantaneous phase difference between the two input signals. Hence, its alternating-current gain is not constant but is a function of the operating point defined by the steady-state phase error. It decreases with increasing phase error, thus reducing the ability of the loop to follow external signals (static-loop-gain limitation).

These remarks apply also to the voltage-controlled oscillator, the nonlinear characteristic of which is a second static-loop-gain limitation.

The shaper, a passive proportional-plus-integral network, has a direct-current transfer function equal to unity; hence, it does not affect the steady-state performance of the loop. Its limitation is of a dynamic nature. The choice of its corner frequencies affects the bandwidth and transient response as well as the stability of the loop.

## 2.2 LINEARIZED LOOP TRANSFER FUNCTION

If the open-loop gain is described by  $G(s)$ , the transfer function  $Y(s)$  relating output phase  $\phi_{vco}$  to input phase  $\phi_s$  is given, in operational notation, by

$$Y(s) = \frac{\phi_{vco}(s)}{\phi_s(s)} = \frac{G(s)}{1 + G(s)} \quad (1)$$

and the error function relating phase error  $E(s)$  to input phase

$$\frac{E(s)}{\phi_s(s)} = \frac{1}{1 + G(s)} = 1 - Y(s). \quad (2)$$

We denote the low-pass-filter transfer function by  $F(s)$ ; the transfer function of the voltage-controlled oscillator by  $K_{vco}/s$ ; the gain of the direct-current amplifier by  $K_d$ ; we replace the nonlinear transfer function of the phase detector  $K_{pd} \sin(\phi_s - \phi_{vco})$  by its linear equivalent  $K_{pd}(\phi_s - \phi_{vco})$ ; then

$$G(s) = K \frac{F(s)}{s} \quad (3)$$

where  $K = K_{vco} \cdot K_d \cdot K_{pd}$ , and accordingly

$$Y(s) = \frac{KF(s)}{s + KF(s)} \quad (4)$$

and

$$\frac{E(s)}{\phi_s(s)} = \frac{s}{s + KF(s)} \quad (5)$$

The error introduced by the linearization of the phase detector is less than or equal to 7 percent for phase angles up to 45 degrees.

Several important considerations determine the selection of  $F(s)$ .

- (A) Input-signal dynamics.
- (B) Signal-to-noise conditions for in-lock operation.
- (C) Predetection signal-to-noise conditions and sweep rate during the frequency-search mode of operation.

The dynamics of the received signal can be described by the maximum rate of frequency variation, which for medium-altitude satellites does not exceed 300 cycles per second per second, and by the maximum doppler shift, which does not exceed  $\pm 100$  kilocycles per second. The noise environment is such that a predetection signal-to-noise ratio of  $-4$  to  $-6$  decibels is obtained during frequency search, the noise being essentially system noise. After phase lock is achieved, an output signal-to-noise ratio of at least  $+10$  decibels is required which will keep the loop in lock and introduce an insignificant amount of noise into the error channels.

The last consideration arises from the minimum speed of frequency search compatible with the frequency range to be covered and the time during which the satellite dwells within the 3-decibel width of the antenna beam.

$F(s) = 1$  describes a first-order loop. Analysis of (4) reveals that in such a case the phase-transfer function of the loop is identical to the voltage-transfer function of a low-pass filter

with a cutoff frequency equal to  $K$ . Loop gain and loop bandwidth are interdependent, and a narrow loop bandwidth can only be achieved at the expense of low loop gain.

The solution appears to be a second-order system that comprises an integrator network. A simple resistance-capacitance network with a transfer function  $F(s) = (1 + s \cdot \tau)^{-1}$  will allow the loop bandwidth to be reduced to any desired degree without affecting the loop direct-current gain. Such a system, however, would be potentially unstable. Its plot of open-loop gain versus frequency would show a slope of 40 decibels per decade at the crossover point, with no means of controlling it. There appear to be two ways to circumvent this difficulty in a second-order system.

(A) Use a resistance-capacitance network having 2 time constants. Such a network (imperfect integrator) would have the transfer function

$$F_1(s) = \frac{\omega_1 + s}{\omega_2 + s} \quad (6)$$

(B) Use a perfect integrator with transfer function

$$F_2(s) = 1 + (a/s) \quad (7)$$

The effect of these three networks on the open-loop gain is shown in Figure 3. In the last two cases, the slope of the gain curve at the unity-gain level is 20 decibels per decade. In the  $F_1(s)$  case, this is achieved by judicious selection of the second corner frequency  $\omega_2$ ; the gain for  $\omega < \omega_2$  and  $\omega > \omega_1$  is 20 decibels per decade. In the  $F_2(s)$  case, the slope at very-low frequencies is 40 decibels per decade and the only breakpoint at  $\omega = a$  is selected so as to ensure 20 decibels per decade at unity-gain level, with the necessary phase margin.

In servo-system terminology, the first two systems, showing a 20-decibel-per-decade slope at the lowest frequencies, must be identified as type-1 servos characterized with one pole at the origin; only the last system would be

## Satellite-Tracking Receiver

identified as a type-2 servo, showing a 40-decibel-per-decade slope at lowest frequencies with two poles at the origin.

It can be predicted from servo analysis that type-1 and type-2 servos will follow a phase step with no steady-state error. Phase ramps, resulting from steps in radial target velocity, will be followed with zero (type-2 servo) or small (type-1 servo) steady-state phase errors. Sustained radial-velocity ramps (steps in radial acceleration) however, will result in finite phase errors in a type-2 system; they will not be followed by a type-1 system over long periods of time.

It is understood that variations in the tangential component of the target velocity will not affect the input signal.

The following discussion is confined to the error response of the linear loop that contains a perfect integrator. The effect of noise on loop performance is reviewed and a brief summary of experimental results is given.

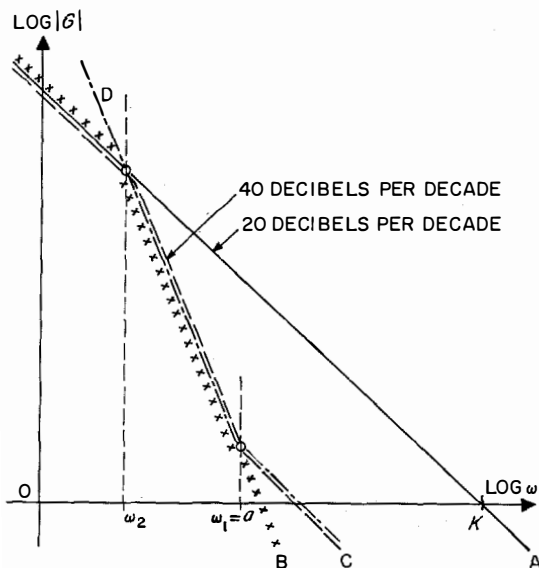


Figure 3—Effect of integrator networks on loop bandwidth and stability. Curve A is for a first-order loop; B, a 1-time-constant passive network; C, a 2-time-constant passive network; and D, a perfect integrator.

### 2.3 LOOP ERRORS

The output of the phase detector is a voltage analog of the loop phase error. It arises essentially from two sources.

(A) The limited ability of the loop to follow the frequency variations of the input signal. A given input time function can give rise to transient or steady-state phase errors, depending on the loop characteristics.

(B) The noise environment from which the signal must be extracted. The resulting errors may cause the loop to lose lock or they may be transferred to the difference channels and give rise to tracking errors.

In a linearized system, these two errors can be evaluated separately. If signal and noise at the loop input are uncorrelated, the resulting mean-square error is the sum of the mean-square errors of these two error components. The phase errors resulting from various input signals can be summarized briefly as follows.

#### 2.3.1 Phase Step Input $\Delta\phi$

From (5), the error  $E(s)$  is given by

$$E(s) = \frac{\Delta\phi \cdot s}{s^2 + Ks + Ka} \quad (8)$$

The final-value theorem, applied to  $E(s)$

$$\lim_{s \rightarrow 0} s \cdot E(s) = 0$$

results in a zero steady-state error. The transient error is given by the inverse Laplace transform of (8)

$$E(t) = \mathcal{L}^{-1}\{E(s)\} = \frac{\Delta\phi}{(1 - \xi^2)^{1/2}} e^{-\xi\omega_0 t} \cdot \sin[(1 - \xi^2)^{1/2}\omega_0 t + \tau], \quad (9)$$

$$\text{with } \tau = \text{tg}^{-1} \frac{(1 - \xi^2)^{1/2}}{\xi}$$

where the response is oscillatory ( $\xi < 1$ ).

2.3.2 Frequency Step  $\Delta F$

$$E(s) = \frac{\Delta F}{s^2 + Ks + Ka} \quad (10)$$

The final-value theorem again yields zero steady-state error and a transient-error time function

$$E(t) = \frac{\Delta F}{\omega_o(1 - \xi^2)^{1/2}} e^{-\omega_o \xi t} \cdot \sin(1 - \xi^2)^{1/2} \omega_o t. \quad (11)$$

$E(t)$  decays to zero in a manner similar to the phase-step case.

2.3.3 Frequency Ramp  $D$

$$E(s) = \frac{D}{s(s^2 + Ks + Ka)} \quad (12)$$

The final-value theorem yields a finite steady-state error equal to  $D/\omega_o^2$  and the transient error is given by the inverse transform of  $E(s)$

$$E(t) = \frac{D}{\omega_o^2} \left\{ 1 - e^{-\omega_o \xi t} \times \left[ \frac{\xi}{(1 - \xi^2)^{1/2}} \sin(1 - \xi^2)^{1/2} \omega_o t + \cos(1 - \xi^2)^{1/2} \omega_o t \right] \right\}. \quad (13)$$

It can be seen that the loop will not follow a higher-order input function. Equation (13) reveals that a frequency parabola will result in an infinite steady-state error, that is, the loop will not be able to maintain phase lock.

It is instructive at this point to review briefly the error behavior of a loop comprised of a passive integrator network instead of a perfect integrator. The passive integrator has a transfer function as given by (6) and an error function given by

$$E(s) = \frac{s^2 + s\omega_2}{s^2 + s(\omega_2 + K) + K\omega_1} \phi_s(s). \quad (14)$$

It can be seen that this expression will yield a zero steady-state error only for a phase step;

a frequency step will result in a finite error

$$s \cdot E(s) \frac{\Delta F}{s^2} = \frac{\Delta F \cdot \omega_2}{K \cdot \omega_1}, \quad (15)$$

$s \rightarrow 0$

and the transient error is given by

$$E(t) = \frac{\Delta F \omega_2}{K \omega_1} \left\{ 1 - e^{-[(\omega_2 + K)/2]t} \times \left\{ \frac{\omega_2 + K}{2} - \frac{\omega_1 K}{\omega_2} \right. \right. \\ \times \left. \left. \left[ \frac{(K + \omega_2)^2}{4} - K\omega_1 \right]^{1/2} \right. \right. \\ \times \left. \left. sh \left[ \frac{(K - \omega_2)^2}{4} - K\omega_1 \right]^{1/2} \cdot t \right. \right. \\ \left. \left. + \left. ch \left[ \frac{(K + \omega_2)^2}{4} - K\omega_1 \right]^{1/2} \cdot t \right. \right. \right\}. \quad (16)$$

In addition to the advantage of zero steady-state error to frequency step inputs, the non-linear analysis by means of phase plane trajectories has shown [1] that the perfect integrator has a very-large (theoretically infinite) pull-in range. The theoretical pull-in range of a loop with imperfect integrator has been shown [2] to be limited to

$$\Delta\omega = (2\xi\omega_o K)^{1/2} \quad (17)$$

which for high-gain narrow-bandwidth loops (for instance,  $\omega_o = 2\pi \cdot 300$  rad/sec,  $\xi = 0.5$ ,  $K = 3 \cdot 10^6$  1/sec) is approximately 12 kilocycles per second.

2.4 NOISE

The effect of noise on the loop performance can be analyzed by assuming that the incoming signal is amplitude and phase modulated by band-limited random noise. Then, using the loop transfer function, the effect of noise can be found at various points of the loop. The points of interest are generally the voltage-controlled-oscillator output (output noise) and the phase-detector output (phase error due to noise).

One significant simplification is generally invoked. The noise amplitude is assumed to be small compared with the signal amplitude. That is, the signal-to-noise ratio is large, so that the amplitude modulation can be neglected, and the signal is assumed to be only phase modulated by noise. The input signal plus noise can be written

$$V = (V_s + X) \cos(\omega_s t + \phi_s) + Y \sin(\omega_s t + \phi_s). \quad (18)$$

Here, the noise is represented by an in-phase component  $X$  and a quadrature component  $Y$ , which are time functions independent of each other. Their instantaneous values are defined by the Gaussian distribution law. Equation (18) describes a signal with center frequency  $\omega_s$  that is amplitude and phase modulated by the random-noise function.  $V_s$  is the signal amplitude and  $\phi_s$  is the signal phase, which may be a time function carrying information. The average noise power  $N$  and the signal-to-

noise ratio  $S/N$  can be written

$$N = \overline{X^2} = \overline{Y^2}$$

$$\frac{S}{N} = \frac{V_s^2}{2N} = \frac{V_s^2}{2\overline{X^2}} = \frac{V_s^2}{2\overline{Y^2}}. \quad (19)$$

It follows from (18) that for

$$X \ll V_s \gg Y \quad (20)$$

$$V = V_s \cos(\omega_s t + \phi_s + \phi_N) \quad (21)$$

where  $\phi_N \cong Y/V_s$ .

The mean-square value of the excursions is the phase jitter

$$\sigma_{\phi_N}^2 = \frac{\overline{Y^2}}{V_s^2} = \frac{N}{2S} \quad (22)$$

where  $S$  is the mean-square signal power.

Although (20) appears too restrictive and apparently precludes the use of (22) in cases where  $S/N \ll 1$ , experimental evidence [3] seems to suggest that (22) will predict with good accuracy the output mean-square phase jitter at input signal-to-noise ratios as low as  $-6$  to  $-8$  decibels.

Since phase jitter is directly proportional to noise power, one should expect that the loop noise bandwidth will be of prime importance in determining the phase jitter of the voltage-controlled oscillator. That this is so can be seen briefly from the following. In analogy to the noise power spectral density, an input phase-jitter density  $\phi_{pj}$  can be defined as the ratio of the mean-square phase jitter and the equivalent noise bandwidth of the loop input circuit  $(BW)_{in}$ .

$$\phi_{pj}(\omega) = \frac{\sigma_{\phi_N}^2}{(BW)_{in}} = \frac{N}{2S(BW)_{in}} = \frac{\phi_N(\omega)}{2S} \quad (23)$$

where

$$\phi_N(\omega) = \frac{N}{(BW)_{in}} \quad (24)$$

is the input noise power spectral density. Then, output phase-jitter spectral density  $\phi_o$  is obtained by using the loop transfer function

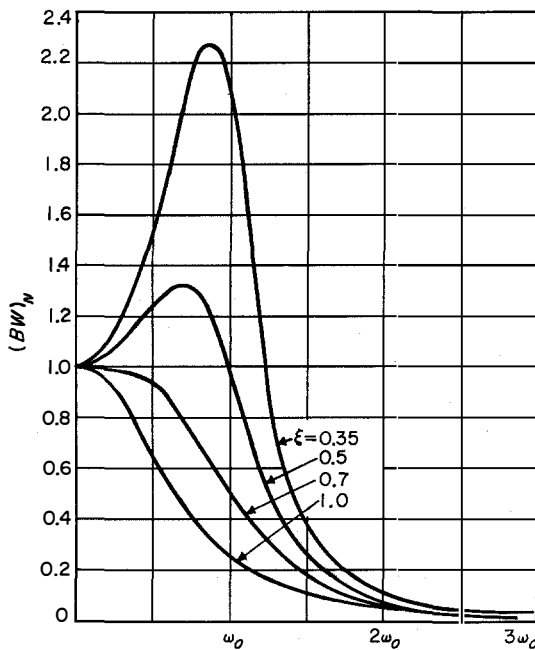


Figure 4—Low-frequency component of loop noise bandwidth (35).

$$\begin{aligned} \phi_o(\omega) &= |Y(j\omega)|^2 \phi_{pj}(\omega) \\ &= \frac{1}{2} |Y(j\omega)|^2 \frac{\phi_N(\omega)}{S} \end{aligned} \quad (25)$$

and the mean-square phase jitter of the voltage-controlled oscillator is found by evaluating the integral

$$\sigma_{vc\phi}^2 = \int_{-\infty}^{+\infty} \phi_o(\omega) d\omega. \quad (26)$$

Using (23) and (24), this can be written

$$\sigma_{vc\phi}^2 = \frac{1}{2} \frac{N}{S} \frac{1}{(BW)_{in}} \int_{-\infty}^{+\infty} |Y(j\omega)|^2 d\omega$$

or

$$\sigma_{vc\phi}^2 = \frac{1}{2} \frac{N}{S} \frac{(BW)_N}{(BW)_{in}} \quad (27)$$

where

$$(BW)_N = \int_{-\infty}^{+\infty} |Y(j\omega)|^2 d\omega \quad (28)$$

is the equivalent noise bandwidth of the loop.

Equation (27) defines the voltage-controlled-oscillator phase jitter under the assumptions made initially. The integral (28) is evaluated in Appendix A for the simplified case  $\xi = 0.7$ . The result obtained is

$$(BW)_N = 1.06 \pi \cdot \omega_o.$$

More-detailed investigations of the noise bandwidth have been undertaken by various authors [2, 4] analyzing a loop with a 2-constant resistance-capacitance network. The results obtained indicate that a minimum noise bandwidth of  $2\pi\omega_o$  can be obtained with a slightly oscillatory system ( $\xi = 0.5$ ). This minimum noise bandwidth is twice as high as the one obtained with a perfect integrator and grows only slowly with  $\xi$ . A  $\xi$  of 0.7 yields an increase of approximately 5 percent;  $\xi = 1$ , however, augments the noise bandwidth by 20 percent.

The trend toward narrow noise bandwidths encounters two important limitations.

(A) The necessity to perform a frequency search at a reasonably high rate during frequency-search operation.

(B) The vulnerability of a narrow-band loop to internal noise. This will be discussed in more detail.

Equation (33) (See Appendix A) can be written

$$\begin{aligned} |Y(j\omega)|^2 &= \frac{K^2 a^2}{\omega^4 + \omega^2(K^2 - 2aK) + K^2 a^2} \\ &\quad + \frac{\omega^2 K^2}{\omega^4 + \omega^2(K^2 - 2aK) + K^2 a^2}. \end{aligned}$$

Introducing  $\omega_o$  and  $\xi$ , and setting

$$K^2 - 2aK = 4\omega_o^2 \xi^2 - 2\omega_o^2 = \alpha$$

or

$$\alpha = \omega_o^2 (4\xi^2 - 2)$$

$$\begin{aligned} |Y(j\omega)|^2 &= \frac{\omega_o^4}{\omega^4 + \alpha\omega^2 + \omega_o^4} \\ &\quad + \frac{4\xi^2 \omega_o^2 \omega^2}{\omega^4 + \alpha\omega^2 + \omega_o^4}. \end{aligned} \quad (29)$$

The last expression, integrated over  $\omega$ , yields the noise bandwidth. It contains a first (low-frequency) term and a second (high-frequency) term. These are depicted in Figures 4 and 5 as functions of  $\omega$ , for various values of  $\xi$ .

The contribution of these terms to the total noise bandwidth of the loop varies with  $\xi$ . It can be seen from Figure 4 that the value of the integral over the low-frequency term increases with decreasing  $\xi$ . It exhibits a well-defined maximum for  $\xi < 0.7$  that will grow and move from  $\omega = 0$  toward  $\omega = \omega_o$  with decreasing  $\xi$ , thus increasing the low-frequency contribution to the noise bandwidth of the system.

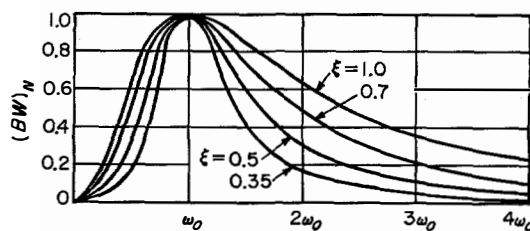


Figure 5—High-frequency component of loop noise bandwidth (35).

For  $\xi$  close to zero (for  $\xi = 0$  the system oscillates and noise bandwidth and voltage-controlled-oscillator phase jitter are meaningless) the large noise-bandwidth contribution is due to frequencies from 0 to  $\omega_o$  for which the phase shifts around the loop are favorable, resulting in sustained action (positive feedback).

The high-frequency term behaves differently. It is zero for  $\omega = 0$  and  $\omega = \infty$ , and has a fixed maximum at  $\omega = \omega_o$ , independent of  $\xi$ . The contribution of this term to the noise bandwidth grows with increasing  $\xi$ . As the system approaches the oscillating state, the curve in Figure 5 becomes a narrow line peaked at  $\omega = \omega_o$ , with a finite maximum and with noise-bandwidth contribution tending toward a single spectral line.

It follows that when noise is introduced into the loop with the input signal, noise components above  $\omega_o$  tend to be suppressed, while noise components with  $\omega < \omega_o$  will be favored to a degree determined by the choice of  $\xi$ .

The loop behavior is different for noise generated in the loop. Figure 6 shows two points at which noise is injected.

(A) Point *a* (output of the phase detector). White noise is injected into the summing network  $\Sigma 1$  to be added to the error signal *e* at the output terminals of the phase detector. This case is quite similar to the case where

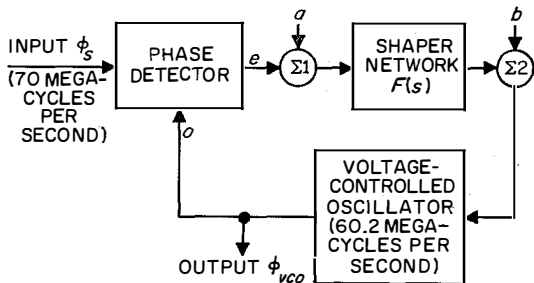


Figure 6—Effect of internal noise on loop performance. Noise is injected at points *a* and *b*. Noise spectral density at point *e* is  $G(j\omega)_e$ . Phase-jitter spectral density at point *o* is  $G(j\omega)_e$  divided by the gain of the phase detector  $K_{pd}$ .

band-limited white noise is introduced into the phase detector with the input signal. The noise phase-modulates the voltage-controlled oscillator (in lock operation) and appears at the output terminals of the phase detector with its spectral density modified by the transfer function of the loop.

$$G(j\omega)_e = |Y(j\omega)|^2 G(j\omega)_i$$

where  $G(j\omega)_e$  is the noise spectral density at point *e* and  $G(j\omega)_i$  is the noise spectral density at point *a*.

The phase-jitter spectral density at point *o* is then  $G(j\omega)_e$  divided by the gain of the phase detector  $K_{pd}$ .

This result is more general than the one obtained in (19) . . . (22) since no restrictions are imposed on the amount of noise delivered to the summing point.

(B) Noise introduced into point *b* is treated differently by the loop. Following the same reasoning as in the previous case, it can be shown that the input noise spectral density has to be multiplied by

$$|Y_1(j\omega)|^2 = \left| \frac{G(j\omega)}{[1 + G(j\omega)]K_{pd} \cdot K_d F(s)} \right|^2 \quad (30)$$

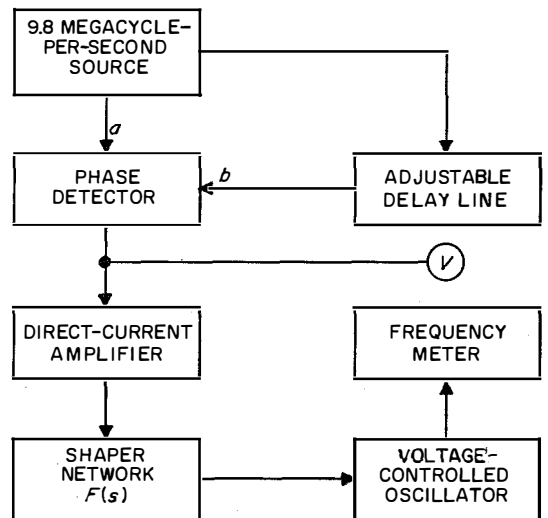


Figure 7—Open-loop arrangement for loop-response test. The signal at port *a* acts as the reference for the adjustable-delay signal supplied at port *b*.

to obtain the phase-jitter spectral density of the voltage-controlled oscillator. This expression differs significantly from (33). Introducing

$$G(j\omega) = K \frac{F(j\omega)}{j\omega}$$

and

$$F(j\omega) = 1 + \frac{a}{j\omega}$$

(30) yields

$$|Y_1(j\omega)| = \frac{K}{K_{pd} \cdot K_d} \left| \frac{j\omega}{Ka + jK\omega + \omega^2} \right|$$

and

$$|Y_1(j\omega)|^2 = \left( \frac{1}{K_{pd} \cdot K_d} \right)^2 \times \frac{4\omega_o^2 \xi^2 \omega^2}{\omega^4 + \alpha\omega^2 + \omega_o^4} \quad (31)$$

which is the second (high-frequency) term of expression (33). Hence, the low-frequency noise is completely suppressed by the loop while high-frequency noise is present to a lesser extent (factor  $(K_{pd}K_d)^{-2}$ ). Physically this can be seen from the fact that the high-frequency noise components appear in full strength in the voltage-controlled-oscillator

phase jitter unaffected by the loop; the low-frequency components are strongly attenuated because of the feedback effect.

### 3. Experimental Results

The loop response has been tested in an open-loop and a closed-loop arrangement. Figure 7 shows the open-loop arrangement.

The loop phase detector receives two signals at  $f = 9.8$  megacycles per second. An adjustable time delay is assigned to the signal supplied to the phase detector at port  $b$ ; the signal at port  $a$  acts as the switching or reference signal.

Curve  $A$  in Figure 8 shows the phase detector output voltage, which is a sinusoidal function of the phase difference between the signals at ports  $a$  and  $b$ ; curve  $B$  shows the frequency deviation of the voltage-controlled oscillator from the center frequency. The slope of curve  $B$  is the differential loop gain. Its maximum value (approximately 100 kilocycles per second per 15 degrees, or 400 kilocycles per second per radian) is constant for phase shifts  $\approx \pm 20$  degrees and decays rapidly for larger phase shifts in the positive direction. This is attributed to the nonlinear characteristic of

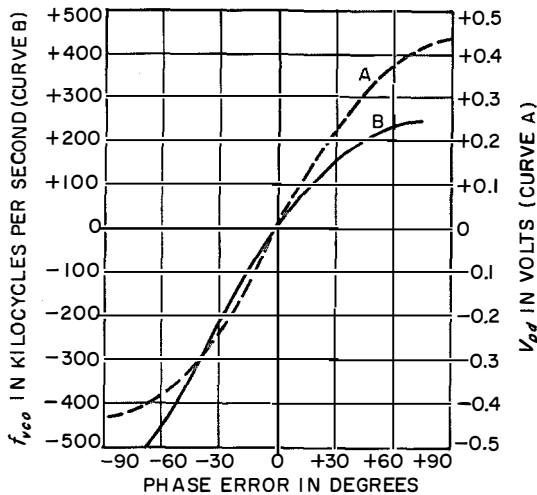


Figure 8—Open-loop response. Curve  $A$  shows the phase-detector response and curve  $B$  the loop gain. The reference voltage is 0.5 volt root-mean-square and the input voltage is 0.140 volt root-mean-square.

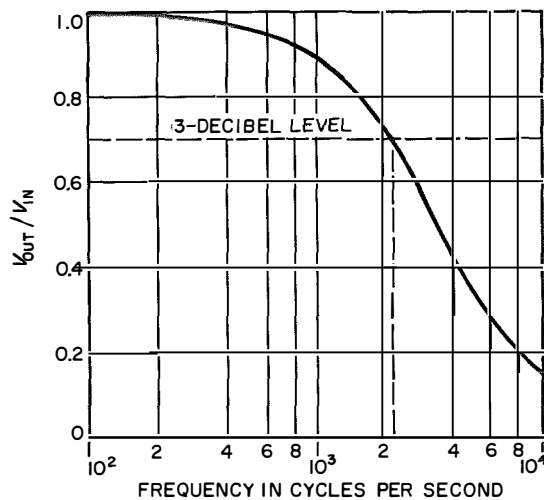


Figure 9—Closed-loop response.

## Satellite-Tracking Receiver

the voltage-controlled element in the oscillator tank circuit. The gain in the negative direction is constant for phase shifts up to 60 degrees.

The closed-loop response is shown in Figure 9. The test was performed with the arrangement shown in Figure 10.

A continuous-wave signal of 70 megacycles per second is applied to the input of the phase-locked loop and lock is achieved by adjusting the free-running frequency of the voltage-controlled oscillator.

A sinusoidal signal is supplied to port *a* of the direct-current amplifier and the loop response is observed at port *b*.

This method of testing loop response departs somewhat from the usual way which introduces a frequency-modulated signal into the loop and permits the voltage-controlled-

oscillator signal to be observed after being discriminated. It is preferable and commonly used because of its simplicity, allowing the tests to be made directly at the modulating low frequency. The loop transfer function can be measured at any point along the loop. It should be borne in mind, however, that this arrangement produces a different distribution of levels at the various points of the loop. The output of the phase detector, for instance, now shows the full output voltage instead of the error voltage. This will not be of further consequence as long as the loop is operated within the linear portion of its response.

### 3.1 ACQUISITION TESTS

The acquisition capability of the loop has been tested under various signal-to-noise conditions. Parameters were the loop bandwidth, the frequency-sweep amplitude (maximum frequency excursion), and the sweep rate. The curves in Figure 11 show the degradation of loop lock-in capability with increasing noise.

The tests were performed by establishing a noise level at the input terminals of the phase detector, then slowly increasing the input signal while frequency-sweeping the voltage-controlled oscillator until phase lock was achieved. The resulting signal-plus-noise root-mean-square voltage was measured and the signal-to-noise ratio determined. The acquisition-signal voltage was plotted as a function of the signal-to-noise ratio. Each measurement was repeated 5 times and the maximum signal voltage was plotted on Figure 11.

Curve *A* shows the degradation of the acquisition capability with increasing noise-to-signal ratio when the frequency sweep is completely eliminated. Curve *B* shows the effect of the frequency sweep on the acquisition capability, all other conditions remaining the same.

Curves *C* and *D* show the effect of a larger loop bandwidth  $(BW)_1 > (BW)_2$ ; the lock-in capability of the loop is increased.

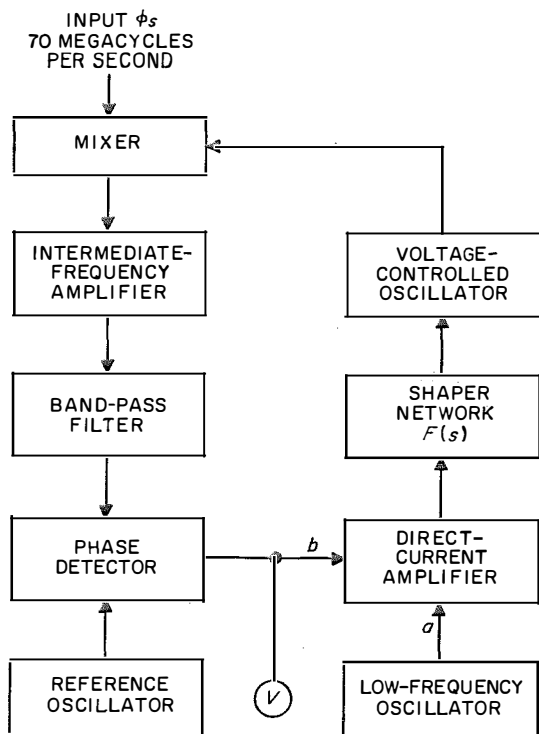


Figure 10—Closed-loop arrangement for loop-response test. A sinusoidal signal is supplied to port *a* and the loop response is monitored at port *b*.

3.2 PULL-IN TESTS

The pull-in capability of the loop was tested by first offsetting the input-signal frequency by several kilocycles per second with respect to its nominal value, then introducing this signal into the loop and observing the pull-in process on a paper recorder and an oscilloscope. Both voltage-controlled-oscillator frequency and input frequency were continuously monitored. The pull-in time was determined from the calibrated speed of the paper recorder.

Figure 12 shows the pull-in time as a function of the initial frequency offset, with a preset

signal strength and signal-to-noise ratio. The bandwidth of the loop remained constant during the tests.

Comparison of Curves *A* and *C* shows the effect of noise on the pull-in time with an input signal kept constant at 10 microvolts.

Curve *A* appears to be in accordance with the theoretical results obtained by Viterbi [1]. The pull-in time has been calculated by a nonlinear loop analysis, and under no-noise conditions, it is

$$t_{\text{pull-in}} = \frac{(\Delta\omega)^2}{2\xi\omega_o^3} \quad (32)$$

where  $\Delta\omega$  is the small initial frequency offset, and  $\omega_o$  is the natural frequency of the loop, both in radians per second. Applying this equation to a frequency offset of  $2\pi 2500$  (rad/sec),  $\xi = 0.7$  and  $\omega_o = 2\pi 300$  (rad/sec) yields a  $t_{\text{pull-in}} = 26$  milliseconds. The equation is not applicable for  $\Delta\omega$  large compared with the loop bandwidth.

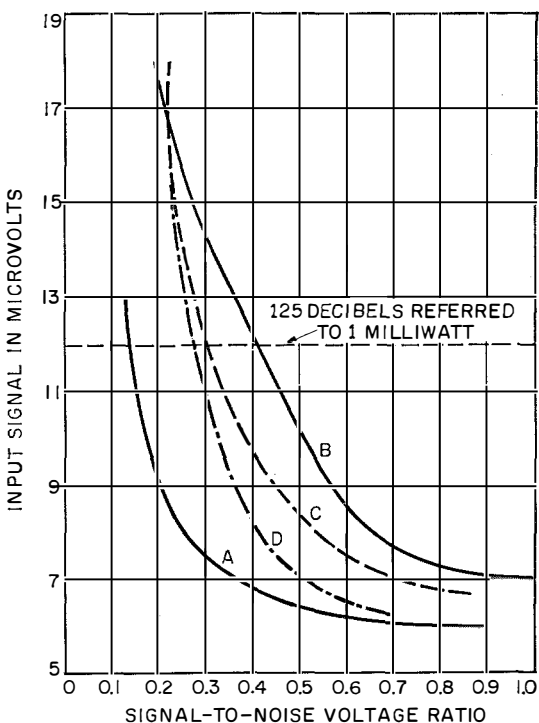


Figure 11—Loop acquisition capability under various signal-to-noise conditions. Curve *A* is plotted for manual acquisition and bandwidth of 2000 cycles per second, curve *B* for the same bandwidth and a  $\pm 100$ -kilocycle-per-second frequency sweep, curve *C* for a  $\pm 200$ -kilocycle-per-second sweep and bandwidth of 5000 cycles per second, and curve *D* for a  $\pm 100$ -kilocycle-per-second sweep and bandwidth of 5000 cycles per second. The sweep frequency for cases *B*, *C*, and *D* is 0.6 cycle per second.

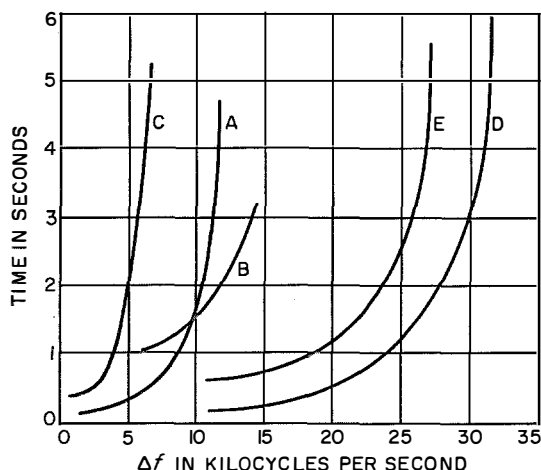


Figure 12—Loop pull-in times at various signal and signal-to-noise levels. Curve *A* is plotted for a constant input signal of 10 microvolts under no-noise conditions, curve *B* is for a 20-microvolt input signal and a signal-to-noise ratio of  $-6$  decibels, curve *C* is for a 10-microvolt input signal and a signal-to-noise ratio of  $-6$  decibels, curve *D* is for a 20-microvolt input signal under no-noise conditions, and curve *E* is for a 20-microvolt input signal and a signal-to-noise ratio of 0 decibels.

### 4. Difference Channels

The two difference channels properly constitute the tracking receiver. Their task is to amplify the positioning errors supplied by the radio-frequency comparator, to extract them from the noise environment, and to convert them into a form acceptable to the servo amplifiers. The importance of this task can be appreciated from the fact that the received signal is at a level of  $-137$  decibels referred to 1 milliwatt for 0.1-degree target offset, with a signal-to-noise ratio of  $-32$  decibels.

The error channel is thus essentially a radio-frequency amplifier. Its last section operates at 9.8 megacycles per second, and this frequency is kept constant by the action of the voltage-controlled oscillator. Here again, a narrow fixed-tuned crystal filter reduces the predetection bandwidth to 30 kilocycles per second, allowing coherent detection to be applied to the radio-frequency signal under favorable conditions. The phase detector is presented with an intermediate-frequency signal of approximately 150 millivolts root-mean-square for a target offset of 0.1 degree, with a signal-to-noise ratio of  $-12$  decibels. A large locally generated switching signal of the same frequency, properly phased, ensures no degradation of the signal-to-noise ratio at the phase-detector output. A low-pass filter with cutoff frequency of 300 cycles per second raises the output signal-to-noise ratio to  $+8$  decibels. This signal is supplied to the servo amplifier.

The difference-channel output exhibits an undesirable feature inherent to the system; it varies with the loop phase error according to a cosine law. To keep this error small, the loop gain has been made high. The maximum expected frequency shift of the input signal ( $\pm 150$  kilocycles per second) results in only 8 degrees loop phase error, which in turn yields a positioning error of only 1 percent in the difference channels.

Since the signal amplitude in the difference channel depends not only on target offset but

also on variations in range, fading in the atmosphere, and orientation of the satellite antenna, automatic gain control must be provided. This is derived from the sum channel, the input signal of which is independent of target position but varies with range, fading, and satellite orientation. The automatic-gain-control voltage applied to the difference channel varies its gain in such a manner as to cancel all signal variations except those caused by target offset. It is understood that this task can be accomplished only at signal levels strong enough to actuate the automatic gain control in the sum channel. Signals below this threshold carry not only target position information but also exhibit undesirable variation with range.

Note that the gain of the difference channel is part of the total gain of the positioning servo loop. Every variation in gain affects not only the positioning accuracy but may also lead to instabilities in case of gain increase beyond safe limits. Such a gain increase can be experienced when the automatic gain control performs unsatisfactorily. Then, a signal increase caused by range reduction is not completely cancelled by the automatic gain control; this results in an increased output signal and increased gain of the error channels. This consideration must be taken into account along with the servo characteristics when deciding on the desired performance of the automatic gain control.

Significant errors in the difference channels can be caused by the noise environment. Any correlation between sum-channel noise and difference-channel noise causes a variation of the amplitude and phase of the 9.8-megacycle-per-second intermediate-frequency signal, which results in a steady-state positioning error. Uncorrelated noise results in a slight oscillation around the steady-state position, the amplitude of which depends on the pass band of the filter or the time constant of the servo system.

These considerations are discussed more fully in Appendix B.

5. References

1. A. T. Viterbi, "Acquisition and Tracking Behavior of Phase-Locked Loops," Jet Propulsion Laboratory, External Publication 673, California Institute of Technology; 14 July 1959.
2. W. J. Gruen, "Theory of AFC Synchronization," *Proceedings of the IRE*, volume 41, pages 1043-1048; August 1953.
3. J. P. Frazier and J. Page, "Phase-Lock Loop Frequency Acquisition Study," *IRE Transactions on Space Electronics and Telemetry*, volume SET-8, number 3, pages 210-227; September 1962.
4. R. Leek, "Phase-Lock AFC Loop" and "Tracking Signals of Varying Frequency," *Electronic & Radio Engineer*, volume 34, number 4, pages 141-146; April 1957, and volume 34, number 5, pages 177-183; May 1957.
5. R. Jaffe and E. Rechtin, "Design and Performance of Phase-Lock Circuits Capable of Near-Optimum Performance over Wide Range of Input Signal and Noise Levels," *IRE Transactions on Information Theory*, volume IT-1, number 1, pages 66-76; March 1955.
6. H. T. McAleer, "New Look at Phase-Locked Oscillator," *Proceedings of the IRE*, volume 47, pages 1137-1143; June 1959.
7. C. S. Weaver, "New Approach to Linear Design and Analysis of Phase-Locked Loops," *IRE Transactions on Space Electronics and Telemetry*, volume SET-5, number 4, pages 166-178; December 1959.

6. Appendix A

6.1 LOOP NOISE BANDWIDTH

The loop transfer function defined by (7) yields

$$|Y(j\omega)|^2 = \frac{K^2 a^2 + \omega^2 K^2}{\omega^4 + \omega^2(K^2 - 2Ka) + K^2 a^2} \cdot (33)$$

Setting  $K^2 - 2Ka = 0$  which corresponds to a critically damped system ( $\xi = 0.7$ ) simplifies this expression to

$$|Y(j\omega)|^2 = \frac{\omega^2}{\frac{\omega^4}{K^2} + a^2} + \frac{1}{\frac{\omega^2}{K^2 a^2} + 1} \cdot (34)$$

The integration of these terms can be performed with the help of integral tables and, on introducing the limits of integration, yields the noise bandwidth

$$(BW)_N = \frac{\pi}{2(2)^{1/2}} \left[ \frac{K^2}{(Ka)^{1/2}} + (Ka)^{1/2} \right]$$

or with  $Ka = \omega_o^2$  and  $K = 1.4 \omega_o$

$$(BW)_N = \frac{3\pi}{2(2)^{1/2}} \omega_o \approx 1.06\pi \omega_o. (35)$$

7. Appendix B

It is assumed that additive white Gaussian noise is present in the sum and difference channels. If  $n_1(t)$  and  $n_2(t)$  are the noise contributions, the signals in the sum and difference channels can be written

$$S = A_v \cos \omega_v t + n_1(t) (36)$$

$$d = A_d \cos \omega_d t + n_2(t) (37)$$

where  $\omega_d$  and  $\omega_v$  are the frequencies of the difference signal and of the voltage-controlled oscillator, respectively.  $n_1(t)$  and  $n_2(t)$  are described by

$$\left. \begin{aligned} \overline{n_1(t)} &= 0 = \overline{n_2(t)} \\ \overline{n_1^2(t)} &= \sigma^2 = \overline{n_2^2(t)} \\ \overline{n_1(t) \cdot n_2(t)} &= \rho \sigma^2 \end{aligned} \right\} (38)$$

where  $\sigma$  is the root-mean-square value of the noise, and  $\rho$  is the normalized correlation function defining the correlation between the noise in the sum and difference channels.  $n_1(t)$  and  $n_2(t)$  can be split into their in-phase and quadrature components

$$\begin{aligned} S &= (A_v + X_v) \cos \omega_v t + Y_v \sin \omega_v t \\ d &= (A_d + X_d) \cos \omega_d t + Y_d \sin \omega_d t. \end{aligned}$$

## Satellite-Tracking Receiver

These two signals are multiplied by each other. Terms in  $\omega_v + \omega_d$  are filtered out and terms in  $\omega_d - \omega_v = \omega_i$  are retained.

$$Sd = \frac{1}{2} \{ (A_v + X_v)(A_d + X_d) \cos \omega_i t + Y_v Y_d \cos \omega_i t + (A_v + X_v) Y_d \sin \omega_i t + (A_d + X_d) Y_v \sin \omega_i t \}.$$

This signal is multiplied by the reference signal  $r = R \cos \omega_i t$  in the phase detector. Retaining only low-frequency terms again yields

$$S_0 = r \cdot S \cdot d = R/4 \times [(A_v + X_v)(A_d + X_d) + Y_v Y_d]. \quad (39)$$

Equation (39) describes quantitatively the steady-state and root-mean-square positioning error at the output terminals of the difference

channel.

$$\overline{S_0} = R/4(A_v A_d + \overline{X_v X_d} + \overline{Y_v Y_d}) \quad (40)$$

indicates a steady-state error  $\overline{X_v X_d} + \overline{Y_v Y_d}$  which is reduced to  $R/4 \cdot \overline{Y_v Y_d}$  if the voltage-controlled-oscillator signal can be considered as only phase modulated by the noise. Furthermore

$$\overline{S_0^2} - (\overline{S_0})^2 = R^2/16 [A_d^2 \overline{X_v^2} + A_v^2 \overline{X_d^2} + \overline{X_v^2 X_d^2} - (\overline{X_d X_v})^2 + \overline{Y_v^2 Y_d^2} - (\overline{Y_v Y_d})^2 + 2A_v A_d \overline{X_v X_d}]. \quad (41)$$

Equation (41) describes the root-mean-square value of the fluctuations around the steady-state positioning error. It can be seen that (41) is a function of the degree of correlation between the noise in the difference channels and the voltage-controlled oscillator.

**W. Janeff** was born in Burgas, Bulgaria, on 13 October 1920. He received a Diplom Ingenieur degree from the Technische Hochschule in Vienna, Austria, in 1942 and a Ph.D. degree in 1945 from the Technische Hochschule in Dresden, Germany.

He joined the engineering staff of ITT Federal Laboratories in 1959 and is now a development engineer in the space-communication laboratory. Dr. Janeff is a member of the Association des Ingenieurs Docteurs de France and a Member of the Institute of Electrical and Electronics Engineers.

# Transportable-Station Operation with Telstar and Relay Satellites

J. E. DRUCKER

ITT Federal Laboratories, A Division of International Telephone and Telegraph Corporation; Nutley, New Jersey

## 1. Introduction

The first transportable space-communication terminal [1] began operation with active satellites on 11 August 1962, when it tracked Telstar 1 pass 298. From this date to June 1963, when this paper was written, two more terminals entered active service, two more communication satellites were placed in orbit, and we have devoted some 25 man-years of activities to satellite-communication operations. In general, operation has closely correlated with theory, while review of logistics, staffing requirements, et cetera, validates the soundness of the station design.

Experimental operation has been tailored to the requirements of both military and commercial programs, the latter concentrating on transmission measurements. The combined objectives of both programs dictated the examination of several areas of interest.

(A) The technical parameters of a single transportable ground station considered as a communication entity.

(B) The technical parameters of a full-duplex communication system consisting of 2 transportable ground stations and an orbiting satellite.

(C) The practical problems encountered in transportation, operation, maintenance, and support in the field.

Two stations were used by the Department of Defense, each staffed by 9 enlisted military technicians under the direction of 3 of our engineers. A third was operated near Rio de Janeiro by 6 engineers of Companhia Rádio Internacional do Brasil. The 12-man teams used in the Department of Defense program exceeded basic operational requirements, but were justified by the need to train military personnel.

The frequencies used in communicating via Telstar and Relay satellites all lie in international treaty bands designated for com-

mercial use. Therefore, operation at sites under control of the United States Federal Communications Commission has been governed by experimental (earth-station-research) licenses issued to Mackay Radio and Telegraph Company. The Brazilian terminal is licensed by the Post and Telegraph Department of Brazil. Since all programs are purely experimental, no toll communications have been authorized by any licensing agency and all information passed during communication tests is considered as dummy traffic for test purposes only.

## 2. Chronology of Operations

Initially, during the August-October 1962 phase, equipment checkout and basic-parameter verification were the primary objectives. By November 1962, checkout was sufficiently complete to permit a shift in program emphasis. Team training and the documentation of operating procedures such as prepass checkout, test, and reporting became the primary efforts. By early 1963, this phase was about complete, station operation had become somewhat routine, and paramount interest was directed toward the analysis of test data.

In the following discussion, satellite passes are designated by satellite name and pass number; for example, T1-175 denotes pass 175 of Telstar 1.

## 3. Test Conditions

Stations 1 and 3 generally communicated during 2 or 3 Telstar passes each week, with typical passes from 15 minutes to 1 hour long. Other passes, not allocated for testing, were used for tracking or receive-only exercises. Station 2 generally used two 20- to 30-minute Relay passes each week. The task of dividing these limited allocations of operating time among the various tests and test areas was

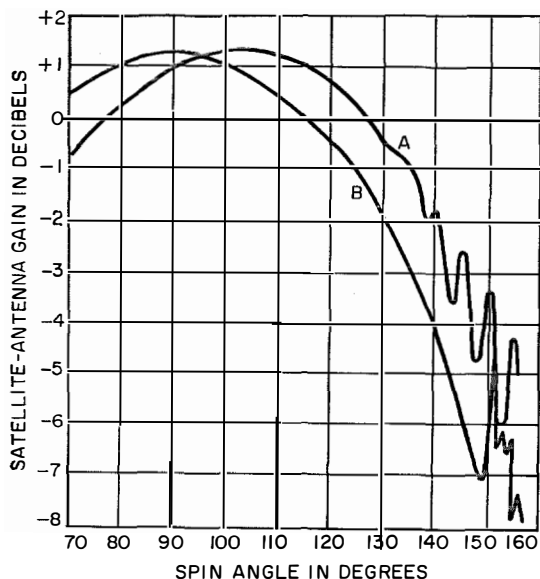


Figure 1—Satellite-antenna polar pattern for Telstar 1 derived from pass 125, as a function of spin angle. Curves A and B are for 4 and 6 gigacycles per second, respectively.

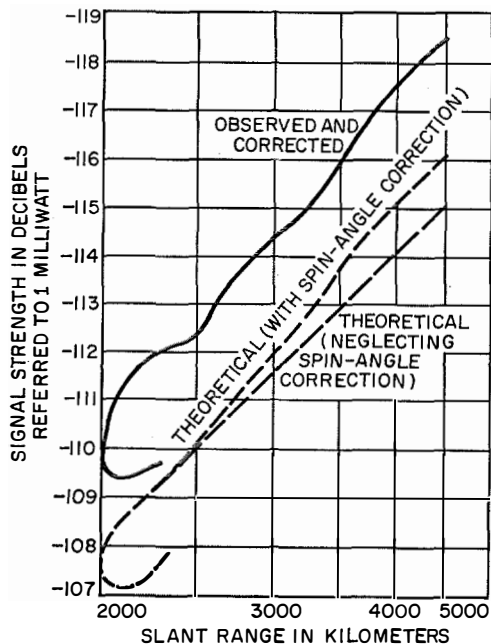


Figure 2—Comparison of theoretical and observed beacon signal strength measured at station 1 during Telstar 1 pass 1187. Note how theoretical plot changes as a result of spin-angle effect on antenna gain.

quite critical. This was further complicated by the requirement that each test be performed under various conditions of weather, radio-frequency signal level, et cetera.

### 3.1 ANCILLARY TESTS

A number of ancillary areas were examined during the periods of operation. Required logistic support, maintainability, staffing, site and transportation requirements, primary power drain, and other operational factors were included. No specific test program was prescribed in this area but data were accumulated for later analyses.

## 4. Performance

Unless indicated otherwise, the data are based on experience at all 3 operating terminals.

### 4.1 PROPAGATION

The 4-gigacycle-per-second propagation from satellite to terminal depends on the following factors.

(A) Output power level of the satellite transmitter. For Telstar 1, it was assumed that the 4080-megacycle-per-second beacon signal was generated in the satellite transmitter at +17 decibels referred to 1 milliwatt and that 1 decibel was lost between generator and antenna.

(B) Satellite-antenna gain. For both Telstar and Relay, effective satellite-antenna gain depended on spin angle, as shown in Figure 1. For Telstar, the spin angle (also called *earth aspect* angle) is defined as "the angle between the line of sight from the ground station to the satellite and the South Pole axis of the satellite. The South Pole is the pole opposite the telemetry antenna" [2]. For Relay, this angle was termed the *look* angle.

(C) Total path loss, which includes free-space, precipitation, ionospheric, and atmospheric losses. In the following analysis, only free-space loss was considered.

(D) Ground-antenna gain and transmission-line loss. This was taken to be a 48-decibel gain followed by a 1-decibel loss. One primary purpose of the 4-gigacycle-per-second analysis is the verification of this composite value of +47 decibels.

The distinctive button-hook shape shown in Figure 2 is occasioned by spin-angle variations that created a marked change in satellite-antenna gain as the slant range decreased and then lengthened during the pass. Figure 2 is derived from pass T1-1187.

The composite average of the 4-gigacycle-per-second curves for station 1 shows observed levels generally about  $2 \pm 1$  decibels below theoretical. The cause of this discrepancy has not been clearly determined, but probably lies in the area of ground-antenna gain, beacon-transmitter output level, or, most likely, terminal calibration procedures. This analysis is continuing for all stations.

The lobes in Figure 1 produce variations in signal level as spin angle changes. This variation pattern (called *spin lobing* for brevity) is clearly evident in the signal trace of Figure 3 taken during pass T1-1811. In about 2 minutes, the tracking-signal level decreased from -125.2 to -132.8 and then dropped below -137 decibels referred to 1 milliwatt, causing loss of phase lock. Typical timing on spin lobes is from  $\frac{1}{2}$  to 5 minutes per lobe, with peak-to-peak amplitudes of 8 decibels or more.

The antenna patterns shown in Figure 4 produce ripples of up to several hundred cycles per second in the received signals. This spin modulation is noticeable in Figure 3 and may be closely examined in Figure 5, where peak-to-peak variations of 7.5 decibels in beacon-signal level were experienced during pass R1-285. Variations up to 8 decibels have been realized. A satellite spin rate of 167 revolutions per minute is calculated from this recording.

Curve B of Figure 1 shows the 6-gigacycle-per-second antenna gain of Telstar 1 as a

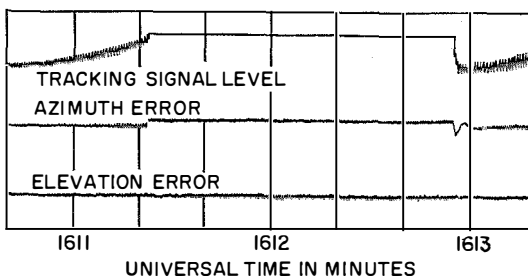


Figure 3—Recording of signals received at station 1 from Telstar 1 on pass 1811.

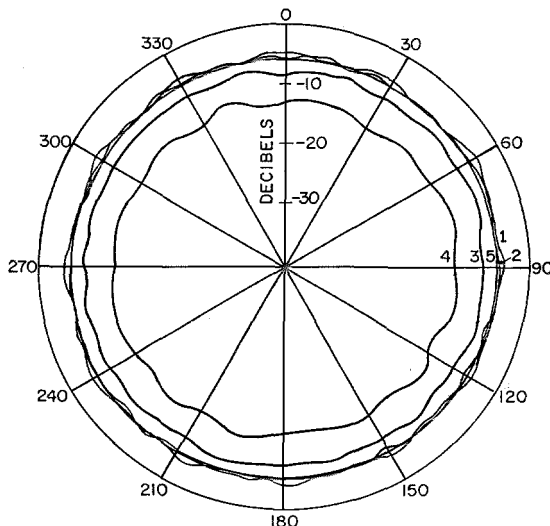


Figure 4—Telstar 1 longitudinal antenna patterns for 4 gigacycles per second. Curves 1 through 5 are for satellite spin angles of 90, 70, 50, 30, and 10 degrees, respectively.

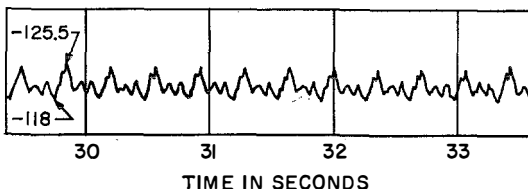


Figure 5—Recording of Relay 1 pass 285 at indicated seconds intervals for 1409 hours universal time. Arrows indicate tracking-signal levels in decibels referred to 1 milliwatt.

## Operation with Telstar and Relay Satellites

function of spin angle. Figure 6 shows the theoretical and observed values of 6-gigacycle-per-second signal level at the satellite as a function of time during pass T1-1187. The shapes of the curves are determined by changing range and spin angle as in Figure 2, with a constant ground-transmitter power level throughout the pass. In the 6-gigacycle-per-second case, the actual received signal data are derived from satellite telemetry equipment that samples and reports the received signal level once per minute.

For station 1, the 6-gigacycle-per-second performance is concluded to be within  $\pm 1$  decibel of the ground-station antenna-gain design target of 52 decibels. Greater discrepancies were noted at rather-low levels ( $-70$  to  $-77$  decibels referred to 1 milliwatt), but this is thought to be caused by an error at the lower limit of the telemetry sensor.

### 4.2 TRACKING ERRORS

Tracking errors are defined here as the angular errors, in degrees of azimuth or elevation, existing between the radio-frequency main-lobe axis of the station antenna and the line of sight to the satellite. The magnitude and sense of these errors were determined from the recorded analogs of the errors, namely the

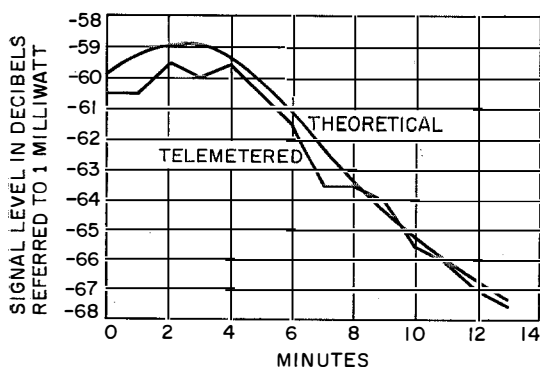


Figure 6—Theoretical and telemetered values of 6-gigacycle-per-second signal received at Telstar 1 during pass 1187. A temperature of 25 degrees centigrade was assumed for the telemetry sensor.

direct-current error output voltage from the azimuth and elevation channels of the tracking receiver.

The station design specifications limit tracking errors to less than  $\pm 0.1$  degree in either axis, even in winds of 35 miles (56 kilometers) per hour with a 25-percent gust factor.

Analysis of 103 satellite passes during 1962 and 1963 reveals that tracking performance has been within specification. Typical errors are between  $\pm 0.01$  and  $\pm 0.03$  degree.

Figure 7 shows recordings of the azimuth and elevation tracking errors that occurred while station 3 tracked pass R1-872. Also shown are the wind speeds, which were recorded at our Space Communication Research Station during the same pass. The stations were approximately 100 feet apart. Wind gusts of up to 58 miles (93 kilometers) per hour produced errors that averaged perhaps  $\pm 0.04$  degree throughout the passage of a local weather front. The peak error discernable occurred at 20 seconds past 2318 hours universal time, when the azimuth axis moved to a maximum error angle of  $-0.15$  degree. The abrupt variations in tracking-signal level were occasioned by technical difficulties at the transmitting station during pass R1-872, not by the tracking performance of station 3.

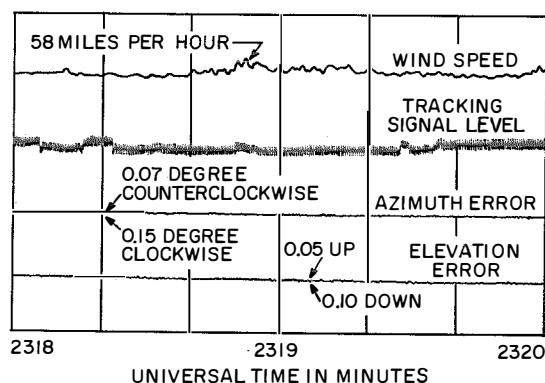


Figure 7—Recordings of azimuth and elevation tracking errors and the wind speeds causing these errors during pass 872 of Relay 1.

Another notable performance occurred during pass R1-269, when station 1 tracked the satellite through an elevation angle interpolated to have been in excess of 89.7 degrees (Figure 8). No calibrated error traces are available for this pass, but analysis of the recorded signal levels (Figure 9) during the period of maximum azimuth variation indicates that the maximum effect of tracking error during this virtual-zenith pass was to momentarily perturb the received signals, with no significant effect on communication capability. The 89.7-degree elevation was the highest noted in the 1500 pass predictions examined to date.

### 4.3 POINTING ERRORS

Pointing errors are defined here as the angular errors, in degrees of azimuth or elevation, existing between the theoretical and observed positions of a satellite. The validity of the pointing-error analysis depends on the accuracy of the azimuth and elevation predictions furnished the station, since these serve as the "theoretical" points for the analysis. We were

fortunate in having predictions furnished, both for Telstar and Relay, by the Tracking Directorate of the National Aeronautics and Space Administration's Goddard Space Flight Center. These predictions normally were accurate to within a few hundredths of a degree and thus made possible analysis of pointing errors to approximately the same magnitude.

Ignoring prediction computation errors, pointing errors can be occasioned by

- (A) Errors in defining the station location or geodetic elevation.
- (B) Inaccuracies in position sensors and readouts.
- (C) Lack of orthogonality between azimuth and elevation axes.
- (D) Lack of coincidence of antenna axes with vertical and North references.
- (E) Collimation error between radio-frequency beam and mechanical readout, and dynamic errors caused by servo lag or lead.

Examination of data from station 1 revealed an azimuth pointing error that followed the

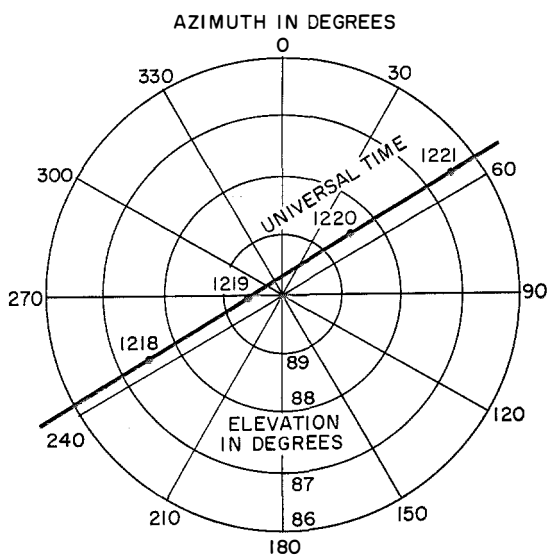


Figure 8—Near-zenith path of Relay 1 pass 269, which attained an elevation of 89.7 degrees at 16 seconds past 1219 hours universal time.

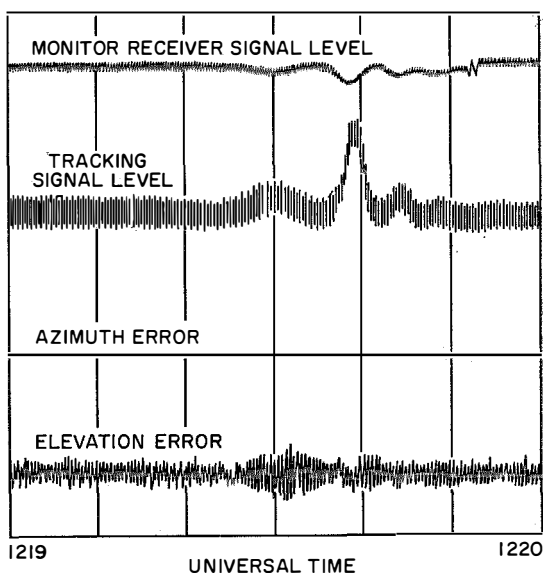


Figure 9—Recording of signal levels during near-zenith pass shown in Figure 8.

## Operation with Telstar and Relay Satellites

shape of curve *A* in Figure 10, when azimuth error was plotted as a function of elevation. A curve of this shape could be occasioned by a static offset plus an azimuth error caused by either a lack of axial orthogonality of magnitude  $E_\phi$ , wherefrom

$$E_{az} = \tan^{-1} (\tan E_L \sin E_\phi) \quad (1)$$

or an azimuth collimation error of magnitude  $E_\theta$ , wherefrom

$$E_{az} = \sin^{-1} (\sin E_\theta \sec E_L) \quad (2)$$

where  $E_{az}$  = azimuth error  
 $E_L$  = elevation error  
 $E_\theta$  = azimuth collimation error  
 $E_\phi$  = axial orthogonality error.

The plots of (1) and (2) are also shown in Figure 10 as curves *B* and *C*, respectively. Both closely resemble the plot of observed error in *A*, with *C* virtually indistinguishable from *A*. Further evaluation of the antenna orthogonality case indicated that such a mechanical error would also cause an elevation error of a type not observed, and it would have been readily detected by physical measurements. It was therefore concluded that the observed azimuth error was occasioned by a static azimuth readout offset of 0.44 degree and a partially compensating azimuth collimation error of 0.22 degree.

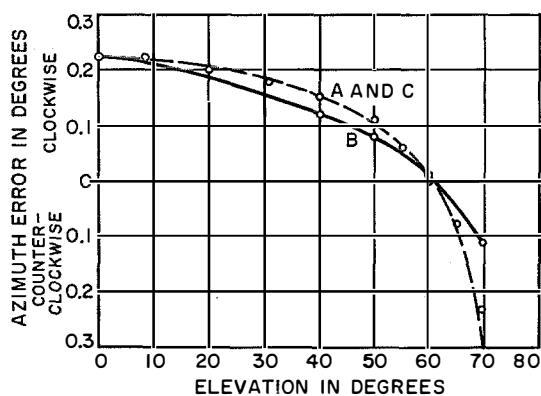


Figure 10—Comparison of observed (curve *A*) and theoretical (curves *B* and *C*) values of azimuth error as a function of predicted elevation.

This type of test analysis and equipment evaluation will continue throughout the experimental life of each station, providing a continuing check on the status of equipment. Particular attention will be paid to the pointing-error data after each station relocation, both to check equipment condition after shipment and antenna assembly, and to verify coordinate accuracy of the new site.

### 4.4 VOICE COMMUNICATION

The ability of the stations to provide multi-channel voice communication via both Telstar and Relay has been demonstrated repeatedly. Specific tests of channel quality confirmed the theoretical predictions.

When using true 4-wire terminal sets with no sidetone feature, the transmission delay of as much as 100 milliseconds encountered with Telstar 1 presented no barrier to conversation. However, when talking over circuits that permitted one to hear the looped return of his own voice, the average person was noticeably affected. A common reaction was a rapid, hesitant change in the rate of speech, as the talker tried to "get away" from his echo. This effect clearly revealed the need for properly terminated voice equipment, possibly assisted by echo-suppression devices.

During those passes when spin modulation momentarily depressed signal levels below the noise threshold, a distinctive low-repetition-rate noise appeared in the voice channels, apparently synchronized with the spin rate of the satellite.

Voice communication was occasionally achieved with very-low radio-frequency signal levels, either by deliberately reducing transmitted signal level, or fortuitously when Telstar 2 ranges exceeded those originally anticipated in the station design. Under these conditions, voice communication degraded in accordance with normal expectations, but only extreme combinations of range and spin angle rendered communication impossible.

4.5 TELEPRINTER COMMUNICATION

Teleprinter communication, using frequency-shift tone keys deviating 85 cycles per second peak to peak for each teleprinter channel, produced results quite similar to that discussed for voice communication. With radio-frequency signals above threshold, teleprinter error rates of 0 to 2 in  $10^5$  bits obtained. Normal teleprinter operation was at 60 words per minute.

4.6 FACSIMILE

The facsimile transceivers used at stations 1 and 3 are capable of reproducing 12 to 14 shades of gray and resolving 70 lines per inch. Typical facsimile transmissions through a voice-multiplex channel produced copy indistinguishable from the best obtainable from the transceiver.

4.7 CHANNEL SIGNAL-TO-NOISE RATIO

The channel signal-to-noise ratio for conditions above threshold may be expressed as

$$S/N = C - F + 20 \log_{10} \frac{W}{f_m} - 10 \log_{10} 2B_c - 10 \log_{10} KT - N_o B_a$$

where

$C$  = carrier input power in decibels referred to 1 watt

$F$  = receiver noise factor

$W$  = maximum peak frequency deviation for the channel in cycles per second

$f_m$  = midfrequency for the channel in cycles per second

$B_c$  = channel bandwidth in cycles per second

$K$  = Boltzmann's constant =  $1.38 \times 10^{-23}$

$T$  = absolute temperature = 290 degrees Kelvin.

$N_o$  = noise level in decibels referred to 1 milliwatt

$B_a$  = intermediate-frequency bandwidth.

Below the carrier threshold level, signal-to-noise ratios range from approximately 10 to 35 decibels for discernible signals with a reliability above 80 percent. Pass T1-1756 with station 1 demonstrated this range of operation. During this pass, signal-to-noise ratios between 27 and 35 decibels were observed for carrier-to-noise ratios below threshold while operation slightly above threshold resulted in signal-to-noise ratios up to 42.5 decibels.

4.8 BASEBAND FREQUENCY RESPONSE

The measured baseband frequency response of station 1, using 3 different pre-emphasis networks, is shown in Figure 11. The curves were derived during loop testing via a satellite simulator. The station uses phase-locked-loop threshold-extension demodulation. The effective noise-bandwidth and base-bandwidth response is therefore a function of signal level. The results of base-bandwidth and intermodulation measurements are unique for each signal level. This requires the assembly of much data to describe the system operation fully.

The baseband width is reduced as signal level is reduced. Intermodulation products are increased with a reduction in base bandwidth. Systems are designed at threshold conditions with a compromise between thermal noise and intermodulation products.

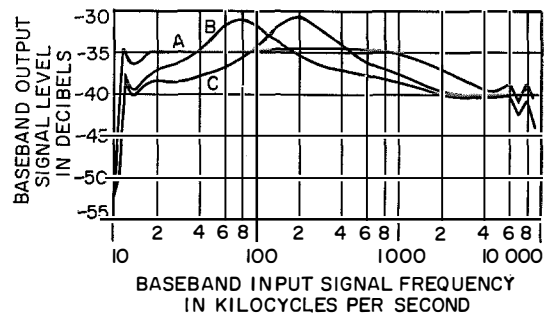


Figure 11—Measured baseband response of station 1 plotted against frequency. Curves A, B, and C illustrate the use of zero, 12-channel, and 36-channel pre-emphasis networks, respectively.

## Operation with Telstar and Relay Satellites

The 2-tone intermodulation test determines the linearity of transmission by examining the harmonics and the cross-modulation sum and difference frequencies generated from an input to the system of 2 tones. Since the system performance may be evaluated in terms of second- and third-order nonlinearities, the levels of these terms reasonably indicate the degree of this linearity. Data taken during two intermodulation tests about 10 minutes apart on pass T1-980 are shown in Figure 12. The input frequencies were 15 and 20 kilocycles per second.

Interchannel noise tests have been conducted to determine the level of noise in the telephone channels under conditions similar to the actual telephone loading conditions. In this experiment, all active channels except one are loaded with white noise. Noise is measured in the idle channel with and without noise on the active channels. The noise contributions are then computed. Because of the change of base-band response as a function of signal level, these results have to be taken at threshold conditions. The phase-locked-loop demodulator has been shown to have the advantage of automatically reducing noise bandwidth as signal level is decreased. This increases intermodulation at the same time as thermal noise increases because of reduced signal level. The

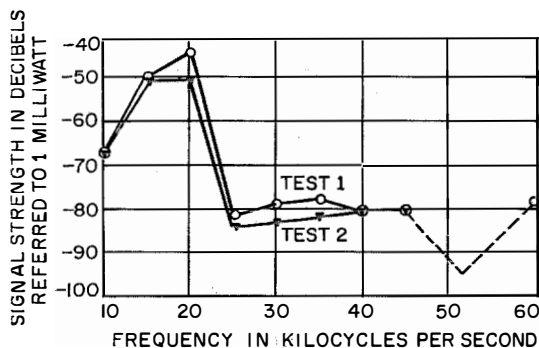


Figure 12—Results of 2-tone intermodulation distortion tests. The broken line indicates interpolation. Using input tones of 15 and 20 kilocycles per second, two measurements were made approximately 10 minutes apart.

problem in equipment design is to maintain the noise contribution from these two sources in the same ratio and to perform accurate measurements at various signal levels.

### 4.9 MEDIUM-SPEED DATA

During pass T2-177, station 1 loop tested medium-speed data communication. Sending 1200-bit-per-second test data for a scheduled 8-minute period, more than 500 000 bits were received, error-free, with radio-frequency signal levels of  $-106$  decibels referred to 1 milliwatt, while channel signal-to-noise ratios ranged between 17 and 19.5 decibels.

### 4.10 GAIN STABILITY

Two-way and loop tests, both through satellite simulators and during actual satellite passes (with radio-frequency levels above threshold) have produced data indicating gain stability of better than  $\pm 0.5$  decibel for periods of many minutes. Only when operation falls below threshold does stability depart noticeably from this value.

## 5. Transportation Requirements

The composition of a station varies with its mission and may be as small as 3 vehicles: a radio van and 2 antenna trailers. However, stations 1 and 3 in the Telstar program used the 6 vehicles listed in Table 1.

To date, two station relocations have been made. A minimum station (V-1, T-1, T-2) was towed from Nutley, New Jersey, to Dover, Delaware, flown to Rio de Janeiro, and then towed to Jacarapaqua, Brazil. A full terminal (6 vehicles) was towed from Nutley to McGuire Air Force Base, New Jersey, flown to Vandenberg Air Force Base, California, and then towed more than 100 miles to Paso Robles, California.

Table 2 shows a number of aircraft-load combinations usable for air-transporting a 6-vehicle station.

**6. Pointing Data Requirements**

The experimental program required prediction of ephemeris data for three purposes.

(A) To permit the location and acquisition of satellites for the purposes of communication and/or tracking.

(B) To permit the comparison of observed results of communication tests with theoretical values based on predicted satellite range and attitude.

(C) To permit analysis of tracking-system performance based on predicted satellite position.

To accomplish tasks (A) and (B) (simple acquisition and communication analysis), range predictions plus azimuth and elevation calculations having accuracies within a few tenths of a degree are necessary. These accuracies are needed when moderate tracking-signal levels (approximately -125 decibels referred to 1 milliwatt) are encountered.

TABLE 1  
STATION CONFIGURATION FOR TELSTAR

Vehicle	Type	Equipment Carried	Gross Weight in Pounds (Kilograms)	Parking Length in Feet (Meters)
V-1	Semitrailer van	Radio terminal	28 000 (12 701)	30 (9.1)
V-2	Semitrailer van	Command and telemetry	24 000 (10 886)	30 (9.1)
T-1	Trailer	Antenna structure	31 500 (14 288)	25 (7.6)
T-2	Trailer	Antenna reflector	9600 (4355)	17 (5.2)
T-3	Trailer	Heat exchanger	4800 (2177)	10 (3)
T-4	Trailer	Diesel generator	14 000 (6350)	12 (3.7)

TABLE 2  
TYPICAL AIRCRAFT-LOAD COMBINATIONS\*

Aircraft	Vehicles Carried	Net Weight in Pounds (Kilograms)	Load Length in Feet (Meters)	Comments
C-124	V-1, T-2	37 600 (17 055)	48 (14.6)	Most-even weight distribution
C-124	V-2, T-4	38 000 (17 237)	41 (12.5)	
C-124	T-1, T-3	36 300 (16 466)	29 (8.8)	
C-124	T-1, T-2	41 100 (18 643)	38 (11.6)	Most-convenient arrival sequence
C-124	V-2, T-4	38 000 (17 237)	41 (12.5)	
C-124	V-1, T-3	32 800 (14 878)	39 (11.9)	
C-124	T-1, T-2†, T-3‡	45 900 (20 820)	46 (14)	Most compact and good arrival sequence
C-124	V-1, V-2	52 000 (23 587)	62 (18.9)‡	
C-124	T-4	14 000 (6350)	10 (3)	
C-133	V-1, V-2, T-1	83 500 (37 876)	83 (25.3)	Poor arrival sequence and few C-133's available
C-124	T-2, T-3, T-4	28 400 (12 882)	35 (10.7)	
C-124	T-1, T-2	41 100 (18 643)	38 (11.6)	
C-124	V-1, V-2	52 000 (23 587)	62 (18.9)‡	
C-130	T-3, T-4	18 200 (8256)§	18 (5.5)	

\* Calculated on basis of one-way mission of 1000 nautical miles (1852 kilometers).

† Loaded sideways.

‡ Clears ramp.

§ Trailer undercarriages removed.

## Operation with Telstar and Relay Satellites

Diminished accuracies will suffice for higher signal levels, as the search and acquisition capability of the tracking system is enhanced. One prediction per minute is adequate for satellites such as Telstar 1 and Relay 1. The time interval between predictions may be lengthened if:

(A) Signal levels are high.

(B) Azimuth and elevation rates are easily interpolated.

(C) Some delay in acquisition may be tolerated.

The requirements for task (C) (analysis of tracking-system performance) are more stringent. As was discussed earlier, the station tracking system exhibits nominal nonsystematic pointing errors on the order of a few hundredths of a degree. The predicted data must be at least as accurate if analysis of predicted-versus-observed data is to be performed. Thus, the stipulated accuracy requirement for azimuth and elevation predictions for analytic use is  $\pm 0.01$  degree. Range accuracies of  $\pm 1$  percent, spin-angle accuracies of  $\pm 1$  degree, and time accuracies of  $\pm 0.5$  second are specified.

### 7. Acknowledgments

The operation of stations 1 and 3 discussed in this article were partially sponsored by the United States Air Force Communication Service and the United States Air Force Electronic Systems Division under Communication Service Authorization AMIZ-BE-60 000.

The author also wishes to acknowledge the work of the military and International Telephone and Telegraph Corporation personnel

responsible for the operation of the transportable stations, whose activities provided the majority of the data for this paper.

### 8. References

1. L. Pollack, W. Glomb, and L. F. Gray, "Medium-Capacity Space-Communication Terminal," *Electrical Communication*, volume 39, number 1, pages 37-48; 1964.
2. "Project Telstar Preliminary Report, Telstar 1," Bell Telephone Laboratories, Murray Hill, New Jersey; 1962.
3. D. Campbell, D. Hershberg, and E. Singer, "Universal Transportable Space Communication Terminal," Technical Memorandum 796-7A, ITT Federal Laboratories, Nutley, New Jersey; 1961.
4. "Telstar Data Book," volumes 1 and 2, Bell Telephone Laboratories, Murray Hill, New Jersey; 1962.

**Joel E. Drucker** was born on 28 January 1928 in New York, New York. In 1951, he received a B.S. degree in electrical engineering from Polytechnic Institute of Brooklyn.

From 1951 to 1955, he served as a first lieutenant in the United States Army Signal Corps. For the next two years, he was employed by Sperry Gyroscope Company.

In 1957, he joined ITT Federal Laboratories and worked on defense communication systems. He is now responsible for technical planning, operations, and data analysis for Project Trade Post, a satellite communication program for the Department of Defense.

# Satellite-Communication Ground Station in Germany

HELMUT CARL

Standard Elektrik Lorenz AG; Stuttgart, Germany

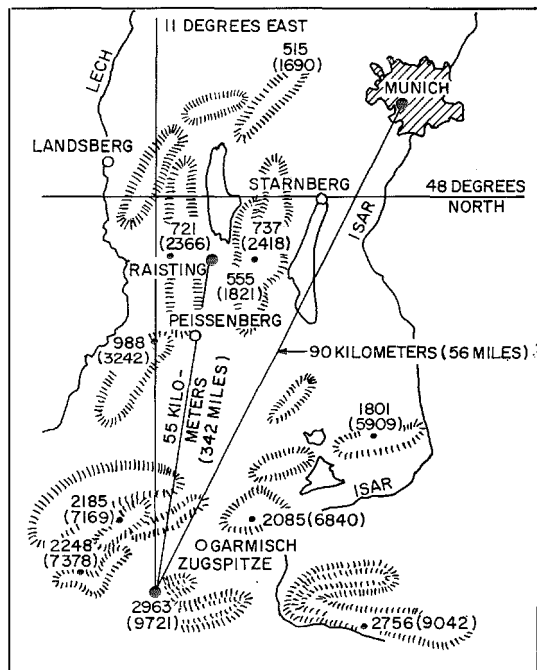


Figure 1—The Raisting satellite-communication ground station is connected to the Munich switching center over a microwave link using Zugspitze as a repeating point. Peak elevations are given in meters (feet).

A transportable satellite-communication ground station of the type described in this issue was manufactured by ITT Federal Laboratories and installed for the Deutsche Bundespost by Standard Elektrik Lorenz in the second half of 1963. The station is located near Raisting, about 40 kilometers (25 miles) southwest of Munich on the same site selected for a large fixed ground-station terminal of the Bundespost.

The general location is given in Figure 1. The site is fairly well shielded against outside interference by the surrounding mountainous terrain, except perhaps from the north. Radio horizon angles range between 0.5 and 2.5 degrees.

The equipment will serve for communication experiments with both the Relay and Telstar satellites. This requires that the 10-kilowatt transmitter and associated feed horns be capable of operation in both the 2- and 6-gigacycle-per-second bands. For interconnection with the German telecommunication network, a line-of-sight 120-channel 2-gigacycle-per-second system was installed between Raisting and the Bundespost switching office in Munich via a repeater at Zugspitze. Experiments are being made of both telephone and telegraph transmissions.

**Helmut Carl** was born in Danzig, then part of Germany, in 1916. He received a doctor of engineering degree from the Technical University of Danzig in 1943.

Dr. Carl joined Standard Elektrik Lorenz in 1939. He has done development work on radar, frequency-modulation broadcast transmitters, and microwave radio systems.

# Transportable Satellite-Communication Ground Station in Brazil

J. C. FONSECA  
C. H. MOREIRA

Companhia Rádio Internacional do Brasil; Rio de Janeiro, Brazil

## 1. Station Description

The Brazilian ground station is located in the southern part of Rio de Janeiro within a non-industrial zone shielded by mountains. It covers approximately 10 000 square meters (109 000 square feet) of flat, dry, sandy soil. The station layout is shown in Figure 1.

Factors determining the choice of site were the horizon profile, ease of access, freedom from radio interference, and proximity to the international traffic center of Brazil.

The horizon profile affects the operating time available during a pass and also how much interference is encountered from nearby microwave and television stations. Table 1 describes these nearby stations. No interference has been noticed from them to date.

Figure 2 shows a polar plot of the horizon profile. Figure 3 is a chart of occurrences of

azimuth paths during satellite communications. It can be seen that 70 percent of the paths were within  $\pm 30$  degrees of north in which the maximum elevation obstacle is about 4 degrees. The highest obstacle, however, is at an elevation of 7 degrees 42 minutes, occurring in a sector used only 10 percent of the time.

Coordinates of the reference mark at the antenna site are 22 degrees 57 minutes  $6.5 \pm 1.2$  seconds South Latitude and 43 degrees 22 minutes  $20.7 \pm 1.3$  seconds West Longitude. It is 4.5 meters (14.8 feet) above mean sea level. The distance to downtown Rio de Janeiro is about 32 kilometers (20 miles).

The ground station was transported by air from the United States, where it was manufactured in Nutley, New Jersey, and arrived in Rio de Janeiro on 8 December 1962. It manually tracked the first orbit of Relay 1 on 13 December, using the 136-megacycle-per-

TABLE 1  
NEARBY MICROWAVE AND TELEVISION STATIONS

Type of Station	Location	Distance From Rio de Janeiro Ground Station in Kilometers (Miles)	Frequencies in Megacycles Per Second	Power Output in Watts
Microwave Link	Mendes	81 (50)	3928.75 3971.25	1 1
Microwave Link	Caxias	21 (13)	3891.25 4008.75	1 1
Microwave Link	Petrópolis	60 (37)	3810 3920	5 5
Television Station	Sumaré	12 (7)	82-88 7036 7250 10 900	30 000 1 1 1
Television Station	Sumaré	12 (7)	186-192 6897.5 6950 7030	20 000 1 1 1
Television Station	Sumaré	12 (7)	210-216 6170 6330 6795 6845 6895	30 000 1 1 1 1 1

second beacon in the satellite. On 12 January 1963, the first voice and teleprinter messages were sent via Relay 1 during its orbit 229 to the ground station at Nutley, New Jersey.

The ground station receives 50-cycle-per-second primary power through a 25-kilovolt aerial line. This is stepped down to 208 volts for 4-wire distribution. The installed capacity is 300 kilovolt-amperes with protection by a 30-kilovolt circuit breaker having an interrupting capability of 1000 megavolt-amperes. Four 208-volt feeders provide for the following kilovolt-ampere capacities: equipment van 140, antenna 70, heat exchanger 40, and office building 50. Emergency power is provided by two diesel engines rated at 125 and 50 kilovolt-amperes.

A satellite simulator, which is a transponder corresponding electrically to the satellite, is located 3 miles from the station reference mark. It is on a hill accessible by road and primary power is available. It is viewed with the antenna pointing at 64.72 degrees in azimuth and 2.96 degrees in elevation.

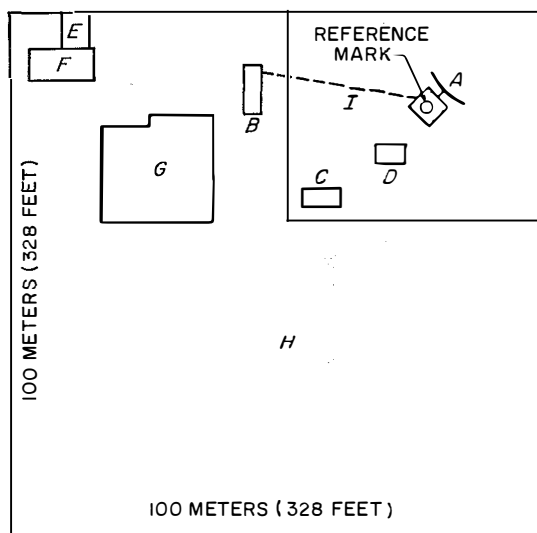


Figure 1—Station layout. The designators are as follows: A antenna, B equipment van, C reflector trailer, D heat exchanger, E power station, F emergency power plant, G office building, H future expansion, and I interconnecting cables.

Support communication facilities include a 50-baud double-current-operation teleprinter, connected by landline to a telex international network; a standard 4-wire telephone channel, for demonstration and service, connected to the downtown international telephone exchange by amplifier-equipped landlines; a 2-wire telephone connected to the local suburban network via a manual switchboard; and a simplex voice-channel 153-megacycle-per-second connection between the equipment van and the satellite simulator.

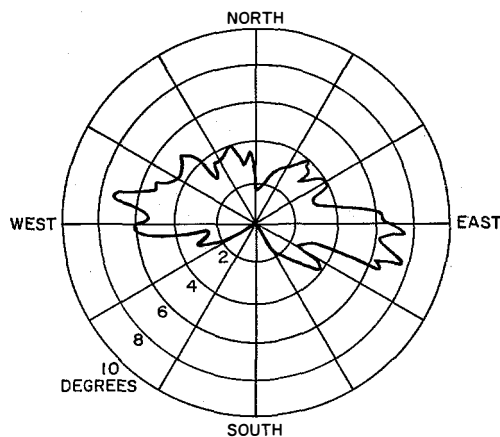


Figure 2—Polar plot of elevation obstructions in degrees.

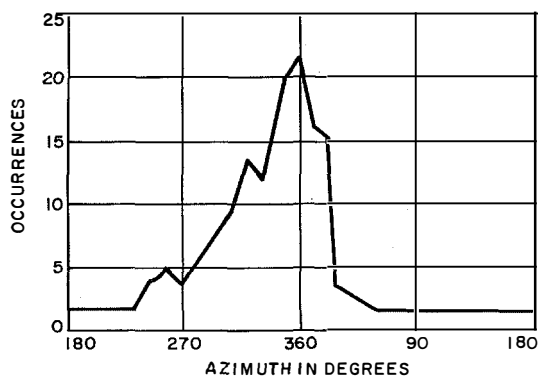


Figure 3—Azimuth directions of satellite paths during communication from December 1962 through March 1963.

## Satellite Ground Station in Brazil

### 2. Tests

Satellite acquisition is made by directing the antenna to predetermined bearings at predicted times. Satellite arrival is first signalled by manual acquisition of the 136-megacycle-per-second beacon. Automatic acquisition of the 4080-megacycle-per-second beacon signal then occurs and tracking continues automatically.

The satellite-to-station loop, station-to-station link, and the station-to-station loop constitute three sequential stages for performance evaluation. As indicated, the station communicates via the satellite with itself, with the distant station, and with itself through the distant station in these tests.

The times of events, automatic-gain-control signals from the receiving system, antenna read-out, transmitter parameters, results of terminal-equipment tests, and other data are recorded during each pass. System demonstrations include connection between the local-telephone and communication-satellite systems, to test the quality of voice, teleprinter, and facsimile operations. During each communication pass, voice is also used to coordinate experiments between the ground stations.

### 3. Test Results

The Rio de Janeiro ground station performed experiments during 44 satellite passes from 9 January to 11 May 1963 with ground terminals at Andover, Maine, and Nutley, New Jersey, in the United States; at Goonhilly Downs, England; Pleumeur Bodou, France; and Fu-

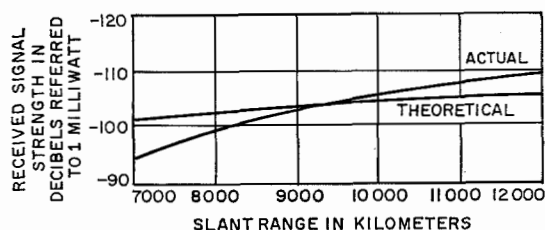


Figure 4—Actual and theoretical received signal strengths as a function of slant range.

cino, Italy. Most tests lasted between 17 and 26 minutes, with the longest being 41 minutes 39 seconds.

Most of the experiments were conducted with Relay 1. Telstar 2 was also tracked manually on very-high frequency and automatically using its 4080-megacycle-per-second beacon signal. A summary of the experiments is shown in Table 2.

TABLE 2  
SUMMARY OF EXPERIMENTS

Type	Occasions
Insertion gain	20
Continuous random-noise measurement	2
Received carrier power	27
Intermodulation distortion	1
Medium-speed data transmission	1
Two-way telephone transmission	25
Teleprinter transmission	4
Facsimile and telephoto transmission	3

Signal strength of the received carrier is plotted in Figure 4 as a function of satellite distance. The theoretical curve assumes a satellite power output of +40 decibels referred to 1 milliwatt, maximum satellite-antenna gain of 1.6 decibels, and a receiver-antenna gain of 48.4 decibels. The majority of actual mean carrier levels were in the range of  $-102$  to  $-106$  decibels referred to 1 milliwatt. Maximum and minimum levels observed were  $-94$  and  $-109$  decibels referred to 1 milliwatt. Theoretical and actual received

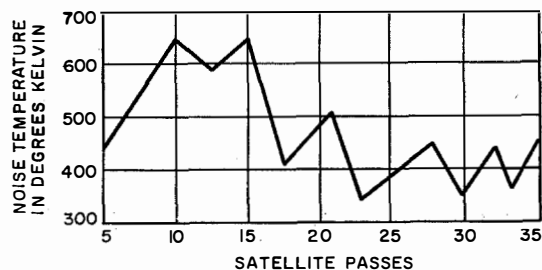


Figure 5—The equivalent system noise temperatures measured with the antenna at a 60-degree elevation at the time of each pass.

carrier signal strengths differ by 3 to 11 decibels. A number of possible sources of error exist, such as assumed satellite output power, satellite antenna gain as a function of look angle, and measurement errors in calibration. The range of signal levels for the tracking receiver extends from  $-109$  to  $-119$  decibels referred to 1 milliwatt.

The continuous random-noise test is used to determine the audio-signal-to-noise ratio. Typical values are 37 decibels on channel 1 and 42 decibels on channel 12 at a carrier level of  $-104$  decibels referred to 1 milliwatt.

Equivalent system noise temperature, shown in Figure 5, averaged between 400 and 600 degrees Kelvin, with a minimum of 350 and a maximum of 640. These figures were measured with the antenna pointing at an elevation of 60 degrees.

Slant range during passes varied from 7000 to 12 500 kilometers (4351 to 7768 miles). The average time of experiments was 21 minutes with a 30-minute maximum. Mutual visibility during April 1963 between Rio de Janeiro and Nutley, New Jersey, varied between approximately 60 and 80 minutes.

The recorded differences between ephemerides and actual tracking data ranged from 0 to  $+0.3$  degree in elevation and from  $-0.1$  to

$-0.4$  degree in azimuth. These are shown in Figures 6 and 7.

In addition to engineering experiments, a number of demonstrations were made via Relay 1. A total of 25 telephone conversations were held between ground terminals, which included calls originated in telephone exchanges. Quality was generally excellent, that is, of commercial telephone quality or better. Two simultaneous telephone conversations were relayed via satellite between Rio de Janeiro and Nutley, New Jersey, and then relayed by microwave to and from Tokyo, Japan, with satisfactory results.

**4. Conclusions**

The following conclusions are based on the results of experiments conducted to date with the Rio de Janeiro ground station.

(A) Multichannel, 2-way, high-quality telephone communications are feasible between South America, the United States, and Europe using low-orbiting satellites.

(B) There is relatively close agreement between theoretical and experimental results.

(C) Good operational performance of a medium-capacity ground station in tropical regions has been demonstrated.

(D) The transportability and flexibility of the ground station have been demonstrated.

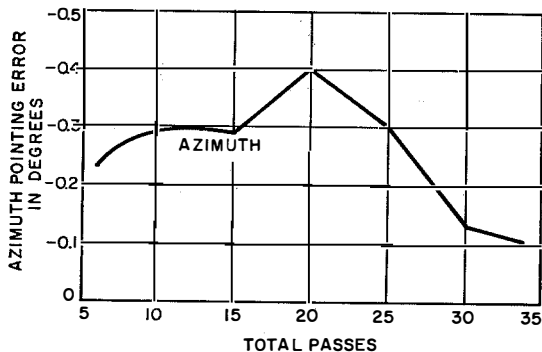


Figure 6—Antenna pointing errors in azimuth.

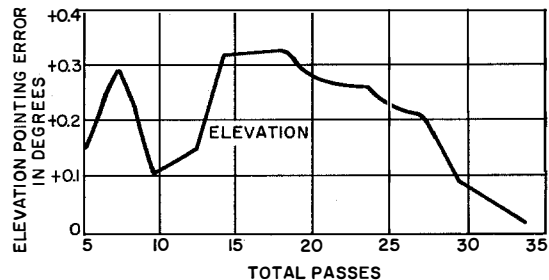


Figure 7—Antenna pointing errors in elevation.

### 5. References

1. Louis Pollack, "Radio Communication Using Earth-Satellite Repeaters," *Electrical Communication*, volume 36, number 3, pages 180-188; 1960.
2. W. J. Bray, "Satellite Communication Systems," *Post Office Electrical Engineers' Journal*, volume 55, pages 1-8; July 1962.

**John Fonseca** was born in Paris, France, on 14 February 1930. In 1955, he received a degree in electrical engineering and in 1959 in telecommunication engineering, both from the University of Brazil.

From 1953 to 1959, he was employed by General Electric S.A. In 1959, he joined Companhia Rádio Internacional do Brasil. In 1962, he received special instruction on satellite

ground-terminal equipment at ITT Federal Laboratories in Nutley, New Jersey. He is presently chief engineer of the Rio de Janeiro space-communication terminal.

Mr. Fonseca is a Member of the Institution of Brazilian Electrical Engineers.

**C. H. Moreira** was born in Ponta Grossa, Paraná, Brazil, on 26 December 1935. He obtained a degree in electronics engineering from the Instituto Tecnológico de Aeronautica in Brazil in 1959.

Since 1959, he has been with Companhia Rádio Internacional do Brasil. He was sent to ITT Federal Laboratories at Nutley, New Jersey, in 1962 to become acquainted with the satellite ground-terminal equipment that he helped to install later in Brazil. He now serves as a senior engineer at this station.

# Radio Transmitter for Satellite Communication from Goonhilly Downs Station of the British Post Office

E. A. RATTUE

Standard Telephones and Cables Limited; London, England

In Cornwall, the extreme southwestern county of England, an experimental satellite-communication station has been established at Goonhilly Downs by the British Post Office. A 10-kilowatt radio transmitter operating at 1725 mega-

cycles per second was put in service early in 1963 for transmission to the Relay satellite. Based on the transmitter design developed for the tropospheric-scatter link between Nassau, Bahamas, and Miami, Florida, it differs in that



Figure 1—Ten-kilowatt transmitter. The power control unit occupies the two open bays at the left, the transmitter drive is next, and at the right end is the klystron cabinet. Behind the power and drive units, with its panel showing at the extreme left, is the extra-high-tension cabinet.

## Radio Transmitter for Goonhilly Downs

it is capable of using either the Eimac *5KM70SF* or the Varian *VA800* klystron. The former is preferred as it has a bandwidth of 15.5 megacycles per second at the 0.5-decibel points, while the latter has a bandwidth of 8 megacycles per second at the 3-decibel points.

The transmitter is housed in three cabinets as shown in Figure 1. The heat exchanger is a separate unit shown in Figure 2.

The power control unit, which contains the auxiliary supplies, overload circuit breakers, fault-indicator lamps, and the mains isolator, is the centre control for the whole transmitter

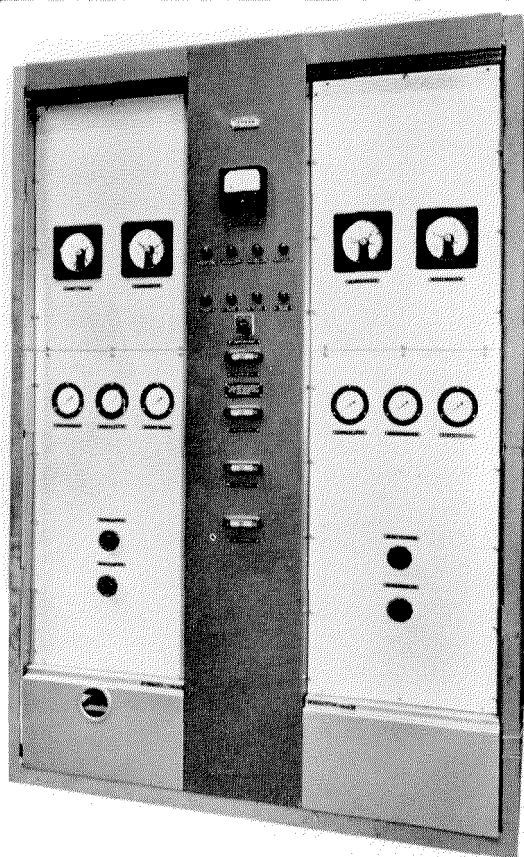


Figure 2—The heat-exchanger unit provides for monitoring the temperature and rate of water flow with provision for removing all high voltages if normal limits are not maintained.

and the heat exchanger. With the exception of the extra-high tension, the transmitter is switched on and off by two push-buttons mounted on its centre control panel.

The drive unit was supplied by the British Post Office. The remainder of the equipment was provided by Standard Telephones and Cables.

The klystron is in the front section of its cabinet with the indicating instruments and controls. Each klystron is mounted on its own trolley and by use of push-on connectors and plugs and sockets a change-over from one type to the other can be effected in approximately 10 minutes.

The output waveguide and cross coupler together with an artificial load are at the rear of this cabinet. The design and mounting of the artificial load permit its being quickly put into service.

The extra-high-tension supply is switched on and off by two push-buttons mounted on a panel above the klystron. They are electrically interlocked with the voltage control so that power can be applied only at near-zero voltage. A specially designed rotary switch controls a voltage divider to vary the grid bias on a *3J/232E* high-vacuum triode from cut-off to a predetermined positive value. The triode is in series with the power supply and a smooth application of voltage to the klystron is effected by it. The power transformer has 3 off-load taps to give outputs of 0, 10, 16, and 20 kilovolts. At the maximum voltage in each range, the positive bias on the triode is predetermined to keep the anode dissipation of the triode to approximately 1.5 kilowatts.

This triode also serves as a protective device to cut off the extra-high tension in the event of excessive current flow, waveguide flash-over, or too high a standing-wave ratio. Being at the output of the filter, the triode also prevents damage from discharge of the filter capacitor into the klystron. Its effectiveness as a voltage stabilizer, with consequent reduction in filter

size, recommends its application to later models of such transmitters.

The extra-high tension is supplied by a 3-phase transformer, vacuum rectifiers, and a filter consisting of a choke and an output capacitor that attenuates the ripple by 60 decibels. The control tube follows.

All doors to compartments giving access to high voltages are interlocked with the mains isolator via a special cable system.

A single heat exchanger is used but duplicate pumps and blowers provide automatic change-over in the event of a fault. All water outlets are monitored on dial-type meters having contacts that will open to disconnect power if the water flow is outside of the set maximum and minimum limits for safe operation. An automatic valve maintains the outlet water temperature within  $\pm 2$  degrees of 55 degrees centigrade for an ambient temperature up to 45 degrees.

**E. A. Rattue** was born in Eastleigh, Hampshire, England, on 15 August 1899. He received a certificate in telecommunications from City and Guilds College in 1928.

He joined the Western Electric Company in 1925 as a radio installation engineer. From 1928 to 1930, he was employed by International Marine Radio Company as engineer-in-charge of radio engineering.

In 1930, he joined Standard Telephones and Cables, where he has been engaged in development and commissioning of medium- and high-power broadcast and communication transmitters.

Mr. Rattue is an Associate of the Institution of Electrical Engineers.

# Graphic Methods for Calculating Coverage Attainable with Communication Satellites

R. HEPPE

ITT Intelcom, Inc.; Falls Church, Virginia

## 1. Introduction

A brief review is presented of methods developed to determine the percentage of the time one or more satellites in various orbits will be usable by a given link. Several techniques and results are included that have not previously appeared in the literature. The techniques described permit satellite coverage problems to be solved graphically, without the aid of a computer.

For a satellite to be used by a given link in a communication network, it must be visible to both ends of the link above the minimum elevation angle  $\alpha$  of the receiving antennas at the terminals. This minimum elevation angle depends on the local topography, on local weather conditions affecting the noise introduced in the receiver at low elevation angles, et cetera, but is usually on the order of 7.5 degrees. In addition, there may be other restrictions on the satellite that affect its use. For example, satellites may not be trackable if they pass directly over the ground station, because of the high azimuth slew rates required. Also, satellites that depend on solar

power supplies are not usable when passing through the earth's shadow.

If a satellite is at an instantaneous altitude  $h$  above the earth and is visible to a ground terminal at an elevation angle greater than  $\alpha$ , then the projection of the satellite on the surface of the earth will be within a circle centered on the terminal and having angular-great-circle radius  $\psi$ , where

$$\psi = \cos^{-1} \left( \frac{R}{R+h} \cos \alpha \right) - \alpha. \quad (1)$$

In this equation, which is plotted in Figure 1,  $R$  is the mean radius of the earth, approximately 3440 nautical miles (6371 kilometers). By drawing on a globe a circle of radius  $\psi$ , centered on the terminal, one can readily see where satellites must be to be visible to the terminal. If circles of this radius are drawn from the two terminals of a link, satellites in the region common to both circles will be visible to both terminals and may be used for communication if all other factors are favorable. The region common to both circles is called the mutual-visibility region.

A single satellite in orbit will have a probability  $p$  of being in the mutual-visibility region at any given instant. If the satellite is extremely high, if the distance between the two terminals of the link is small, and if an  $\alpha$  of zero is used, then the value of  $p$  may approach 0.5; if the distance between terminals is large, the value of  $p$  may be zero. The value of  $p$  associated with a given link and orbit may be found with the aid of a visibility chart. This chart also shows how long a given satellite can be expected to remain inside the mutual-visibility region during any pass, the probability that the satellite will be in sunlight and not almost overhead at one of the stations, et cetera.

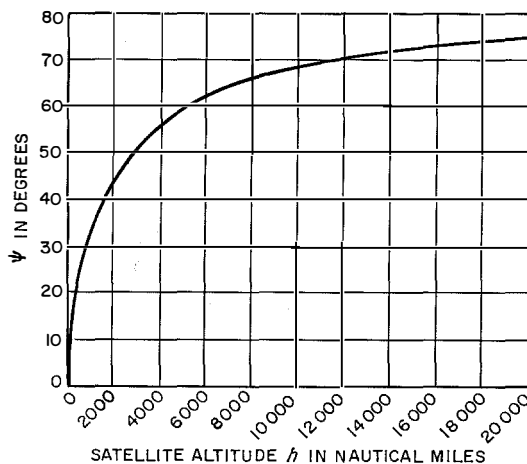


Figure 1— $\psi$  plotted as a function of satellite altitude  $h$ , assuming a ground-terminal elevation angle of 7.5 degrees and earth radius of 3440 nautical miles (6371 kilometers).

## 2. Visibility Charts

To obtain the value of  $p$  by graphic methods, it is desirable to map the world, and the

mutual-visibility region, using a map projection that gives the satellite an equal probability of being at any point of the map. For example, if a satellite is in a polar orbit, it moves at a constant rate in latitude. Since it spends an equal amount of time at every latitude, the latitude lines should be equally spaced on the map. If the period of the satellite is not an exact multiple or sub-multiple of the earth's rotational period, it will be equally likely to be at any given longitude at a particular instant and therefore the longitude lines should be equally spaced. (As explained in Section 2.8, it is possible to use this map even when the satellite period is an exact submultiple of the earth's period.)

For a satellite in circular polar orbit, therefore, the earth may be drawn as a series of equally spaced longitude lines from 0 to 360 degrees, crossed at right angles by equally spaced latitude lines from -90 to +90 degrees. Such a projection superficially resembles a Mercator map, except that in a

Mercator map the latitude lines are not equally spaced.

The region of mutual visibility on this map may be found by drawing the visibility circles associated with each terminal of the link. Although these areas are circles on the surface of the earth, they are badly distorted in the projection. The latitudes and longitudes of points on the circumference of each circle, or on the circumference of the mutual-visibility region itself, may be found by drawing the visibility circles on a globe, reading the latitudes and longitudes of points along the boundaries of the circle, and plotting them on the chart, or they may be calculated and plotted without the aid of a globe using

$$\theta = \theta_T \pm \cos^{-1} \left( \frac{\cos \psi - \sin \phi \sin \phi_T}{\cos \phi \cos \phi_T} \right) \quad (2)$$

- where  $\theta$  = longitude, positive west
- $\theta_T$  = longitude of the ground terminal
- $\phi$  = latitude, positive north
- $\phi_T$  = latitude of the ground terminal.

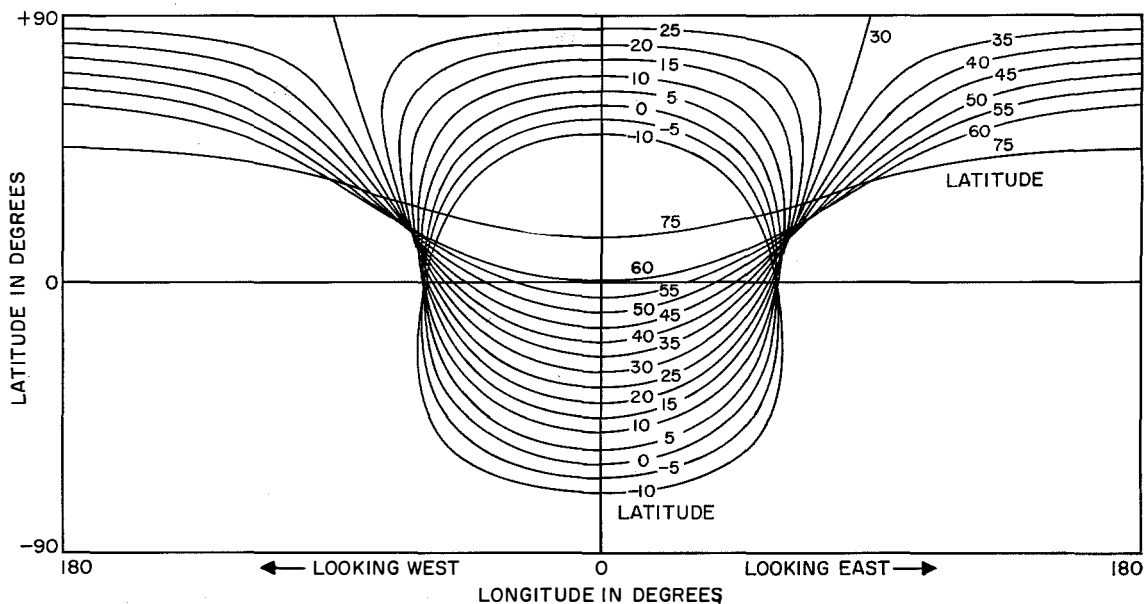


Figure 2—Template of satellite visibility contours for circular polar orbits. The numbers on the curves indicate the latitudes in degrees of various ground terminals for a minimum elevation angle of 7.5 degrees and a satellite altitude of 5472 nautical miles (10 134 kilometers). Zero degrees longitude corresponds to the actual longitude of the ground terminal.

## Graphic Methods for Calculating Coverage

If many visibility areas are to be drawn for a single orbital altitude, inclination, and ellipticity, it is convenient to make a template by plotting the contours defined by (2). Once the template is available, the visibility areas of any pair of stations may be drawn quickly.

Figure 2 shows such a visibility template for stations at latitudes from  $-10$  to  $+75$  degrees, using satellites in circular polar orbits such that  $\psi = 60$  degrees. One example of such an orbit is the combination  $\alpha = 7.5$  degrees,  $h = 5472$  nautical miles (10 134 kilometers). This orbit has a period of 5.87 hours and will be called nominally a 6-hour orbit.

To use the template, the locations of the two terminals of the link are plotted on a latitude-longitude grid of the earth, drawn on translucent paper to the same scale as the template. This grid need not show the continental outlines and it is usually more convenient to omit them. The central vertical line of the template is then placed directly under the terminal whose visibility contour is to be drawn. The

visibility contour corresponding to the latitude of the terminal is then traced, interpolating if necessary. Figure 3 shows the visibility contours for Honolulu, Hawaii, and Santa Barbara, California. The mutual-visibility region is that region common to both contours. The value of  $p$  is simply the ratio of the size of this mutual-visibility area to the size of the whole world, on the map. The size of the mutual-visibility area is readily measured with the aid of a planimeter, or by using a Bruning areagraph, and is found in this case to be 0.145.

This same chart can be used for equatorial satellites at the same altitude. Since these satellites never depart from the equator, the probability that they will be within the mutual-visibility area is simply the ratio of the length of that portion of the equator inside the mutual-visibility area to the total length of the equator. For the link shown, the value of  $p$  for equatorial satellites is 0.200.

If equatorial satellites are to be maintained with equal rather than random spacing, the

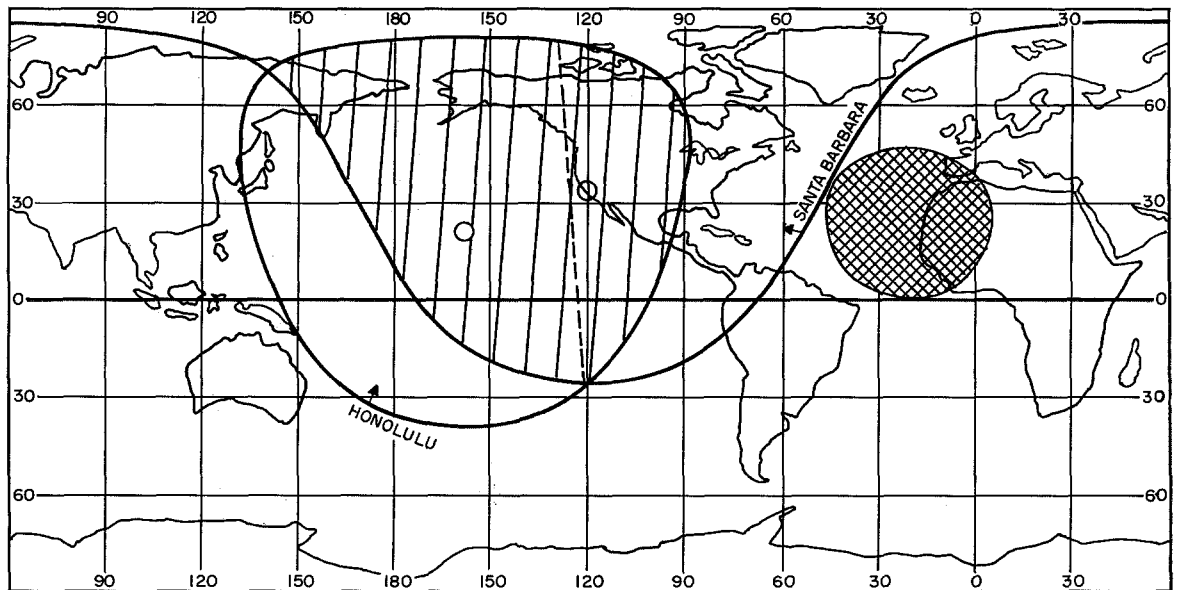


Figure 3—Visibility contours for Honolulu, Hawaii, and Santa Barbara, California. The arrows point into the visibility regions and the mutual-visibility region is common to both contours.

visibility chart shows the maximum allowable separation between satellites if 100-percent coverage is to be maintained. The minimum number required is  $1/0.2$ , or 5.

Instead of thinking of the visibility contour of radius  $\psi$  as a region of the world centered about a terminal, it is sometimes useful to think of it as a circular cap centered on earth directly beneath the satellite and moving with the satellite. If two stations are within this subsatellite cap simultaneously, they can communicate through the satellite. Thus two stations more than 120 degrees apart can never communicate on a single-hop basis through a 6-hour satellite. This concept is especially useful in the case of synchronous satellites; by drawing the visibility contours centered about the subsatellite points of a proposed arrangement of synchronous satellites, it is evident which stations can communicate directly, which links must use two satellites and an intermediate ground relay station, and which terminals cannot see any satellites. The cap concept is also useful in a medium-altitude random-satellite system in assessing the maximum number of links that can use the same satellite at the same time.

Polar satellites move across the chart in two parallel sets of inclined straight lines, since they always move a constant number of degrees per minute north or south, and at  $\frac{1}{4}$  degree per minute to the west. The inclined lines in the mutual-visibility region in Figure 3 are parallel to the paths of southbound satellites. When they come to the top or bottom of the chart, they suddenly shift 180 degrees in longitude and reverse their north-south direction. By measuring the maximum dimension of the mutual-visibility area in directions parallel to the satellite tracks, the maximum time a satellite can spend within the mutual-visibility region is readily obtained. A maximum-duration northbound pass is shown as the dashed line in Figure 3. Since the satellite track is within the mutual-visibility area from approximately 25 degrees South to about 80 degrees North latitude, and

since a satellite at this altitude travels about 1 degree per minute north or south, the maximum time any satellite will spend within the mutual-visibility region is about 105 minutes.

Extensions of the technique for drawing visibility charts for inclined and elliptical orbits are described in Sections 2.6 and 2.7.

### 2.1 RANDOM-SATELLITE COVERAGE AS A FUNCTION OF $p$

In a random-satellite system, as it is usually proposed, one or more satellites are launched in each of several orbital planes. The attitudes of these planes can be fixed with reasonable accuracy before launch, but the position of each satellite along its orbit at any future time  $t$  is not controllable in advance. Therefore, if there are more than one satellite in a ring, at certain times most of them will be closely bunched and at other times they will be relatively uniformly spread. At times when they are bunched, there may be no satellites over some parts of the world and outages will occur. These outages, although predictable once the satellites are established in orbit, will have many characteristics of random occurrences.

If all the satellite positions were statistically independent of each other, the probability  $P_D$  that no satellites were within a mutual-visibility region of normalized area  $p$  would be simply

$$P_D = (1 - p)^N \quad (3)$$

where  $N$  is the number of satellites.  $P_D$  thus represents the fraction of the time that the link will be down.

Because of the fact that several satellites will probably be launched in each of several discrete planes in a medium-altitude random system, the positions of the satellites are not statistically independent. If a mutual-visibility region such as that shown in Figure 3 were only, say, 90 degrees wide, and all satellites were put in one polar orbit, the value

## Graphic Methods for Calculating Coverage

of  $P_D$  could not be less than 0.5 no matter how many satellites were used, because the plane in which the satellites travel would be over the mutual-visibility region only half the time. Links with usable values of  $p$  almost always have mutual-visibility regions considerably wider than 90 degrees, however, and if several approximately equally spaced planes are used, the error introduced by using (3) is negligible. Reference [1] shows that if 24 satellites are distributed equally among 4 planes, the results are indistinguishable from complete randomness, and even as few as 2 planes are enough to approximate randomness closely on all but the low-latitude links. If it

is necessary for some reason to use a link having a mutual-visibility region that is narrow compared with the angular separation between orbital planes, (3) should not be used. Instead,  $1 - P_D$  should be calculated by computing the probability that an orbital plane intersects the mutual-visibility region, then multiplying this by the conditional probability that one or more satellites are within the region, given that the plane intersects the region.

It may be noted from (3) that if  $N$  satellites yield 10-percent downtime,  $2N$  satellites will yield 1-percent downtime, and  $3N$  satellites will yield 0.1-percent downtime.

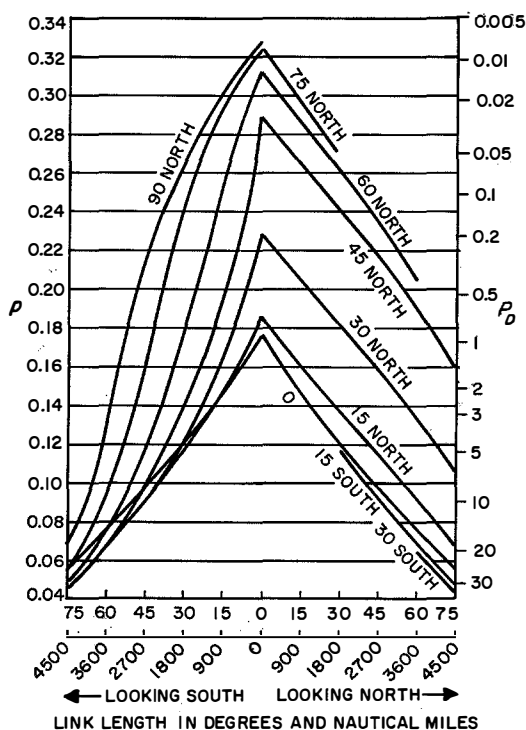


Figure 4—The effects of the lengths of north-south links on the probability of communication for random circular polar orbits at an altitude of 5023 nautical miles (9304 kilometers) and  $\alpha$  of 7.5 degrees.  $p$  is the probability of both terminals of the link having a single satellite in view.  $P_D$  is the percentage of time that the link will be down for a system of 24 satellites. The numbers on the curves are values of  $\phi_T$ , the latitude in degrees of one terminal.

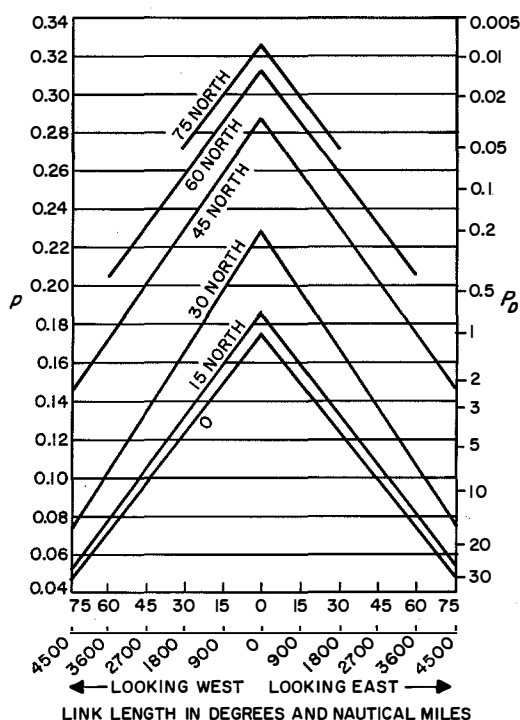


Figure 5—The effects of the lengths of east-west links on the probability of communication for random circular polar orbits at an altitude of 5023 nautical miles (9304 kilometers) and  $\alpha$  of 7.5 degrees.  $p$  is the probability of both terminals of the link having a single satellite in view.  $P_D$  is the percentage of time that the link will be down for a system of 24 satellites. The numbers on the curves are values of  $\phi_T$ , the latitude in degrees of one terminal.

The value of  $p$  associated with a link of a given length depends strongly on the latitudes of the terminals of the link and the direction of the link, as well as on the orbital altitude, orbital inclination, and the value of  $\alpha$ . In general, polar orbits are best for most links except east-west links near the equator and north-south links crossing the equator. In reference [2] the values of  $p$  for 156 different links are plotted as a function of inclination, with several values of altitude and  $\alpha$  as parameters. Even for the same link, one inclination may be best when using satellites at one altitude, and a substantially different inclination may be best at a different altitude. Because of the fact that polar orbits give some coverage to near-equatorial links, while equatorial orbits give no coverage to northerly links, it would be best to choose an inclination of around 80 or 90 degrees for the worldwide system discussed in [2] if all its satellites had to be placed in orbits of the same inclination.

Values of  $p$  as a function of link length are shown in Figures 4 and 5 for north-south and east-west links with terminals at various latitudes, using satellites in random circular polar

orbits. A scale is also given indicating the associated values of  $P_D$  in percent, if  $N = 24$ . These graphs are based on [2] and correspond to an orbital altitude of 5023 nautical miles (9303 kilometers) if  $\alpha = 7.5$  degrees ( $\psi = 58.7$  degrees). It is apparent that when polar satellites are used, terminals at high latitudes have a considerable advantage over those at low latitudes.

Furthermore, at a given latitude in the northern hemisphere, visibility looking north is much better than visibility looking south, while visibility looking east or west is somewhere in between. This is to be expected; if polar 6-hour orbits are used, a satellite will pass over the north pole on the average of once every 15 minutes. Therefore it is highly probable for any two stations that can see the region over the north pole to have a satellite in their mutual-visibility area. For this reason a relay station in Alaska, for example, may be more useful than a relay station at a lower latitude. This is shown graphically in Figures 6 and 7, in which equal-downtime contours

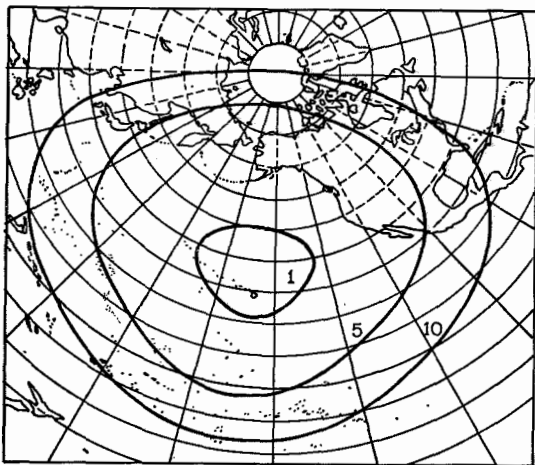


Figure 6—Equal-visibility contours for Honolulu, Hawaii, using a 24-satellite system in random circular polar orbits.  $\alpha = 7.5$  degrees and  $h = 5472$  nautical miles (10 134 kilometers). The numbers in the figure show the percentages of downtime for links operating within the various encircled areas.

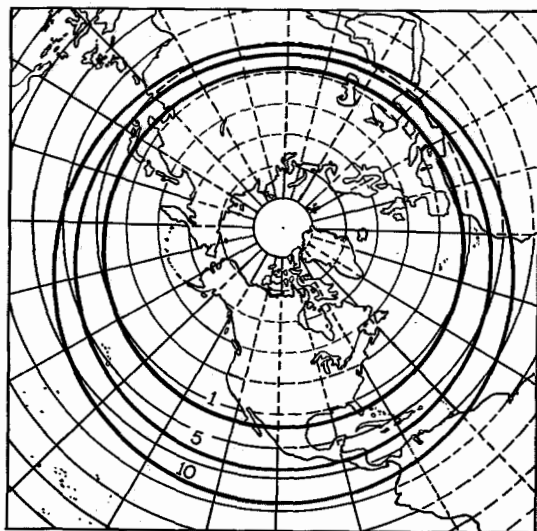


Figure 7—Equal-visibility contours for Anchorage, Alaska, using a 24-satellite system in random circular polar orbits.  $\alpha = 7.5$  degrees and  $h = 5472$  nautical miles (10 134 kilometers). The numbers in the figure show the percentages of downtime for links operating within the various encircled areas.

are drawn for Honolulu and Anchorage, Alaska, in a 24-satellite system using 6-hour random polar orbits. It can be seen that the downtime of links connecting Anchorage to almost any part of the United States, Europe, Japan, and large parts of Asia is less than 1 percent, whereas the downtime of a link connecting Honolulu with the western United States is more than 1 percent and downtime is more than 5 percent of links to Japan or the eastern United States.

In a network that must service links having a variety of lengths, latitudes, and orientations, it may be better to place some satellites in equatorial orbits and some in polar orbits. The downtime for any link in such a mixed inclination system may be calculated by multiplying the probability that none of the equatorial satellites are visible by the probability that none of the polar satellites are visible.

$$P_D = (1 - p_e)^{N_e}(1 - p_p)^{N_p} \quad (4)$$

where  $p_e$  = the value of  $p$  for the link when equatorial satellites are used

$p_p$  = the value of  $p$  for the link when polar satellites are used

$N_e$  = the number of equatorial satellites

$N_p$  = the number of polar satellites.

However, in deciding what is the optimum mix of satellites, a clear definition is required of what is meant by optimum. Optimum may mean that the worst link has a downtime no greater than a certain value, that the downtime averaged over all links is no greater than a certain value, or various links may be weighted differently. Furthermore, it may sometimes be preferable to use a double hop, through two satellites and one relay station, to service a link, rather than tailor the number and inclination of satellites in the system to make one-hop service feasible on that link. Finally, due allowance must be made for the fact that it will probably be possible to launch more satellites per booster into polar orbits

than into equatorial orbits, in calculating the optimum mix.

Satellites at inclinations other than equatorial and polar should also be considered, of course. In particular, satellites at inclinations of about 30 degrees give good service to those links that are served well by equatorial satellites, and are much easier to launch from the United States than equatorial satellites.

The advantage of sticking to polar and equatorial orbits for medium-altitude satellites, on the other hand, is that it may be possible to use simple spin stabilization without a command link or active attitude control, keeping the earth within the toroidal pattern of the satellite antenna by initially spinning the satellite about an axis perpendicular to the orbital plane. If inclinations other than equatorial or polar are used, the orbital plane will not remain perpendicular to the spin axis, and the satellite antenna pattern may point away from the earth at times, if no command link and attitude control were used. Furthermore, the rate of rotation of the orbital plane about the earth's axis is very low in a near-polar orbit, minimizing the possibility that the planes may bunch together if they have slightly different inclinations.

## 2.2 OUTAGE DURATIONS

In a system using random satellites, it is desirable to know not only the percentage of the time outages will occur, but also the distribution of the durations of outages and innages, where innages are defined as the periods between outages. Reference [3] shows that the average duration of an outage is given by

$$t_o = (1 - p)(T/N) \quad (5)$$

where  $T$  is the average time between successive appearances of a particular satellite. If the mutual-visibility region includes one of the earth's poles,  $T$  for polar orbits is approximately equal to the orbital period  $P$ .  $P$  may be

found by

$$P = 6.9726 \times 10^{-6} a^{\frac{3}{2}} \quad (6)$$

where  $a$  is the semimajor axis of the orbit in nautical miles and  $P$  is in hours.

If the mutual-visibility region does not include one of the earth's poles, a particular satellite may make many orbits before reappearing within the mutual-visibility region. Therefore the value of  $T$  will be larger than  $P$  by some factor that depends on the width of the mutual-visibility region normal to the direction of motion of the satellites, and to some extent on the length and location of the region. To find the approximate value of  $T$  to use in this case, the following procedure may be used for polar orbits.

Prepare a visibility chart and join it along its top to an inverted identical chart displaced 180 degrees to the right or left, as shown in Figure 8. A satellite track will now be a continuous straight line across the two charts, as indicated. This type of visibility chart is referred to as double-valued, since each area is mapped twice. Project the two mutual-visibility areas onto a line normal to the satellite track, and find the total projected length  $D$  of these areas, counting any overlap region twice. In Figure 8,  $D = D_1 + D_2$ .

If the orbital plane of the satellite is swept through all possible values of longitude of the ascending node from 0 to 360 degrees, the point of intersection of the satellite track and the normal to the satellite track would move along the normal for its total length  $L$  from one edge of the chart to the other. There is therefore a probability of  $D/L$  that the satellite orbit will intersect the mutual-visibility area at any instant. In Figure 8,  $D/L$  is about 0.47; therefore the satellite will intersect the mutual-visibility area, on the average, about once every two orbits. The value to use for  $T$  is correspondingly

$$T = LP/D. \quad (7)$$

For equatorial orbits having the same direc-

tion of rotation as the earth

$$T = \frac{P}{1 - (P/24)}. \quad (8)$$

The average time between outages is given by

$$t_i = \frac{(1 - P_D)t_o}{P_D}. \quad (9)$$

The fraction of outages longer than  $t$  is approximately  $\exp(-t/t_o)$ , and the fraction of innages longer than  $t$  is approximately  $\exp(-t/t_i)$  [4].

### 2.3 EQUALLY SPACED SATELLITES

The use of the visibility chart to find the minimum number of equally spaced equatorial satellites for 100-percent coverage of a given link has already been described. The chart is equally adaptable for finding the minimum number of equally spaced polar satellites. In this case, however, it is helpful to think of the latitude and longitude lines on the chart as representing celestial latitude and longitude. A polar orbital plane will therefore be a pair

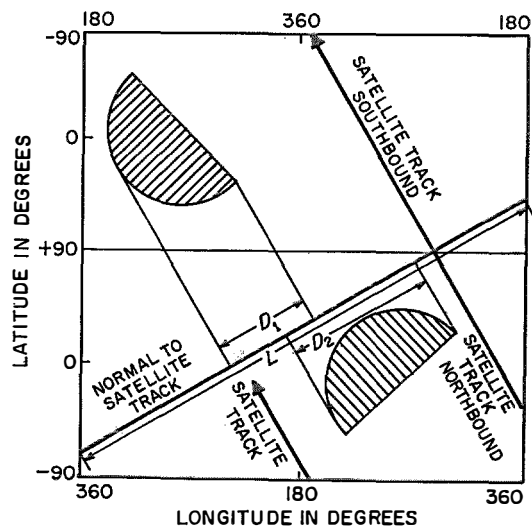


Figure 8—Method for finding the average time  $T$  between successive appearances of a particular satellite when the mutual-visibility region does not include one of the earth's poles.

of fixed vertical lines 180 degrees apart on a chart such as Figure 3, and the mutual-visibility area will move eastward across the chart once per day. The maximum separation between planes that will still permit an intersection with the mutual-visibility region 100 percent of the time can be seen to be equal to the maximum width of the mutual-visibility area in an east-west direction. However, if the planes were actually this far apart, the satellites within each plane would have to be very close together to maintain coverage at the moment the area is just getting out from under one ring and barely touching the trace of the next ring.

At any instant, a link will have a satellite visible to both terminals if satellites in the same ring are separated no farther than the height of the intersection of the orbital trace and the mutual-visibility region. If the region is intersected by several traces, the longest may be used. By trying several different numbers of planes and sliding a template in the shape of the mutual-visibility region east and west, it is possible to quickly find the optimum combination of number of planes and number of satellites per plane.

Although equal spacing of satellites theoretically permits 100-percent coverage with  $\frac{1}{3}$  to  $\frac{1}{4}$  the number of satellites that give acceptable service in a random system, it must be remembered that the effect of a satellite malfunction is considerably more severe in an equally spaced system. Replacement of failed satellites in an equally spaced system poses some difficult problems, especially if it is necessary to launch many satellites with one booster for economic reasons. Therefore, rather than think in terms of being able to use a much-smaller number of satellites if equal spacing proves technically feasible, it is probably more realistic to think of using almost the same number of satellites, but getting better coverage for a period of time until malfunctions make the system appear somewhat random.

### 2.4 EFFECT OF ECLIPSES ON BATTERYLESS SATELLITES

Satellites can be made considerably smaller and lighter by designing them without batteries. Not only is the weight of the battery eliminated, but the weight of the solar cells needed to recharge the battery while the satellite is in sunlight is saved, and there is also some weight saving in the voltage-regulating circuit. It therefore may be possible to put up more satellites per booster if they contain no batteries. However, the satellites will not operate without batteries while in the earth's shadow and the effect of this reduction in capability must be weighed against the improved coverage resulting from a larger value of  $N$ .

To calculate the effect of the earth's shadow on downtime if batteryless satellites are used, the region in which satellites will be in the shadow is projected on the visibility chart as shown by the crosshatched area in Figure 3. Within a few thousand miles of the earth the shadow is almost cylindrical with a diameter equal to the earth's mean diameter, 6880 nautical miles (12 742 kilometers). Figure 3, however, includes an extra 84 miles in the shadow diameter, which is the amount the penumbra widens out between the surface and an orbital altitude of 5472 nautical miles (10 134 kilometers).

Projected on the surface of the earth, this shadow region is a circle with a radius of 1400 nautical miles (2593 kilometers) or 23.2 degrees, the center of which is 23.5 degrees north of the equator on December 21, 23.5 degrees south of the equator on June 21, and on the equator at the equinoxes. The shadow moves across the visibility chart from east to west once per day. It is shown in Figure 3 as it would appear on December 21. It can be seen that in a few hours it will enter the Honolulu-Santa Barbara mutual-visibility region, decreasing the usable area of the region. Although the area of the crosshatched region is

constant on the surface of the earth, it is slightly variable in the cylindrical projection used, being at its maximum (for this altitude) of 0.0284 on December 21 and at its minimum of 0.0263 at the equinoxes. Therefore, when it is a few hours either side of local midnight at the center of the Honolulu-Santa Barbara link on December 21, the  $p$  of the link will decrease by 0.0284. During other times of the year the decrease will be less, partly because the area of the shadow of this projection is slightly less, but much-more importantly because only a part of the shadow area will overlap the mutual-visibility region. For many more-northerly links, the shadow region overlaps the mutual-visibility region very little during most of the year.

Thus, considering the trade-offs of leaving batteries out of the satellite, one must decide whether a moderate decrease in coverage on some links during the nighttime hours for a few months a year is more than balanced by better coverage on all links at other times, attainable by loading more satellites into each booster.

If equatorial orbits are used, the worst time for batteryless satellites is at the equinoxes, when the earth's shadow is right on the equator. Since the diameter of the shadow is 46.4 degrees, the value of  $p$  for equatorial 6-hour satellites must be reduced by 0.129 at this time.

By cutting a paper template in the shape of the crosshatched area of Figure 3, moving it east and west to represent various times of day, and moving it north and south to represent various seasons of the year, one can rapidly determine the effect of the earth's shadow on the coverage of any given link, if batteryless satellites are used. It should be noted that the size of the shadow area on the map projection will vary with altitude, just as the shapes of the visibility contours shown in Figure 2 are functions of altitude.

## 2.5 EFFECTS OF OVERHEAD PASSES

Some types of tracking antennas are unable to track satellites passing directly overhead, since they must slew 180 degrees in azimuth just as the satellite reaches the zenith. A circle can be drawn on the visibility chart to represent this forbidden region around each terminal. These circles have been drawn in Figure 3 to represent antennas that cannot track satellites passing at elevation angles higher than 85 degrees. This 10-degree-diameter cone of silence as measured at the surface of the earth intercepts an arc of 6 degrees at satellite altitude, as measured from the center of the earth. These 6-degree-diameter circles are shown around both terminals in Figure 3. As can be seen, together they decrease the usable area of the mutual-visibility region by only about 0.001, which is negligible.

If it is desired to eliminate the need for another satellite when the one in use enters the forbidden region, an allocation doctrine may be applied to prevent use of a satellite that enters the forbidden region during its pass. Here, instead of just removing the forbidden circle from the mutual-visibility region, a slice the width of this circle and parallel to the satellite track should be removed from the region. Since northbound and southbound satellites have tracks that slope in opposite directions, the length of the subtracted slice is the average between that parallel to the northbound and that parallel to the southbound tracks. For mutual-visibility regions that include one of the earth's poles, it is easiest to visualize this slice by preparing a double-valued chart as shown in Figure 8; for other regions a single-valued chart is adequate. Even if the whole slice is removed, the effect in most cases is relatively small.

Long links, which can ill afford to have their mutual-visibility regions reduced, often have mutual-visibility regions that do not include the terminals. In such cases there will never be overhead passes when the link is in use.

## Graphic Methods for Calculating Coverage

### 2.6 VISIBILITY CHARTS FOR INCLINED ORBITS

Calculations similar to those illustrated previously may be made readily for inclined orbits. The principal change in preparing the mutual-visibility charts is that the separations between parallels of latitude must be non-uniform, so that the space between two parallels is proportional to the fraction of its time that the satellite spends between those two latitudes. Since a satellite at inclination  $i$  never passes over any point on the earth north or south of  $i$  degrees, regions beyond latitude  $\pm i$  may be omitted from the chart.

Longitude lines may be drawn as equally spaced vertical lines perpendicular to the latitude lines, if desired, since the satellite is equally likely to be at any particular longitude at any moment. This type of chart is easy to prepare and is adequate for measurement of mutual-visibility areas. However, if some of the other properties of the chart are used that depend on the satellite track being a straight line, the longitude lines must be properly distorted so that they are still equally spaced but no longer straight or vertical. Once templates similar to Figure 2 have been prepared in either of these ways for a particular inclination and altitude, they are as easy to use as the polar templates.

### 2.7 VISIBILITY CHARTS FOR ELLIPTIC ORBITS INCLINED AT 63.4 DEGREES

If a satellite is placed in an elliptic orbit with apogee over the northern hemisphere, it can spend much more than half its time over the northern hemisphere. It will also be at a higher altitude, for a given booster power, than it would be in a circular orbit. Both of these factors improve coverage. Most elliptic orbits experience a rotation of the line connecting apogee and perigee, caused by the oblateness of the earth. This would place the apogee for about as much time above the southern hemisphere as above the northern hemisphere, over a long period of time. However, for orbits inclined close to 63.4 degrees,

this rate of rotation is small or zero, and the apogee can remain over the northern hemisphere for years. Thus elliptic orbits at this inclination are of particular interest.

In such an orbit, the satellite will always pass over a given latitude at a particular altitude. Knowing the apogee and perigee altitudes above the surface, the semimajor axis and eccentricity of the orbit can be calculated from

$$a = \frac{q_1 + q_2}{2} + 3444 \quad (10)$$

and

$$e = (q_2 - q_1)/2a \quad (11)$$

where  $q_1$  and  $q_2$  are respectively perigee and apogee altitudes above the surface in nautical miles.

From these, the instantaneous satellite altitude and latitude may be calculated as functions of time by use of (12) through (15). One can plot latitude as a function of altitude from these results. The visibility chart can then be prepared as before, using (2), except that  $\psi$  will now be a function of latitude instead of a constant.

$$E - e \sin E = 2\pi t/P \quad (12)$$

$$\tan \frac{v}{2} = \left( \frac{1+e}{1-e} \right)^{\frac{1}{2}} \tan \frac{E}{2} \quad (13)$$

$$h = \frac{a(1-e^2)}{1+e \cos v} - 3444 \quad (14)$$

$$\phi = \sin^{-1} [\sin i \sin (\omega + v)] \quad (15)$$

where  $e$  = eccentricity

$t$  = time, in hours ( $t = 0$  occurs as satellite passes through perigee)

$E$  = eccentric anomaly

$v$  = true anomaly

$\omega$  = argument of perigee (if perigee occurs at maximum southerly latitude,  $\omega = 270$  degrees)

$\phi$  = latitude.

Equations (12) through (15) need be solved for only enough values of  $t$  to get the shape of

the curve for latitude as a function of altitude. If perigee occurs at maximum southerly latitude and apogee occurs at maximum northerly latitude, which is usually the case of interest, the end points of the curve are known immediately, and use of about 4 intermediate values of  $t$  in (12) through (15) will permit the curve to be drawn. The values of  $\psi$  as a function of latitude may then be found from this curve with the help of Figure 1.

Since the orbit is inclined, the parallels of latitude on the chart will have to be non-uniformly spaced.

#### 2.8 USE OF VISIBILITY CHARTS WHEN PERIOD IS AN EXACT SUBMULTIPLE OF EARTH'S PERIOD

If a satellite makes an integral number of revolutions around the earth in a small number of days, it will repeat certain tracks on the mutual-visibility chart time after time. To investigate the behavior of such a system, a series of charts similar to Figure 8 should be prepared, except that they should be  $n$ -valued rather than double-valued, where  $n$  is the number of half orbits the satellite makes before passing over its starting point again in the same direction. Alternate charts in this vertical array will be right side up, with the intervening ones inverted and displaced 180 degrees in longitude. The satellite track can then be drawn from top to bottom across the vertical series of charts. Assuming that its integral relationship can be perfectly main-

tained, the satellite will cross the mutual-visibility regions only along the single track indicated on the  $n$  charts. The periods during each day when the satellite will be visible can then be noted readily.

#### 3. Acknowledgment

The author is indebted to Mr. F. J. Altman for his many valuable ideas that contributed substantially to this paper.

#### 4. References

1. H. K. Karrenberg and R. D. Luders, "Orbital Aspects of Nonsynchronous Communication Satellite Systems," Aerospace Corporation Report TDR-169(3550-01)TN-1; September 1962.
2. F. V. Bennett, "Further Developments on the Required Number of Randomly Spaced Communication and Navigation Satellites," National Aeronautics and Space Administration Report TN D-1020; February 1962.
3. J. D. Rinehart and M. F. Robbins, "Characteristics of the Service Provided by Communications Satellites in Uncontrolled Orbits," *Bell System Technical Journal*, volume 41, number 5, pages 1621-1670; September 1962.
4. O. S. Rice, "Intervals Between Periods of No Service in Certain Satellite Communication Systems—Analogy with a Traffic System," *Bell System Technical Journal*, volume 41, number 5, pages 1671-1690; September 1962.

**Robert Heppe** was born in New York, New York, on 16 June 1926. In electrical engineering, he received a B.S. degree with honors from California Institute of Technology in 1948 and an M.S. degree from Columbia University in 1955. He served with the United States Navy during the second World War.

After employment with Sylvania Electric Prod-

ucts Corporation, Arma Corporation, and Reeves Instrument Corporation, he joined ITT Federal Laboratories in 1952. In 1962, he transferred to ITT Intelcom, and has specialized in studies of satellite coverage and replenishment statistics.

Mr. Heppe is a member of the American Institute of Aeronautics and Astronautics.

# Spacecraft Technology for Satellite Communication Systems

M. E. BRADY

ITT Intelcom, Inc.; Falls Church, Virginia

## 1. Introduction

There is a wide range of choices for selecting the technical approach in each space subsystem area. A sophisticated technical approach often gives clear performance advantages over a simpler one, but this improved performance is usually obtained by increasing system complexity, cost, and development time.

The best technical approach is determined by the design constraints of the over-all requirements, the time schedule for system implementation, economic factors, and the relative development risks. Thus selection of the best approach for the design of spaceborne systems cannot be accomplished without reference to a specific situation. This paper reviews several of the alternatives and compares their risks and advantages.

## 2. Synchronous System

The required spacecraft characteristics of a synchronous satellite communication system are generally well known.

Because of orbital perturbations introduced by the triaxiality of the earth, such a spacecraft requires a small propulsion subsystem to remain on its assigned longitude station throughout its mission life. To keep the spacecraft on station, based on present knowledge, requires ground tracking, command, and control of the satellite.

To direct the propulsion thrusts correctly, attitude control is required. The attitude-control subsystem, however, can also point a pencil-beam antenna at the earth. At synchronous altitude, the most-direct approach is 4-axis stabilization of the satellite attitude with respect to the geocentric direction and the satellite-to-sun vector. This may be achieved by means of an active self-contained control system using earth and sun sensors, plus torque devices such as reaction wheels and gas jets. Several major problems must be solved if this method is to be useful for operational systems. These are:

(A) High reliability in a complex subsystem that must operate throughout the mission life of the spacecraft.

(B) Sensing devices that can determine the geocentric direction reliably and precisely.

(C) Injection maneuvers to attain with high reliability the required initial attitude and velocity vectors at deployment.

(D) The weight and complexity associated with the system of sensors, torque devices, and logic circuits.

An alternative to full stabilization at synchronous altitudes is the Syncom approach [1]. This uses spin stabilization to keep one axis of the spacecraft fixed in inertial space. It also employs a system of on-board logic to derotate a pencil-beam antenna pattern electronically and to pulse-modulate the reaction jets in the proper phase when necessary for spin-axis reorientation or orbit control.

This approach is relatively complex, requiring both a telemetry and a ground command link for operation. If a photovoltaic power system is employed, it also causes a reduction in area efficiency of the solar array mounted on the cylindrical surface of the spinning satellite to about 30 percent of that achievable with a fully oriented solar array.

Because of the continuous coverage afforded by each synchronous satellite to a large geographical area and the relatively large investment in orbit-control and attitude-control equipment, it is most efficient to provide a relatively small number of synchronous satellites to serve a large number of communication links. Our presently available launch vehicles can place a maximum weight of about 700 pounds (318 kilograms) into synchronous orbit. This weight corresponds to a transmitter power output of 16 to 25 watts, possibly shared by a number of repeaters as required by the modulation, multiplex, and multiple-access features of the communication-link design. It is estimated that launch vehicles in the next few years will permit spacecraft weights of 1000 to 2000 pounds

(454 to 908 kilograms) for synchronous systems, with corresponding increases in available power.

The primary advantages of the synchronous system are the continuous coverage furnished to the large heavily populated areas of the earth and the concomitant simplicity of the system control and ground-terminal design. Such a system will enjoy a relatively high communication efficiency when it can use highly directive spacecraft antennas. The statistical characteristics of the traffic loads imposed at widely separated ground terminals will have diurnal variations that peak at different times, resulting in efficient system utilization.

A spacecraft at synchronous altitude also has the advantage of operating in a relatively radiation-free environment, compared with that encountered at medium altitudes.

### 3. Medium-Altitude Systems

In its simplest form, the spacecraft portion of a medium-altitude satellite communication system will consist of a relatively large number of small spin-stabilized satellites deployed randomly in a number of circular polar orbital rings. Each spacecraft will consist essentially of a power system, a communication repeater, and the necessary support structure.

To irradiate the earth, the spin axis of the satellite must be perpendicular to the orbital plane so that the toroidal antenna pattern always lies in the plane of the orbit. However, unless means such as magnetic torque is provided to reorient the spin axis, the choice is restricted to polar or near-equatorial orbital planes. With inclined orbits, the nodal regression of the orbital plane will cause the nulls of the antenna pattern to point at the earth part of the time.

For a satellite in a 6-hour polar orbit, the gain of the earth-coverage toroidal antenna pattern, with a reasonable allowance for spin-axis misalignment, is approximately that of an ideal isotropic radiator.

To achieve the efficiencies possible with the injection of a number of satellites into each orbital ring by a single currently available launch vehicle, the weight of each satellite is limited to the 120-pound (54-kilogram) class. Such satellites can carry single communication repeaters that provide approximately 4 watts of transmitter output power.

For development in the near future, the medium-altitude system has several significant advantages. The experience already gained with Relay and Telstar is directly applicable to such a system. Consequently, the dollar cost and time required for spacecraft development would be much less than for the more-complex synchronous system.

Furthermore, the inherent reliability of such a system is much higher than that of a synchronous system because of the simpler design of the spacecraft and its smaller number of parts. It can be shown that the mean-time-to-failure of a medium-altitude satellite will be three or more times that of the synchronous satellite, assuming that production processes and component parts of the same quality are used in each system. This difference can have a profound effect on over-all system reliability and cost, as will be discussed later.

One additional reliability feature of the medium-altitude system is the fact that each satellite is not permanently associated with a particular geographical area. Because of this permutability of the satellites in the system, the failure of individual satellites will cause a small average increase in link outage times but will not result in complete disruption of certain links, as in the case of the synchronous stationary satellite. This feature of gradual service deterioration is particularly important in military systems.

### 4. Gravity Gradient Stabilization

An attractive alternative to spin stabilization for attitude control at medium altitudes is gravity gradient stabilization, whereby the

spacecraft axis of inertia attempts to align itself along the gradient of the earth's gravitational field. Thus a pencil-beam antenna may be pointed toward the earth without an active control system. It has the further advantages of permitting the use of inclined orbits, providing improved coverage for communication links in the medium and equatorial latitudes, and permitting slightly larger launch-vehicle payloads than polar orbits. There are, however, several significant problems in the use of gravity gradient stabilization.

The first of these is whether the gravity gradient torque is of sufficient magnitude at useful orbital altitudes to ensure the continuous dynamic alignment of the required satellite axis with the earth vertical, considering internal and external disturbance torques such as solar pressure and outgassing. The gravity gradient effect varies as the cube of the distance from the geocenter, being extremely small compared with other torques at the altitudes of interest. Figure 1 illustrates this by showing the variation with satellite altitude of the aligning torque on a body possessing typical moments of inertia. This torque must be able to overcome the other misaligning torques.

The second significant problem is that of damping the librational energy of the gravity-gradient-stabilized satellite, considering the extremely small energy content of the dynamic system.

The third problem is that of initial deployment, during which it is necessary to remove unwanted turning rates and ensure that the 180-degree ambiguity in position will be correctly resolved so that the satellite finally stabilizes with the antenna pointed toward the earth. It is also necessary to ensure that the orbit eccentricity is sufficiently small so that introduced perturbing forces, which are very close to the natural frequency of the system and are very difficult to damp, do not result in large librational motions.

### 5. Precise Spacing in Orbital Rings

A fundamental characteristic of random-orbit systems is that there will always be a probability of outages on particular links regardless of the number of satellites in the system. The percentage of outage time, however, can be made quite small if enough satellites are used. One way of eliminating outages is to carefully match the orbital speeds of the satellites in each ring and establish their initial phasing in the ring. They will then remain uniformly spaced and thus avoid the occasional clustering that produces outages in a random-orbit system.

This precise spacing may be achieved for a number of satellites deployed from a single launch vehicle by using extremely precise vernier speed control of the final stage of the launch vehicle to achieve the required equispacing and identical speeds. This technique involves a rather-large weight penalty because of the vernier propulsion and control equipment. The probability of successful deployment is also much less than for a random-orbit system because of the sequential effects on the launch vehicle resulting from the injection maneuvers.

This method of deployment creates a problem with regard to the replacement of failed satellites, since the orbital speed and position of each replacement must be matched exactly to that of the failed satellite. Under these conditions, injection of a single satellite into an established orbital ring requires a much-higher order of guidance and timing accuracy than the initial precise deployment of a ring of satellites from a single vehicle. It also requires the availability of a large launch vehicle for initial deployment of each ring and a smaller vehicle for the replacement of single satellites. An alternative replenishment philosophy would be to establish new rings of equispaced satellites from time to time rather than try to fill the holes in the initial rings left by failed satellites.

Another method of achieving precise spacing is to deploy one or more satellites from a launch

vehicle with the approximate desired injection conditions and to rely on a propulsion capability within the spacecraft to achieve the final set of precise conditions. The synchronous satellite, of course, is a special case of a controlled orbit. The necessity for spacecraft propulsion, ground command, and attitude control to achieve precise spacing introduces the same problems of size, weight, and complexity to the spacecraft design that were discussed for the synchronous stationary system.

The last-described method has the advantage that the orbit-control capability is available for subsequent corrections to remove the effects of perturbing forces and the accumulated effects of initial errors. This would relax somewhat the accuracy requirements for initial deployment.

## 6. Phase-Steered-Array Antennas

An interesting consideration is the use of phase-steered-array antennas to direct the energy radiated by the satellite toward the earth or, ideally, toward the desired receiving ground station. One possible way to accomplish this is based on the principles of the active Van Atta array [2]. Such a system uses amplifiers, preferably with small frequency offsets, inserted into the connections between the conjugate Van Atta array elements, to form an antenna beam electrically and to provide gain. Best use of such an array to relay communications between ground stations requires the development of techniques to direct each signal toward the desired ground receiving terminal. The use of a large number of small identical amplifiers connected between the antenna elements provides for graceful degradation of the satellite performance with component failures, since a number of amplifiers may fail in a random manner with only minor effect on the directivity and strength of the antenna beam.

## 7. Communication Capacity

Communication capacity of a satellite for a given ground receiving system is limited by

the received power at the ground terminals, which is a function of both the effective radiated power of the satellite and the propagation path losses.

Figure 2 shows the received ground power for a number of the satellite-antenna configurations previously discussed, as a function of the allowance that must be made in the antenna beamwidth because of uncertainty in the satellite attitude. The received powers in this figure are referenced to that from a perfectly stabilized synchronous satellite using an antenna beam that illuminates the portion of the earth from which the elevation angle of the satellite is greater than 5 degrees. This is designated point *A* on the figure. The convergence near point *A* of the curves for satellites at 24-hour, 12-hour, and 6-hour altitudes with similar earth-coverage antennas illustrates the fact that, if attitude-control uncertainty is not

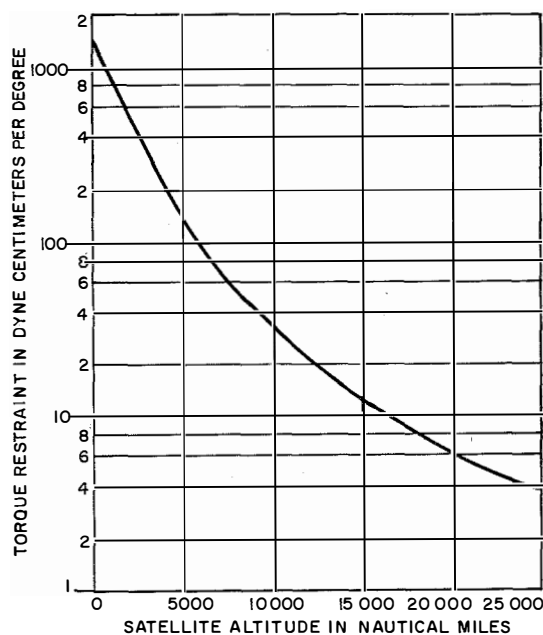


Figure 1—Torque restraint as a function of altitude for a typical gravity gradient satellite. The transverse moments of inertia  $I_x$  and  $I_y$  each equal 2000 slug-feet squared. The moment of inertia about the longitudinal axis  $I_z$  equals 20 slug-feet squared.

considered, increase in space loss as satellite altitude is increased is almost exactly compensated by the decrease in the required antenna beamwidth for earth coverage and the consequent increase in gain.

The picture for earth-coverage pencil-beam antennas changes somewhat if the necessity of allowing for the effects of attitude-control uncertainty on the required antenna beamwidth for earth coverage is recognized. Point *B* shows the 2-decibel loss encountered when the antenna beamwidth of a synchronous satellite is broadened enough to account for a  $\pm 2.0$ -degree uncertainty in attitude. Points *C* and *D* indicate the received power that might be expected from gravity-gradient-stabilized satellites at 6-hour and 12-hour altitudes, respectively, where additional antenna beamwidth of  $\pm 5$  degrees provides for the undamped librational motion or static misalignment of such a satellite.

Point *E*, at a relative level of  $-9$  decibels, is the expected received power from a spin-stabilized satellite in a 6-hour orbit when misalignment of  $\pm 15$  degrees between satellite spin axis and the orbit plane is taken into account in the toroidal earth-coverage antenna pattern. Although the effects of nodal regression and perturbing forces are decreased as the satellite altitude is increased, the net communication performance for a spin-stabilized satellite decreases sharply as the orbital altitude is increased. Point *F*, the received power from a spin-stabilized satellite at 12-hour altitude with attitude uncertainty of  $\pm 10$  degrees, is approximately 3 decibels below that of the 6-hour satellite.

The three upper curves illustrate spin-stabilized satellites at 6-hour, 12-hour, and 24-hour altitudes where the radiation from a cylindrical phase-steered array  $2.5\lambda$  in diameter and  $2.5\lambda$

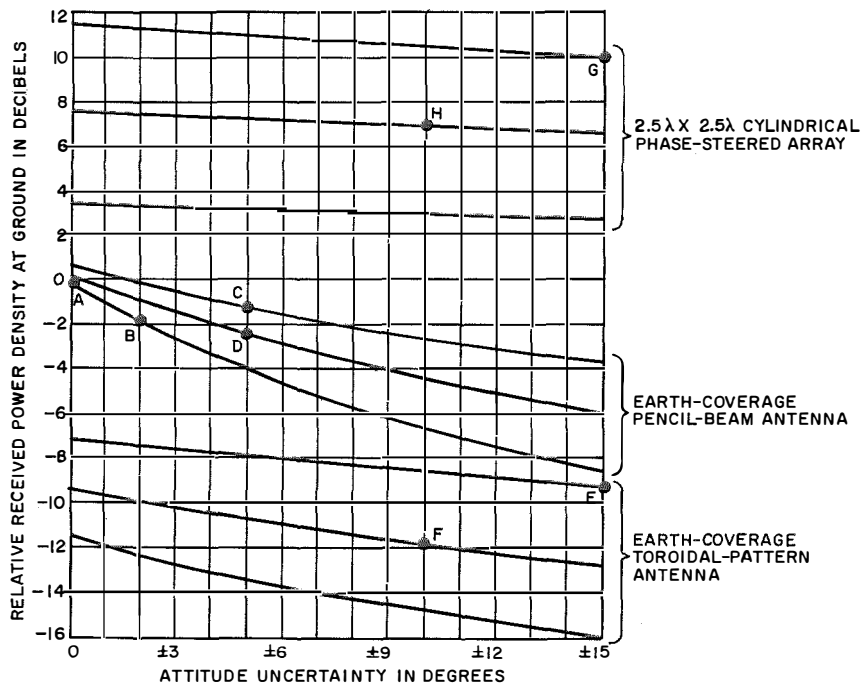


Figure 2—Relative received power density at the ground terminal for various spacecraft antenna configurations and altitudes. For each antenna configuration, the top curve is for a 6-hour satellite, the middle curve for a 12-hour satellite, and the bottom curve for a 24-hour satellite. Corresponding altitudes are 5600, 10 900, and 19 300 nautical miles (10 371, 20 187, and 35 744 kilometers), respectively.

in length is directed toward the receiving ground station. The axis of the cylindrical array is assumed to be nominally at right angles to the orbital plane. Points *G* and *H* illustrate the performance achieved for 6-hour and 12-hour satellites using spin-attitude errors of  $\pm 15$  degrees and  $\pm 10$  degrees, respectively, as before.

At 4 gigacycles per second, such an array would be only 7.5 inches (19 centimeters) in both diameter and length, would contain 48 to 64 elements, and would require the same number of identical microwave amplifiers. The performance in terms of received power from such a system at 6-hour altitude, however, is 19 decibels above that of the same spin-stabilized satellite with a toroidal earth-coverage pattern. Even if the over-all efficiency of the phase-steered-array amplifiers was 10 to 12 decibels poorer than the efficiency of the conventional system using a single receiver and a travelling-wave-tube amplifier, the net improvement in communication capacity would be highly significant.

### 8. Reliability

The impact of spacecraft reliability on total costs of a satellite communication system is illustrated in Figure 3, which shows for a 6-year period the total cost of launch vehicles, launch operations, and spacecraft for establishment and replenishment of a synchronous satellite system and a medium-altitude satellite system. The following assumptions are used.

- (A) Each launch costs 10 million dollars.
- (B) Launch operations are at a rate of 8 per year until the systems are established. Replenishment launches are made whenever the number of functioning synchronous satellites in orbit falls to 6 or the number of functioning medium-altitude satellites in orbit falls to 27.
- (C) The launch success probability for the synchronous system, because of the additional sequences and/or vehicle stages involved, is 0.50.

The launch success probability for the medium-altitude system is 0.70.

(D) Each launch vehicle places 1 spacecraft in synchronous stationary orbit or 6 spacecraft in medium-altitude random orbits.

As was noted previously, using presently available high-reliability components, mean-time-to-failure of a medium-altitude satellite is estimated to be a little longer than 3 years. Using similar components and processes, the mean-time-to-failure of the synchronous satellite would be approximately 1 year because of the increased complexity and larger number of components.

For the first 6 years of system operation, these reliability figures result in space-system costs of 470 million dollars for the synchronous system and 190 million dollars for the medium-altitude system. Under these conditions, the synchronous system does not appear to be economically attractive now and must await advances in component reliability, launch-vehicle capability, and space-system technology.

### 9. Spacecraft Power Systems

The capacity and performance of a satellite communication system are limited by transmitter

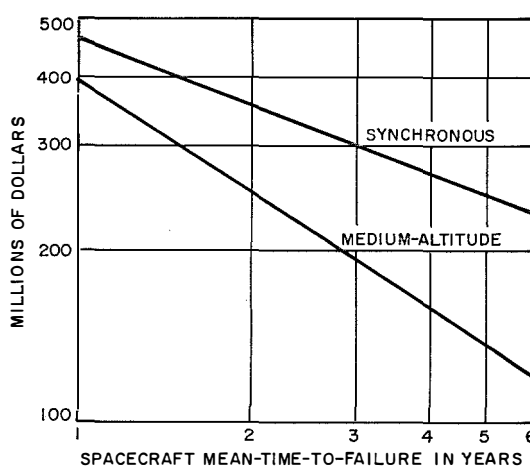


Figure 3—Total space-subsystem cost of satellite communication systems as a function of mean-time-to-failure for a 6-year period.

## Spacecraft Technology for Satellite Systems

power output from the satellite, which is in turn directly controlled by the available primary power.

The comparative performances of several spacecraft power systems, ranging from the conventional solar cell and battery to a projected 100-kilowatt reactor and turbine, are given in Table 1. It shows that the specific power output of these systems increases rapidly with size.

System *A*, comprising solar cell and battery such as might be employed in the spacecraft of a military communication network, has a specific power output of only 0.5 watt per pound. A degradation factor of 50 percent is included in the design because of the radiation environment that might be created by a high-altitude nuclear explosion. A commercial network might allow a degradation factor of only 20 percent and would perform as described in system *B*.

If the batteries are omitted from a medium-altitude polar-orbit satellite so that it does not operate during eclipse periods, as much as 20

pounds of weight might be saved from a 125-pound satellite, allowing a proportionate increase in the number of satellites orbited by each launch vehicle. System *C* describes this. The omission of batteries would result in each satellite being incapacitated an average of only 2 percent of the time. However, the impact of these outages will always be felt by the communication links in the region of local midnight.

System *D* gives the improvement in specific performance achieved with a fully stabilized synchronous satellite using an oriented solar array in a more-benign radiation environment.

Systems *E*, *F*, and *G* describe power systems using nuclear-isotope heat sources and thermoelectric converters. Such systems offer advantages with regard to spacecraft weight, size, and attitude control. For example, it is not necessary to provide an exterior surface for the mounting of solar cells, nor to orient the solar array to the sun. If alpha-emitting fuels, such

TABLE 1  
SPACECRAFT POWER SYSTEMS

Power Supply	Application	Direct-Current Power in Watts	Power-System Pounds Per Watt	Remarks
A. Solar cell and battery	Medium-altitude spin-stabilized satellite	25	2.0	50-percent degradation allowance for natural- plus artificial-radiation environment.
B. Solar cell and battery	Medium-altitude spin-stabilized satellite	25	1.6	20-percent degradation allowance for natural-radiation environment.
C. Solar cell	Medium-altitude spin-stabilized satellite	25	0.8	20-percent degradation allowance. 2-percent average annual outage during eclipse periods.
D. Solar cell and battery	Synchronous satellite, oriented solar array	100	1.2	10-percent degradation allowance for artificial-radiation environment and solar flare protons.
E. Isotope-thermoelectric	Medium-altitude satellite	25	1.2	Use of $\beta$ -emitting fuel may require component shielding.
F. Isotope-thermoelectric	Synchronous satellite	100	1.0	Use of $\beta$ -emitting fuel may require component shielding.
G. Isotope-thermoelectric	Large synchronous satellite	500	0.7	Use of $\beta$ -emitting fuel may require component shielding.
H. Reactor-thermoelectric	Large synchronous satellite	500	1.1	Shielding of radiation-sensitive components required.
I. Reactor and mercury turbine	Very-large synchronous satellite	3000	0.25	Shielding of radiation-sensitive components required.
J. Reactor and mercury turbine	Communication space station	100 000	0.02	Isolation and shielding of personnel and radiation-sensitive components required.

as plutonium-238, are used, handling and component-shielding problems are greatly reduced. Beta-emitting fuels, such as strontium-90, are presently more-readily available, but introduce serious problems of safety and irradiation of the spacecraft components. These problems must be solved before the use of such supplies is feasible for satellite communication systems.

Systems *H*, *I*, and *J* are reactor-powered supplies, using thermoelectric, thermionic, or Rankine-cycle conversion. For very-large spacecraft power systems, such as those required for a communication space station, reactor systems have no competitors.

Systems using solar collectors and thermoelectric or thermionic conversion are feasible up to 10 kilowatts. Although calculations demonstrate a very-high specific power output, the solar collector so influences the design of the rest of the spacecraft, such as the basic structural configuration and the attitude-control system, that it is difficult to determine realistic typical performance. For the near future, solar collector systems do not appear to be practical for satellite communication space stations because of the problems in erecting and orienting the collector.

**10. Space Radiation Environment**

Communication satellites orbiting the earth at various altitudes will be exposed to the deleterious effects of natural space radiation, such as charged particles trapped in the earth's mag-

netic field, solar flare particles, and cosmic particles from galactic space. The charged particles entrapped in the magnetic field are a mixture of electrons and protons of various energy levels, while the solar and galactic particles are primarily protons. In addition to this natural environment, the satellites may be exposed to an enhanced electron-radiation environment in the magnetic field due to high-altitude nuclear detonations.

The radiation level is a function of position in space. Satellites orbiting the earth in this environment will encounter varying particle dosage rates, depending on their orbits. In polar orbits, the satellites will encounter the solar and galactic protons as well as the charged particles entrapped in the magnetic field. In equatorial or low-inclination orbits, the satellites will remain within the magnetic field and encounter only the entrapped particles, since the magnetic field will keep out most of the protons from outer space. The entrapped-radiation environment varies with altitude, the most-intense area being located approximately 2000 nautical miles (3704 kilometers) above the geomagnetic equator. The intensity diminishes rather rapidly at higher altitudes. Present radiation environment estimates are given in Tables 2 and 3.

The radiation environment degrades the performance of satellite solar cells and transistors. In the case of solar cells, a reduction in their power output is experienced as a function of

TABLE 2  
ELECTRON FLUX RADIATION ENVIRONMENT ESTIMATES

Energy Level in Millions of Electron-Volts	Particles Per Square Centimeter Per Year for Polar Orbit of 5600 Nautical Miles (10 371 Kilometers)	Particles Per Square Centimeter Per Year for Equatorial Orbit of 19 300 Nautical Miles (35 744 Kilometers)
Total	$6.9 \times 10^{14}$	$1.6 \times 10^{12}$
>1.0	$3.5 \times 10^{13}$	$5.0 \times 10^{11}$
>1.6	$9.0 \times 10^{12}$	$1.2 \times 10^{11}$
>2.0	$3.5 \times 10^{12}$	$4.0 \times 10^{10}$
>3.0	$6.9 \times 10^{11}$	$1.0 \times 10^{10}$

TABLE 3  
PROTON FLUX RADIATION ENVIRONMENT ESTIMATES

Energy Level in Millions of Electron-Volts	Particles Per Square Centimeter Per Year for Polar Orbit of 5600 Nautical Miles (10 371 Kilometers)
$0.1 < E < 5$	$1.0 \times 10^{14}$
> 20	$3.3 \times 10^9$
> 50	$7.0 \times 10^8$
>100	$1.3 \times 10^8$
>200	$1.2 \times 10^7$

the total particle dosage encountered. In the case of transistors, the performance characteristics are altered as a function of both dose rate and total dosage. Fortunately, since transistors can be located well-inside the satellite structure, they can be shielded adequately from most of the radiation environment. Solar cells, on the other hand, are shielded by glass, quartz, or sapphire, with limited effectiveness. Low-energy particles can be kept out by reasonably thick shielding, on the order of 0.030 inch (0.762 millimeter). However, higher-energy particles are difficult to keep out and it becomes necessary to provide a sufficient margin of cells over the number required for satellite operation to allow for the degradation effect.

Figure 4 shows the degradation in short-circuit current of a number of commercially available *n-p* solar cells when irradiated with 1-million-electron-volt electrons. Also shown are the equivalent total dosages caused by the natural-radiation environment encountered at several altitudes over a 3-year period. These equivalent dosages include the effects of electrons and protons of various energy levels that would not be kept out by about 0.030 inch (0.762 millimeter) of glass or quartz. From these figures, it is evident that the higher altitudes provide greater security from the radiation environment.

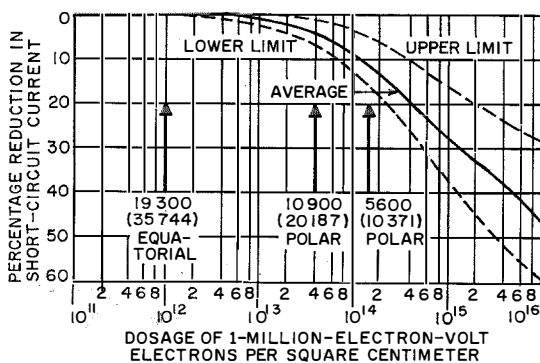


Figure 4—Percentage reduction in short-circuit current of typical *n-p* solar cells irradiated by 1-million-electron-volt electrons. The arrows indicate equivalent 3-year dosages for the altitudes in nautical miles (kilometers) and the orbits stated.

A more-serious effect is the introduction of high-energy electrons into the magnetic field by high-altitude nuclear detonations. Fission-produced electrons have an energy spectrum up to 7 million electron-volts, and the total number of electrons that would be trapped in the magnetic field would be a function of the altitude and yield of the detonations. The effect of these injected electrons on semiconductors could be far-more serious than the natural-radiation environment. To date, only a few nuclear devices have been detonated above the atmosphere, and these were at relatively low altitudes compared with anticipated communication-satellite altitudes. These detonations introduced electrons of sufficient quantity and speed to have deleterious effects on satellites in orbit at the time.

To estimate the total potential effect of high-altitude detonations on semiconductors, an examination of the maximum level of injected electrons that could be entrapped by the magnetic field reveals the order of magnitude of this effect. The magnetic energy density of the magnetic field is  $B^2/8\pi$ , where  $B$  is in gauss. A rough upper estimate of the omnidirectional intensity of entrapped electrons at an altitude of approximately 6000 nautical miles (11,112 kilometers) might be  $5 \times 10^{10}$  electrons per square centimeter per second, if it is assumed that the magnetic field is capable of confining 20 percent of this energy density in the form of the fission-product spectrum. Although the decay rate of these entrapped particles would be rather rapid, the exposure in one day could be on the order of  $4 \times 10^{15}$  electrons per square centimeter and approaching  $10^{18}$  over several days, or approximately two orders of magnitude higher than the 3-year exposure caused by the natural-radiation environment. It is estimated that such a level of radiation might be achieved at this altitude by a 10-megaton total yield. This level of radiation would seriously degrade solar cells and greatly increase the shielding requirements for transistors.

However, the total entrapment would decrease at the higher altitudes, since the strength of the

TABLE 4  
LAUNCH-VEHICLE TRENDS

Vehicle	Approximate Payload in Pounds (Kilograms) at Synchronous Altitude		Approximate Vehicle and Launch Costs in Millions of Dollars	Operational Availability
	28-Degree Orbit	Equatorial Orbit		
Atlas-Agena D*	300 (136)	100 (45)‡	6.0	Now
Thrust-Augmented Thor-Delta†	150 (68)	—	2.4	1964
Atlas-Centaur*	1400 (635)	900 (408)	10.0	1965
Titan III-C	3000 (1361)	2000 (907)	12.0	1966

\* Multiple restart required.  
 † Solid injection stage required.  
 ‡ With addition of solid third stage, approximately 700 pounds (318 kilograms).

magnetic field at the equator decreases as the inverse cube of the distance from the center of the earth. Hence, again the higher altitudes would provide greater security from entrapped electrons created by nuclear detonations.

11. Launch-Vehicle Trends

The performance of satellite communication systems is controlled essentially by the satellite-to-ground-link budget, which is controlled in turn by the size and weight of the satellites as determined by launch-vehicle capabilities and costs.

Table 4 gives comparative performance estimates of several launch vehicles in terms of their payload capability for synchronous inclined and equatorial orbits, plus the approximate vehicle and launch costs. These do not include the costs of the payload. Figure 5 plots these data in terms of the cost per pound of payload at synchronous altitude.

Note that the launch-vehicle portion of the over-all costs will trend sharply downward with the larger vehicles available in the near future, such as Atlas-Centaur and Titan III-C.

Figure 5 also shows the approximate cost of using a solid rocket stage with the Atlas-Agena D to place a satellite in synchronous orbit. This results in a much-lower cost per pound in orbit, but it also introduces an additional uncontrolled stage that must be spin stabilized. The satellite

orbit-control system is thus burdened with removing the injection errors introduced by this stage.

12. References

1. "Advanced Syncom, Syncom II Summary Report," Hughes Aircraft Company; 31 March 1963.
2. R. C. Hansen, "Communications Satellites Using Arrays," *Proceedings of the IRE*, volume 49, number 6, pages 1066-1074; June 1961.

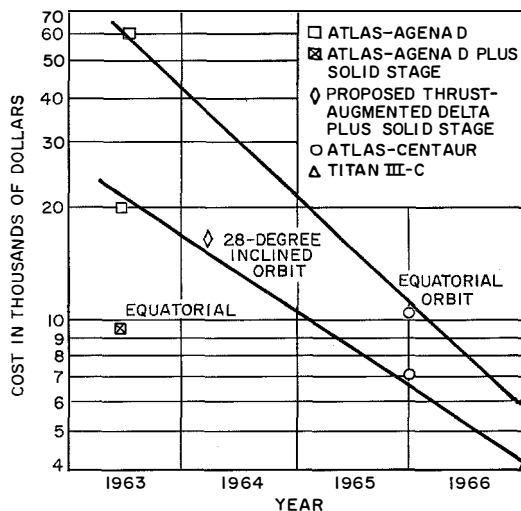


Figure 5—Curves of vehicle and launch costs per pound of payload at synchronous altitude.

## Spacecraft Technology for Satellite Systems

**M. E. Brady** was born in Los Angeles, California, in 1924. He received a B.S. degree in electrical engineering in 1945 and a Master of Engineering degree from the University of California at Los Angeles in 1959.

From 1947 to 1954, he was an electronics scientist with the United States Navy Electronics Laboratory developing long-range underwater sound detection and signaling systems. From

1954 to 1962, he was with the Ramo Wooldridge Corporation and Space Technology Laboratories, working on communication, navigation, guidance, and space probe systems. In 1962, he joined ITT Intelcom, where he is now director of the Space Systems Division.

Mr. Brady is a Senior Member of the Institute of Electrical and Electronics Engineers.

# Terrestrial Navigation by Artificial Satellites

P. C. SANDRETTO

International Telephone and Telegraph Corporation; New York, New York

## 1. Introduction

Our recently acquired ability to orbit artificial satellites around the earth has permitted the development of a novel system of navigation. This system [1] was developed by the Applied Physics Laboratory of Johns Hopkins University for the United States Navy. Many American industrial laboratories, including those of the International Telephone and Telegraph Corporation, participated in this development.

The system employs a stable oscillator in the satellite and a receiver at the location where position is to be determined. The receiver has the ability to measure the doppler shift in the transmitted frequency. An ephemeris lists the position of the satellite as a function of time.

The approach of the satellite transmitter increases the number of waves that pass the receiving antenna in a given interval of time, causing an apparent change in the wavelength. This change is given by

$$\lambda_r = \frac{c - v \cos \theta}{f_t} \quad (1)$$

where  $c$  is the velocity of radio waves in free space,  $v$  is the linear velocity of the satellite,  $f_t$  is the frequency of the satellite transmitter, and  $\theta$  is the angle between the direction of travel of the satellite and a line connecting the satellite and the observer (see Figure 1). The received frequency  $f_r$  will be

$$f_r = \frac{c}{\lambda_r} = \frac{f_t c}{c - v \cos \theta}. \quad (2)$$

If  $X$  is the path traveled by the satellite from some initial point to its closest approach to point  $P$  and  $R$  is the distance from the point of closest approach to point  $P$ , then

$$\cos \theta = \frac{X}{(X^2 + R^2)^{1/2}}. \quad (3)$$

By substituting (3) in (2), the expression for the received frequency becomes

$$f_r = \frac{f_t c}{c - vX/(X^2 + R^2)^{1/2}}. \quad (4)$$

The rate of change of the received frequency when the satellite is closest to the observer can be found by differentiating (4) and giving  $X$  a value of zero. Accordingly

$$\frac{df_r}{dX} = \frac{f_t v}{cR}. \quad (5)$$

If the velocity of the satellite is constant during the time it is within observation range, then it follows that the rate of frequency change is the same with distance as with time; therefore  $df_r/dt$  may be substituted for  $df_r/dX$  in (5). If this equation is then rearranged, the distance from the satellite to the observer at the time of its closest approach is expressed as

$$R = \frac{f_t v}{c(df_r/dt)}, \text{ for } t = 0. \quad (6)$$

Equation (6) shows that it is possible to obtain the position of the observer by:

- (A) Knowing the exact position of the satellite when the doppler frequency shift is zero ( $f_r = f_t$ ),
- (B) Knowing the exact velocity of the satellite, and
- (C) Calculating the distance from the satellite to the observer at the time of its nearest approach.

The Transit\* system broadcasts a signal that gives corrections to the orbital data in the

\* The name of the system discussed in this paper.

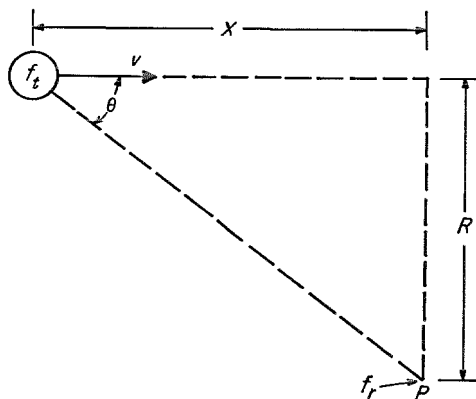


Figure 1—Principle of Transit system.

ephemeris. In addition, the satellite broadcasts time signals.

Figure 2 shows the geometry of the orbit. It is seen that the observer may be at either of two positions located at right angles to the projection of the orbit on the surface of the earth for any observation of the doppler frequency. This ambiguity can be resolved by taking readings on two successive passes of the satellite, by taking readings on more than one satellite, or by using an approximate position determined by dead reckoning.

## 2. Relationship of Transit to Earlier Technology

It is desirable to determine how this navigation system relates to or how radically it departs from the mass of electronic technology employed by earlier systems. It then becomes possible to forecast the performance that may be expected. All of the earlier navigation systems may be classified as self-contained or classical [2]. The self-contained systems (see Figure 3) are essentially computers that extend a past position to a present position and then correct the calculation by making an observation of some natural phenomena. There

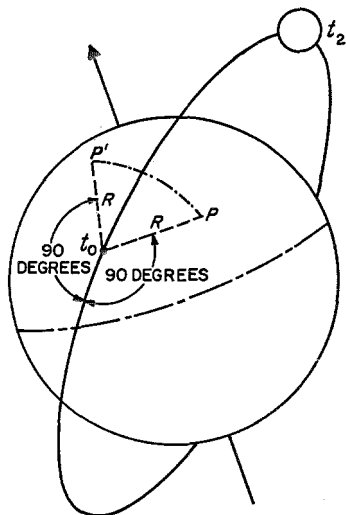


Figure 2—Geometry of the orbit.

are only four known types of self-contained systems. These make observations on celestial bodies, the atmosphere's pressure system, doppler phenomena, and inertial space. Clearly, Transit is not a self-contained system. The classical systems (Figure 3) all employ radio transmission between the known and unknown positions. These systems all make some observation on the time or times of transmission. The simplest (from the standpoint of the phenomenon used but not the instrumentation) is the single-path one-way system used in Navarho and Dectra. The most-accurate designs produced thus far have been the single-path round-trip systems commonly used to determine distance with conventional radar and distance-measuring equipment. Accuracies of the order of 3 feet are not unknown with these systems. Historically, the oldest are the multiple-path systems such as are used with direction finders consisting of two dipoles attached to a common crossarm and rotated together. Loran and Decca, despite their far-more-complex instrumentation, operate on the multiple-path principle of the simple dipole pair.

The satellite system relates to the classical systems and yet it differs to some extent. At first consideration it appears to be a single-path system, but this is not the case, for observation of the transmission over only one path would yield no usable information. What actually occurs is the comparison of the transmission over one path with that over a second path that is present between the satellite and observer an instant later, then with a third path present an instant later, et cetera. In this respect, it is a true multiple-path system with the transmission over the various paths made sequentially rather than simultaneously. It is not unlike Loran, for with that system also the bursts of transmission do not occur simultaneously. Transit is the approximate reciprocal of the latest doppler direction finders, which rotate a single dipole and measure the resulting doppler frequencies. If our

conclusion is correct that it is a multipath system, then its figure of merit is given by

$$d\phi/d\theta = 2\pi n \cos \theta. \quad (7)$$

In (7)  $d\phi/d\theta$  expresses the possible accuracy of a system where  $n$  is the number of wavelengths between the collectors or radiators and  $\theta$  is the angle between a line connecting them and the direction to the receiver or transmitter (that is, depending on whether multiple radiators or multiple collectors are in use with the particular system). Assuming that observations are used over a period of 1.5 minutes, velocity is 27 369 kilometers per hour (456 kilometers per minute), and frequency is 200 megacycles per second ( $\lambda = 1.5$  meters),

the figure of merit is approximately 2 860 000. This figure of merit compares with about 19 000 for standard Loran and about 240 for Decca. Thus, it would appear that the Transit system is capable of the highest accuracy yet attained with multiple-path systems. Since the satellite system uses very-high frequencies, it is free from the effects of atmospheric static, the aurora borealis, and sunspots, and yet it furnishes worldwide coverage.

### 3. Satellite

The first Transit satellite to achieve successful orbit was launched on 13 April 1960. The fifth was launched on 15 November 1961. All

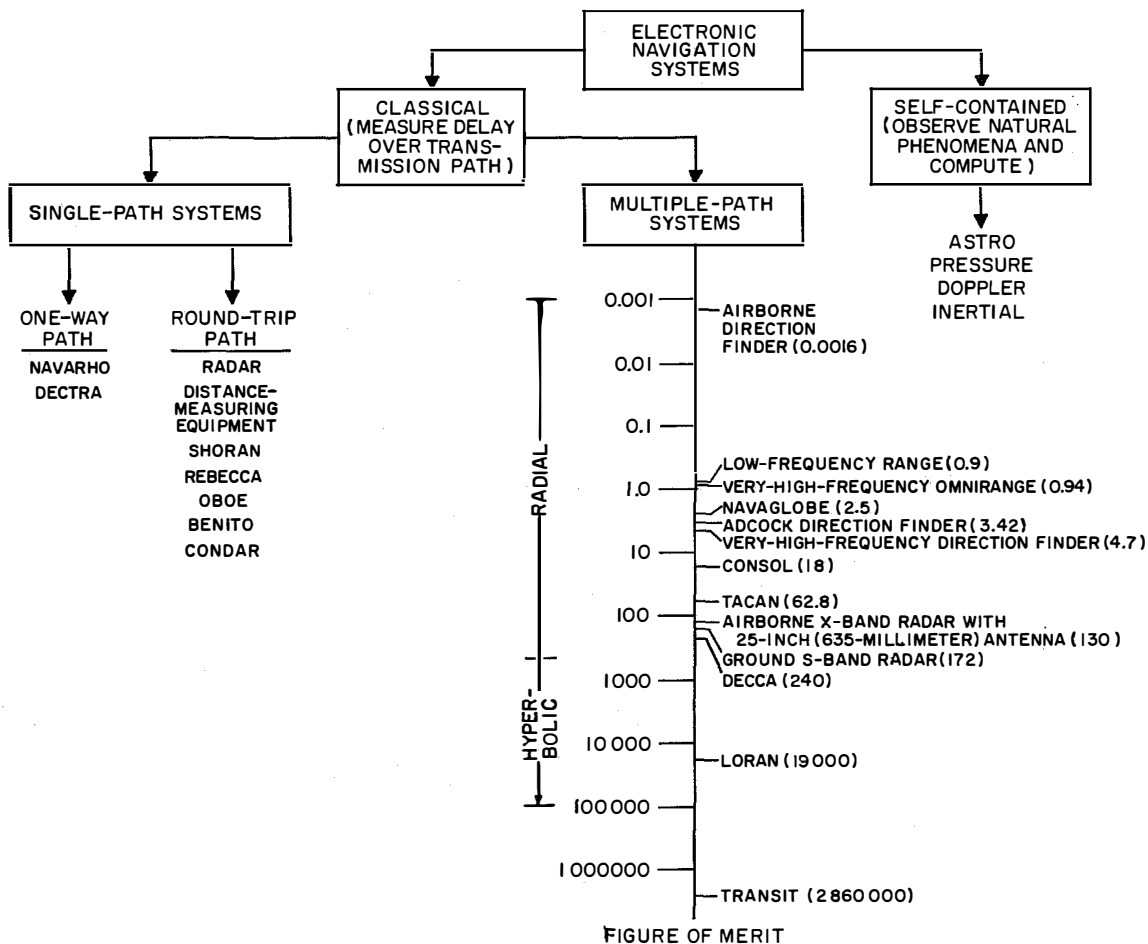


Figure 3—Classification of electronic navigation systems.

## Terrestrial Navigation by Artificial Satellites

five satellites have different designs. Figure 4 shows Transit satellite *IB*, which is representative of these devices.

Transit *IB*, the first navigation satellite to achieve successful orbit, was a 36-inch (914-millimeter) sphere that weighed 265 pounds (120 kilograms). This sphere was encircled by several banks of solar cells that charged storage batteries containing fluid electrolyte. The launching vehicle imparts a spin to the satellite that causes undesirable fluctuations in the received frequency. To remove the spin, it is first necessary that the satellite have no wobble or nutation motion [3]. The amplitude of the nutation motion can be reduced to approximately zero by a nutation damper. In this satellite, nutation damping was accomplished by the electrolyte in the battery. When the nutation was removed, the spin was

eliminated by releasing a weight attached to a cord wrapped around the equator of the satellite. After the cord is played out, it is cut and the weights fly off into space. For dynamic balance, two cords and two weights are employed.

To ensure long life for the satellite, reliability was emphasized in its design. In addition to meticulous selection of components, redundancy was incorporated by employing two crystals, two amplifiers, two power supplies, double wiring, et cetera.

Four transmitters were included in satellite *IB*. These transmitters had an output power of approximately 100 milliwatts and operated on harmonically related frequencies of 54, 162, 216, and 324 megacycles per second. Two receivers were incorporated for receiving and recording the orbit data. An infrared scanner

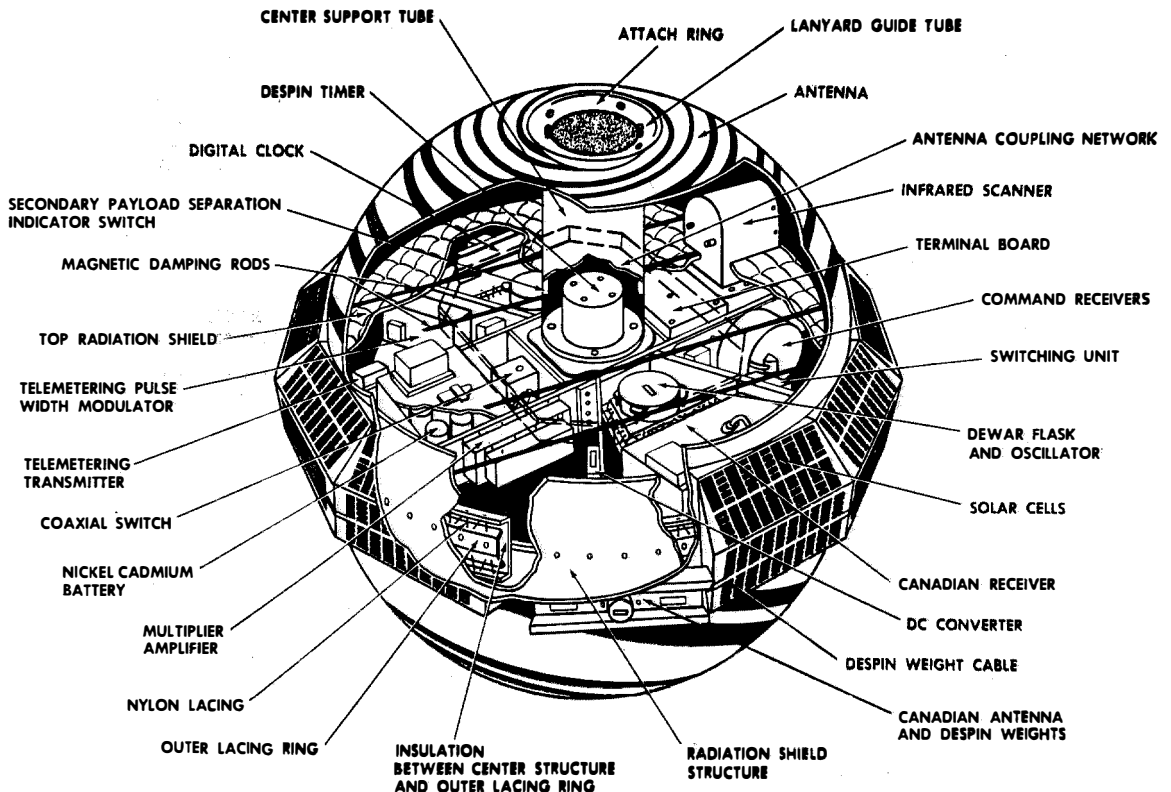


Figure 4—Transit *IB* satellite, cutaway view.

was used to monitor the satellite's rotation during the first four days of its flight. In addition, telemetry equipment was included to transmit satellite performance data to the launching site.

Every effort was made to produce a design that would protect the quartz crystals, which originate the frequencies, from temperature changes. Maximum use was made of the vacuum environment of space. Since the shell of the satellite experiences the greatest variations in temperature as it passes in and out of the earth's shadow, it was separated from the internal instrumentation platform by several inches of space. The platform was attached to the shell by nylon lacings, which are poor conductors of heat. The platform was supported against the launching force by a fiberglass tube. The instrumentation platform was surrounded by both an insulation blanket and a radiation shield. The crystals were housed in gold-plated multiple flasks that were connected to the platform by nylon cords. The crystal frequency is 3000 kilocycles per second and a stability of 1 part in  $10^8$  has been obtained. It was decided that oscillators with higher stability were not practical within the satellite.

In satellite *IVA*, a radioisotope thermoelectric generator weighing 4.5 pounds (2 kilograms) was used for power in addition to solar cells [4]. This unit generates 3 watts of power for an estimated period of 5 years.

Orbit corrections are transmitted to the satellite twice every 24 hours and stored within its magnetic memory. Every 11.18 seconds, precise position of the satellite is broadcast in binary notation, that is, coded as phase modulation of the basic transmission. This modulation consists of a 60-degree phase advance followed by a 60-degree phase lag and does not interfere with measurement of the doppler frequency. These broadcasts are triggered by a frequency divider consisting of 25 transistor circuits controlled by the highly stable oscillator previously mentioned. In addition to transmitting orbit parameters, the satellite trans-

mits a time-synchronizing pulse from its stable oscillator. A signal-injection ground station monitors the time pulses from the satellite and compares them with an arbitrary standard. It then transmits to the satellite a digitized time correction. Thus, the satellite constitutes a self-contained system in that it transmits a correction to the ephemeris as well as the accurate time, so that there is no need for the observer to correct his time standard from some other source, such as station *WWW*.

#### 4. Ground-Station Receiver

Figure 5 is a photograph of the model 1002 ground receiver developed for the United States Navy for use with the Transit navigation system. This receiver [5] differs from conventional designs in the following respects:

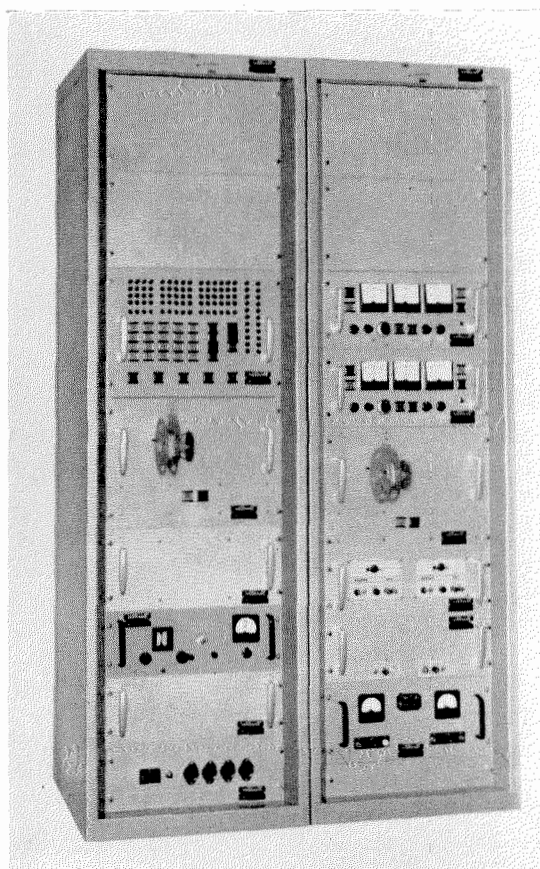


Figure 5—Model 1002 satellite doppler tracking station.

## Terrestrial Navigation by Artificial Satellites

(A) It incorporates a so-called phase detector to limit the apparent noise bandwidth and thus gives very-high performance.

(B) It receives simultaneously on two harmonically related frequencies and computes a refraction correction.

(C) Its output is a punched paper tape capable of being inserted directly into a digital computer. The tape is a record of doppler frequency versus real time.

Figure 6 is a block diagram showing the essential elements of one-half of the radio-frequency section of the receiver, which is designed to operate at 162 and 216 megacycles per second. An essential element of the receiver is a highly stable (1 part in  $10^{10}$ ) crystal oscillator connected to a frequency synthesizer that is the source of several stable frequencies used in the operation of the dual receiver. The receiving antenna is connected to a radio-

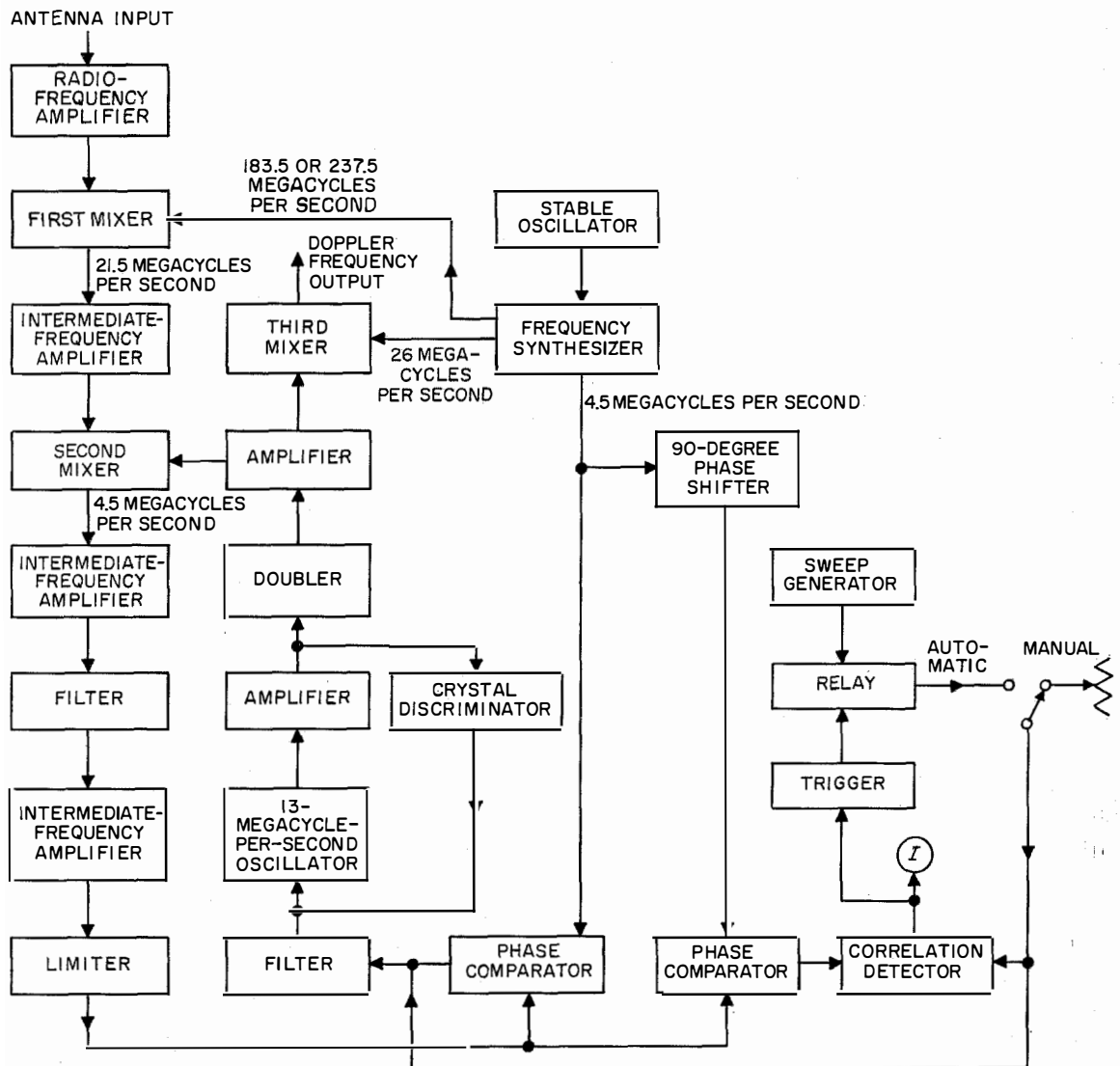


Figure 6—One half of the radio-frequency section of the model 1002 receiver.

frequency amplifier, the output of which is mixed with either 183.5 or 237.5 megacycles per second from the synthesizer to produce a beat frequency of 21.5 megacycles per second. This intermediate frequency is passed to an amplifier and then to the second mixer, where it is mixed with a frequency from a voltage-controlled oscillator. This oscillator is of the inductance-capacitance type and operates at a frequency of 13 megacycles per second. Its stability is maintained by the use of a crystal discriminator. This is a well-known technique, but in the equipment under discussion, the discriminator uses quartz crystals to form the frequency-determining elements. The output of the voltage-controlled oscillator is amplified and then doubled, the output frequency being 26 megacycles per second. This frequency, beating with the first intermediate frequency of 21.5 megacycles per second, produces a second intermediate frequency of 4.5 megacycles per second. There are two 4.5-megacycle-per-second intermediate-frequency-amplifier stages with a crystal filter between them.

This intermediate-frequency amplifier has a bandwidth of 3 kilocycles per second for a response of -6 decibels. At 5 kilocycles per second above or below the center frequency, the response is attenuated by more than 60 decibels. After amplification and limiting, the 4.5-megacycle-per-second output is connected to a phase comparator that requires a second frequency for its operation. This frequency is supplied from the frequency synthesizer. The output of the phase comparator is essentially a direct voltage that is passed through a resistance-capacitance filter. Actually, any one of four such filters can be selected. These give equivalent noise bandwidths of 5, 15, 50, or 100 cycles per second. The output of the selected filter is the voltage that controls the voltage-controlled oscillator. Thus it is seen that the 4.5-megacycle-per-second intermediate frequency will always be in phase with the frequency output of the synthesizer.

Note the absence of a conventional detector. The output of the receiver is derived by novel means. The frequency that is being injected into the second mixer will vary as a function of the carrier frequency being received at that moment. This oscillator frequency is also mixed in the third mixer with 26 megacycles per second from the synthesizer. The difference between the two frequencies is the doppler beat that constitutes the output of the receiver. The input noise figure of the receiver is less than 6 decibels for a 127-decibel gain.

The circuit described for phase locking the receiver would be satisfactory if the range of operation were unlimited or had very-wide limits. Actually it is necessary that there be some way to lock the voltage-controlled oscillator approximately to the incoming signal at the time of initial reception. This function requires several additional circuits. The lock-on circuits begin with a second phase comparator that makes use of the 4.5-megacycle-per-second frequency also used by the phase comparator that was previously described. In the auxiliary comparator, however, the 4.5-megacycle-per-second frequency is shifted in phase by 90 degrees. Thus, when the output of the first comparator is maximum, that of the auxiliary comparator is zero. By comparing the outputs of the two comparators, an indication of signal strength is obtained and presented on a meter located on the receiver panel. A voltage introduced into the voltage-controlled oscillator by a manually controlled adjustable resistor can control the phase of the injected frequency and adjust it to a value to produce maximum output. For automatic control, a sawtooth generator may be substituted for the manually controlled adjustable resistor. The voltage from this generator is applied through a relay actuated from the correlation detector. When lock-on occurs, the sweep generator is disconnected.

The doppler output of the receiver just described is combined with that of a second similar receiver operating on a harmonically related frequency in a refraction-correction

unit that will be discussed later. The single output is passed to the data-reduction unit, shown simplified in Figure 7. This unit records the parameters necessary to derive the position data on a paper tape that may be inserted into the input of a digital computer programmed in accordance with the equation of the phenomena on which the system is based. The tape must show Greenwich civil time plus the received doppler frequency as a function of time. The basic quantity required for the operation of the data-reduction unit is a 1-megacycle-per-second signal. This signal is supplied to a time-signal generator (not shown) that may be inserted to test the equipment. During operation, however, the 1-megacycle-per-second signal goes to a time encoder that may be connected to a receiver that is receiving either radio station *WWV* or the time transmissions from the satellite itself. The time encoder generates a series of synchronized control signals for other parts of the data reduction unit, such as the doppler control, punch readout, et cetera.

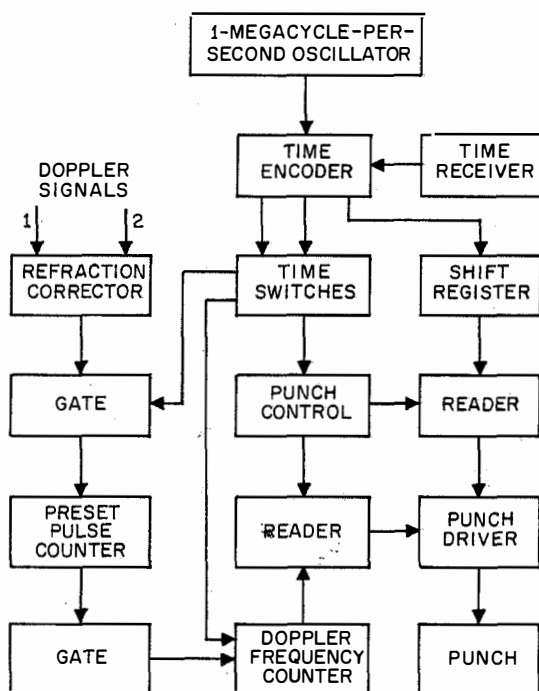


Figure 7—Data-reduction unit.

One of the outputs of the time encoder is a digital output corresponding to Greenwich civil time. This output is stored in a shift register and, on command of a signal from the time switches, is recorded on the paper tape. Provisions are also made for including on the paper tape a suitable heading indicating the station at which the tape was made and other significant data, but this feature is also not shown in the figure.

The time switches control a gate that passes doppler cycles to a preset pulse counter. The counter is preset in that it will accept only 1024 positive-going doppler cycles. On receipt of this number of cycles, it operates through another gate to a doppler frequency counter. "Doppler frequency counter" is a misnomer, for this unit actually counts not the doppler frequency but the number of 1-megacycle-per-second pulses from the previously mentioned oscillator. It therefore counts the number of 1-megacycle-per-second time intervals that occur during the reception of 1024 doppler frequency cycles. The time and the output of the doppler frequency counter are read out on a standard telegraph paper tape once every two seconds.

### 5. Accuracy and Instrumentation

It was indicated earlier that the Transit system had a large figure of merit so it would be expected to have a very-high order of accuracy. It is now necessary to consider those factors in the system that introduce error or a departure from the system's intrinsic accuracy. One of the most important is diffraction of the radio waves through the propagation medium. The theory discussed earlier was based on the hypothesis that the radio waves from the satellite traveled in a straight line to the receiving station. The medium actually causes some severe bending of the waves and makes it appear that the satellite is traveling on a different path than it really is. The observed doppler shift has been approximated by a power series [6] as

$$\Delta f^{(i)} = \Delta f_o^{(i)}(t) + \mu(t)/f_i \quad (8)$$

where  $\Delta f^{(i)}$  is the doppler shift as observed at the receiver

$\Delta f_o^{(i)}(t)$  is the doppler frequency that would have been present if the transmission had been in a vacuum

$\mu(t)$  is the power coefficient of  $1/f_i$ ; where  $f_i$  is the transmitting frequency.

The Transit system makes use of transmissions on two harmonically related frequencies, one of which is 3 times the other. Equation (2) shows that  $\Delta f_o^{(i)}(t)$  should be 3 times as large for 162 as for 54 megacycles per second. The term, because of diffraction, is one-third as large for the higher as for the lower frequency. With this information, therefore, it is possible to construct a passive network that solves two simultaneous equations and abstracts the doppler frequency as if the transmission had been in a vacuum; that is, to a first approximation. This passive network is called a refraction-correction unit and uses standard available adders, subtractors, and multipliers.

Before considering the problem of instrumental accuracy, it is desirable to review again the procedure for determining position by the satellite system, which is as follows:

- (A) The exact time when the doppler frequency becomes zero is observed.
- (B) The exact projected position of the satellite on the surface of the earth and its altitude are determined for the time of zero doppler frequency from an ephemeris.
- (C) The slant distance from the satellite to the receiver is determined through an observation of the rate of change of doppler frequency (at the time that the frequency becomes zero) and the use of (6).

A curve giving the doppler frequency [7] as a function of time is shown in Figure 8. This curve is for the 74th orbit of satellite Beta 1957 for the combined frequencies of 20 and 40 megacycles per second. It is seen that the steeper and linear portions of the curve oc-

curred during a period of about 1.5 minutes. Satellite *IB*, for example, was traveling at a velocity of approximately 17 006 miles (27 363 kilometers) per hour or about 4.724 miles (7.6 kilometers) per second. An error of only one second in reading the time of zero doppler frequency would result in an error of 4.724 miles in reading the position from the ephemeris. Unlike other navigation systems, in which the information cycle is repeated again and again at rates which may be of the order of 30 per second, the Transit system produces only one information cycle each time the satellite passes the observer. To extract accurate information from this single passage, it is necessary to use all parts of the information cycle. Accordingly, the model 1002 receiver prints out values of the doppler cycle as a function of time for the entire cycle. The procedure used to determine the information consists of preplotting doppler curves and determining which one best fits the curve recorded from the satellite pass [8]. This type of computation has been performed with digital computers for apparent reasons.

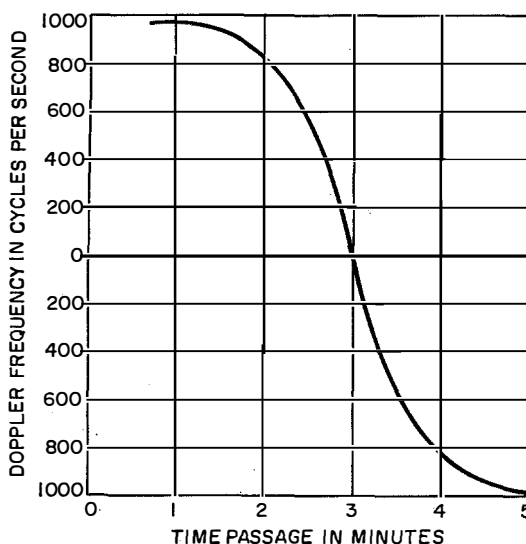


Figure 8—Curve of doppler shift. The curve was drawn from combined 20- and 40-megacycle-per-second observations of satellite  $\beta$  during orbit 74 on 8 November 1957, starting at 1019 Greenwich civil time.

TABLE 1  
HISTORY OF TRANSIT SATELLITES

Model	Launch Date	Perigee in Miles (Kilometers)	Apogee in Miles (Kilometers)	Period of Orbit in Minutes	Inclination of Orbit to Equator in Degrees	Comments
<i>IB</i>	13 April 1960	234 (376)	478 (770)	96	51	Ceased radiating because of power-supply difficulties
<i>IIA</i>	21 June 1960	386 (621)	665 (1070)	102	66.7	Still effective
<i>IIIB</i>	21 February 1961	111 (178)	605 (974)	117	28	Life less than 6 weeks because of highly elliptical orbit
<i>IVA</i>	28 June 1961	542 (872)	610 (982)	94	67	Still effective
<i>IVB</i>	15 November 1961	542 (872)	685 (1102)	105.9	32.4	Still effective

Frequency-measuring accuracies of the receiving system require special consideration. Random frequency errors introduced by the receiving equipment must be held to a root-mean-square value of less than 1 part in 10<sup>9</sup> of the received frequency. The other major sources of these errors are:

(A) Phase shifts in the automatic-gain-controlled stages of the receiver during received signal amplitude variations.

(B) Phase errors introduced by the phase-locked tracking loop because of the time rate of phase and its derivatives.

(C) Phase noise originating in the frequency standard and frequency synthesizer.

(D) Frequency jitter in the voltage-controlled oscillator that provides the narrow-band output from the phase-locked loop.

(E) Counting errors in the digital frequency-sampling equipment.

## 6. Performance

As stated previously, a total of 5 Transit satellites have been orbited successfully or with sufficient success to produce useful results. These satellites are listed in Table 1. As an example of the performance of these devices, satellite *IB* produced a signal on each side of its orbit (as projected on the face of the earth) of approximately 1600 miles; therefore, it produced navigational coverage over nearly 80 million square miles of the earth's

surface per orbit. It did not, however, produce navigational information continuously, since it had a period of 96 minutes. At each pass, its position advanced eastward at the equator by 24 degrees, or approximately 1600 statute miles. It was possible, therefore, for an observer at the equator to obtain between 4 and 6 readings in a period of 24 hours.

Observations made at a known location with the model 1002 receiver gave the following results:

Percent of Readings	Error in Miles (Kilometers)
38.5	0.02 to 0.05 (0.03 to 0.08)
34.5	0.05 to 0.10 (0.08 to 0.16)
23.15	0.10 to 0.50 (0.16 to 0.80)
3.85	0.50 to 0.65 (0.80 to 1.05)

Only one error was recorded in excess of 0.41 mile (0.66 kilometer) and this was an error of 0.65 mile (1.05 kilometers). Considering that this system was free from static and other propagation effects that cause signal loss, the results are truly remarkable [9].

## 7. Critique of Transit System

Let us analyze whether the Transit system constitutes a practical means for navigation or whether it is merely an interesting scientific demonstration. One of the major practical considerations, of course, is that of cost. One author [10] has expressed the opinion that a launch and booster stage based on the intermediate-range-ballistic-missile design might be reduced to the order of 2.3 million dollars.

The cost of launching is difficult to estimate because the launch facilities in existence today have been erected for other purposes. One cost estimate of a launch facility is between 15 and 20 million dollars. For our purposes, however, it is assumed that existing launch facilities will be available without cost. The cost of launching, however, cannot be disregarded and is estimated at 1.5 million dollars per launch. After development, the satellite itself may cost \$500 000. The total cost of a satellite in orbit thus might be 4.3 million dollars. It has been shown, however, that to obtain service at approximate intervals of 1.5 hours (at the equator) at least 3 such satellites would be required. Not all launchings would be successful and, assuming 50-percent failure, the cost would be approximately 25.8 million dollars. If a 3-year life is assumed, the cost per year would be 8.6 million dollars. To this cost must be added the cost of 3 ground injection stations that would be manned only on an 8-hour basis. The total cost of operating these three stations can bring the total yearly cost of the system to 8.8 million dollars. The net, therefore, is approximately 5.1 cents per navigational square mile per year.

Cost may be reduced by the use of higher-altitude satellites. It has been estimated that satellites operating at an altitude of 2000 miles may be developed with a life of 20 years. The period of such a satellite, however, would be 2 hours and 36 minutes. This system (at the equator) would provide coverage at distances of more than 4500 miles on either side of the terrestrial projection of the satellite's orbit. Three such satellites in polar orbits, therefore, might provide a preferable configuration. To increase the frequency of the readings, however, it might be desirable to use two satellites on the same orbit. This plan would be more costly than that previously discussed since an intercontinental-ballistic-missile launching stage would be required. An estimated figure is 5.3 million dollars each, plus \$500 000 for the satellite. Again assuming

50-percent failure in launching, the total cost would be 69.6 million dollars. On a 20-year-life basis, the yearly cost, including the operation of three signal-injection stations, would be 3.68 million dollars per year. Worldwide coverage would be obtained at a net cost of 1.9 cents per square mile.

A hyperbolic system [11] operating at frequencies of the order of 10 kilocycles per second is under development. This system will give coverage over the surface of the entire globe by the use of 8 stations. The cost of this system based on the best experience available is as follows:

8 Equipments.....	\$ 8 300 000
8 Buildings at 0.8-4.0 million dollars each, average of 2.0 million dollars.....	16 000 000
8 Power generators, 2250 kilovolt-amperes at \$150 per kilovolt-ampere.....	2 700 000
Land, 2000 acres per station at \$1000 per acre.....	16 000 000
Antennas.....	40 000 000
	<hr/>
Total.....	\$83 000 000

Approximate cost per year, amortized over a period of 20 years.....	\$ 4 150 000
Salaries, 28 men per station at \$168 000 per year.....	1 344 000
Replacement parts at \$250 000 per station per year.....	2 000 000
Power at 3 cents per kilowatt hour.....	4 153 000
	<hr/>

Total Operating Cost Per Year \$11 647 000

The cost per square mile of navigational coverage is 5.9 cents.

Table 2 compares the two satellite systems and the hyperbolic system.

## Terrestrial Navigation by Artificial Satellites

TABLE 2  
COMPARISON OF SATELLITE AND HYPERBOLIC SYSTEMS

Criterion	300-Mile (483-Kilometer) 50-Degree Orbit	2000-Mile (3218-Kilometer) Polar Orbit	Hyperbolic Ground-Based System
Frequency range	Very high and ultra high	Very high and ultra high	Very low
Coverage in millions of square miles (square kilometers)	174 (450.66)	Entire earth's surface or 197 (510.23)	Entire earth's surface or 197 (510.23)
Readings	Every 1.5 hours	Every 1.3 hours	Continuous
Ambiguity	None	None	Every 10 miles
Accuracy	See text	See text	0.25-0.5 mile
Initial cost in millions of dollars	25.8	69.6	83
Life in years	3	20	20
Cost per year in millions of dollars	8.8	3.68	11.65
Cost per square mile per year in cents	5.1	1.9	5.9

### 7.1 RECEIVER

It is evident from Figure 5 that the Transit ground receiver is an elaborate equipment. The necessity to correct for refraction requires the use of a 2-frequency receiver. If transistors become available that would operate on the higher frequencies, it may be possible to operate the system at a frequency of 1600 megacycles per second. This frequency has already been assigned for worldwide navigation use by the International Telecommunications Union. At 1600 megacycles per second, the refractive index would be sufficiently small so that it could be disregarded. The receiver is complicated because of the use of phase-locking techniques. These techniques are employed because of the very-low power that is used in the satellite. They could be eliminated if the transmitter power could be increased appreciably. The data are now extracted by the use of a data-reduction unit and a digital computer. Clearly, these techniques are impractical if the equipment is to be used on small ships and fishing boats. It is possible to incorporate at the receiver output a recorder that will plot directly the doppler frequency as a function of time. It may be possible to obtain fair accuracy by using a plastic scale engraved with a number of pre-calculated doppler curves. It appears, there-

fore, that with further development, the cost of receivers may be reduced to a level meeting the market requirements of small shipowners. Nothing has been said about use of the Transit system for aircraft navigation. With aircraft that will be capable of traveling from New York to Europe in about 2 hours, a system that produces only one reading in a period of 1 hour is not very helpful, although it may be usable for correcting doppler navigators.

From the foregoing discussion, it has been shown that the Transit system has a cost of the same order as a worldwide ground-based system and, with further development, may be substantially lower in cost. The transmitting system has the advantage of requiring low power. The complete system is virtually unmanned. Its greatest field of application, however, appears to lie with ships rather than with aircraft. The United States Navy has announced that it will place its Transit system in operational use [12].

### 8. Acknowledgments

The author gratefully acknowledges the assistance of Dr. Maurice Arditi in the development of equation (6); Mr. P. D. Rodgers for the material describing the model 1002

receiver; Commander Robert T. Swenson, United States Naval Reserve; and Mr. John Nicolaidis for information on the Transit satellite.

## 9. References

1. R. F. Freitag, "Project Transit; A Navigation Satellite," *Journal of the Institute of Navigation*, volume 7, numbers 2-3; Summer-Autumn 1960; page 106.
2. P. C. Sandretto, "Principles of Electronic Navigation Systems," *IRE Transactions on Aeronautical and Navigational Electronics*, volume ANE-6, number 4, page 221; December 1959.
3. J. D. Nicolaidis, "Project Transit; Earth and Aerospace Navigational Satellite System," *Aerospace Engineering*, volume 20, number 2, pages 20-21, 60, 62-65; February 1961.
4. L. Booda, "Transit," *Aviation Week*, pages 26-28; 10 July 1961.
5. "Operation and Maintenance Manual for Doppler Systems, Model 1002," ITT Federal Laboratories, Fort Wayne, Indiana, 1960; Sections 4 and 6.
6. G. C. Weiffenbach, "Measurement of Doppler Shift of Radio Transmission from Satellites," *Proceedings of the IRE*, volume 48, number 4, pages 750-754; April 1960.
7. H. P. Hutchinson, "Slant Range at the Nearest Approach," *IRE National Convention Record*, Part V, pages 65-66; 23-26 March 1959.
8. O. R. Spies, "The Problem of Satellite Navigation by Use of a Doppler Receiver," *Ballistic Missile and Space Technology*, Academic Press, New York and London, 1960; pages 73-101.
9. R. B. Kershner, "Transit Program Results," *Astronautics*, volume 6, number 5, pages 30-31, 106, 108-110; May 1961.
10. B. Graham, "Commercial Application of Satellite Boosters," Institute of the Aeronautical Sciences 29th Annual Meeting, New York; 23-25 January 1961.
11. C. J. Casselman, D. P. Heritage, and M. L. Tibbals, "VLF Propagation Measurements for Radux-Omega Navigation System," *Proceedings of the IRE*, volume 47, number 5, part 1, pages 829-839; May 1959.
12. R. Hawkes, "Transit System," *Aviation Week and Space Technology*, pages 57-59; 1 January 1962.

**Peter C. Sandretto** was born on 14 April 1907 in Pont Canavese, Italy. He received from Purdue University a B.Sc. degree in 1930 and the degree of electrical engineer in 1938. He graduated from the Command Staff School of the United States Army.

From 1930 to 1932, he designed aircraft radio equipment at Bell Telephone Laboratories. He was superintendent of the communication laboratories of United Air Lines from 1932 to 1942. From 1942 to 1946, he served in the United States Air Force, advancing to the rank of brigadier general.

In 1946, he joined International Telephone and Telegraph Corporation and later became vice president and technical director of Federal Telecommunication Laboratories. In 1960, he became deputy executive of the U. S. Defense Group. In 1963 he transferred to the North American Area Staff of International Telephone and Telegraph Corporation. He served temporarily as acting president of ITT Kellogg Telecommunications Division.

General Sandretto is a Fellow of the Institute of Electrical and Electronics Engineers, a vice-president of the Institute of Navigation, and Member of the Institution of Electrical Engineers. He has lectured extensively in many parts of the world and is the author of two books, the more recent being *Electronic Avigation Engineering*.

**Radio Communication and  
Navigation Via Artificial  
Earth Satellites**

**VOLUME 39 • NUMBER 1 • 1964**